



The
University
Of
Sheffield.

**Binding of bacteria to highly branched poly (*N*-isopropylacrylamide) modified with antibiotics:
Comparison of behaviour of linear and highly branched
conformation**

Pavintorn Teratanatorn

A thesis submitted for the Degree of Doctor of Philosophy

Department of Clinical Dentistry

The University of Sheffield

May 2018

Acknowledgments

I would like to express my gratitude to my supervisors, Prof Charles W. I. Douglas and Prof Stephen Rimmer who provided me with an opportunity to pursue my PhD. I am grateful for all their consistent support, guidance and encouragement throughout this project. I would like to thank Dr David Williams, who was my advisor from the Chemistry Department for his advice, and Dr Daniel Lambert, who also gave me warm welcome when I moved to the department of Clinical Dentistry.

I am truly grateful for all support and valuable guidance from Dr Joanna Shepherd, Dr Richard Hoskins, Dr Thomas Swift, Dr Marc Daigneault and Dr Natalya Doroshenko. Special thanks to Dr Abigail Pinnock, Dr Aunwaya Kaewpitak, Jason Heath and Brenka McCabe who gave me kind support and helpful guidance on the biological work. I would also like to thank to Dr Colin Gray who assisted me with confocal imaging, Jenny Louth for training me to use microDSC and Dr Esther Karunakarun for allowing me to use ZetaPALS.

Thanks to all the members of the biomaterials group (F Floor) and oral and maxillofacial pathology unit for their assistance and making the department such an enjoyable place to work particularly Dr Saran Canning, Dr Laura Shallcross, Dr Richard Plenderleith and Dr Laura Platt.

I am thankful to Dr Sawaporn Siripanthana, Dr Matthana Khangkhamano, Dr Rungrote Kokoo and Dr Supatthra Narawatthana and other Thai friends for all kinds of support during these years.

I would like to thank Abdullah Khalid for always being there for me and making my life in Sheffield so memorable.

Lastly, I would like to express profound gratitude to my parents and to my brother for financial support and endless encouragement throughout my studies and my life.

Abstract

Poly (*N*-isopropylacrylamide) (PNIPAM) polymers are thermo-responsive and change conformation above their lower critical solution temperature (LCST). However, there is evidence that highly branched PNIPAM can be driven through a conformational change from open chain to globule at temperatures below the LCST by interaction of groups placed on the chain ends with a compatible molecule/ligand. It is less clear how the linear analogue would behave and our hypothesis is that it would collapse but with the chain ends shielded within the globule. In this study we explored the behaviour of a highly branched PNIPAM and a linear analogue that had the antibiotic vancomycin placed at the chain ends. Vancomycin binds to residues in the cell wall of Gram-positive bacteria so binding to bacteria should result in the highly branched PNIPAM undergoing a conformational change. The aim of the work reported in this thesis, therefore, was to compare the behaviour of linear and highly branched PNIPAM functionalised with vancomycin when interacting with *Staphylococcus aureus* with a view to better understand the role of conformation in polymer responsiveness.

The reporting systems employed were the ability of the polymers to cause aggregation of bacteria and the response of the fluorescent solvatochromic dye, Nile red. The highly branched PNIPAM (HB-PNIPAM) was synthesised via self-condensing vinyl polymerisation (SCVP)-reversible addition-fragmentation chain transfer (RAFT) polymerisation using 4-vinylbenzyl-1-pyrrolocarbodithioate as the chain transfer monomer. The polymer chain ends were functionalised with vancomycin via activation of carboxylic acids to succinimidyl derivative. A linear analogue of the polymer was synthesised using vinyl benzoic acid as comonomer to provide the same fraction of repeating units and aryl groups, because HB-PNIPAM consists of aryl branching points. The coil-to-globule conformational transition of the two polymers was studied by micro differential scanning calorimetry (microDSC) and turbidimetry. It was found that the LCSTs of highly branched polymers with pyrrole and carboxylic acid chain ends could be measured by turbidimetry (cloud point) and by microDSC. A cloud point for vancomycin-ended PNIPAM could only be detected for the linear version, not the HB-PNIPAM-van. However, the LCST of both polymers could be measured by microDSC.

In aggregation tests with bacteria in aqueous suspension, the L-PNIPAM-van and HB-PNIPAM-van behaved very differently. Even though both polymers contained the same amount of vancomycin, only the HB-PNIPAM-van caused aggregation of *S. aureus*. These

observations support a concept that the HB-PNIPAM-van has a core-shell structure above its LCST, with the densely packed core originating from desolvated PNIPAM and the outer shell stemming from solvated polymer that is swollen because of the presence of vancomycin. In contrast, when the L-PNIPAM-van initially bound to *S. aureus* and desolvation occurred, most of the vancomycin residues become shielded within the globule so are not available to stabilise the collapse and consequently bind more bacteria. It is suggested that the outer shell swelling is stabilised by electrostatic repulsion of adjacent vancomycin residues. However, a further complexity was identified which was the degree of hydrophobicity and charge of the bacterial cells.

We also sought to confirm that vancomycin end groups of both linear and highly branched polymers were still functional and able to bind to their targets. The data presented here indicate that as the vancomycin residues on the chain ends of the polymers bind to their targets D-Ala-D-Ala and the two polymers did not differ in this respect.

To probe the solvation state of the polymers when interacting with the target for vancomycin, two approaches were taken. First in the presence of the D-Ala-D-Ala peptide, hydration was disrupted by binding to vancomycin so that less energy was required to drive the polymer through its LCST. Second, a solvatochromic dye, Nile red, provided information on the environmental polarity of the polymer. The hypothesis was that Nile red could provide information on phase transition because loss of water should shift the emission wavelength or fluorescence intensity. It was found that in the presence of 10^8 cfu/ml of *S. aureus* and HB-PNIPAM-van Nile red fluorescence increased with the number of bacteria almost in a dose dependent manner, whereas there was relatively little change in fluorescence with the L-PNIPAM-van. This supports a model of change in the solvation of only the microenvironment around the chain ends of HB-PNIPAM-van, rather than of the whole polymer segment.

Finally, we have shown that highly purified vancomycin functionalised L-PNIPAM and HB-PNIPAM, which bind to the cell surface of *S. aureus* without killing activity. We conclude, therefore, that the binding interaction primarily involves surface-located D-Ala-D-Ala on the bacterial cell wall.

List of Abbreviations

ACVA	4, 4-azobis (4-cyanovaleric acid)
Ala	alanine
ATRP	atom transfer radical polymerisation
BHI	brain heart infusion
CDCl ₃	deuterated chloroform
CIP	cell-imprinted polymer
CRP	controlled-radical polymerisation
CTA	chain transfer agents
Đ	dispersity
DB	degree of branching
DMAC	dimethylacetamide
DMF	dimethylformamide
DMSO	dimethyl sulfoxide
DNSBA	(3-(5-(dimethylamino naphthalene-1-1sulfonamido) phenyl) boronic acid)
D ₂ O	deuterium oxide
DSC	differential scanning calorimetry
ELP	elastin-like polypeptides
ELISA	enzyme-linked immunosorbent assay
ECM	extracellular matrix
Gly	glycine
Glu	glutamic acid

GPC	gel permeation chromatography
HB	highly branched
HRP	horseradish peroxidase
LCST	lower critical solution temperature
LPS	lipopolysaccharide
LTA	lipoteichoic acid
Lys	lysine
MIP	molecular-imprinted polymers
M_n	number-average molecular weight
M_w	weight-average molecular weight
MIC	minimum inhibitory concentration
MRSA	methicillin-resistant <i>Staphylococcus aureus</i>
MSCRAMM	Microbial Surface Components Recognising Adhesive Matrix Molecules
NAG	<i>N</i> -acetyl-D-glucosamine
NAM	<i>N</i> -acetylmuramic acid
NIPAM	<i>N</i> -isopropylacrylamide
NR	Nile red
OPD	o-phenylenediamine dihydrochloride
PBS	phosphate buffered saline
PDA	polydiacetylene
PDI	polydispersity
PMVE	poly (methyl vinyl ether)
PNIPAM	poly (<i>N</i> -isopropylacrylamide)

Pro	proline
PVCL	poly (<i>N</i> -vinylcaprolactam)
RAFT	reversible addition-fragmentation chain transfer polymerisation
RI	refractive index
SCVP	self-condensing vinyl polymerisation
SEC	Size exclusion chromatography
SNAPP	structurally nano-engineered antimicrobial peptide polymer
TRAMS	time-resolved anisotropy measurement
Val	valine
VBA	vinyl benzoic acid
Van	vancomycin
VISA	vancomycin-intermediate <i>Staphylococcus aureus</i>
VRE	vancomycin resistant Enterococci
WTA	wall teichoic acids

Table of Contents

Acknowledgments.....	i
Abstract.....	ii
List of Abbreviations	iv
Table of Contents.....	vii
Chapter 1 : Introduction	1
1.1 Detection of microorganisms and applications	3
1.2 <i>Staphylococcus aureus</i> and vancomycin antibiotic.....	7
1.3 Thermo-responsive polymers used in biological applications	19
1.3.1 Poly (<i>N</i> -vinylcaprolactam) (PVCL).....	20
1.3.2 Poly(methyl vinyl ether) (PMVE)	21
1.3.3 Elastin-like polypeptides (ELP).....	22
1.3.4 Naturally-derived polymers and synthetic thermo-responsive polymer system	24
1.3.5 Poly (<i>N</i> -isopropylacrylamide) (PNIPAM) and lower critical solution temperature (LCST) 26	
1.3.6 Thermodynamics of low critical solution temperature	28
1.4 Reversible addition-fragmentation chain transfer (RAFT)-mediated self-condensing vinyl polymerisation (SCVP).....	30
1.4.1 Factors that affect RAFT polymerisation	33
1.4.2 The success of highly branched PNIPAM synthesised by reversible addition- fragmentation chain transfer (RAFT) mediated self-condensing vinyl polymerisation (SCVP) polymerisation used in biological studies	37
1.5 Ideal features of a detection system for binding bacteria to polymers functionalised with antibiotics.....	39
1.6 Hypothesis, Aims and Objectives	42
Chapter 2 : Materials, methods and polymer characterisations.....	44
2.1 Materials	44
2.2 Synthesis	44
2.2.1 Synthesis of 4-vinylbenzyl pyrrolicarbodithioate	44
2.2.2 Highly branched PNIPAM (HB-PNIPAM-pyrrole)	45
2.2.3 Carboxylic acid terminated highly branched polymer (HB-PNIPAM-COOH).....	47
2.2.4 Synthesis of HB-PNIPAM with vancomycin at the chain ends (HB-PNIPAM-van).....	48
2.2.5 Synthesis of linear poly (<i>N</i> -isopropylacrylamide)-co-vinylbenzoic acid (L-PNIPAM)	50
2.2.6 Synthesis of linear poly (<i>N</i> -isopropylacrylamide)-co-vinylbenzoic acid functionalised with vancomycin (L-PNIPAM-van)	51
2.3 Polymer characterisation.....	53

2.3.1 ¹ H NMR spectroscopy	53
2.3.2 Fourier Transform Infrared Raman spectroscopy (FTIR)	53
2.3.3 Size Exclusion Chromatography (SEC)	53
2.3.4 Determination of LCST	53
2.3.5 Zeta potential measurements	54
2.3.6 Particle sizing analysis.....	54
2.4 Results and discussion	54
2.4.1 Nuclear Magnetic Resonance (NMR).....	57
2.4.2 Fourier Transform Infrared Raman spectroscopy (FTIR)	62
2.4.3 Size Exclusion Chromatography (SEC) analysis.....	64
2.4.4 Low critical solution temperature and cloud point of the polymers	71
2.4.5 Electrostatic charge of HB-PNIPAM-van and L-PNIPAM-van.....	79
2.4.6 Development of assay for quantifying amount of vancomycin in polymers	86
2.5 Conclusions.....	101
Chapter 3 : Determination of the killing capability of polymers functionalised with vancomycin	102
3.1 Introduction.....	102
3.2 Materials	103
3.3 Methods.....	103
3.3.1 Determination of Minimum Inhibitory Concentration (MIC)	103
3.4 Results and Discussion	104
3.5 Conclusions.....	110
Chapter 4 : The effect of hydrophobicity and electrostatic charge of bacteria on binding ability of the polymers	111
4.1 Introduction.....	111
4.2 Hydrophobicity test of <i>S. aureus</i> strains	112
4.2.1 Materials	112
4.2.2 Methods	112
4.2.3 Results and discussion	113
4.3 Assessment of polymer binding to bacteria	114
4.3.1 Materials	114
4.3.2 Methods	114
4.3.3 Results and discussion	116
4.4 Bacterial surface charge.....	137
4.4.1 Materials	138
4.4.2 Methods	138

4.4.3 Results and discussion	138
4.5 Comparison of D-Ala-D-Ala binding sites on <i>S. aureus</i> strains using fluorescent vancomycin	150
4.5.1 Materials and Methods	150
4.5.2 Results and discussion	150
4.6 Conclusions.....	152
Chapter 5 : Development of a reporter system for Gram-positive bacteria based on L-PNIPAM and HB-PNIPAM modified with vancomycin using Nile red dye as a probe.....	153
5.1 Introduction.....	153
5.2 Materials	154
5.3 Methods.....	154
5.3.1 Bacteria preparation.....	154
5.3.2 Mat/button aggregation – rapid method for assessing bacterial binding to PNIPAM-van polymers	154
5.3.3 Addition of Nile red to polymer incubated with bacteria	154
5.4 Results and discussion	155
5.4.1 Aggregation assay of HB-PNIPAM-van and L-PNIPAM-van incubated with <i>S. aureus</i> at various bacterial concentrations and incubation times	155
5.4.2 Development of a detection system for the binding of <i>S. aureus</i> to HB-PNIPAM-van and L-PNIPAM-van at various bacterial concentrations with Nile red as a probe	157
5.5 Conclusions.....	168
Chapter 6 : Comparison of the interactions of HB-PNIPAM-van and L-PNIPAM-van with D-Ala-D-Ala peptide: Investigation of enthalpy change and LCST of the polymers.....	169
6.1 Introduction.....	169
6.2 Materials and Method	170
6.3 Results and Discussion	172
6.4 Conclusions.....	183
Chapter 7 : Summary, and Conclusions	184
7.1 Summary and Conclusions.....	184
Chapter 8: Future Work	189
References.....	190

List of Figures

Figure 1.1 Gram-positive cell wall structure	7
Figure 1.2 Schematic diagram of Peptidoglycan of <i>S. aureus</i>	9
Figure 1.3 Model of virulence determinant synthesis in infection of <i>S. aureus</i>	11
Figure 1.4 The structure of vancomycin	15
Figure 1.5 (A) The formation of the stoichiometric complex between vancomycin and D-Ala-D-Ala dipeptides terminus of precursors, (BI) Phase contrast image of <i>S. aureus</i> cells (BII) An image of the same sample with fluorescent vancomycin viewed with fluorescent microscope. Fluorescence is concentrated at recent division sites [62].....	16
Figure 1.6 Structural aspects of vancomycin involved in dimerisation [70]	17
Figure 1.7 Schematic of the replacement of D-Ala with D-Lac in resistant strain, leading to a decrease in binding affinity with vancomycin due to the repulsion between oxygen atoms [55].....	18
Figure 1.8 The chemical structure of poly (<i>N</i> -vinylcaprolactam) (PVCL).....	20
Figure 1.9 The chemical structure of poly (methyl vinyl ether) (PMVE)	21
Figure 1.10 The chemical structure of PNIPAM	26
Figure 1.11 The mechanism of SCVP [115].....	30
Figure 1.12 Mechanism of RAFT polymerisation [124]	31
Figure 1.13 A scheme showing the possible fragmentation of IR [124]	34
Figure 1.14 The structure of vinyl RAFT agents synthesised by Carter et al.....	38
Figure 1.15 The structure of Nile red dye.....	40
Figure 2.1 The chemical structure of 4-vinylbenzyl pyrrolocarbodithioate	45
Figure 2.2 ¹ H NMR spectrum of HB-PNIPAM with pyrrole end groups, with the expanded region showing the peaks due to the pyrrole groups (m and l) and the peaks due to the styryl groups (e and f)	46
Figure 2.3 ¹ H NMR spectrum of HB-PNIPAM-COOH , with the expanded region showing the peaks due to the carboxylic acid groups (k).....	48
Figure 2.4 ¹ H NMR spectrum of HB-PNIPAM-van in D ₂ O	49
Figure 2.5 The chemical structure of L-P(NIPAM-co-VBA).....	50
Figure 2.6 ¹ H NMR spectrum of L-PNIPAM-van in D ₂ O.....	52
Figure 2.7 Schematic diagram showing synthesis of HB-PNIPAM-van.....	55
Figure 2.8 Schematic diagram showing synthesis of L-PNIPAM-van.....	56
Figure 2.9 Examples of ¹ H NMR of (A) HB-PNIPAM-van and (C) L-PNIPAM-van in D ₂ O and (B) magnified region from 6-8.5ppm and (D) Expanded ¹ H NMR of (D1) HB-PNIPAM-van and (D2) L-PNIPAM-van	60
Figure 2.10 FTIR spectra of (A) HB-PNIPAM and (B) linear PNIPAM (1500-1900cm ⁻¹) during chain end modifications (original = red, acid modified = dashed red, succinimide modified = blue, vancomycin modified = black).....	63
Figure 2.11 The universal calibration curve of methanol-SEC generated by retention time of series of PNIPAM standard polymer	65

Figure 2.12 Molar mass distributions of HB-PNIPAM-van (—) and L-PNIPAM-van (--) from determined by methanol SEC	67
Figure 2.13 Molar mass distributions of HB-PNIPAM with different type of chain ends	67
Figure 3.1 Schematic showing the layout of the 96 well plates with the range of the concentration of vancomycin.....	103
Figure 3.2 MICs of vancomycin of four strains of <i>S. aureus</i> . The lowest concentrations of vancomycin required to inhibit the visible growth of bacteria are the concentration between the last wells in which there is no bacterial growth and the first well showing growth (cloudy) after overnight incubation.	105
Figure 3.3 Example images of antimicrobial activity testing of L-PNIPAM-van and HB-PNIPAM-van with Oxford (NCTC 6571) strain which show that neither polymers had any detectable inhibitory activity toward <i>S. aureus</i>	106
Figure 3.4 A model explaining how HB-PNIPAM with vancomycin chain ends could interact with D-Ala-D-Ala peptides in the cell wall without influencing the integrity of the cell wall (not to scale).....	110
Figure 4.1 %Hydrophobicity of four strains of <i>S. aureus</i> , namely Oxford (NCTC6571), S235, Newman and L9897.....	113
Figure 4.2 The scheme of rapid Mat/button assay for HB-PNIPAM-van and L-PNIPAM-van	116
Figure 4.3 Images captured under UV light of HB-PNIPAM-van and L-PNIPAM-van incubated with <i>S. aureus</i> (1×10^8 cfu/ml) for 2, 4 and 24 h	117
Figure 4.4 Images captured under UV light of HB-PNIPAM-van and L-PNIPAM-van incubated with <i>S. aureus</i> S235, L9879 and Newman (1×10^8 cfu/ml) for 24 h.....	119
Figure 4.5 Confocal images of <i>P. aeruginosa</i> and <i>S. aureus</i> Oxford (NCTC6751) (both 1×10^8 cfu/ml) incubated for 24 h at 37 °C.	122
Figure 4.6 Confocal images of <i>S. aureus</i> strain S235 (1×10^8 cfu/ml) incubated at 37°C for 24 h in (G) PBS; (H) L-PNIPAM-van; (I) HB-PNIPAM-van. (J) Zoom in of HB-PNIPAM-van incubated with <i>S. aureus</i> S235.....	124
Figure 4.7 Confocal images of HB-PNIPAM-van and L-PNIPAM-van incubated with <i>S. aureus</i> Newman (10^8 cfu/ml) in PBS at 37°C for 24 h.....	125
Figure 4.8 Confocal images of HB-PNIPAM-van and L-PNIPAM-van incubated with <i>S. aureus</i> L9879 (10^8 cfu/ml) in PBS at 37°C for 24 h.....	126
Figure 4.9 Images of <i>S. aureus</i> strains (1×10^8 cfu/ml) incubated with HB-PNIPAM-van and L-PNIPAM-van for 24 hours in PBS at room temperature (22°C)..	127
Figure 4.10 Binding of vancomycin to Alanine-D-Alanine of bacteria cell wall.....	129
Figure 4.11 The interaction of polymer modified with vancomycin to D-Ala-D-Ala in Gram-positive <i>S. aureus</i> cell wall peptidoglycan.....	130
Figure 4.12 Schematic representation of the mat formation of bacteria-HB-PNIPAM-van polymer complex	134
Figure 4.13 Schematic representation of the mat formation of Bacteria-L-PNIPAM-van complex.....	135
Figure 4.14 Images of the mat/button assay and confocal microscopy of HB-PNIPAM-van and L-PNIPAM-van incubated with <i>S. aureus</i> Oxford (NCTC6751) in PBS for 24 h (composite of sections of figs 4.4 & 4.8).....	136

Figure 4.15 Bar charts showing the zeta potential values of four strains of <i>S. aureus</i> suspended in three different buffers.....	139
Figure 4.16 Summary of zeta potential values of all stains used in this study in potassium phosphate buffer (0.12M), PBS (0.164M) and PUM buffer (0.602M).....	141
Figure 4.17 Cross-sectional representation of a bacterial cell illustrating the various layers of ions surrounding the cell surface	142
Figure 4.18 Images of aggregation assays of HB-PNIPAM-van and L-PNIPAM-van incubated with Oxford (NCTC6751), S235, L9879 and Newman strain labelled with Et/Br in potassium phosphate buffer (navy line) and in PBS (green line) at 37°C for 24 hours.	146
Figure 4.19 Schematic diagram presenting the interactions that occur between bacteria and HB-PNIPAM-van polymer. Hydrogen bonding occurs between the vancomycin groups at the chain ends of the polymers and D-Ala-D-Ala in the bacterial cell wall.	149
Figure 4.20 Chemical structure of fluorescent vancomycin (BODIPY®FL).....	150
Figure 4.21 Relative fluorescence intensity of bound fluorescent vancomycin to two <i>S. aureus</i> strains.	151
Figure 5.1 Nile red solution in various types of solvents (n-hexane, acetone).....	153
Figure 5.2 Mat/button assay of <i>S. aureus</i> Oxford (NCTC6751) with PNIPAM-van polymers for varying times and with varying number of bacteria.....	156
Figure 5.3 Bar chart showing relative fluorescent intensity of HB-PNIPAM-van and L-PNIPAM-van with Nile red solution incubated with 10^8 cfu/ml <i>S. aureus</i> at 37°C for 2, 4 and 24 hours.....	158
Figure 5.4 Fluorescence intensity of HB-PNIPAM-van and L-PNIPAM-van solutions incubated with 10^5 - 10^8 cells/ml <i>S. aureus</i> and nile red at 37°C at 2 h	159
Figure 5.5 Fluorescence intensity of HB-PNIPAM-van and L-PNIPAM-van solutions incubated with 10^5 - 10^8 cells/ml <i>S. aureus</i> and nile red at 37°C at 4 h	160
Figure 5.6 Fluorescence intensity of HB-PNIPAM-van and L-PNIPAM-van solutions incubated with 10^5 - 10^8 cells/ml <i>S. aureus</i> and nile red at 37°C at 24 h	161
Figure 5.7 Fluorescence intensity of L-PNIPAM-van and HB-PNIPAM-van with increasing number of bacterial cells (10^5 - 10^8 cfu/ml) at 2, 4 and 24 hours using nile red as probe with excitation at 550 nm and emission at 640 nm.....	163
Figure 5.8 A Schematic diagram showing non-homogeneous response of HB-PNIPAM-van on binding to bacteria (via its binding site D-Ala-D-Ala) in presence of nile red.....	166
Figure 6.1 The microDSC curve of L-PNIPAM-van solution with various concentrations of D-Ala-D-Ala peptide on heating from 10 to 40°C.	173
Figure 6.2 The percentage enthalpy decrease of L-PNIPAM-van and HB-PNIPAM-van in the presence of D-Ala-D-Ala peptides at various concentrations.....	174
Figure 6.3 Changes in enthalpy of L-PNIPAM-van compared with the ratio of peptide: vancomycin.	176
Figure 6.4 Changes in enthalpy of HB-PNIPAM-van as the ratio of peptide: vancomycin increase.	176
Figure 6.5 A schematic diagram showing a non-homogenous response of HB-PNIPAM-van to binding to the D-Ala-D-Ala dipeptide and relation to the LCST.	180

Chapter 1 : Introduction

With the emergence of bacterial resistance to antibiotics, early diagnosis of infections is critical. If not treated appropriately, wound infections can become chronic and/or severe, leading to a decrease in healing rate and increased morbidity/mortality in serious cases [1-3]. Furthermore, many clinical research papers have shown that wound infections affect not only the quality of patients' lives, but also there is financial loss for the healthcare system. Data from the World Health Organization revealed that there are more than a hundred million patients around the world each year who are affected by bacterial infections, especially *Staphylococcus aureus*, which is a common wound pathogen [4, 5]. One of the main factors that plays a crucial role in wound healing is the number of bacteria that colonise the wound. This is closely linked to how the status of the wound can be precisely diagnosed [6-9].

The classical ways to diagnose wound infection rely on signs and symptoms of wounds such as local warmth, redness and swelling of the area, obvious wound breakdown [2, 8] and conventional microbiology. The latter is not readily available in all countries and it is difficult to diagnose the stages of wound infections accurately using clinical methods alone. Consequently antibiotics are often prescribed, even though the wound might only be becoming colonised by bacteria rather than infected [10]. To minimise the use of antibiotics, effective early detection of pathogens is one of the challenging goals in all areas of infection treatment. Therefore, the development of simple-to-use devices for identification of pathogenic bacteria would be a very useful addition to the clinician's armament.

One approach to devising a simple diagnostic device is to capitalise on the behaviour of certain polymer systems. For example, efforts are being made to develop the properties of poly (*N*-isopropyl acrylamide) (PNIPAM) by modifying it with high-affinity ligands for bacteria. PNIPAM has been extensively used in a wide range of biomedical areas because it shows a number of advantages for biological applications, such as biocompatibility, thermal-responsiveness properties close to human body temperature and availability of a number of molecular architectures [11-14]. One group of high-affinity ligands for the bacteria are antibiotics themselves. The idea behind their use is that placement of the antibiotic at the chain ends of the PNIPAM could produce materials that respond to the presence of bacteria and that response could form the basis of a detection system. Polymer-based systems have attracted significant attention in the field of microorganism detection because a variety of

types of architecture can be designed, and also desirable functionalities can be obtained such as the star structure of a co-peptide polymer, which can enhance antimicrobial activity against bacteria [15]. Recently, highly branched PNIPAM with integrin binding peptides, arginine–glycine–aspartic acid (GRGDS), showed the capability of binding to integrins on human cells above its LCST. Moreover, previous work by our group (Shepherd et al.) has shown that highly branched PNIPAM (HB-PNIPAM) functionalised by the addition of antibiotics at the chain ends can bind bacteria, resulting in a phase transition in the polymer from a solvated expanded coil to a desolvated collapsed structure, also called coil-to-globule transition [16, 17]. However, little is known of the factors by which this system works, which is necessary to develop this material into a bacterial detection system.

This work, therefore, focuses on understanding the behaviour of antibiotic-functionalised, highly branched thermo-responsive PNIPAM in the presence of *S. aureus*. As a comparator, we prepared the linear analogue version of the PNIPAM-vancomycin to investigate the effect of polymer architecture on their interactive behaviour. In addition, the influences of key features of the bacteria on interaction with the PNIPAMs were investigated.

With the emergence of methicillin-resistant *S. aureus* (MRSA) and other antibiotic resistant bacteria, it is important that polymers used for detection should not themselves have antimicrobial activity. Consequently, this was assessed at various stages of purification of the polymers.

1.1 Detection of microorganisms and applications

Early detection of pathogens is an important concern for the health sector and is a major hurdle in the treatment of infectious diseases. For example, infected wounds can cause considerable morbidity if not treated properly [1, 2]. In most cases, the infected wound results from bacteria, originating from either the skin or the outside environment, that have colonised the site [4]. The intact skin surface is essential for the protection of tissue against infection and also the preservation of body fluid homeostasis. However, when such a protective barrier is injured, e.g. during surgery or an accident, bacteria can colonise the wound area, resulting in damage to the host tissues and further inflammation [18]. In fact, local inflammation leads to a low wound healing rate and deterioration of the patient's condition. Also, delay of the wound healing process can cause severe pain for the patient and contribute to increased likelihood of mortality [4, 19, 20] through cellulitis, osteomyelitis or the spread of bacteria to blood vessels and other parts of body [21]. The conventional approach for treating bacterial infections is the use of antibiotics. However, unguided use of antibiotics due to inaccurate or slow identification of the causative bacteria can lead to selection for drug resistance.

These serious problems have brought about considerable efforts to discover novel methods for rapid diagnosis and identification of the causative pathogens. The conventional methods based on antibodies have several drawbacks, such as poor stability at high temperature and strain-to-strain variation of reaction with immune-diagnostics [22]. Consequently, a range of alternative methods have been explored, such as the use of a biosensor based on (3-(5-(dimethylamino naphthalene-1-sulfonamido) phenyl) boronic acid) (DNSBA) [3]. Amin et al. showed that such a sensor could rapidly bind to *Escherichia coli* and be detected by an increase in fluorescence intensity as the number of bacterial cells increased. They suggested that the increase in fluorescence of DNSBA in the presence of *E. coli* is owing to the binding to the *E. coli* membrane consisting of lipopolysaccharides (LPSs) with diol groups [23].

Polymeric materials are one of the most interesting platforms for use in the field of diagnostics. They have been applied in various areas of bacterial infection, treatment and diagnosis, most of which has involved a colour change of the material to aid 'bed-side' detection and diagnosis. For example, self-selective bacterial binding and labelling using bacteria-instructed polymers has recently been shown to be possible [24]. Polymers have even been used to promote phagocytosis of opsonised bacteria using a bifunctional polyacrylamide. The polymer was functionalised with vancomycin and fluorescein hapten for

specific recognition of Gram-positive bacteria and binding of anti-fluorescein antibody respectively leading to enhanced phagocytosis of bacteria that bound the polymer [25]. There are several advantages to polymer-based materials and these have attracted considerable interest in the field of microbial detection. Firstly, various functionalities (polyvalency) can be provided, using different types of functional chemistry [26]. Moreover, a variety of architectures can be designed, such as star diblock copolymers and highly branched polymers. In the last decade, numerous polymeric materials used for reporting the presence of bacteria were developed. However, their mechanisms of detection differ according to their applications. Silbert et al. presented a new method for the visual detection of bacterial contamination in food. This system was based on the chromatic transition of agar-embedded nanoparticles composed of polydiacetylene (PDA) and phospholipids with a blue-to-red transition, due to their interaction with membrane-active molecules released from proliferating bacteria. They demonstrated that such a biomimetic polymer sensor could be a new platform for detecting bacteria, which could be rapidly identified by a visual colour change. However, this biosensor is still not able to differentiate between types of bacteria [27]. Sun et al. also exploited the intrinsic properties of chromatic transition from blue to red of polydiacetylene (PDA) in terms of signalling the presence of bacteria. They found that synthesised liposomes composed of mannose-glycolipids and PDA, mixed with *E. coli* caused a change in colour from blue to red. Binding between bacteria and PDA resulted in a change in side chain conformation from acetylene to butatriene, which led to the colour change [28, 29].

Glycopolymers are synthetic polymers that were developed and used for specific interactions with bacteria thanks to high-affinity ligands incorporated into the structure, such as pendant carbohydrates [30, 31]. Disney et al. exploited a fluorescent glycopolymer functionalised with carbohydrate groups, which act as active sites for binding to bacteria. In their study, poly(*p*-phenylene ethylene) coupled with mannose was synthesised and used as a bacteria detector. The binding of bacteria to such a fluorescent polymer was observed as fluorescent clusters of bacteria in the mixture that were visible to the naked eye. It is obvious that this fluorescence-based detection could be a powerful quantitative technique in a microbiological study [32]. Xue et al. also synthesised highly water-soluble glycopolymers for the detection of *E. coli*. This glycopolymer was based on poly(ethylene glycol) conjugated with a fluorescent group. They suggested that some of the neutral conjugated glycopolymers exhibited low solubility in water owing to strong hydrophobic interactions between polymer

backbones. Thus, they developed a structure of glycopolymers comprising flexible poly(ethylene glycol) as a tethered segment in order to increase spaces between polymer backbones, so that high solubility could be obtained and the tethered spacer could decrease the effect of steric hindrance between polymer chains, resulting in an enhancement of cellular recognition. They showed that the fluorescent conjugated fluorine-based glycopolymers interacted strongly with *E. coli* pili [30].

Not only do the types of high-affinity binding sites play a vital role in the properties of polymeric materials for specific interaction with bacteria, but also the location of binding sites on the polymer. Consequently, polymer architecture is a significant factor in the binding process. Kim et al. showed that spherical micelles of amphiphilic polyphenylene derivatives, composed of tetra (*p*-phenylene) (hydrophobic part) and oligo ethylene oxide (hydrophilic part), showed higher potential for interaction with *E. coli* compared with cylindrical micelles. They explained that, in aqueous solution, the binding sites of spherical molecules (carbohydrate groups) were located at the outer surface, leading to a higher chance that they would be exposed to their targets [33].

Glycopolymers are not the only systems that have been developed for the detection of microorganisms. Molecular imprinted polymers (MIPs) are also used for specific recognition of microorganisms and detecting low molecular weight analytes. Molecular printing is a technique that can introduce selective recognition sites on polymers to sense their targets. It can be synthesised by copolymerising with the desired and appropriate functional comonomers to provide specific recognitions such as peptides and organic molecules. The simplicity of the synthetic process and the stability of MIPs make them suitable for use as biosensors. However, they are not without limitations, particularly for imprinting large and complex structures such as bacteria. There are also several parameters that have an impact on the selectivity of imprinted polymers, such as the interaction between the polymer and target molecules, and the properties of the polymers themselves [34, 35]. Xue et al. successfully synthesised the *S. aureus* protein A imprinted polyacrylamide polymer, which exhibited a good specific recognition for *S. aureus* protein A [34]. Tokonami et al. also successfully developed MIPs from polypyrrole to specifically recognise anionic bacteria using electrochemical polymerisation. They suggested that the polypyrrole template was capable of distinguishing between Gram-positive and Gram-negative bacteria depending on the types of bacteria used to create the templates. However, the size distribution of each bacterium could cause problems and have an effect on the selectivity [35]. In addition, Golabi et al. were

recently successful in synthesising cell-imprinted polymer (CIP) using 3-aminophenylboronic acid (3-APBA) as a functional monomer. Their data suggested that CIP could specifically bind to *Staphylococcus epidermidis* when present above 10^3 cfu/ml, and could differentiate between the bacterial target and structures of a similar shape. However, high non-specific binding was still found because of the presence of boronic acid groups in the imprinted cavities and on the polymer surface [3].

Another approach to detect pathogens with high sensitivity and that exhibit antimicrobial activity without an increase in drug resistance is to use multivalent polymers. Recently, there have been numerous efforts attempting to overcome these difficulties by developing new materials consisting of functionalities that can detect, bind and inactivate pathogens but not to induce antibiotic resistance. Lam et al. revealed that structurally nano-engineered antimicrobial peptide polymer (SNAPPs) exhibited antimicrobial activity against all types of Gram-negative bacteria used in their study without observable emergence of multiple drug-resistant strains. They explained that binding SNAPPs to bacterial cell walls caused destabilisation of bacterial membranes, leading to unregulated ion movement and cell death. SNAPPs were synthesised from poly(amido amine) (PAMAM) dendrimers, in which the terminal amine groups of the polymer were functionalised with lysine and valine *N*-carboxyanhydrides (NCAs) via ring-opening polymerisation. They showed that SNAPPs were capable of forming stable star shaped nanoparticles containing lysine and valine peptide residues in solution, resulting in an efficiency enhancement in binding to their targets [15]. Indeed, Arimoto et al. prepared polyvalent polymers with vancomycin pendants using ring-opening methathesis polymerisation which increased antimicrobial activities against vancomycin resistant Enterococci (VRE) and other multi-resistant bacteria [36]. Magennis et al. also proposed a new polymeric material that seemed to exhibit properties that could be used for diagnostic application. Two types of monomer, namely (2-(methacryloyloxy)-*N,N,N*-trimethylethanaminium chloride (TMAEMA), which is a cationic monomer, and 2-(*N*-3-Sulphopropyl-*N,N*-dimethyl ammonium) ethyl methacrylate (MEDSA) were used for preparing the bacterial template. TMAEMA was chosen because they expected electrostatic attraction between negatively charged bacterial surfaces and the positive charge of the polymer. Also, MEDSA was used due to the expectation that it would behave as a spacer and increase the solubility of the polymer. The template was synthesised using bacteria-mediated atomic transfer radical polymerisation (b-ATRP) in presence of bacteria. Phase contrast and fluorescence microscopy showed that bacteria-template polymer caused formation of large

aggregates of their matched bacteria [24]. Li et al. designed multifunctional micellar nanoparticles with fluorescent sensing, which were fabricated from negatively charged segments and cationic diblock copolymers. The anionic part originating from tetraphenylethylene (TPE) sulfonate derivatives and the cationic segment stemmed from poly (ethylene oxide)-b-quaternised poly (2-dimethylamino) ethyl methacrylate (PEO-b-PQDMA). They found that in the presence of *E. coli* the binding of a negatively charged bacterial surface to positively charged PQDMA resulted in the disruption of micellar formation leading to reduction of tetraphenylethylene fluorescence intensity due to the loss of aggregation-induced emission effect. Moreover, the polyions micellar nanoparticles were tested with *S. aureus* in order to prove their versatility. The same pattern that occurred in *E. coli* samples was found. They concluded that this material potentially exhibited optical detectors for pathogenic bacteria [37].

1.2 *Staphylococcus aureus* and vancomycin antibiotic

S. aureus

S. aureus has remained a dangerous pathogen, causing diseases in most parts and systems of the body [5]. It is also a major cause of nosocomial infection [6, 38]. It is therefore a useful model pathogen with which to explore systems for detection of infection.

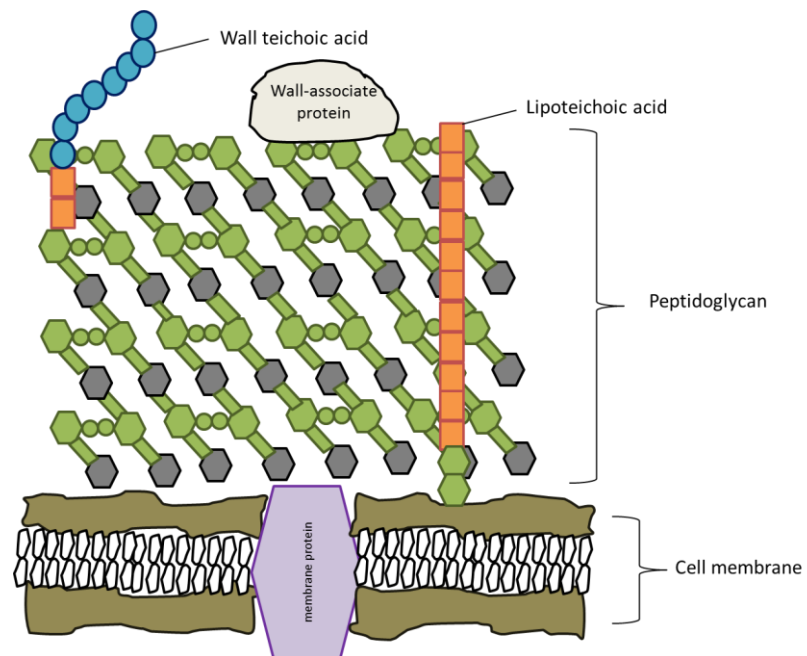


Figure 1.1 Gram-positive cell wall structure

S. aureus is a Gram-positive, spherical bacterium of approximately 0.5-1.5 μ m in diameter and which grows in clusters due to its cell division in multiple planes. The Gram-positive cell wall differs from Gram-negative cell envelopes in several ways. Firstly, there is no outer membrane, which protects Gram-negative bacteria from the environment and to which the thin peptidoglycan layer is linked. Gram-positive bacteria have a much thicker layer of peptidoglycan and this thickness provides the protection from the environment. It is however, porous to allow passage of essential compounds [5, 10, 39].

In this study we have focused on *S. aureus*. *S. aureus* is commonly found on the human skin, which is an exceptional barrier against any pathogenic microorganisms. However, if the skin is broken due to surgery or trauma, *S. aureus* can easily access the tissue underneath and cause invasive infection. Mortality in relation to skin infection is most often associated with *S. aureus* [5, 40, 41].

The *S. aureus* cell wall is about 20-40nm thick, comprising about 50% w/w peptidoglycan and 40% anionic polymers. The anionic polymers thread through the peptidoglycan layers and are classified into two types, namely teichoic acids and lipoteichoic acids. Both anionic polymers are considered to make up 50% of the mass of the bacterial cell wall, which has an influence on the overall structure and the functions of the bacteria (discussed in more detail below). Underneath the peptidoglycan is the cytoplasmic membrane. The Gram-positive cell wall also contains a range of proteins and these can change in response to growth conditions [39]. The major structural components of *S. aureus* are illustrated as follow.

Peptidoglycan

The *S. aureus* peptidoglycan comprises *N*-acetyl-D-glucosamine (NAG) and *N*-acetylmuramic acid (NAM) joined by 1, 4- β linkages. A tetrapeptide chain is attached to the MurNAc and is crosslinked to adjacent peptide chains via a pentaglycine bridge to form a meshlike network [10]. The tetrapeptide chain comprises L-Alanine, D-Glutamic acid, L-Lysine and D-Alanine in most organisms but the degree of crosslinking varies depending on the type of bacteria. The proportion of peptide crosslinks in *S. aureus* peptidoglycan is about 80-100% of the total glycan strand [10, 39]. These peptide substitutes serve as binding sites for covalently-associated proteins, in which the crosslinking process can be halted by the removal of terminal D-Alanine through the action of carboxypeptidases. Additionally, these peptide substitutes are also associated with the action of certain antibiotics, particularly the β -lactam antibiotics and the glycopeptides, vancomycin and teichoplanin. Both classes of

antibiotic inactivate the crosslinking process of peptidoglycan synthesis [10, 39]. A schematic diagram of peptidoglycan of *S. aureus* is shown in Figure 1.2.

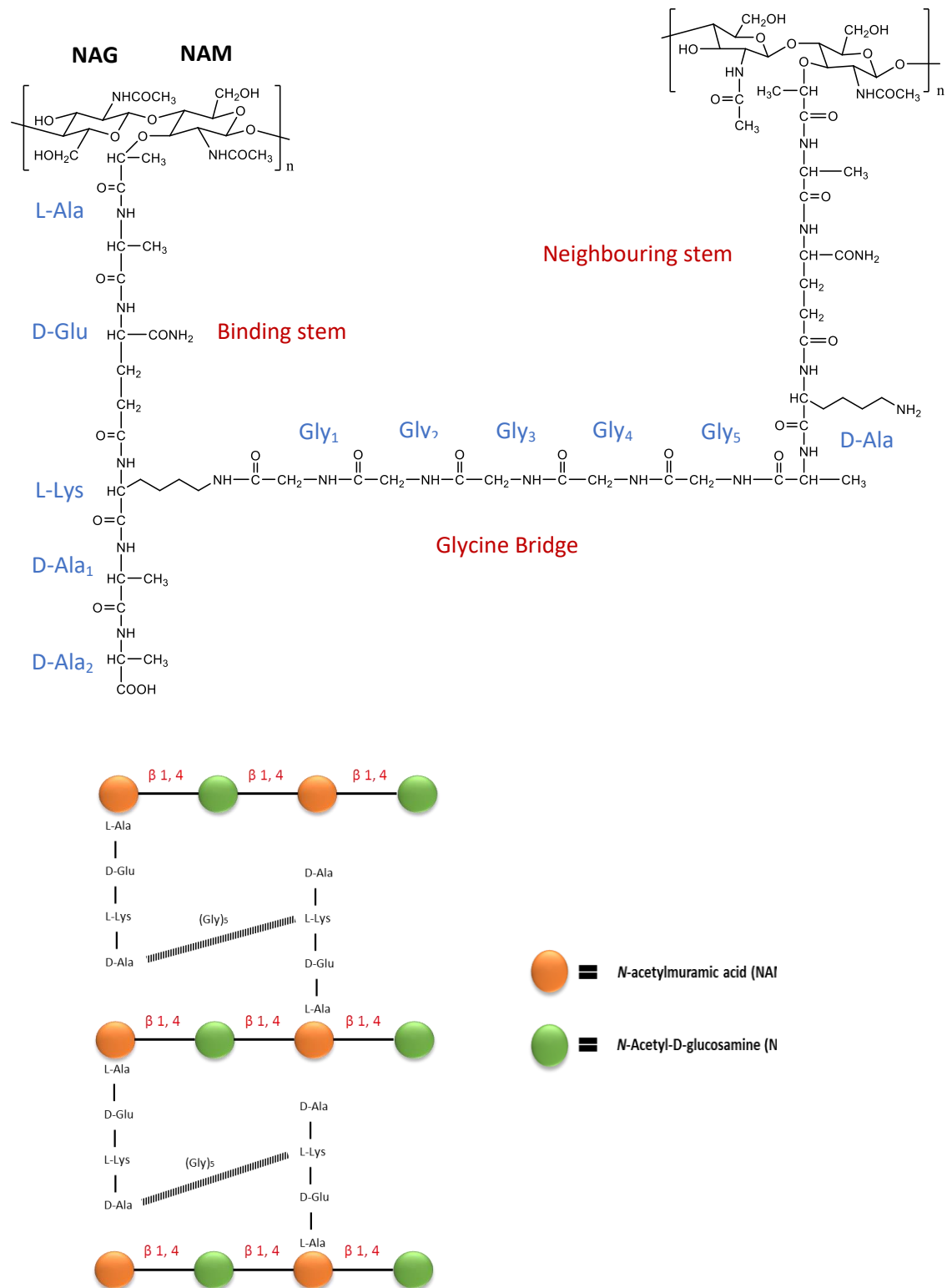


Figure 1.2 Schematic diagram of Peptidoglycan of *S. aureus*

Wall Teichoic Acids (WTAs) and Lipoteichoic Acids (LTAs)

Teichoic acids are anionic polymers consisting of large repeating units of glycerol phosphate (polyglycerol phosphate, polyGrop) or ribitol phosphate (polyribitol phosphate, polyRboP), which is commonly found in the cell wall of *S. aureus*. Teichoic acids are divided into two groups, which are wall teichoic acids (WTAs) and lipoteichoic acids (LTAs). WTAs are covalently coupled to peptidoglycan via phosphodiester linkage to hydroxyl groups of NAM, while LTAs are anchored to the head groups of lipids in cytoplasmic membrane. LTAs are similarly composed of polyglycerol phosphate, but they are functionalised with D-Alanine and their chirality is different. WTAs are located perpendicularly through networks of peptidoglycan, whereas LTAs insert into the mesh and lipid membrane of the bacteria, which can be seen in Figure 1.1. Teichoic acids are considered a significant component of the bacterial cell wall because of their negative charge which influences both cation homeostasis and interaction with other charged structures such as surfaces. Thus, teichoic acids are involved in the localisation of metal ions between the network of WTAs and metal ions, which affect the porosity and strength of the bacterial cell wall. The charge of the cell wall can be modified by introducing a positive charge, which has a significant effect on the interaction between the cells and other molecules. For instance, coupling D-Alanine with free hydroxyl groups on polyribitol phosphate in *S. aureus* causes the bacteria to be more susceptible to cationic antimicrobial peptides due to the lack of D-Alanine esters [39, 42]. As mentioned above, WTAs also play a role in colonisation, such as mediating binding to the epithelium of the nose [39, 43].

Surface proteins

For adhesion to host tissue or other molecules, several parameters are involved. These include teichoic acids, as mentioned previously, as well as surface proteins, which specifically adhere to a number of host proteins, for example the extracellular matrix proteins (ECM), elastin, fibronectin, and collagen [5]. The surface proteins acting as adhesins are often referred to as Microbial Surface Components Recognising Adhesive Matrix Molecules (MSCRAMMs) [44, 45].

The particularly important MSCRAMMs in *S. aureus* is protein A, which plays a role in adhesion to surfaces and in pathogenesis of disease. Protein A consists of an *N*-terminal fraction with immunoglobulin (Ig) binding sites and a *C*-terminal threonine-containing portion which links to the peptidoglycan. Protein A is capable of binding to the Fc fragment of Igs

during infection, resulting in prevention of the opsonisation process [44, 46] and is a major component that is responsible for the hydrophobic property of *S. aureus* [46, 47].

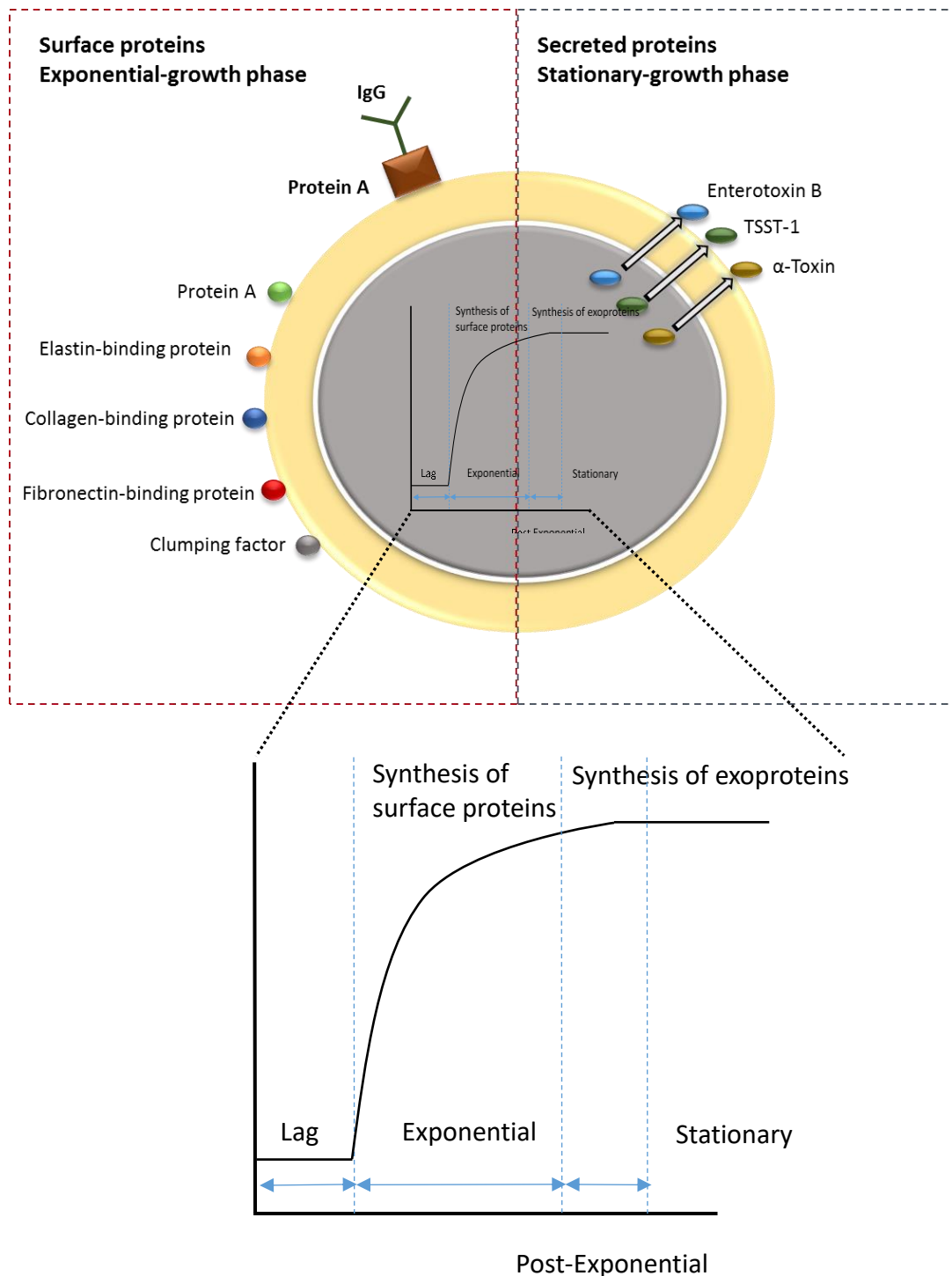


Figure 1.3 Model of virulence determinant synthesis in infection of *S. aureus*.

Synthesis of surface proteins and other types of proteins, which is essential for adhesion and cell division, occurs during the exponential phase, while toxins and exoproteins are produced in the post-exponential phase leading to relocalisation to new places during the stationary phase. MSCRAMMs produced during the exponential phase mediate adherence to components of host tissues, resulting in colonisation of host tissue sites, whereas expression of secreted proteins such as α -toxin and enterotoxin B are produced during the stationary phase.

While the cell-wall components of Gram-positive bacteria are related to virulence and resistance to antibiotics, other factors, such as the hydrophobicity of the cell surface and the surface charge of bacteria, will have a significant influence on interaction with polymer surfaces [5, 44].

Functional properties of bacterial cell wall components and their role in relation to adhesion

Bacterial surface charge

Adhesion to host tissues and ECM is considered the initial stage of bacterial infection. There are several functional properties of bacterial cell surfaces that are related to bacterial adhesion to the host cells, such as bacterial surface charge. Gram-positive bacteria consist of both negatively and positively charged groups. However, the net surface charge is negative at physiological pH. This is due to phosphate and carboxyl groups from proteins in the bacterial cell wall. In many Gram-positive bacteria, including *S. aureus*, teichoic acids are present and provide a negative charge. In aqueous suspension, *S. aureus* cells therefore have a negative charge, which results in electrostatic repulsive force between the bacterial cells. However, not only does surface charge play a role in the interaction between the cells, but also the hydrophobicity of the bacteria can contribute to specific binding between the bacteria and target molecules/or biomaterial surfaces, such as biomaterial implants [48]. The degree of hydrophobicity depends on the type of strains and the age of the culture [47]. Gristina et al. found that, at a certain distance (about 15nm) from a negatively charged substrate surface, hydrophobic forces could overcome electrostatic repulsion between *S. aureus* bacteria and the substrate leading to adhesion. While bacterial surface constituents confer physical properties that influence adhesion, other surface structures can also play a role e.g. the extracellular capsule [48, 49].

Extracellular capsule

The extracellular capsule of bacteria is composed of polysaccharide and other types of exopolymers such as uronic acids and protein or hyaluronic acids. Although, the capsule is involved in the attachment of cells to surfaces, its primary function appears to be protective by reducing phagocytosis and by providing a barrier for antimicrobial agents [50].

S. aureus-associated infections and antibiotic resistance in S. aureus

S. aureus was one of the most common pathogens causing surgical wound infection and bloodstream infection [5, 50]. Generally, the human nose and skin are considered to be natural reservoirs for *S. aureus*. Infection occurs when the skin barrier is broken, allowing access to the underlying tissue and blood vessels. The effect of bacteria in a wound can be described in three stages: contamination, colonisation and infection [5]. Contamination is the first step where there is the presence of bacteria in the wound but no harm to the tissue. After that, the number of bacteria will multiply, this is called colonisation but at this stage there are no signs or symptoms. Bacteria can then either remain localised or spread to nearby areas through the tissue [51, 52] due to the production of extracellular toxins and proteases [53]. Cellulitis is a spreading form of infection progressing through the fat layers below the dermis. Localised infections present as abscesses, often associated with hair follicles but can also be more deep seated and more severe [40]. *S. aureus* has several mechanisms to protect itself from the host response during an infection. For instance, it can produce antiphagocytic microcapsules. Abscess formation can be induced by the zwitterionic capsule comprising a WTA of ribitol phosphate, *N*-acetylglucosamine and D-Ala repeating units. Weidenmaier et al. compared the biological activity of strains exhibiting a zwitterionic WTA with strains having negatively charged WTAs. They found that strains with the zwitterionic WTA resulted in larger skin abscesses in mice than strains with a negatively charged WTA [54].

Antibiotic resistance is the term most commonly used for when an antibiotic loses its ability to control bacterial multiplication and allow the bacteria to continue to grow in the presence of a therapeutic level of drug. More recently the term antibiotic non-responsiveness has become used to help explain why some bacteria are not controlled by an antibiotic but do not display the same genetic features of fully resistant strains. These are referred to as showing antibiotic tolerance since they are not killed by antibiotics but they are not growing either. In other words they are in a state of dormancy. However, sometime later after a therapeutic

regime is finished the bacteria can emerge from their dormant state and start growing as 'normal'. This state of affairs pertains particularly to bacteria growing in a biofilm, where their physiology differs markedly from that of planktonic bacteria.

Conventional antibiotic resistance arises from mutation or the acquisition of resistance genes from other bacteria and is selected for by Darwinian evolution in an environment that is relatively high in the drug. The acquisition of resistance genes is mediated by uptake of free foreign DNA (e.g. plasmids), by conjugation between bacteria or by viral transfer (transduction). An important example of plasmid mediated resistance is the acquisition of β -lactamase by *S. aureus*, which hydrolyses the β -lactam ring of the penicillin group of antibiotics. This leads to drug inactivation but there are other mechanisms of providing resistance including, the alternation of drug target sites, decreased uptake of drugs, expulsion of drugs from the cytoplasm, over production of the drug target and by genetic modification of the drug target. An example of the latter is a change in the structure of penicillin binding proteins (PBPs) which leads to low binding affinity for the drug.

The significance of antibiotic resistance is that it makes many healthcare and surgical procedures that we currently take for granted almost impossible. Resistance has now become a worldwide problem and its effects are made worse by increased human and animal transport from place-to-place and country-to-country which allows efficient spread of resistance strains and their genes. Also, there is a significant economic cost of resistance through treatment complications, longer hospital stays and loss of working days. Several approaches can be taken to reduce the incidence of antibiotic resistance, including the development of new classes of antibiotic, the control of public access to antibiotics, improved prescribing of antibiotics and improving the speed and accuracy of diagnosis of infection. This thesis addresses one aspect of the latter approach.

Vancomycin antibiotics

As mentioned above, resistance to benzylpenicillin antibiotics in *S. aureus* had emerged by the late 1950s due to the production of the β -lactamase enzyme. To combat this methicillin was synthesised, which consisted of phenol groups disubstituted with methoxy groups, providing a steric hindrance effect on amide bonds, so reducing access of the β -lactamase to the sensitive β -lactam bond. However, in the 1980s methicillin-resistant *S. aureus* (MRSA) strains began to appear, the mechanism of resistance this time being due to the production of low affinity penicillin-binding protein 2, which is involved in transpeptidation (cross-linking) of new peptidoglycan units. The main drugs left to treat infections caused by MRSA were glycopeptide antibiotics [55, 56].

Several types of natural glycopeptide antibiotics are known, in particular vancomycin and teicoplanin. Vancomycin is classed as a Type I glycopeptide antibiotic because it contains valine-1 and asparagine-3, or glutamine-3 residues in its structure [55].

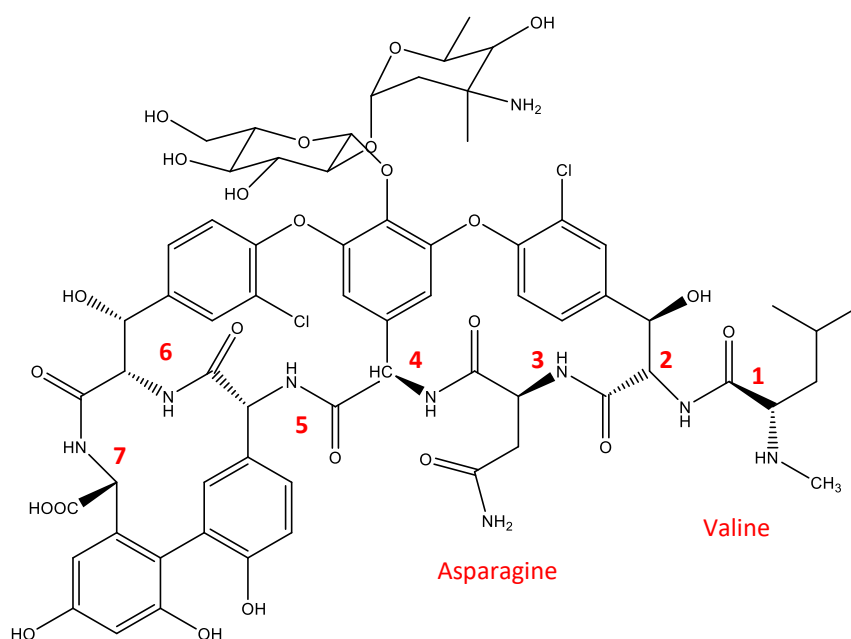


Figure 1.4 The structure of vancomycin

Vancomycin is a product of *Amycolatopsis orientalis* and was discovered by Eli Lilly (Indianapolis, USA) in 1953. A few years later, two more related species from India were found to be able to produce vancomycin. In the early use of vancomycin, side effects, such as nephrotoxicity, were noted which was due to the presence of impurities, resulting in its

nickname of “Mississippi Mud”. However, optimisation and purification of vancomycin preparations enabled it to be a more useful therapeutic and in 1958 it was clinically certified for MRSA infection [55, 57]. However, it was not until 1982 that the structure of vancomycin was described by Harris using X-ray crystallography [58]. Biochemical studies revealed that glycopeptide antibiotics inhibit the synthesis of peptidoglycan. Vancomycin interferes with the transpeptidation reaction by forming a complex with D-Ala-D-Ala dipeptides via five hydrogen bonds (shown in Figure 1.5(A) as dashed lines) with the backbone of the glycopeptides [59-61].

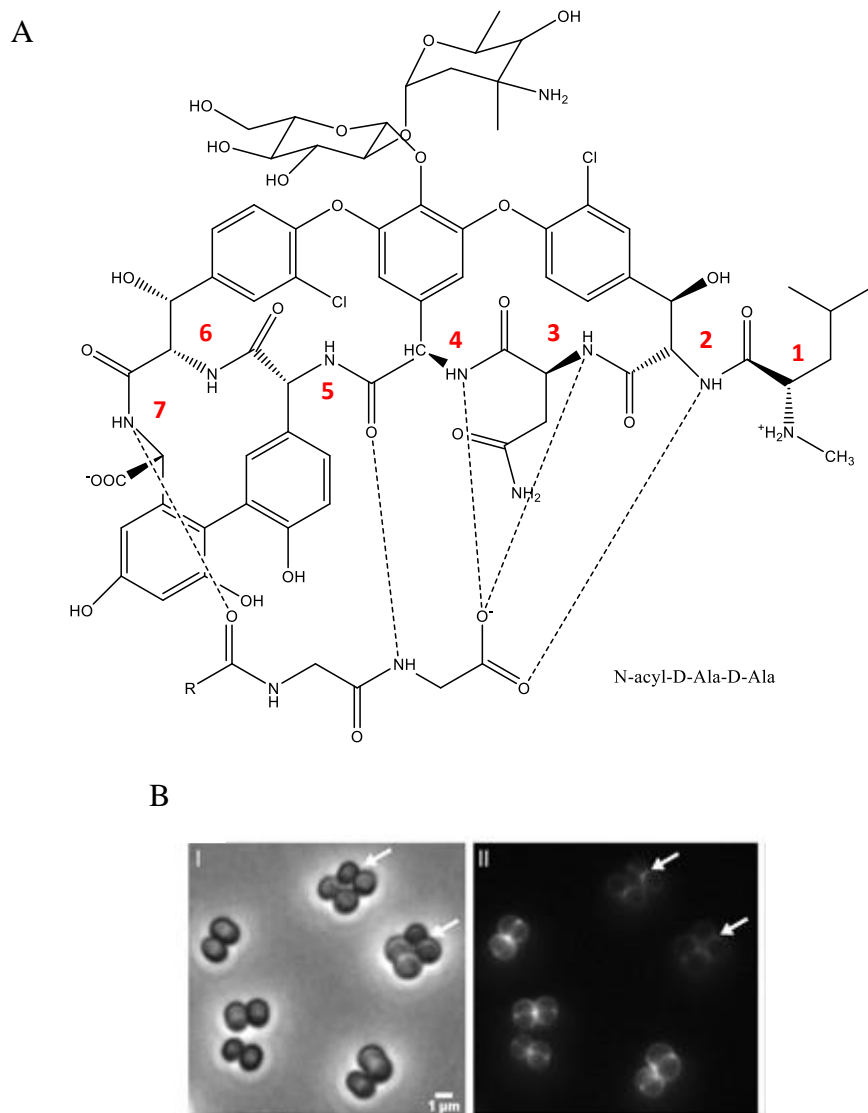


Figure 1.5 (A) The formation of the stoichiometric complex between vancomycin and D-Ala-D-Ala dipeptides terminus of precursors, (BI) Phase contrast image of *S. aureus* cells (BII) An image of the same sample with fluorescent vancomycin viewed with fluorescent microscope. Fluorescence is concentrated at recent division sites [62]

This results in a weak cell wall and osmotic cell lysis [63, 64]. The strength of interaction between vancomycin and the D-Ala-D-Ala binding site can be increased if the vancomycin is in a dimeric form. Beauregard et al. showed that cooperativity between dimers of vancomycin provided rigidity to the structure fixing the binding pocket of vancomycin into the right conformation for maximum interaction with its target [65].

Mackay et al. suggested that the presence of a chlorine atom in the meta-aromatic substituent can increase dimer formation of vancomycin because the electrostatic attraction between partially positively charged hydrogen atoms of the amino group on vancomycin and the negatively charged carboxylate anion of D-Ala-D-Ala peptide plays a vital role in initial binding. Thus, the presence of a chlorine atom near the binding region directly affects the activity resulting in an increased in vitro activity of vancomycin [56, 66, 67]. Moreover, Kaplan et al. stated that the addition of sugar to position 6 in vancomycin enables vancomycin to form dimers more efficiently because the sugar residues can provide a hydrophobic interaction between the disaccharides of each vancomycin. This results in a limited conformational freedom of vancomycin molecules leading to increased cooperative ligand binding and ligand affinity [56, 68, 69]. Also, introducing a lipophilic tail to vancomycin can enable the drug to remain close to its target adjacent to the cell membrane because it becomes anchored in the membrane near to where the new disaccharide-pentapeptide is transported out of the cell [56, 65, 70].

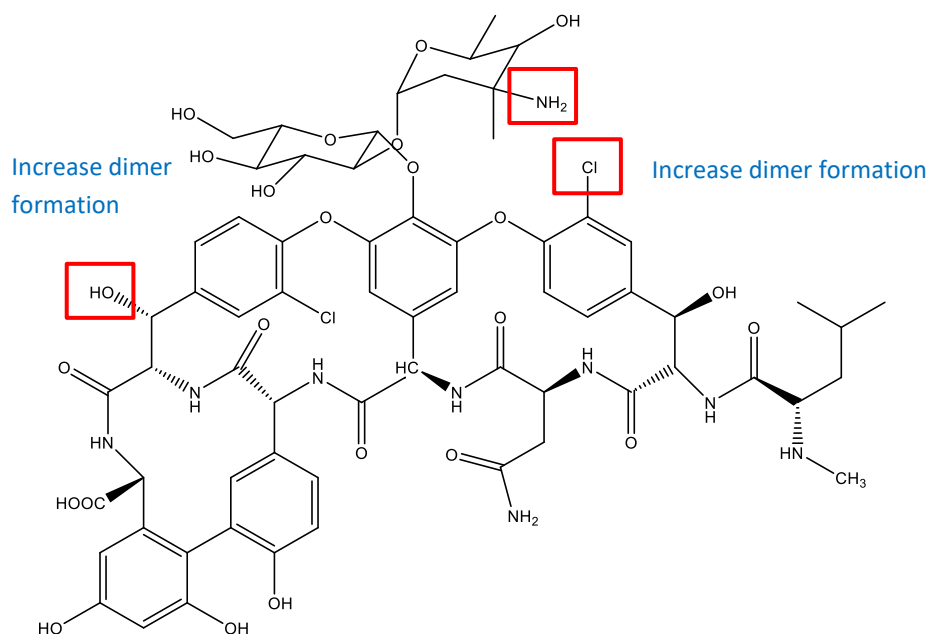


Figure 1.6 Structural aspects of vancomycin involved in dimerisation [70]

Mechanism of resistance

Despite vancomycin still being a useful therapeutic antibiotic, resistant strains of *S. aureus* and other species have been reported. The mechanism of vancomycin resistance is due to substitution of one of the D-Ala groups in the terminal dipeptide by either D-Lactose or D-Serine. Such substitutions reduce the number of hydrogen bonds between the vancomycin and the terminal moieties of the pentapeptide and changes the conformation resulting in lower binding affinity [55, 71]. The replacement process of D-Ala with D-Lac is shown in Figure 1.7.

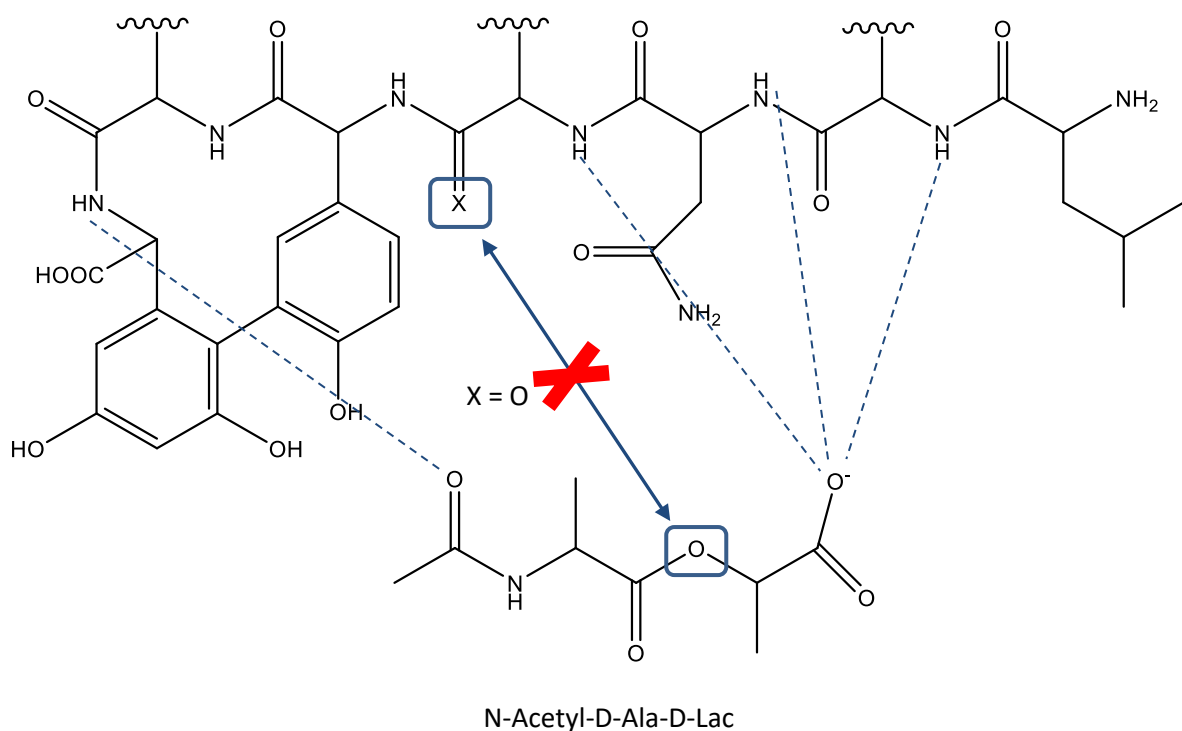


Figure 1.7 Schematic of the replacement of D-Ala with D-Lac in resistant strain, leading to a decrease in binding affinity with vancomycin due to the repulsion between oxygen atoms [55]

An alternative form of vancomycin resistant *S. aureus* first appeared in the form of vancomycin-intermediate *S. aureus* (VISA) with increased minimum inhibitory concentration (MIC) values. VISA exhibits a thicker cell wall with a higher amount of D-Ala-D-Ala termini but less pattern [72]. It enables peptidoglycan to cage vancomycin molecules and prevent their reaching the cytosolic membrane. However, if the dose of vancomycin is increased higher than the number of D-Ala-D-Ala residues, VISA strains can also no longer resist

vancomycin. Additionally, because VISA has to export a greater amount of peptide precursors than sensitive strains, their cell wall strength in an antibiotic-free environment is affected and in the absence of vancomycin the selective advantage is lost and so reversion occurs. This is called the hetero-VISA phenotype (hVISA) [55, 57, 71].

Antibiotic resistance to vancomycin or any antibiotic will inevitably arise in an environment of high usage of the drug. As mentioned earlier, part of the approach to managing this important healthcare problem is to improve detection and diagnosis of infection, particularly in communities or situations where the technology and infrastructure to achieve this routinely is lacking. In this regard, the study reported in this thesis investigates aspects of thermoresponsive polymers that have been suggested could be used as a detection system.

1.3 Thermo-responsive polymers used in biological applications

In the last few decades, “smart materials” have aroused interest due to their properties. They can undergo reversible physical or chemical changes in response to the environment, such as changes in pH, temperature or ionic strength. Additionally, some of them are bio-compatible and so are able to be used in biomedical applications [73-76].

Thermo-responsive polymers are one of the smart polymers, which have attracted considerable attention for biological applications, such as multivalent molecular recognition by bifunctional polyacrylamide, protein and bacteria absorption. Cunliffe et al. were interested in surface-grafted PNIPAM copolymers for the use of bacterial attachment. PNIPAM was grafted to an amine functionalised glass surface via carboxyl terminated groups on PNIPAM. They found that there was an increase in bacterial absorption on the surface-grafted PNIPAM above the LCST of the polymer. This was explained by changes in the surface property of the polymer due to an increase in hydrophobicity of the grafted polymer when the temperature was raised above its LCST [77]. Krishnamurthy et al. designed multivalent polyacrylamide polymers and employed them for modifying bacterial cell surfaces which resulted in an antibody-mediated opsonisation and subsequent phagocytosis. The binding functionality for bacteria was mediated by vancomycin groups and a fluorescein moiety in the polymer provided a means of visualisation [25]. Approaches of this type hold promise as the basis for diagnostic systems. Although not stated by the authors, it is assumed that because the vancomycin was tethered to a surface that there would be less chance of direct killing of bacteria and less chance of selecting an antibiotic resistant population.

Thermoresponsive polymers, which have a Lower Critical Solution Temperature (LCST), switch from soluble to insoluble upon heating to above their LCST. The change in solvation state is associated with intra- and inter-molecular hydrogen bonding between polymer and water molecules. The critical miscibility behaviour can be divided into three categories, namely the classical Flory–Huggins miscibility behaviours Type I, Type II and Type III. The critical point of miscibility of Type I is dependent on the polymer chain length. Increasing molecular weight shifts the critical point to a lower value. At the limit of infinite chain length, it is specified by a limiting critical concentration, with the volume fraction of the solute in solution being zero at theta condition. In contrast, the critical point of Type II is independent of the chain length of the polymers. For Type III, at low concentration of the polymer, the critical point of miscibility is characterised by the limiting critical concentration, which is similar to Type I. However, at high concentration of the polymers, it behaves like Type II and the polymer chain length does not affect the critical point.

There are several types of thermoresponsive polymers that have been studied and here comparisons will be drawn between a selection of them, including PNIPAM, poly(*N*-vinyl caprolactam) (PVCL), poly (methyl vinyl ether) (PMVE) and natural polymer e.g. elastin-like-oligo and polypeptides. These polymers have LCSTs within the physiological range [12].

1.3.1 Poly (*N*-vinylcaprolactam) (PVCL)

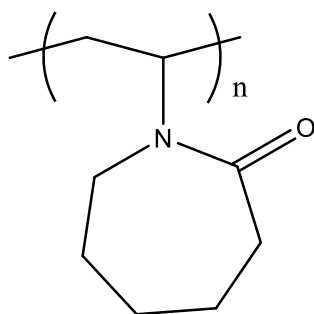


Figure 1.8 The chemical structure of poly (*N*-vinylcaprolactam) (PVCL)

PVCL is a temperature sensitive polymer, and its LCST in pure water is close to human body temperature (34°C), leading to some significant attention in the field of biomedical applications. It also has high solubility in water and various types of organic solvents, and biocompatible properties that are attractive. PVCL has also been used as a model in biomedical studies such as controlled drug release because it does not produce toxic low molecular weight amines under strongly acidic conditions due to the amide group being

directly connected to a carbon-carbon backbone [78]. Although the phase transition temperature of PVCL is close to PNIPAM, the mechanisms are different to those of PNIPAM. PVCL shows continuous phase transition behaviour, which depends on the molecular weight and the polymer concentration. During heating, the phase transition of PVCL is driven by the transformation of hydrogen bonded carbonyls with water to release one, and followed by the hydrophobic dehydration of side groups [79]. PVCL mesoglobules can continuously expel water molecules upon further increase of temperature according to the absence of self-associated hydrogen bonds in the dehydrated state. On the other hand, the globular form of PNIPAM exhibits self-associated hydrogen bonds without a distribution gradient of water molecules. Thus, PNIPAM shows discontinuous phase transition behaviour and does not change when the temperature increases [80, 81]. Both PNIPAM and PVCLs exhibit unique properties for biomedical applications due to their adjustable size and LCST. However, PNIPAM has been more extensively studied because functional group modification can be designed, while it is easy for VCL monomers to be hydrolysed and turned into caprolactam and acetaldehyde under acidic environment. Therefore, copolymerisation with other comonomer such as acrylic acid has to be taken into account due to the presence of carboxylic acid groups in comonomer [80].

1.3.2 Poly(methyl vinyl ether) (PMVE)

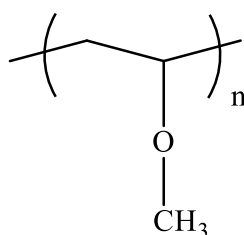


Figure 1.9 The chemical structure of poly (methyl vinyl ether) (PMVE)

Poly (methyl vinyl ether) (PMVE) has a LCST at 37°C, which makes it potentially useful in biomedical applications. It can be synthesised only by cationic polymerisation under inert conditions [12]. Aqueous solutions of PMVE can be transformed to hydrogels by irradiating with electrons, leading to crosslinking between radicals from water molecules and PMVE molecules. The hydrogel of PMVE shows thermo-responsive properties as it shrinks above its LCST. The kinetics of the volume transition of PMVE is controlled by the cooperative diffusion coefficient of the polymer chains (cm²/second) [82]. Thus, a decrease in network

dimensions results in a dramatic increase in shrinking rates of the polymer. Suzuki et al. showed that PMVE gels with fine pores responded to a change in temperature quicker than other gels with comparable dimension [83]. PMVE is often used in hydrogel formation, the shape and conformation of which are limited due to its three-dimensional network. Copolymerisation with other types of polymers such as maleic anhydride or PNIPAM to enhance its properties is essential to improve and provide broader ranges of physico-chemical properties of PMVE used in biomedical applications [84]. The copolymer of PMVE typically is a widely used thermo-stimulus material as a cell scaffold for tissue engineering [84-86].

For wound care applications, PMVE has drawn interest due to its ability to absorb exudate and balance the hydration of the wound. Recently, Calo et al. exploited unique properties between polyvinyl alcohol (PVA) and poly (methyl vinyl ether-alt-maleic anhydride) (P(MVE-alt-MA)) for developing hydrogels exhibiting antimicrobial activity against *S. aureus*. It was found that such an antimicrobial hydrogel could be synthesised by autoclaving the mixture of PVA and P(MVE-alt-MA) resulting in good mechanical and adhesive properties, which can be proposed for novel wound dressing [85]. Nonetheless, copolymers of chemically cross-linked PNIPAM and radiation cross-linked PVME hydrogels have also often been used as a model to investigate the responsive swelling behaviour [82].

However, there are some limitations of PMVE in terms of synthesis because only cationic polymerisation under inert conditions can be used for synthesising PMVE because nucleophiles used in the reaction are not able to be tolerated [12]. Moreover, a purification step is needed because unreacted monomer and crosslinking agents are normally toxic [85]. Even though electron irradiation used to provide three-dimensional networks has been developed to avoid the use of any additives for the preparation of PMVE hydrogels, this technique requires expensive facilities and generates heat [82].

1.3.3 Elastin-like polypeptides (ELP)

ELP is an attractive thermo-responsive material used in biomedical and tissue engineering applications because it displays an LCST in aqueous solution similar to that seen with PNIPAM. ELP is composed of repeats of pentapeptides of which repeating units are valine-proline-glycine-valine-glycine called Val-Pro-Gly-Val –Gly [87, 88]. ELP consists of both hydrophobic and hydrophilic parts, which are isopropyl side chains, hydrocarbon backbone and amide groups, respectively. They can undergo a phase transition upon heating depending

on the hydrogen bonding interaction between polymer chains and water molecules and the effect of hydrophobicity of the polypeptides, which are similar to the behaviours of PNIPAM [89]. Below the LCST of ELPs, the polypeptide chains are fully hydrated and opened. As the temperature is increased above its LCST, the ELP chains fold into a β -spiral formation as a result of the hydrophobic dehydration of valine. However, the dehydrated conformation of ELP above LCST is different from PNIPAM in aqueous solution. The collapsed form of PNIPAM chains are disordered whereas the chain formation of ELP is a uniform β -spiral conformation stabilised by a hydrophobic effect [90]. The LCST of ELP is 20-30°C, where the initial dehydrated form of ELP still contains water of about 63% w/w. However, the irreversible transition takes place when the temperature is raised to 80°C, at which the water content is decreased to 32% w/w. The LCST of ELP is dependent on the overall hydrophobicity of peptide sequences, which can be adjusted by the change in residue group composition in the peptide sequences [89]. This is one of the most interesting features for the design of ELP used in thermo-responsive systems. To date, ELP has attracted intense interest for the promise of incorporating into polymer side chains or polymer backbones for various biomedical applications, such as cancer therapy, thanks to its biocompatibility and biodegradable properties. Dreher et al. synthesised an ELP block copolymer functionalised with RGD and NGR tripeptides, used for tumour vascular targeting. They showed that these ELPs block copolymer self-assembled into multivalent micelles at about 40°C that exhibited higher affinity for the targets compared with freely soluble polymer, which displays monovalence with low-avidity for target cells [91]. Bitton et al also found that the topology of polypeptides plays a significant role in the LCST of ELP. They proposed that dendritic ELP showed a higher phase transition temperature than linear polypeptides which indicates that the phase transition temperature of ELP can be tuned by not only the ratio of hydrophobicity/hydrophilicity, but also the conformation of ELP [87]. The results from Bo et al also showed that thermo-responsive polymer based on ELP is tuneable by the structure of the polymer [87]. It is clear that polymer architecture of thermo-responsive polymer plays a role in phase transition behaviour and its properties, especially in terms of binding to targets. ELP remains a promising material to be developed for further biotechnological applications.

There are several other types of thermo-responsive polymers such as poly(ethylene oxide) (PEO), and poly(*N*-vinyl pyrrolidone) (PVP). However, their LCSTs are very high, above 100°C. Therefore, they will not be discussed in this review.

1.3.4 Naturally-derived polymers and synthetic thermo-responsive polymer system

Dzwolak et al. revealed that a poly (L-lysine) chain formed an α -helix structure below its phase transition temperature and displayed anti-parallel β -sheets when the temperature was raised [92]. Polypeptides can exhibit three different secondary structures, namely α -helix, β -sheet and β -turns. The α -helix formation is stabilised by hydrogen bonds between C=O and HN groups in the residues, leading to a helical conformation. β -sheet is composed of β -strands, in which the backbone is fully extended. Two stands of β -strands can be linked via hydrogen bonding resulting in the stabilisation into β -sheet [89]. In the case of β -turns, they are aligned in inverse direction to the polypeptide chains and are stabilised by hydrogen bonds from amide nitrogen and carbonyl oxygen.

Collagen and gelatin

Collagen is the main component of the ECMs of several mammalian tissues and synthesised by fibroblasts and osteoblasts. It is composed of triple helixes assembled into complex structures. Moreover, collagen contains Arg-Gly-Asp (RGD) adhesion domains, which is one of the key motifs for the interaction between ECMs and various cells that enable it to be widely used for skin repair [93, 94]. Even though collagen is not classified as a thermo-sensitive polymer, the single chain molecules of gelatin, are. Gelatin is a naturally thermo-responsive polymer, which can be obtained by the hydrolysis of collagen into single chain molecules. Amide groups of asparagine and glutamine of the triple helix of collagen can be hydrolysed resulting in carboxyl groups that provide a negative charge for the gelatin. Gelatin exhibits reversible phase transition at 35°C. Above the phase transition temperature of gelatin, unimer chains are in random coils. As the temperature decreases, the gelation process occurs. The gelatin chains form left-handed helixes held together by hydrogen bonding [93]. Van Den Bulcke et al. showed the modification of gelatin by using the addition of methacrylate to the side chains leading to photo-crosslinkable synthetic polymers [95].

The folding structure of proteins is mainly driven by hydrophobic interaction. It is well-known that mostly protein is denatured and undergoes irreversible changes upon heating. The higher-order structures of proteins, the secondary and tertiary structures, can be perturbed by several factors such as pH and temperature. As temperature increases, a breakage of hydrogen bonds between the water network surrounding proteins occurs. Protein denaturation generally occurs, leading to the loss of biological activity and a change in its structure, such as an unfolding. The unfolding structure of proteins upon heating originates from

hydrophobic interaction between hydrophobic amino acid residues in aqueous environment, resulting in irreversible protein precipitation or aggregation [96, 97].

In contrast, an increase in temperature of a thermo-responsive polymer causes polymer aggregation. However, the thermoresponsive system is switchable. The polymer undergoes conformational change from insoluble to soluble form in response to a decrease in the temperature. Therefore, the development of protein stabilisers to exploit their properties has become an important subject in biochemical engineering. There are several studies showing that the incorporation of natural polymers into thermo-responsive-based polymers in order to obtain the reversible nature of synthetic thermo-responsive polymers exhibits advantageous properties compared with the use of each alone. Rimmer et al. also exploited the properties of the RGD peptide by linking it to the chain ends of stimulus-responsive highly branched PNIPAM to provide a cell adhesive property. They firstly revealed the effect of peptide-functional end groups on particle dispersion above its LCST. They found that functionalisation of HB-PNIPAM with RGD at the chain ends led to stable dispersion of sub-micron particles in aqueous solution above the LCST thanks to the polarity of the chain groups [98].

Moreover, in order to make use of some globule proteins that have a potential for biomedical applications, such as bioelectronics, some properties should be improved (i.e. stability and three-dimensional orientation). Lam et al. exploited globular proteins for synthesising self-assembly block copolymers by conjugating with two kinds of proteins, which have similar structure but different chemical compositions. They found that both protein conjugated PNIPAM showed slight differences in the LCST of PNIPAM compared with homo PNIPAM. The phase transition temperature of mCherry-PNIPAM displayed a two-phase region and was lower than EGFP-PNIPAM while EGFP-PNIPAM formed a homogenous structure. It suggested that the self-assembly of mCherry protein conjugates were preferential for the dehydration state of the polymer compared with EGFP owing to the effect of chemical composition, which are responsible for solubility and surface property of the polymer [99]. It is obvious that non-switchable phase transition behaviour of a natural polymer is less useful for potential biomedical applications. Incorporation with synthetic thermo-reversible polymers is necessary so that desirable properties can be obtained.

1.3.5 Poly (*N*-isopropylacrylamide) (PNIPAM) and lower critical solution temperature (LCST)

PNIPAM is a smart polymer that has generated considerable interest since it can be easily synthesised by conventional free radical polymerisation and also its LCST can be tuned by copolymerising with different types of comonomers, consequently changing the balance between hydrophilic and hydrophobic domains. As its behaviour changes in response to temperature at 32°C, it provides a number of potentially useful biomedical applications, including in regenerative medicine and tissue engineering [11]. Over many decades, PNIPAM has become one of the well-known prototype thermo-responsive polymers due to reversible liquid-solid phase transition behaviour at its LCST. For instance, several workers have shown that hydrogel wound dressings synthesised from thermo-responsive polymers provide moisture locally, which has a vital effect on wound healing [100, 101]. Mi et al. have worked on the synthesis of thermo-responsive multifunctional hydrogels to be used as a wound dressing. The polymer was synthesised via reversible addition-fragmentation chain transfer polymerisation (RAFT polymerisation) in order to obtain triblock copolymers, of which one of the blocks is an antimicrobial drug and is hydrolysable. Their ideas were that the polymer solution could change into a non-sticky gel at body temperature and release the drug into the wound. They concluded that the PNIPAM block copolymer is biocompatible and has the potential to be used as a hydrogel wound dressing [8, 102]. This useful thermal behaviour of PNIPAM can be explained by its structure.

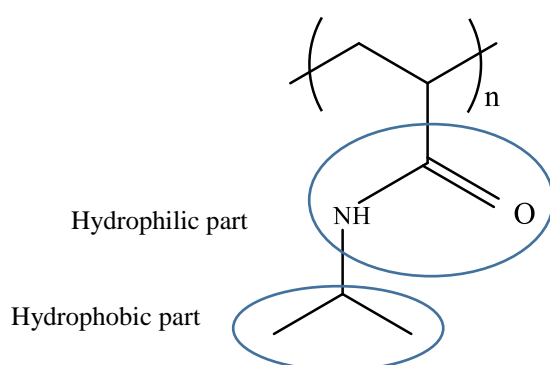


Figure 1.10 The chemical structure of PNIPAM

PNIPAM consists of both hydrophilic and hydrophobic segments. The backbone and isopropyl groups are hydrophobic while the hydrophilic part results from the side chain amide groups. When PNIPAM is dissolved in water, there are three possible interactions: polymer-water, polymer-polymer and water-water interaction. The switching from soluble expanded coil structure to insoluble compact globule form of PNIPAM chains is in response

to the LCST. Below the LCST (32°C), PNIPAM is soluble in water due to the formation of hydrogen bonds between water molecules and amide groups of the polymers. This results in two types of hydrated shells, namely a thin shell of water molecules around a hydrophilic section, and an ice-like structure of water molecules around hydrophobic groups of the polymer, called the solvated stage [74, 103-107]. The change in aqueous solution temperature makes PNIPAM-water interaction unfavourable. Above the LCST, increasing temperature leads to the cleavage of hydrogen bonds between water molecules and the amide groups in the PNIPAM. It brings about the release of the water molecules from the hydrated shell. Then, hydrophobic interaction originating from isopropyl groups becomes dominant. This stage is called a coil-to-globule transition of the polymer. Hydrophobic parts in the molecule induce the chain collapse in order to minimise water contact, resulting in compact globule conformation [104, 108]. There are two stages relevant to the collapse of PNIPAM chains, which are the intramolecular and intermolecular stages. The conformational switch of PNIPAM can be physically verified in several ways, such as investigation of the solution viscosity or turbidity measurement. The viscosity of PNIPAM solution decreases dramatically when the temperature reaches the LCST [74, 105, 109]. Ringsdorf reported that there are two steps in the phase separation mechanism of PNIPAM, which can be confirmed by time-resolved anisotropy measurement (TRAMS). The first step of the mechanism involves intramolecular chain collapse, and the second step consists of the intermolecular aggregation of hydrophobic collapsed units [110]. The conformational change of PNIPAM, resulting in the change in turbidity of solution, can be determined by UV-Vis spectroscopy. The temperature at which PNIPAM is no longer soluble and so aggregates, resulting in an observed increase in turbidity of the solution is usually called the cloud point. The cloud point is defined as the temperature at which the first sign of cloudiness occurs and corresponds to the absorbance at a specific wavelength, which is 450nm in the case of PNIPAM [111]. The turbidimetry measurement can determine the LCST at the macroscopic level because the information is obtained by detecting the clouding of the polymer owing to the hydrophobic interaction of the polymer chains [111]. However, micro differential scanning calorimetry (microDSC) is also one of popular techniques used for observing phase transition behaviour of PNIPAM. Both techniques will be discussed in Chapter 2.

1.3.6 Thermodynamics of low critical solution temperature

In order to explain the favourability of a polymer solution, the Gibbs free energy equation, set out below, can be used [105]. A detailed discussion is outside the scope of this study; however, an understanding of this system is certainly valuable.

$$\Delta G_{mix}(T) = \Delta H_{mix}(T) - T\Delta S_{mix}(T) \quad \text{Equation 1.1}$$

Where, ΔG_{mix} is Gibbs free energy of the system

ΔH_{mix} is enthalpy change of mixture

ΔS_{mix} is entropy change of mixture

T is temperature (K)

The favourable polymer solution occurs when the Gibbs free energy of the system is negative. Therefore, there are two main factors related to the system, which are entropy and enthalpy. The enthalpy change (ΔH_{mix}) is related to bond formation and cleavage between polymer molecules and water molecules, which are used for explaining the favourability of the system. In terms of the general polymer in aqueous solution, the entropy change (ΔS_{mix}) is always positive and small, which does not have a significant impact on the system, while hydrogen bonding interaction between the polymer and water molecule provides negative enthalpy. Therefore, in order to obtain the negative ΔG_{mix} , which is the solubilisation of the polymer, it is essential to increase the temperature [104, 105, 112].

In contrast, a change in the entropy of water is the main driving force for the phase transition behaviour of the thermo-responsive polymer, PNIPAM, at the LCST. Below the LCST, the thin shell ordering structure of the water molecules around hydrophilic parts stemming from hydrogen bonding between the polar amide units and water molecules is a favourable interaction and leads to the negative value of enthalpy of the solution process at a low temperature. Moreover, the ice-like formation of water molecules around the nonpolar regions of the polymer leads to a decrease in enthalpy change (ΔS). Therefore, Gibbs free energy of the system is negative and makes the polymer able to dissolve in water at a temperature below the LCST. When the temperature rises to 32°C, the entropy function becomes dominant. The H-bond interactions are cleaved and the formation of the ice-like structure of water is destabilised, which results in an increase in ΔS and an increase in enthalpy changes. Therefore, positive Gibbs free energy at LCST leads to the phase

separation of the polymer [105, 113, 114]. Nonetheless, there are several factors that have significant effects on the LCST of PNIPAM not just the local temperature.

Li et al. showed that the molecular weight and end groups of polymer structures crucially affect PNIPAM properties. One of the most influential factors is the architecture of polymers. Recently, many scientists have attempted to take advantage of these properties in order to overcome the limitation of the LCST so that wide ranges of applications can be obtained. Chee et al. studied the effect of the balance of hydrophobicity of the polymer on the LCST. It was found that the LCST of the poly(*N,N*-dimethylacrylamide) PDMAC-g-PNIPAM was lower than the PDMAC homopolymer due to the PNIPAM being grafted to the polymer. They concluded that the change in hydrophobicity balance in the polymer directly affected the phase transition behaviour of thermo-responsive polymers. Moreover, the degree of branching had an insignificant effect on the conformation of change of PNIPAM-g-PNIPAM, and that it would be interesting to study the effect of the degree of branching, highly branched PNIPAM on the phase transition behaviour of PNIPAM. Finally, an interesting suggestion was that variation of enthalpy and entropy of the stimulus responsive polymer with polar or non-polar end groups could be used to manipulate the LCST of the polymers [105].

1.4 Reversible addition-fragmentation chain transfer (RAFT)-mediated self-condensing vinyl polymerisation (SCVP)

Self-condensing vinyl polymerisation (SCVP) is considered a versatile synthetic method used for preparing highly branched polymers from vinyl monomers that can be synthesised via radical polymerisation. The process of SCVP combines vinyl polymerisation and polycondensation. Vinyl polymerisation provides oligomeric species, which contributes to growth of the polymer, followed by a step-growth reaction between two oligomers and initiation from a side chain initiating group, eventually forming a highly branched architecture [115]. The mechanism of SCVP polymerisation is illustrated in Figure 1.11.

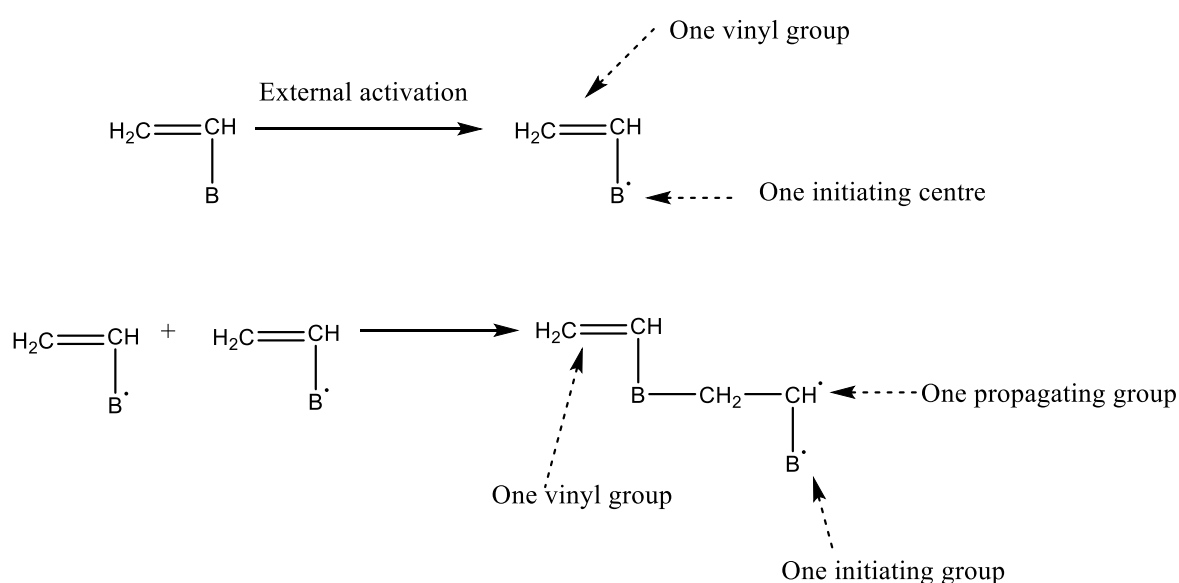


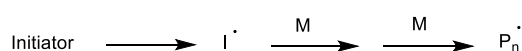
Figure 1.11 The mechanism of SCVP [115]

SCVP can be accomplished using several kinds of polymerisation techniques, such as cationic/or anionic polymerisation [116], photo-mediated polymerisation [117] and reversible addition-fragmentation polymerisation (RAFT) that depend on the types of initiating group [118]. RAFT polymerisation is one the foremost controlled radical polymerisation (CRP) techniques, having attracted interest for over a decade due to its many advantages [119]. Firstly, it can be used for synthesising a variety of polymers and copolymers with complex architectures, such as grafted copolymers and highly branched polymers. In addition, this technique can avoid the drawbacks of the conventional free radical polymerisation by providing narrow polydispersities with high conversion [120]. This is because, at the main equilibrium of the reaction, the probability of both actively propagating radicals and the dormant macro chain transfer agent compounds to fragment is equal, therefore allowing all

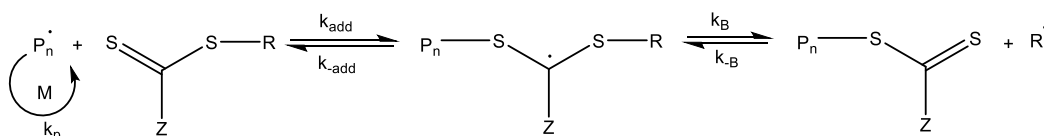
polymer chains to grow equally [121, 122]. Nonetheless, RAFT is compatible with various different functional monomers and can be conducted under mild conditions [115]. RAFT polymerisation is considered a versatile technique for synthesising complex architecture polymers and copolymers with diverse kinds of functional groups due to the use of different types of chain transfer agent (CTA) [120]. Moreover, the degree of branching can also be controlled by the ratio of monomer to CTA [115].

The process of RAFT polymerisation is similar to the conventional free radical polymerisation involved in homolytic or addition substitution. However, an essential difference is the presence of chain transfer agents in the system, which is a key component in the process [123]. Introducing a polymerisable vinyl group to chain transfer agents, resulting in chain transfer monomer, is one of the crucial steps in SCVP to create highly branched PNIPAM used in this study. However, to understand the process of RAFT-SCVP, it is essential to consider the basic mechanism of RAFT, as shown in Figure 1.12 [123].

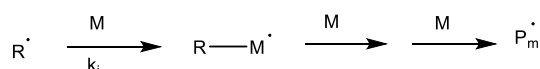
Initiation



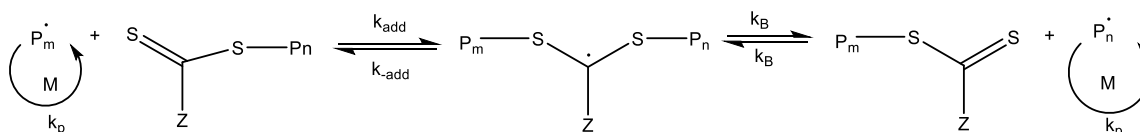
Chain transfer



Reinitiation



Chain equilibration



Termination

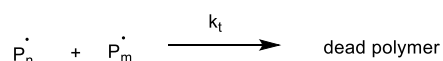


Figure 1.12 Mechanism of RAFT polymerisation [124]

From the above scheme (Figure 1.12), the mechanism of RAFT polymerisation can be explained as follows. As in conventional free radical polymerisation, initiators decompose into two free radicals so that they are able to react with susceptible carbon double bond of monomers, resulting in propagating polymer radicals (P_n^\bullet). This stage can be called the

addition stage. In order to start the polymerisation, the appropriate amount of initiating radicals from a suitable source is essential. Generally, the ratio of the initial concentration of chain transfer agents to the initial concentration of initiator $(CTAs)_0/(I)_0$ is higher than one, ensuring that there is a greater amount of chain transfer agents than free radicals in the solution. The number of chains is controlled by the concentration of the CTA whereas the concentration of free radicals is controlled by the degree of initiator fragmentation. Furthermore, the key stage of RAFT polymerisation is the reversible equilibrium of addition-fragmentation, of which a small amount of initiator fragmentation allows chain transfer agents to be activated. It is necessary for the activation step that primary radicals from the initiators react with the chain transfer agents, resulting in the releasing of new primary radicals. At this stage, propagating radicals (P_n^\cdot) react with the thiocarbonylthio compounds ($RSC-(Z)=S$) and then the fragmentation of the intermediate radicals occurs. The products from these steps are a new radical (R^\cdot) and a polymeric thiocarbonylthio compound ($P_nSC-(Z)=S$). After that, a new propagating radical (P_m^\cdot) will be formed by the reaction between the new radical from the previous step and monomers in the system. This is called reinitiation. In order to obtain efficient re-initiation, new radicals (R groups, R^\cdot) of the chain transfer agents need to effectively fragment and be able to reinitiate the reaction, because almost all of chains in RAFT polymerisation are initiated by these radicals. Only a few chains are generated by initiators. One of the key characteristics of this system is the equal probability of the polymeric thiocarbonylthio compounds and the active propagating radicals (P_n^\cdot , P_m^\cdot) at rapid equilibrium for all chains to grow, which leads to uniform chain growth [121, 124].

At moderate conversion, living chain ends can be extended and made to react with a second monomer to provide block copolymers. It is apparent that RAFT polymerisation can provide homopolymers or polymers with advanced architectures, such as star, multi-block and statistical polymers. However, when the polymerisation is completed, the products still consist of thiocarbonylthioate in the end groups (ω -ends) leading to odour and colour in the polymers, which may have an effect on many applications. The removal of the ω -end groups from polymers have recently been explored [125]. End group elimination could be an issue because the degradation of the polymer comprising of thiocarbonylthioate cause odorous materials due to the presence of sulphur. However, the end groups can be removed or

functionalised by a number of techniques such as ω -End modification, thermal elimination, radical induced end group removal [120, 125].

There are several important factors that have an influence on RAFT polymerisation. In order to obtain efficient control over the molecular weight distribution, some requirements need to be fulfilled. Firstly, it is vital for the chains to be initiated in a short period of time, similar to ideal living polymerisation. Moreover, it must be ensured that the number of monomer units in each active/dormant cycle is low so that every chain grows at a similar rate. Thirdly, any factors that bring about the chain termination need to be minimised. Moad et al. reported that retardation of RAFT polymerisation occurred when high concentrations of RAFT agents were used [123]. Thus, the concentration of the active species must be as low as possible so that the possibility of termination reactions will be minimised [124].

1.4.1 Factors that affect RAFT polymerisation

In this review, factors influencing RAFT polymerisation is briefly described and considered separately in both the addition and fragmentation stages.

1.4.1.1 The structure of chain transfer agents (CTA)

1) The influence of CTA structure on addition reactions

The structure of chain transfer agents (CTA) is one of the factors that play a crucial role in the addition reaction of radicals to double bonds in the system. The addition rate coefficient (k_{add}) depends on the reactivity of the radicals and the chain transfer agents. There are several parameters involved in this reactivity, such as polarity, resonance and steric hindrance of CTA [126]. The different types of substituent CTA directly affect the double bond activation, which results in an increase of the k_{add} in the system. The substituent consisting of a π -orbital, such as phenyl groups, will have a higher addition rate coefficient than the CTA comprising a substituent that bears an atom with a lone pair such as -OR, -NR₂ or halogen. In addition, the polarity of the Z substituent also contributes to the rate of addition reaction. The substituent which bears the electron withdrawing groups, such as halogens, cyano or carboxyl group brings about an increase in k_{add} value because almost all of the attacking radicals are nucleophilic. Finally, steric hindrances of Z groups can also decrease the k_{add} value. Therefore, CTA transfer activity needs to be considered in order to obtain an

appropriate condition because too bulky a structure of the substituent group can cause a reduction in the transfer activity [121, 124].

In this work, the main monomer chosen was one of the acrylamide families, which is NIPAM monomer. Therefore, this review will focus on the Z and R groups that are used for NIPAM in RAFT polymerisation.

2) The influence of CTA structure on fragmentation

Generally, fragmentation is an intra-molecular reaction that is completed by an intermolecular reaction, where the rate of fragmentation relies on the intermediate radical substituent and the conditions of the experiment, such as steric hindrance of intermediate radicals, monomer concentration or experimental temperature. In the case of RAFT polymerisation, a weak bond between carbon and sulphur next to intermediate tertiary radicals induces the fragmentation reaction (See Figure 1.13 below).

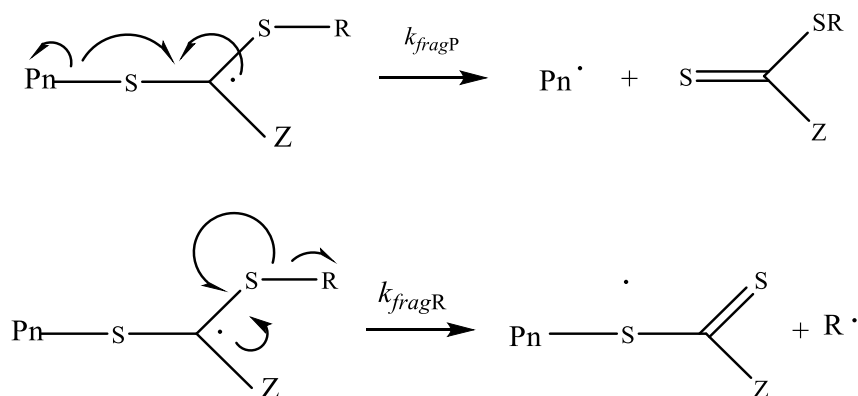
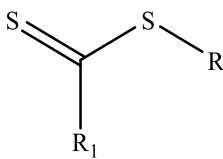
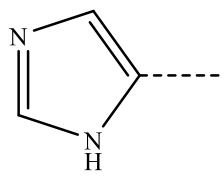
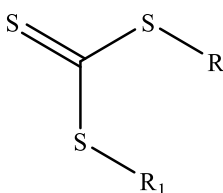
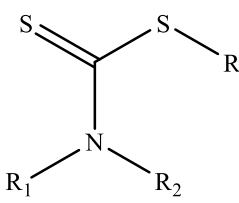
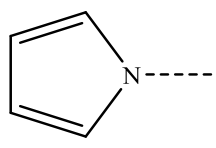


Figure 1.13 A scheme showing the possible fragmentation of IR [124]

The fragmentation rate coefficient (k_{frag}) depends on two factors. The first is the weakness of the S-C bond, which is directly related to the R group. Another factor is the stabilization of intermediate radicals, which stems from the Z group. However, for the polymerisation of acrylates or acrylamides, the fragmentation rate coefficient (k_{frag}) may be low when strong stabilizing Z groups such as dithiobenzoates are used. This is due to the high strength of the S-P_n bond. Therefore, dithiobenzoates are not suitable for polymerisation of acrylates/acrylamides and vinyl esters [127]. One of the important roles of the Z group is to activate the thiocarbonyl groups in RAFT agents and stabilize the intermediate radical such that the addition reaction is able to compete with the propagation reaction [124].

The R group is the main factor in terms of the effect on the fragmentation and re-initiation reaction in RAFT polymerisation. The main role of the R group is to make the S-R bond as weak as possible so that a high fragmentation rate can be obtained. Furthermore, the R radical ($\dot{\text{R}}$) originating from fragmentation should be a good leaving group rather than a propagating radical [128]. To obtain fast and effective initiation of new polymer chains, it is necessary to ensure that the R radical ($\dot{\text{R}}$) is not too stabilized. Rimmer et al. synthesised HB-PNIPAM using a CTA possessing an imidazole functionality, which exhibited a decrease in phase transition temperature (LCST) compared with a linear analogous version. They suggested that a decrease in LCST of the polymer resulted from the aggregation of hydrophobic chain ends because of the imidazole groups [129].

Table 1.1: Types of Z and R groups of CTAs used in RAFT polymerisation for NIPAM monomers [124]

Types of CTAs used in RAFT polymerisation for NIPAM	Structure of Z groups
Z= R ₁ Dithioesters	  Ph- PhCH ₂ -
Z= R ₁ Trithiocarbonates	 C ₁₂ H ₂₅ S- (HO(CH ₂) ₂ O ₂ C)(Et)CHS-
Z= NR ₁ R ₂ Dithiocarbamates	 

1.4.1.3 Influence of the concentration of the polymerisation medium

The viscosity of the system resulting from the concentration of the monomer and the percentage of the conversion affects the kinetics and the control of molecular weight

distribution. The high viscosity of the polymerisation medium decelerates the reaction between the active chains and the dormant species, leading to a reduction in the number of active/dormant cycles and broad molecular weight distribution [124].

1.4.1.4 Impurities

Impurities originate from chain transfer agent synthesis or from chain transfer degradation. They can cause retardation of the polymerisation process. In order to prevent the oxidation of RAFT agents (such as thiocarbonylthio compounds) by air it is essential to store them in an inert substance [130].

1.4.2 The success of highly branched PNIPAM synthesised by reversible addition-fragmentation chain transfer (RAFT) mediated self-condensing vinyl polymerisation (SCVP) polymerisation used in biological studies

Many workers have concentrated on developing not only the properties of PNIPAM, but also the architecture of the polymer. Ideally, changes in architecture of PNIPAM could provide different physical and biological properties of the polymer, leading to various types of polymer applications. Comparing the linear and advanced branched structure of the PNIPAM polymer, it is obvious that the latter is more useful and attractive than the linear polymer for many reasons, such as lower viscosity of polymer melt, higher solubility and more functionalities in structures that are ready to be modified to obtain desirable end groups [8, 16, 17, 104, 131-133]. However, the linear polymer is easier to synthesise and so cheaper. Despite this the unique properties of branched PNIPAM makes them of particular interest for maximum development.

There are several methods for synthesising branched polymers, such as condensation polymerisation, self-condensing ring-opening polymerisation and self-condensing vinyl polymerisation (SCVP). However, in this work, only SCVP will be discussed. SCVP can be accomplished by many types of polymerisation techniques, such as atom-transfer radical polymerisation (ATRP) or RAFT polymerisation. RAFT polymerisation has been studied especially for the PNIPAM [129]. The polymerisable RAFT agent was designed in order to produce a highly branched polymer by using the SCVP-RAFT polymerisation technique. Carter et al. created two kinds of polymerisable RAFT agents, which are 4-vinylbenzyl-1-imidazolecarbodithionate and 4-vinylbenzyl-1-pyrrolicarbodithionate, i.e. RAFT1 and RAFT2 respectively. The structure can be seen in Figure 1.14. Both kinds of these RAFT

agents are appropriate for polymerisation of NIPAM because dithioate group, which is leaving group, is located at chain ends rather than the branch point so that further chain end modifications can be carried out [129, 132, 134]. However, RAFT1 was chosen to use in this work because, according to Carter et al, it was found that polymer with imidazole end groups can only dissolve in DMF and has limited solubility due to considerable H-bonding between imidazole groups, whereas polymer with pyrrole ends can dissolve in water and other solvents.

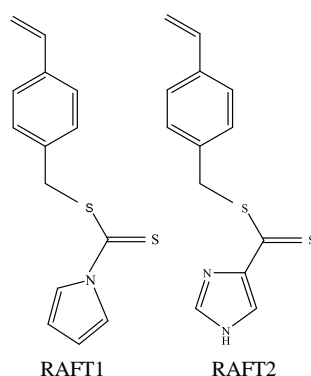


Figure 1.14 The structure of vinyl RAFT agents synthesised by Carter et al.

With the emergence of such advanced techniques, RAFT polymerisation has been used for synthesis of different types of polymer used in biotechnology including PNIPAM. Vogt et al. synthesised branched PNIPAM with varying M_N from 5,000-12,000 g/mol using the RAFT technique. They showed that the phase transition temperature of the polymer decreased with an increase in degree of branching [135, 136]. Plenderleith et al. also found that the LCST of highly branched PNIPAM with varying degree of pyrrole chain ends prepared by SCVP-RAFT polymerisation decreased with increased branching [137]. This information is one of the key values for the use of PNIPAM in biological and pharmaceutical applications because its LCST can be tuned and used over a wide range of temperature by varying the degree of polymer branching. Recently, Wang et al. synthesised PNIPAM via RAFT polymerisation in order to study the interaction between PNIPAM and piceatannol, which is a polyphenol having anti-inflammatory and chemopreventive properties. PNIPAM was chosen in their studies because piceatannol is a natural compound with high hydrophobicity and low bioavailability leading to some limitations for its direct use in pharmacology. They found that, below the LCST of PNIPAM, piceatannol firstly bound to the hydrophilic part of PNIPAM, which is the amide group, followed by hydrophobic interaction with the isopropyl

group and the backbone of PNIPAM. However, above the LCST (37°C), hydrophobic interaction between piceatannol and the polymer occurred first, followed by hydrophilic interaction site. They suggested that phase transition behaviour of PNIPAM has a significant influence on the binding of its target [138]. PNIPAM architecture and properties have continued to attract interest and be developed in various types of applications. Sub-micron PNIPAM particles with cell-adhesive peptide (RGD) chain end was prepared via SCVP-RAFT technique and used as substrates for transferring cultured cells to another substrate thanks to the thermally responsive behaviour of PNIPAM [139]. Following the success of Carter et al. developing the two kinds of polymerisable RAFT agents, Shepherd et al. have applied this knowledge in microbiological applications. Interestingly, they found that binding bacteria to HB-PNIPAM functionalised with vancomycin, which is one kind of antibiotic used for Gram-positive bacteria, can reduce the coil to globule transition temperature from above 70°C to 24 °C. It could be concluded that the binding of the bacteria to the polymer causes the collapse of the polymer coils and the formation of insoluble complexes of polymer and bacteria. From this work, it was also discovered that the number of bacteria in a wound could be decreased when such a polymer was applied and removed from the wound [16]. To confirm that the HB-PNIPAM-vancomycin was binding directly to the bacteria, Shepherd *et al.* incorporated the fluorescent probe anthracene into the polymer. It was found that the bacteria and the polymer were present in the same complex. These findings indicate that HB-PNIPAM has the potential to be an alternative, clinically useful material for wound dressings [16, 17]. It is evident that SCVP-RAFT technique is one of the promising methods used for developing the polymer properties such as chain end functionality, polymer architecture [132, 134] that could be appropriate for each application.

1.5 Ideal features of a detection system for binding bacteria to polymers functionalised with antibiotics

The classical diagnosis of wound infection relies on the recognition of symptoms, such as redness and swelling of the infected area, and of conventional microbiology to optimise treatment but this takes a minimum of 24 hours. Furthermore, clinical diagnosis of the stages of wound infection is difficult because a range of factors can influence the overtness of the symptoms, and this can lead to misdiagnosis. There is therefore a clear clinical need for an improved and more rapid test for the presence of infection. Recently, there have been many attempts to develop materials for the identification of Gram-positive or Gram-negative bacteria, such as the bacterial-instructed synthesis of polymers that can bind to specific

pathogens or fluorescent sensors, and which could provide a rapid probe for increased bacterial load and possibly to bacterial identification.

Simple colourimetric or fluorescent change of the polymer indicating binding of bacteria would be the most valuable. There are several chemicals that have previously been used as fluorescent markers, such as anthracene, but this does not change in character with change in the microenvironment. Therefore, the addition of alternative fluorochromes to the polymers that do change with the microenvironment needs to be investigated.

In this work, Nile red, a polarity-sensitive chemical, has been introduced to act as a fluorescent probe to investigate the system. Nile red (9-diethylamino-5H-benzophenoxazine-5-one) is an uncharged hydrophobic chemical, on which the polarity of the environment has a direct effect on its fluorescence behaviour. The colour and fluorescence change with the polarity of environment due to the electron donor and acceptor groups in its structure. In non-polar solvents, it fluoresces with a high quantum yield at an emission maxima of about 530nm, whereas the quantum yield is significantly less in a polar solvent falling by 50nm [140]. Furthermore, this dye is considered photochemically stable and capable of working in a wide range of wavelengths and pHs (between 4.5 and 8.5). One of the interesting properties of Nile red dye is its high partition coefficient in a broad range of solvents, from hydrophilic to hydrophobic solvents, such as methanol and cyclohexane. The mechanism of Nile red fluorescence in different polarity environments can be explained by its chemical structure [141].

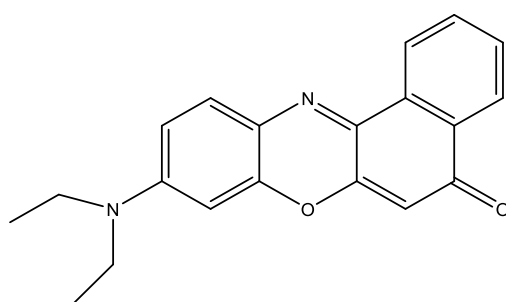


Figure 1.15 The structure of Nile red dye

From the above figure, it can be seen that Nile red consists of an efficient electron acceptor and a donor group, leading to the expectation that it is potentially excited in the dipole moment and it is this that results in sensitivity to the change in the polarity of its environment. Additionally, the chemical structure shows that Nile red has poor solubility in

polar solvents [140, 141]. Dan et al. found that Nile red showed different emission spectra in various kinds of solvent mixtures [141] and the emission maxima of the Nile red decreased when the polarity of its environment changed from hydrophilic (methanol) to hydrophobic (dioxane). Furthermore, the shift in the emission maxima of Nile red does not occur only in dioxane, but in various solvents [142].

Table 1.2: Emission maxima of Nile red in various types of solvents [144]

Type of solvent	Emission max. (nm)	Index of polarity	Dielectric constant
Water	665	94.6	80
30% Ethanol	657	91.6	64
50% Methanol	655	90.9	58
40% Dioxane	653	88.4	44
Diethylene glycol	652	85.1	37
60% Dioxane	644	85	27
methanol	642	83.6	34
Dimethyl sulfoxide	635	71.1	44
Ethanol	635	79.6	24
Butanol	633	77.7	18
80% Dioxane	633	80.2	11
2-propanol	628	76.3	18
Acetonitrile	627	71.3	38
Dimethyl formamide	625	68.5	37
Acetone	615	65.7	21

In recent times, Nile red derivatives have been used as a stain for intracellular lipids and they can interact with various kinds of protein such as β -lactoglobulin [141, 143]. Moreover, recently, Nile red has been used to probe the relative polarity of various degrees of branching of HB-PNIPAM with carboxyl end groups across the temperature range (10-45°C) [137].

In this study, it was hypothesised that addition of Nile red into HB-PNIPAM-van polymer could provide a change in emission maxima and a decrease in fluorescence intensity when bound to bacteria due to the change in micro-environment of the dye from polar to non-polar. Moreover, development of a detection system for bacteria bound to thermo-responsive polymers, based on PNIPAM functionalised with vancomycin and using Nile red as reporter, could provide important applications for this material such as an improvement in efficiency of infection diagnosis. However, in order to develop the system to its full potential, understanding of the factors that have an effect on binding of bacteria to the polymer modified with antibiotics is necessary.

1.6 Hypothesis, Aims and Objectives

The development of new devices for the detection of bacteria seeks to reduce the unnecessary use of antibiotics and so minimise the rise of drug-resistant bacteria. PNIPAM is one such material and recently highly branched (HB) PNIPAM has been modified to respond to the presence of bacteria by addition of antibiotics at the chain ends. However, until now, the behaviour of HB-PNIPAM with antibiotic end groups has not been explored fully and it has not been directly compared to a linear version (L-PNIPAM) that would be easier to manufacture.

When starting this work certain parameters about the HB-PNIPAM-van were known from previous work in this laboratory. This included the observation that in the presence of lower concentrations of HB-PNIPAM-van (1mg/ml), aggregates of *S. aureus* were formed in suspension but they were only small. However, the size of the aggregates increased in a dose-dependent manner with polymer concentration and for ease of observation the optimum concentration appeared to be 5mg/ml [17]. Consequently, this work was not repeated directly and most work was performed at this concentration. Furthermore, we needed a rapid and simple assay for monitoring interaction of the polymer with bacteria and we settled on the aggregation assay (mat/button assay), which had also been described previously [17]. However, the method suffers from requiring relatively high numbers of bacteria to visualize a button or a mat, which limited the range of bacterial number we could use to study polymer interaction. Nonetheless, using microscopy, Shepherd had shown that the size of bacterial aggregates varied not only with polymer concentration but also with bacterial number (the higher the number the larger the aggregates) and around 10^8 bacteria per ml was optimal [17]. Again, we did not seek to merely repeat that work but to use varying bacterial number of concentration of target for vancomycin to explore the behaviours of HB-PNIPAM-van and its linear homologue in more detail. Indeed, until the work of this thesis, little work had been done using linear PNIPAMs with functionalized end groups and in particular their behaviour with bacteria. Consequently, taking into account the concept that linear NIPAMs are thought to collapse above their LCST but with the end groups folding in on the polymer globule [144], so being hidden, and that end group interaction with target ligand results in desolvation of the polymer as well, we hypothesized that L-PNIPAM-van should not be able to bind to bacteria very effectively because the van groups would become hidden early in the interaction.

This project focuses, therefore, on understanding the behaviour of HB-PNIPAM functionalised with vancomycin at the chain ends in the presence of bacteria and a linear analogous polymer as a comparator. The hypothesis to be explored was that the HB-PNIPAM-van can be driven through a coil-to-globule transition when the vancomycin binding groups interact with bacteria, whereas the L-PNIPAM, which has pendant vancomycin groups would dissociate because the ligand-target interactions become shielded when the polymer collapses to the globular form. Furthermore, since the response to the bacteria is a desolvation process, it was expected that bacteria that are more hydrophobic might interact with the polymer more efficiently.

To test this hypothesis, both types of polymer were prepared with equivalent vancomycin composition but because of their different architectures, their behaviour was compared in a number of ways. These included the ability to bind to a range of *S. aureus* strains that have varied features (hydrophobicity and charge) both below and above the LCST of the polymers, the effect of D-Ala-D-Ala on the polymers as a low molecular weight target for the vancomycin, and exploration of their phase transition behaviour in the presence of bacteria using Nile red as a reporter system. The latter aimed to confirm that desolvation does occur when the PNIPAMs interact with bacteria.

The specific objectives of the project were:

1. To investigate the effect of chain architecture on the phase transition behaviour (LCST) of HB-PNIPAM modified with antibiotics and the linear version of the polymer
2. To confirm that vancomycin end groups of both linear and highly branched polymers are still functional and able to bind to their targets using D-Ala-D-Ala
3. To develop and optimise techniques for determining the amount of vancomycin binding sites in both types of polymer
4. To determine any antimicrobial activities of polymers functionalised with vancomycin on strains of *S. aureus*
5. To examine the effect of hydrophobicity and electrostatic charge of the bacteria on the binding ability of the polymers
6. To investigate the change in the LCST caused by interaction with bacteria and the potential for Nile red to act as fluorescence reporter

Chapter 2 : Materials, methods and polymer characterisations

2.1 Materials

N-isopropylacrylamide (Sigma-Aldrich, 97%) was recrystallised three times from *n*-hexane/toluene (60:40). Vinyl benzoic acid (Sigma-Aldrich, 97%) was used as received. 1, 4-dioxane (AnalaR NORMAPUR) and *N,N*-dimethylformaldehyde (DMF) (AnalaR NORMAPUR) and diethyl ether (AnalaR NORMAPUR) were obtained from VWR and used as purchased. 4, 4'-azobis (4-cyanovaleric acid) (Alfa Aesar, 98%), *N*-hydroxysuccinimide (Sigma-Aldrich, 98%) and *N,N*-dicyclohexylcarbodiimide (Sigma-Aldrich, 98%) were used as supplied. Vancomycin-hydrochloride hydrate (Sigma-Aldrich) was used as received. Pyrrole (Sigma-Aldrich, 99%) was distilled over calcium hydride (CaH₂) to obtain a colourless liquid. Carbon disulfide (Sigma-Aldrich, 99%), sodium hydride (60% in mineral oil) and 4-vinyl benzyl chloride (Sigma-Aldrich, 90%) were used as supplied. Nile red (Sigma-Aldrich) was used as supplied. Toluene (AnalaR NORMAPUR) and ethyl acetate (AnalaR NORMAPUR, reagent grade) were used as received.

2.2 Synthesis

2.2.1 Synthesis of 4-vinylbenzyl pyrrolecarbodithioate

A 250ml 3-neck round bottomed flask (RBF) was purged with nitrogen in order to remove any moisture. Sodium hydride (2.98g, 74.53mmol, (N.B in mineral oil dispersion)) was added to the RBF and followed by DMF (80ml) to form a suspension. Pyrrole (5.00g, 74.53mmol) with DMF (10ml) was added dropwise at room temperature to the rapidly stirring suspension of sodium hydride over a period of 30 minutes to obtain a yellow foam. This solution was continuously stirred at room temperature for 30 minutes. Then, the product was cooled to 0°C in an ice bath. Carbon disulphide (5.68g, 4.50ml, and 74.53mmol) with DMF (10ml) was added dropwise for 10 minutes using a pressure equalising funnel. A dark red solution was produced. This solution was stirred at room temperature for 30 minutes and then cooled again to 0°C on ice. 4-vinylbenzyl chloride (11.37g, 10.50ml, and 74.53mmol) with DMF (10ml) were added dropwise over a period of 20 minutes using a pressure equalising funnel. The solution was stirred for a further 16 hours at room temperature. In order to obtain the product, a 1 litre separating funnel was used to separate the product with diethyl ether (80ml) and distilled water (80ml). The organic layer, containing 4-Vinylbenzyl-Pyrrolecarbodithioate, was recovered whereas the aqueous

layer consisting of residue was extracted with diethyl ether (160ml) three times. The extracts were dried over magnesium sulphate and filtered. The solvent was removed by rotary evaporation to yield a brown oil.

The product was purified by flash chromatography using 100% hexane or petroleum ether as an eluent. The R_f value of the product (bright yellow oil) is 0.180 in 100% hexane. The solvent was removed by rotary evaporation and the final product was stored at -18°C under an atmosphere of N_2 .

4-vinylbenzyl pyrrolecarbodithioate: ^1H NMR (CDCl_3 , ca. 5% CD_3OD , 250 MHz): δ/ppm : 7.7 (2H, m, N-CH=, pyrrole); 7.4 (4H, s, C_6H_4 -); 6.7 (1H, dd, $J_{cis} = 10.9\text{Hz}$, $J_{trans} = 17.6\text{Hz}$, vinyl); 6.3 (2H, m, =CH-, pyrrole); 5.8 (1H, d, $J_{trans} = 17.6\text{Hz}$, vinyl) ; 5.3 (1H, d, $J_{cis} = 10.9\text{Hz}$, vinyl) ; 4.6 (2H, s, Ar- CH_2 -S-).

^{13}C NMR (CDCl_3 , ca. 5% CD_3OD , RT, 62.5 MHz): δ/ppm : 199.5 (1C, S-C=S); 137.5 (1C, aromatic C- CH_2 -S); 136.5 (1C, Ar-CH=CH₂, vinyl); 134.12 (1C, aromatic C-CH=CH₂); 129.8 (2C, aromatic); 126.74 (2C, aromatic); 120.85 (2C, -N-CH=CH, pyrrole); 114.55 (1C, -CH=CH₂ vinyl); 114.42 (2C, -N-CH=CH, pyrrole); 41.68 (1C, S- CH_2 -Ar). The ^1H NMR and ^{13}C NMR spectra were similar to the prior literature [145].

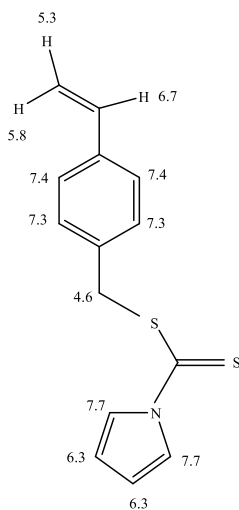


Figure 2.1 The chemical structure of 4-vinylbenzyl pyrrolecarbodithioate

Elemental Analysis, % found (expected): Carbon 65.30% (64.83%); Hydrogen 5.00% (5.05%); Nitrogen 5.30% (5.40%); Sulphur 22.4% (24.72%).

2.2.2 Highly branched PNIPAM (HB-PNIPAM-pyrrole)

Recrystallised *N*-isopropyl acrylamide (NIPAM) (5 g, 44mmol) was dissolved in dioxane (25cm³) 4-vinylbenzyl-1-1-pyrrolecarbodithioate (RAFT monomer) (0.435g,

1.7mmol) and 4, 4-azobis (4-cyanovaleric acid) (ACVA) (0.4704g, 1.7mmol) were dissolved in dioxane (5cm³) and the solution was added to each other. The mixture was transferred to a glass ampoule and degassed by four freeze-pump-thaw cycles under vacuum. Then, the ampoule was sealed and the reaction was conducted at 60°C for 48h. To obtain solid polymer, the viscous reaction mixture was precipitated from dioxane into diethyl ether three times. Then, the polymer (HB-PNIPAM-pyrrole) was dried overnight in a vacuum-oven at room temperature (% yield = 92.8%).

HB-PNIPAM-pyrrole:

¹H NMR (400 MHz, CDCl₃) (ppm): d 0.9-1.1 (6H, s, -N(CH₃)₂), d 1.3-1.7 (2H, m, -CH₂-CH-Ar-), d 1.8-2.5 (2H, m, -CH₂-CH-CO-NH-) and (1H, m, CH₂-CH-CONH -), d 3.8 (1H, s, (CH₃)₂CH-), d 6.4 (H₂, s, *N*-pyrrole-H), d 6.6-7.6 (m, -Ar-), d 7.7 (2H, s, *N*-pyrrole-H). The ¹H NMR spectra were similar to the prior literature [137].

FTIR: 3200 cm⁻¹ (sp² aromatic C-H), 1630 cm⁻¹ (sp² amide C=O), 1570 cm⁻¹ (sp² benzene C=C), 1540 cm⁻¹ (sp³ pyrrole C-N), 1500 cm⁻¹ (sp³ C-C).

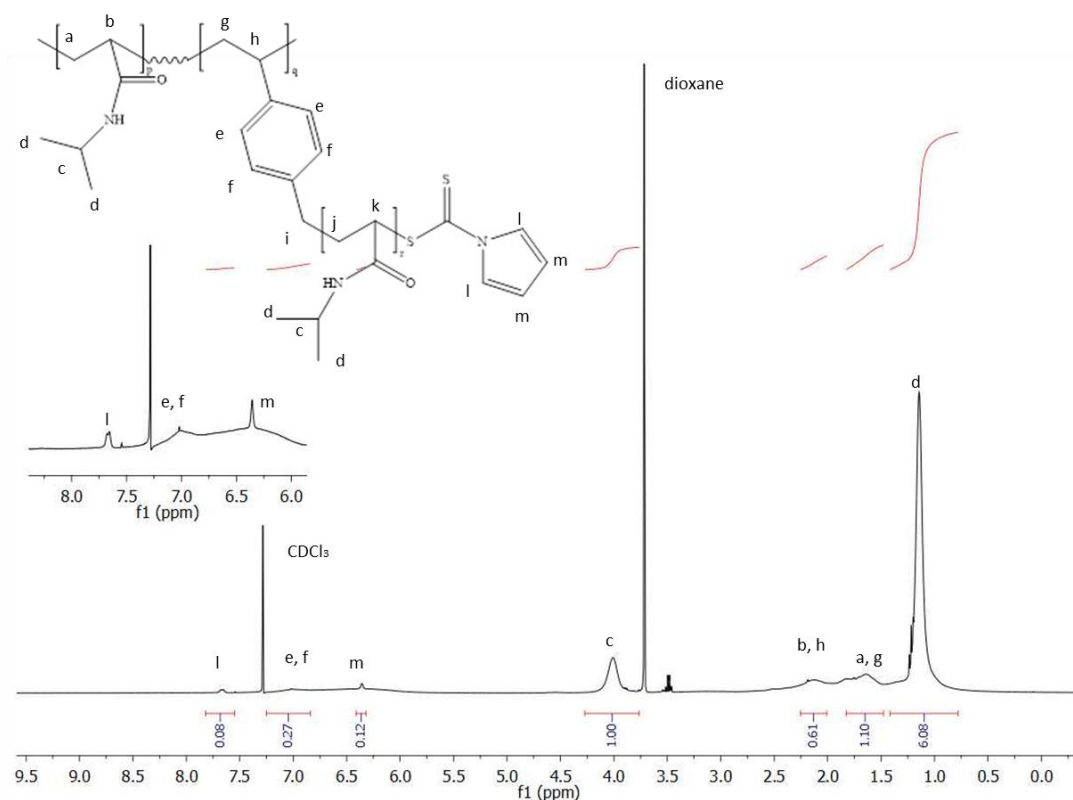


Figure 2.2 ¹H NMR spectrum of HB-PNIPAM with pyrrole end groups, with the expanded region showing the peaks due to the pyrrole groups (m and l) and the peaks due to the styryl groups (e and f)

2.2.3 Carboxylic acid terminated highly branched polymer (HB-PNIPAM-COOH)

HB-PNIPAM with pyrrole end groups were converted to a polymer with carboxylic acid chain ends by using 20eq of 4, 4-azobis (4-cyanovaleic acid) (ACVA). 3g of HB-PNIPAM-pyrrole was dissolved in DMF (10cm³). Then, 20eq.mol of AVCA (5.22 g) was added. The reaction was carried out at 60°C under nitrogen for 24 hours. Then, the addition of AVCA was repeated two more times. To obtain the final HB-PNIPAM-COOH preparation, the polymer was precipitated in diethyl ether three times and purified by ultrafiltration three times in a mixture of acetone and ethanol (9:1) (200cm³). The solvent was removed by rotary evaporation, then HB-PNIPAM-COOH was dried under vacuum at room temperature overnight (% yield = 80%).

HB-PNIPAM-COOH:

¹H NMR (400 MHz, DMSO) (ppm): d 0.9-1.1 (6H, s, -N(CH₃)₂), d 1.3-1.7 (2H, m, -CH₂-CH-Ar-), d 1.8-2.5 (2H, m, -CH₂-CH-CO-NH-) and (1H m, CH₂-CH-CONH-), d 3.8 (1H, s, (CH₃)₂CH-), d 6.4 (2H, s, *N*-pyrrole-H), d 6.6-7.6 (m, -Ar-), d 7.7 (2H, s, *N*-pyrrole-H), d 12.0 (m, COOH). The ¹H NMR spectra were similar to the prior literature [137].

FTIR: 3400 cm⁻¹ (O-H), 3200 cm⁻¹(sp² aromatic C-H), 1710 cm⁻¹ (sp² carboxylic acid C=O), 1630 cm⁻¹ (sp² amide C=O), 1570 cm⁻¹ (sp² benzene C=C), 1500 cm⁻¹ (sp³ C-C)

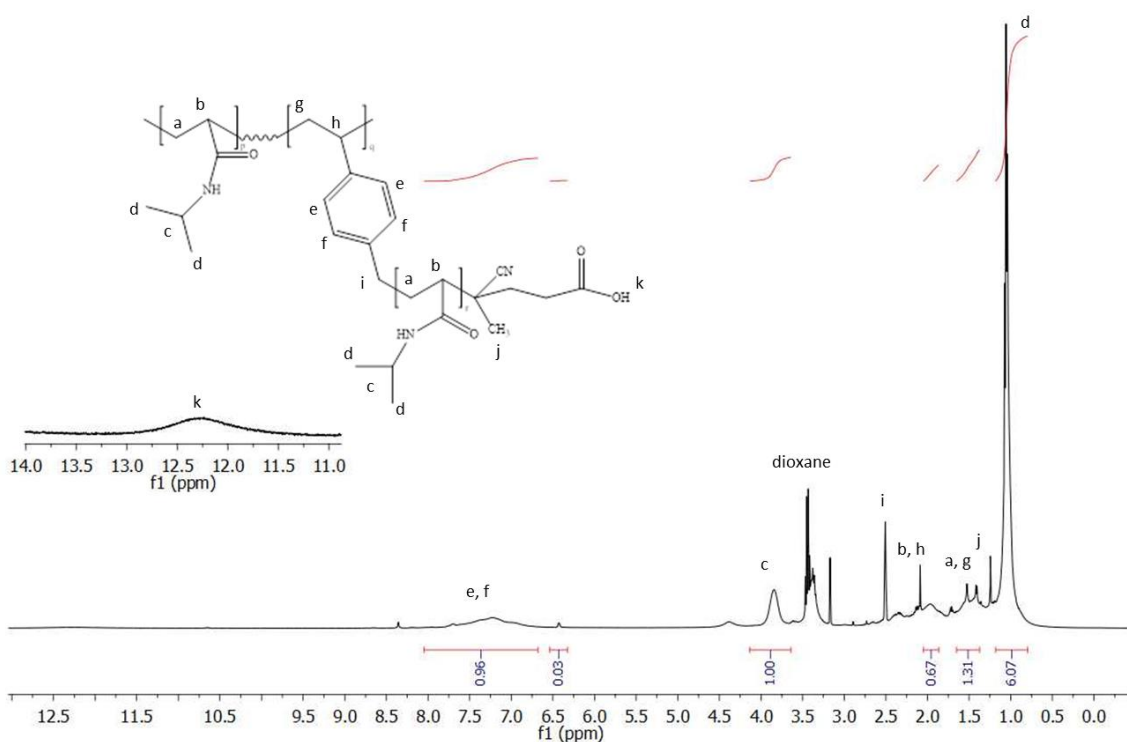


Figure 2.3 ^1H NMR spectrum of HB-PNIPAM-COOH , with the expanded region showing the peaks due to the carboxylic acid groups (k)

2.2.4 Synthesis of HB-PNIPAM with vancomycin at the chain ends (HB-PNIPAM-van)

HB-PNIPAM-COOH (1g) was dissolved in DMF (10cm^3). *N*-hydroxysuccinimide (NHS) (0.1636g, 1.4mmol) and *N,N*-dicyclohexylcarbodiimide (DCC) (0.2930g, 1.4mmol) was dissolved in DMF (5cm^3) and then added to HB-PNIPAM-COOH in DMF solution. The reaction was conducted under an atmosphere of nitrogen overnight. DMF was removed by rotary-evaporation and the product was precipitated in diethyl ether. The solid (HB-PNIPAM-succinimide) was purified by ultrafiltration three times (1 hour each) in a mixture of acetone and ethanol (9:1). To obtain a solid product, the solvent was removed by rotary evaporation and the polymer was dried under vacuum at room temperature. HB-PNIPAM-succinimide (100mg) was dissolved in deionised water (5cm^3) over ice and then vancomycin (30mg, 0.02mmol) solution in deionised water (2cm^3) and phosphate buffer pH 8.5 (2cm^3) was added. The pH was adjusted with sodium hydroxide (0.1M) to obtain a final pH of 9.5. The solution was stirred over ice for 24 hours. Following the reaction, the HB-PNIPAM functionalised with vancomycin (HB-PNIPAM-van) was purified by ultra-filtration

with deionised water three times and freeze-dried to obtain the final solid polymer, which was stored at -20°C (% yield = 68%).

HB-PNIPAM-van:

$^1\text{H NMR}$ (500 MHz, D_2O) (ppm): d 0.9-1.1 (6H, s, $-\text{N}(\text{CH}_3)_2$), d 1.3-1.7 (2H, m, $-\text{CH}_2-\text{CH}-\text{Ar}-$), d 1.8-2.2 (2H, m, $-\text{CH}_2-\text{CH}-\text{CO}-\text{NH}-$) and (1H, m, $\text{CH}_2-\text{CH}-\text{CONH}-$), d 3.9 (1H, s, $(\text{CH}_3)_2\text{CH}-$), d 6.4 (H2, s, *N*-pyrrole-H), d 6.5-7.6 (m, $-\text{Ar}-$), d 7.7 (2H, s, *N*-pyrrole-H).

FTIR: $3300\text{-}3500\text{ cm}^{-1}$ (phenol O-H), 3200 cm^{-1} (sp^2 aromatic C-H), 1630 cm^{-1} (sp^2 amide C=O), 1570 cm^{-1} (sp^2 benzene C=C), 1500 cm^{-1} (sp^3 C-C)

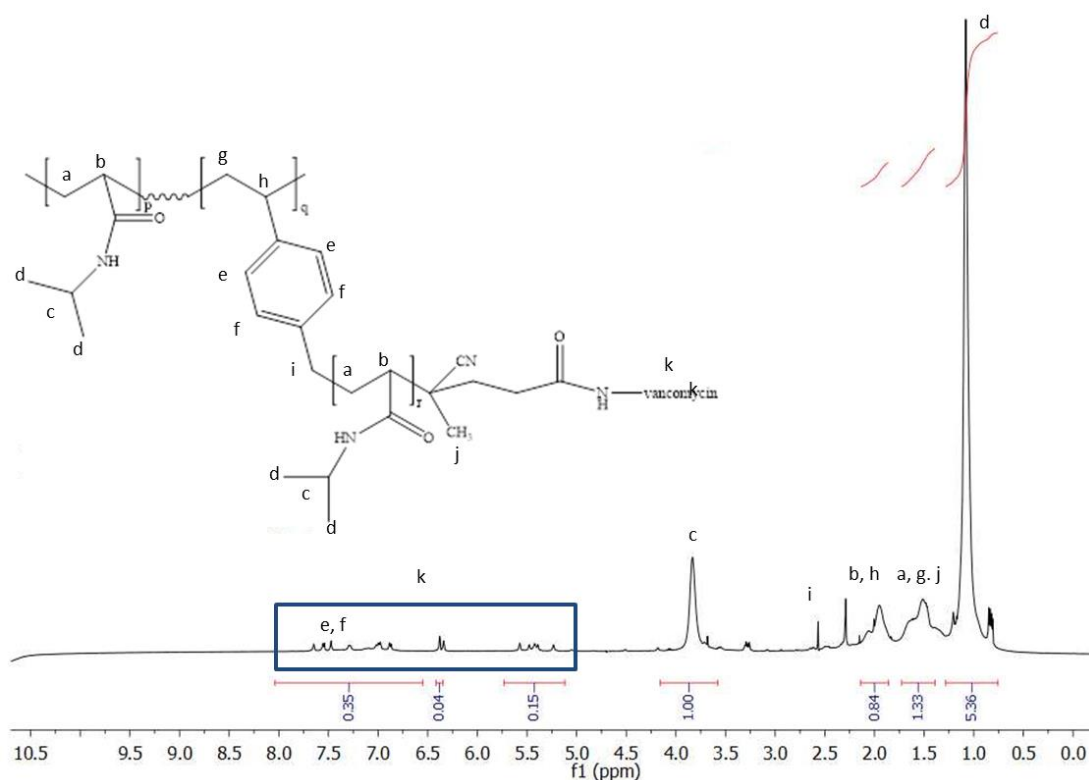


Figure 2.4 $^1\text{H NMR}$ spectrum of HB-PNIPAM-van in D_2O

2.2.5 Synthesis of linear poly (*N*-isopropylacrylamide)-co-vinylbenzoic acid (L-PNIPAM)

The linear analogue of the carboxylic acid terminated poly (*N*-isopropylacrylamide) was synthesised by copolymerising NIPAM with vinyl benzoic acid (VBA) using 4, 4-azobis (4-cyanovaleric acid) as initiator. Recrystallised NIPAM (5g, 44mmol) and VBA (0.249g, 1.7mmol) were dissolved in dioxane (25cm³). AVCA also was dissolved in dioxane (5cm³) and added into the mixture. The solution was transferred to a glass ampoule and four cycles of freeze-pump thaw were carried out. Following the degas step, the ampoule was sealed and the reaction was conducted at 60°C. To obtain a solid polymer (L-PNIPAM), it was precipitated in diethyl ether three times and dried at room temperature in a vacuum oven overnight. In order to obtain the same amount of vancomycin groups along the main chains as the highly branched polymers, modification of carboxylic chain ends was achieved using *N*-hydroxysuccinimide (NHS) and *N,N*-dicyclohexylcarbodiimide (DCC) in the same way as for the HB-PNIPAM method (% yield = 92%).

L-P(NIPAM-co-VBA):

¹H NMR (400 MHz, DMSO) (ppm): d 0.9-1.1 (6H, s, -N(CH₃)₂), d 1.3-1.7 (2H, m, -CH₂-CH-Ar-), d 1.8-2.2 (2H, m, -CH₂-CH-CO-NH- and 1H, m, CH₂-CH-COONH-), d 3.9 (1H, s, (CH₃)₂CH-), d 6.6-7.6 (br m, -Ar-), d 12.2 (br m COOH).

FTIR: 3300 cm⁻¹ (O-H), 1710 cm⁻¹ (sp² carboxylic acid C=O), 1630 cm⁻¹ (sp² amide C=O), 1570 cm⁻¹ (sp² benzene C=C), 1500 cm⁻¹ (sp³ C-C)

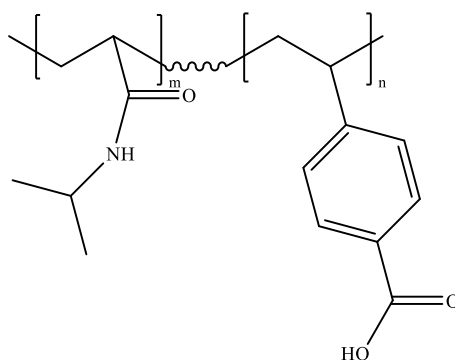


Figure 2.5 The chemical structure of L-P(NIPAM-co-VBA)

2.2.6 Synthesis of linear poly (*N*-isopropylacrylamide)-co-vinylbenzoic acid functionalised with vancomycin (L-PNIPAM-van)

L-PNIPAM (1g) was dissolved in DMF (10cm³). N-hydroxysuccinimide (NHS) (0.1636g, 1.4mmol) and *N,N*-dicyclohexylcarbodiimide (DCC) (0.2930g, 1.4mmol) was dissolved in DMF (5cm³) and added to the L-PNIPAM solution. The mixture was stirred under nitrogen atmosphere overnight. Following the reaction, DMF was removed by rotary-evaporation and the product was precipitated in diethyl ether. L-PNIPAM-succinimide was purified by ultrafiltration over three times (1 hour) in a mixture of acetone and ethanol (9:1). Then, the solvent was removed by rotary evaporation and the polymer dried under vacuum at room temperature.

L-PNIPAM-succinimide (100mg) was dissolved in deionised water (5cm³) over ice. Vancomycin hydrochloride hydrate (30mg, 0.02mmol) was dissolved in deionised water (2cm³) and added into the polymer solution. Phosphate buffer pH 8.5 (2ml) also was added. The pH of the mixture was adjusted with sodium hydroxide (0.1M) to obtain a final pH of 9.5. The solution was stirred over ice for 24 hours. Following the reaction, the L-PNIPAM functionalised with vancomycin was purified by ultrafiltration with deionised water (200cm³) three times and freeze-dried to obtain the final solid polymer. The L-PNIPAM-van was stored at -20°C, (% yield = 70.8 %).

L-PNIPAM-van:

¹H NMR (500 MHz, D₂O) (ppm): d 0.9-1.1 (6H, s, -N(CH₃)₂), d 1.3-1.7 (2H, m, -CH₂-CH-Ar-), d 1.8-2.2 (2H, m, -CH₂-CH-CO-NH- and 1H, m, CH₂-CH-COONH-), d 3.9 (1H, s, (CH₃)₂CH-), d 6.5-7.6 (m, -Ar-).

FTIR: 3300-3500 cm⁻¹ (phenol O-H), 3200 cm⁻¹(sp² aromatic C-H), 1630 cm⁻¹ (sp² amide C=O), 1570 cm⁻¹ (sp² benzene C=C), 1500 cm⁻¹ (sp³ C-C)

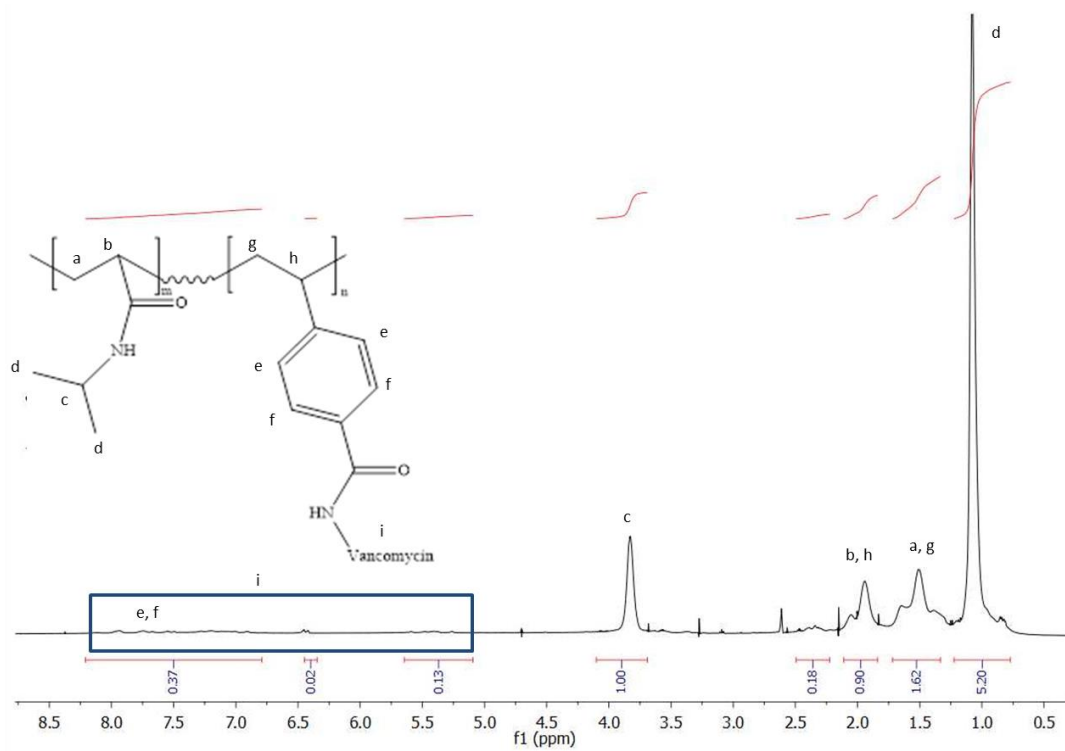


Figure 2.6 $^1\text{H NMR}$ spectrum of L-PNIPAM-van in D_2O

2.3 Polymer characterisation

2.3.1 ^1H NMR spectroscopy

All ^1H NMR spectra were measured and recorded on Bruker AC250 and AC500 which were operated at 250MHz and 500MHz with CDCl_3 , DMSO, D_2O as the solvent at 20mg/ml concentration.

2.3.2 Fourier Transform Infrared Ramen spectroscopy (FTIR)

FT-IR measurements were carried out on a Thermo Scientific Nicolet iS10 FT-IR Spectrometer. Solid samples were dried in a vacuum oven overnight before use.

2.3.3 Size Exclusion Chromatography (SEC)

The average molecular weight (M_n) of polymers was determined by SEC with methanol as eluent. Samples were prepared in pre-filtered methanol at 1mg/ml and injected through two Agilent PolarGel columns at a rate of 1ml/min, maintained at a constant 30°C. They were analysed via comparison to a universal calibration using PNIPAM standards via Agilent Refractive Index and Viscometric (Agilent 1260 Infinity detector Suite) detectors to give absolute molecular weight averages (M_n , M_w/M_n and two forms of dispersity (\mathcal{D}) M_w/M_n and M_z/M_w).

2.3.4 Determination of LCST

Micro Differential Scanning Calorimetry (MicroDSC) was conducted using a VP-DSC microcalorimeter. The transition temperature (LCST) of polymer preparations was defined as the temperature corresponding to the peak of the thermogram. The samples were prepared in deionised water at 1mg/cm³, degassed using ThermoVac. The LCST was determined over a range of temperatures from 10-40°C at a heating rate of 0.5°C/min. The vancomycin-modified polymer concentration was 10mg/cm³. Turbimetry was used to measure the cloud point of polymers with a Cary 300 bio UV-Visible spectrophotometer. The cloud point was determined at 550nm over a range of temperatures from 10-70°C. For this the samples were prepared in deionised water at a concentration of 1mg/ml and a heating rate of 1°C/min. The onset temperature was defined as the first stage of onset of turbidity. In the case of vancomycin-derivatised polymers, the concentration was 10mg/cm³.

2.3.5 Zeta potential measurements

Zeta potentials were measured on a Brookhaven Instruments Corporation ZetaPALS Zeta potential analyser. Samples were prepared at 0.1% w/v concentration (1mg/ml) in ultrapure H₂O. 15µl of sample was added to 1485µl of 1mmol KCl solution. Measurements were carried out at 25°C in triplicate for each polymer in 5 cycles.

2.3.6 Particle sizing analysis

Particle size analysis was carried out on a Brookhaven Instrument Corporation ZetaPALS 90Plus. Samples were prepared at 0.1% w/v concentration (1mg/ml) in ultrapure H₂O. 30µl of sample was added to 2970µl of 1mmol KCl solution. Measurements were carried out at 25°C in triplicate for each sample in 5 cycles.

2.4 Results and discussion

HB-PNIPAM-van was synthesised via SVCP-RAFT polymerisation, with a 25:1 ratio of NIPAM to RAFT monomer, which is 4-vinylbenzyl-1-pyrrole carbodithioate containing alkene functionality. The styryl group of RAFT monomer provides a branching point while the pyrrole groups located at the polymer chain end facilitates further chain end functionalisation. Highly branched polymer with pyrrole end groups can be achieved thanks to the dual action of the RAFT monomer because copolymerisation can occur via the dithioate group and the styryl double bond of RAFT monomer. The pyrrole end groups were then converted to carboxylic acids by radical addition-fragmentation-coupling with radicals obtained from ACVA. This was then modified with vancomycin to achieve binding to Gram-positive bacteria through the surface uncrosslinked D-Ala-D-Ala groups in the peptidoglycan. The synthesis pathway of HB-PNIPAM-van followed the previously report route (Figure 2.7).

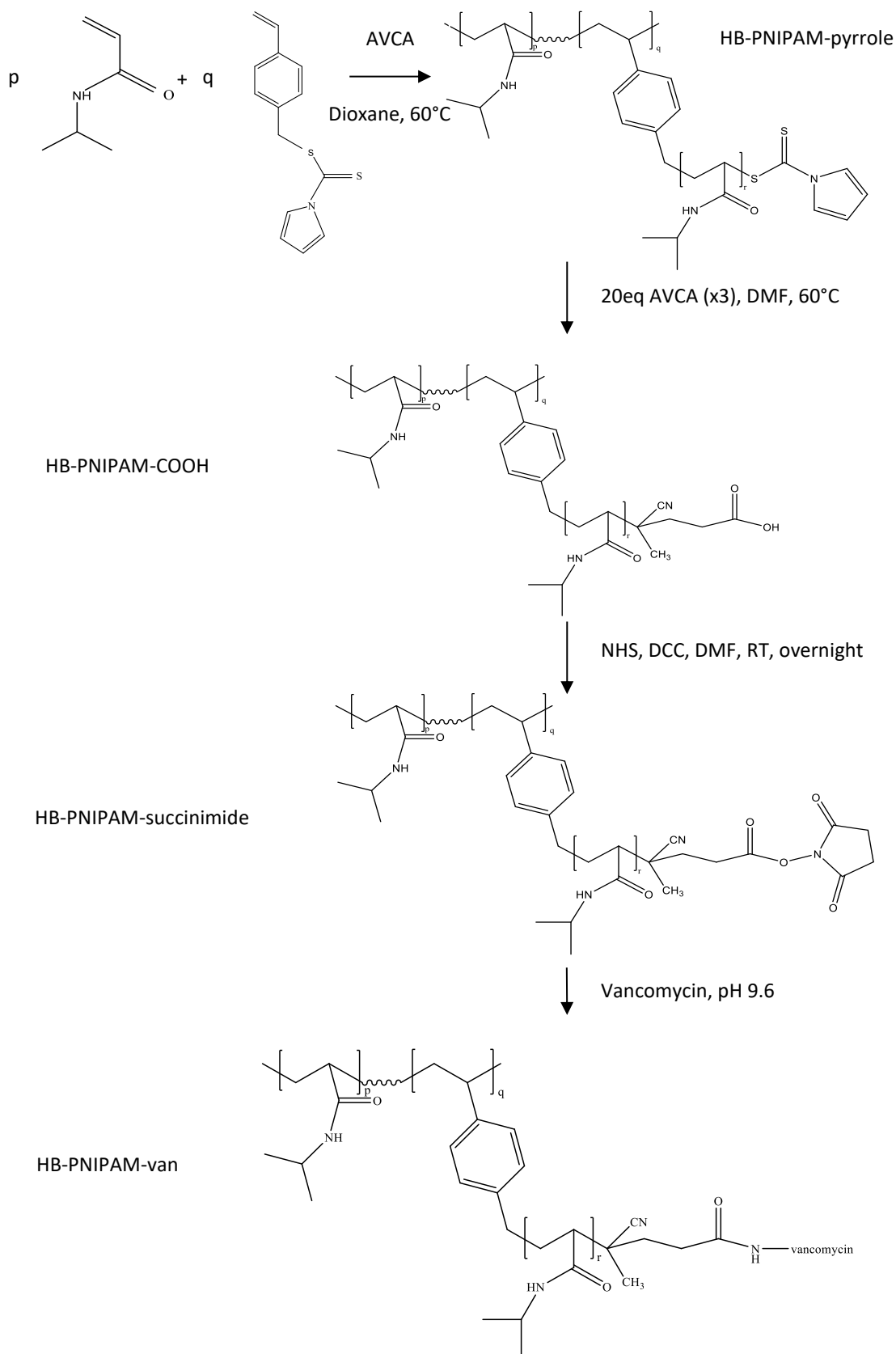


Figure 2.7 Schematic diagram showing synthesis of HB-PNIPAM-van

The first step of the L-PNIPAM-van synthesis was copolymerisation of NIPAM and VBA to form a statistical copolymer and so that the polymer contains the same fraction of repeating units of aryl groups as the HB-PNIPAM. The carboxylic acid groups were activated using dicyclohexyl carbodiimide (DCC) to provide the NHS ester, which was then reacted with vancomycin. The synthetic pathway to L-PNIPAM-van is shown in Figure 2.8

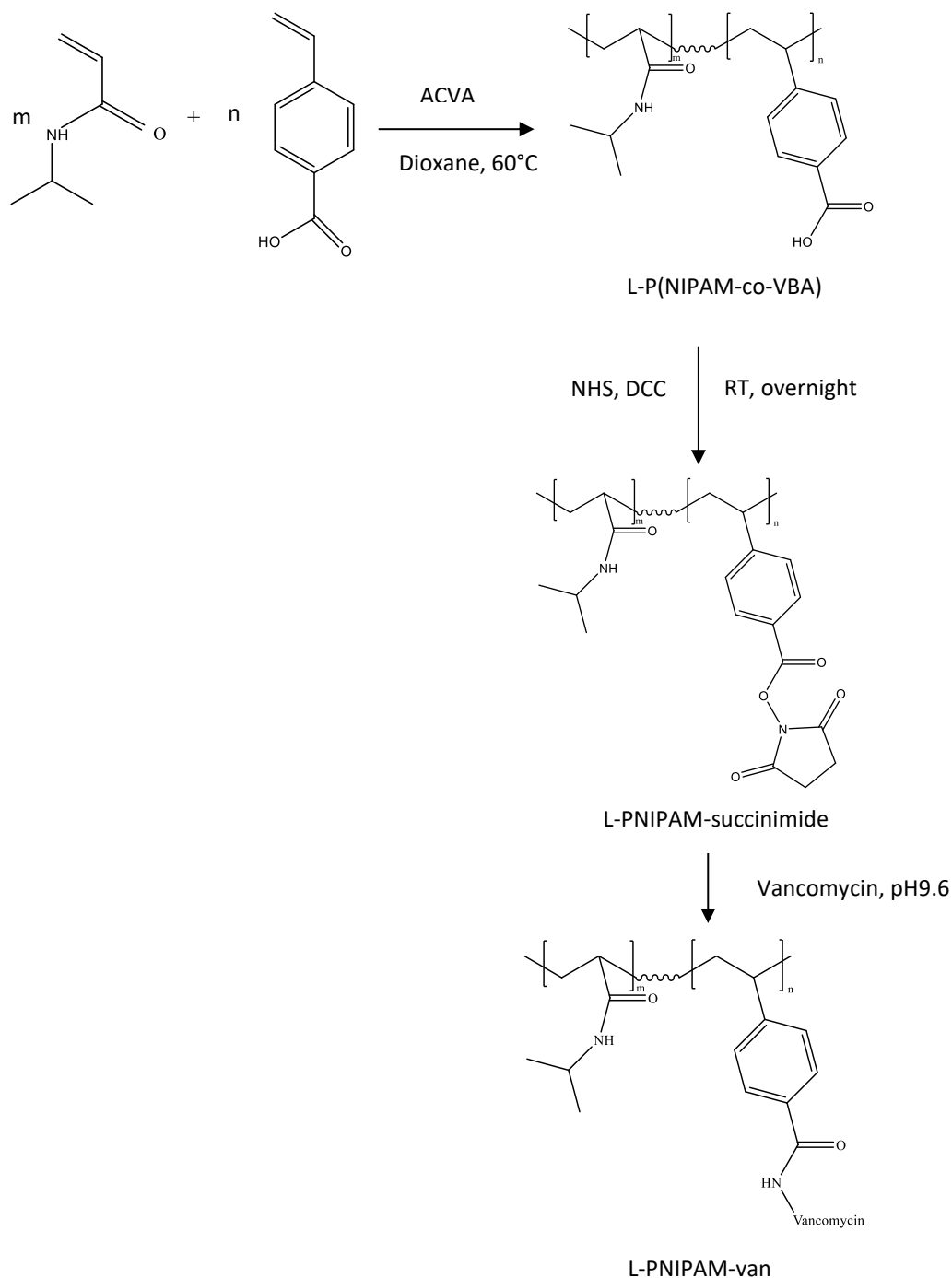


Figure 2.8 Schematic diagram showing synthesis of L-PNIPAM-van

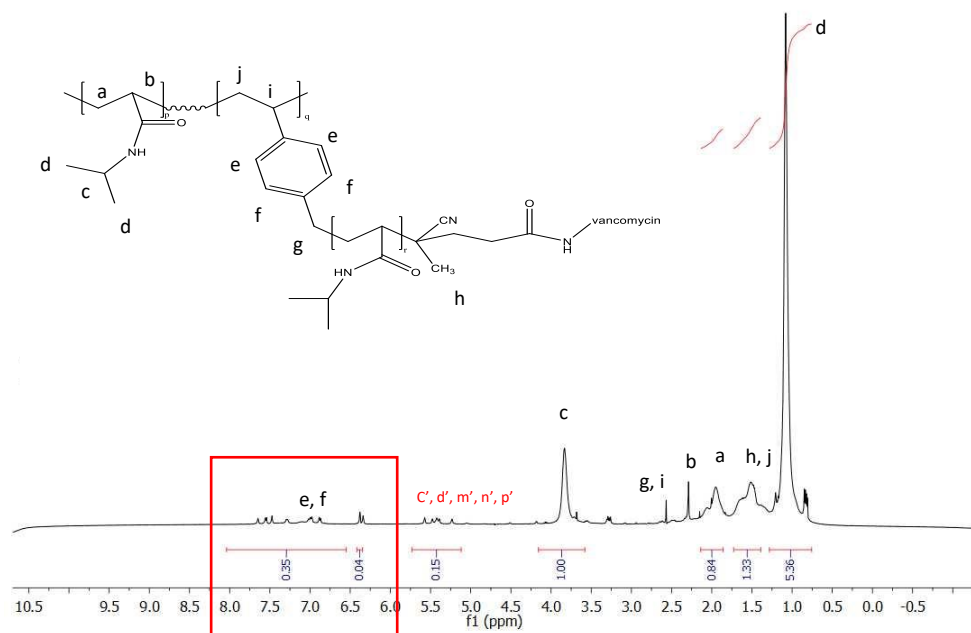
Highly branched polymers can often be prepared in a one-pot reaction using a variety of synthetic methods. SCVP is one of the versatile techniques because vinyl monomers can be used and polymerised by various techniques depending on types of initiating groups [115]. In this work, we synthesised HB-PNIPAM via SCVP-RAFT polymerisation and L-PNIPAM via free radical polymerisation with an equal amount of vancomycin using VBA as a comonomer. SCVP-RAFT polymerisation is a promising technique, having been used to prepare highly branched polymers with controlled branching point and functionalised end groups and resulting in unique properties thanks to the controlled nature of RAFT polymerisation [115, 146]. An advantage of the RAFT technique is that chain end modification/or removal can be achieved due to functional group tolerance of the RAFT monomer. In this work, pyrrole end groups were removed by using an excess amount of ACVA ($\geq 20:1$ molar ratio of ACVA to PNIPAM) called radical addition-fragmentation-coupling resulting in carboxylic acid end groups. This technique involves heating 60-90°C a solution of the polymer with large excess of azo-initiator [98, 147]. NHS/DCC carbodiimide chemistry was used to produce active sites for the attachment of vancomycin. DCC is used to activate carboxylic acid groups by forming highly reactive activated acid intermediate and NHS is used to improve efficiency of acid intermediate for conjugating to primary amine on vancomycin to yield stable product. Both types of polymers were analysed by ^1H NMR to investigate functional modification of pyrrole, carboxylic acids, and vancomycin [16, 137].

2.4.1 Nuclear Magnetic Resonance (NMR)

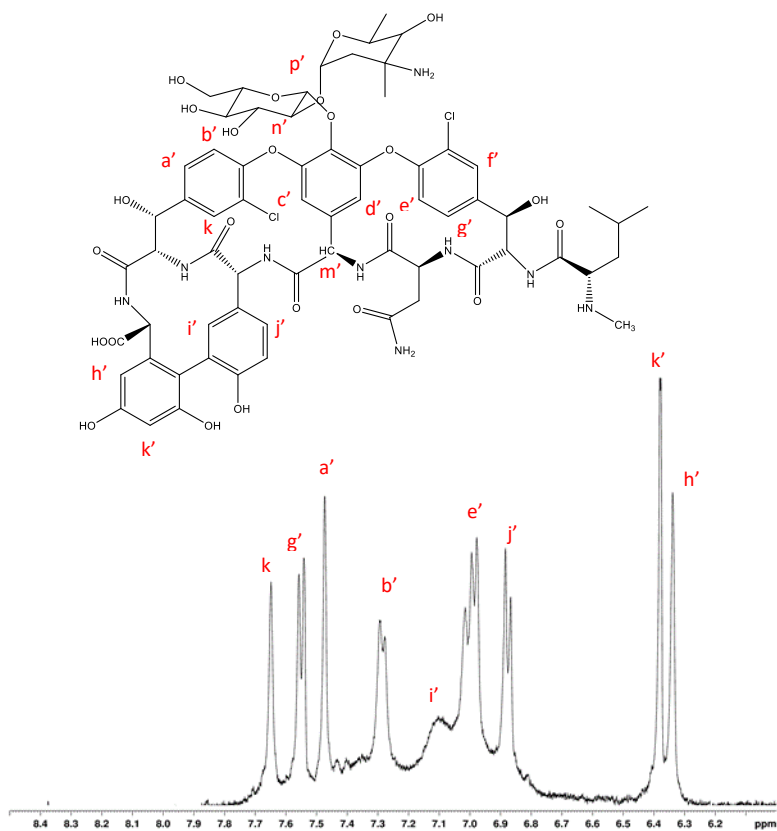
NMR is a well-known technique for calculating functionalities, measurement of polymerisation conversion and degree of branching. Integration of ^1H NMR spectra was used to determine the average molar ratios of comonomers incorporated into the polymers by comparing the integrals of the PNIPAM methylene peak against the benzyl peak of comonomers. The actual ratios of RAFT agent to NIPAMs in the HB-PNIPAM were 0.04, which were similar to the monomer feed ratio. The presence of pyrrole groups was demonstrated by the pyrrole CH resonances at $\delta 6.4$ and $\delta 7.7$ ppm in ^1H NMR spectra, as shown in Fig 2.2. The %pyrrole functionality of HB-PNIPAM was 59.3%, which was calculated from ^1H NMR spectra and the calculation was followed from previous work by Plenderleith et al [137], as shown in appendix 1. Then, the pyrrole end groups were converted to carboxylic acid ends. The chain end modification was confirmed by the decrease in the CH resonances at $\delta 6.4$ ppm and the presence of broad carboxylic acid region around 12-13 ppm, as shown in Fig 2.3. Elemental analysis was also used since the polymers should not contain

sulphur. The degrees of branching (DB), which is number of branch points per number of NIPAM monomer, were also calculated from ^1H NMR spectra and the calculation is shown in appendix 1. DB of HB-PNIPAM was 0.06. For a statistical linear random copolymer, ^1H NMR (Fig 2.4) showed that the actual ratios of benzyls groups to NIPAMs in L-P(NIPAM-co-VBA) were similar to the molar feed ratios. Integration of ^1H NMR spectra was also used to estimate the percentage vancomycin functionality incorporated into the polymers by a rise of the peak at 5.2-5.6ppm (1H integrals per vancomycin) compared to the isopropyl peak (1H integrals per backbone unit) from ^1H NMR of purified products in D_2O . Figure 2.3 shows the spectra of (A) HB-PNIPAM-van and (C) L-PNIPAM-van. To more clearly show the chemical shifts of aromatic hydrogen from vancomycin, expanded regions are shown of the spectrum traces in Fig 2.3 of (B) HB-PNIPAM-van; of (D) L-PNIPAM-van both at δ 6-8ppm. As can be seen, the ^1H NMR spectra of both polymers included the usual resonance for PNIPAM along with the resonances ascribable to the aryl groups and vancomycin. The signals from the hydrogen atoms of the benzene rings in the vancomycin and styryl comonomer were observed in both HB-PNIPAM-van and L-PNIPAM-van at δ 6-8 ppm. However, calculation for functionality of the polymers with vancomycin ends by this approach could be limited because the hydrogen from vancomycin functional unit are broad and overlaps the benzyl peak. For this reason, an alternative technique was developed which is shown in section 2.4.6.

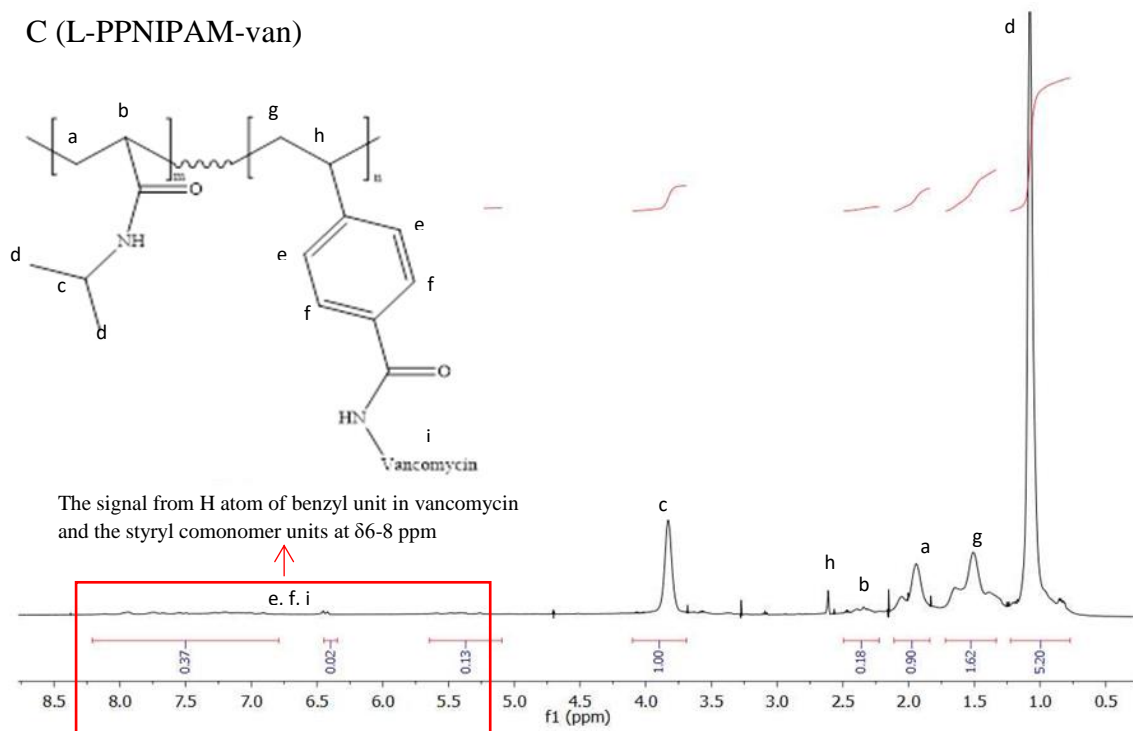
A (HB-PPNIPAM-van)



B (HB-PPNIPAM-van) ($\delta=6.4-8.0$)



C (L-PNIPAM-van)



D Expanded ^1H NMR of (D1) HB-PNIPAM-van and (D2) L-PNIPAM-van

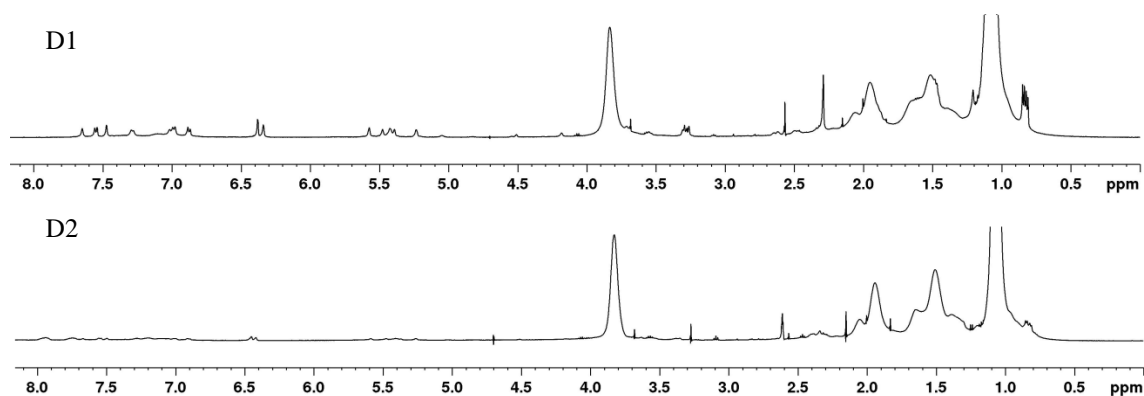


Figure 2.9 Examples of ^1H NMR of (A) HB-PNIPAM-van and (C) L-PNIPAM-van in D_2O and (B) magnified region from 6-8.5ppm and (D) Expanded ^1H NMR of (D1) HB-PNIPAM-van and (D2) L-PNIPAM-van

Table 2.1 Ratio of benzyl groups: NIPAMs and % vancomycin from ¹HNMR

Polymer	Conversion ^a (%)	B-ratio ^b	Van loading ^c (%)
L-PNIPAM-van	96	0.043	2.6
HB-PNIPAM-van	92	0.040	3

^a Percentage conversion based on ¹HNMR

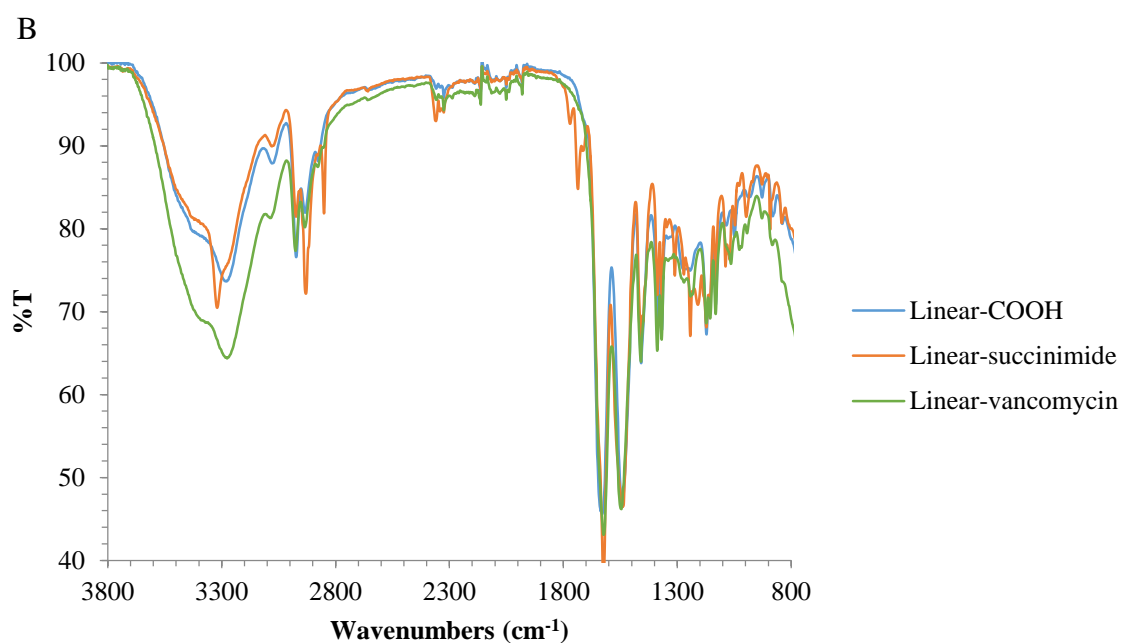
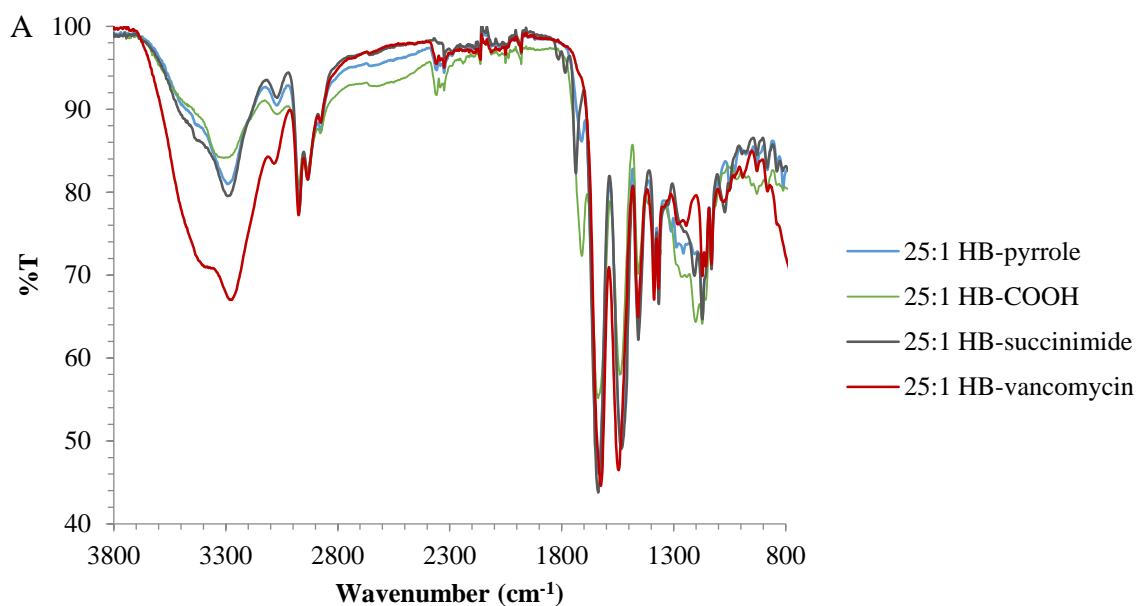
^b Ratio of benzyl groups: NIPAMs calculated from ¹HNMR of purified products, by comparing the integrals of benzyl group at 7.0-7.2ppm to the integrals of the isopropyl NIPAM at 4.0 ppm

^c Percentage vancomycin functionality estimated by rise of peak at 5.2-5.6ppm (1H integrals per vancomycin) compared to the isopropyl peak (1H integrals per backbone unit) from ¹HNMR of purified products in D₂O

¹HNMR is considered to be a useful technique for analysing the chain end structures of polymers and estimating their M_n. However, this technique is restricted by the requirement that the end group signals do not overlap with polymer signals. Thus, analysis of vancomycin functionality and estimation of M_n by ¹HNMR of the polymers in this work could be limited because the signals of benzyl group at the polymer backbone overlap the pyrrole peak and also vancomycin unit at 7.0-8.0 ppm. Therefore, in this work, to monitor chain end modification and obtain reliable estimation of vancomycin functionality, FTIR and an ELISA were utilised respectively to compare the polymers. Also, the average molar mass was determined by SEC instead.

2.4.2 Fourier Transform Infrared Raman spectroscopy (FTIR)

FTIR is a useful analytical technique which is simple and widely used for identification of functional groups. Also it is suited to qualitative analysis of both the starting materials and final products. Modification of chain ends and pendant functionalities to HB-PNIPAM-van and L-PNIPAM-van were observed via infrared spectroscopy as shown in figure 2.10.



C

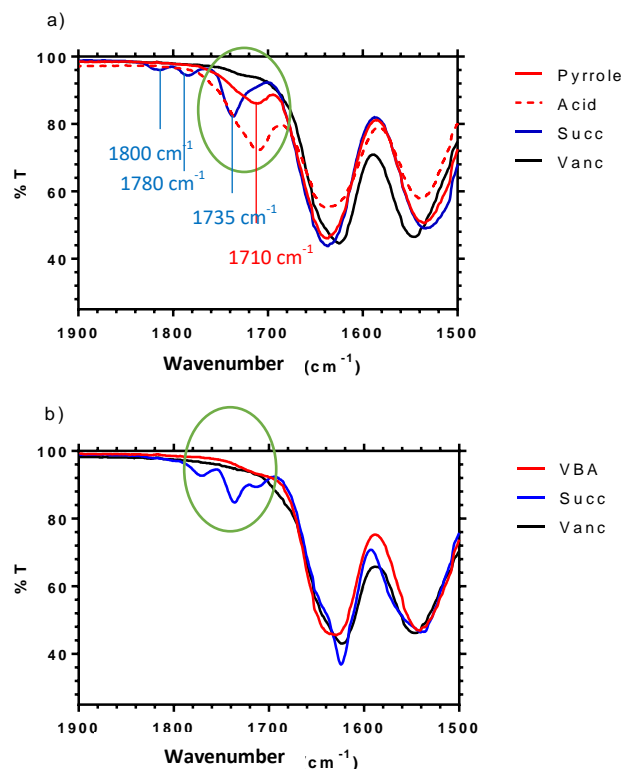


Figure 2.10 FTIR spectra of (A) HB-PNIPAM and (B) linear PNIPAM (1500-1900cm⁻¹) during chain end modifications (original = red, acid modified = dashed red, succinimide modified = blue, vancomycin modified = black).

The chain end modifications of HB-PNIPAM-pyrrole to HB-PNIPAM-van and L-PNIPAM to L-PNIPAM-van were investigated via infrared spectroscopy. The FTIR spectra of HB-PNIPAM-pyrrole showed C-C stretching of pyrrole at 1540cm⁻¹, then when pyrrole ends were converted to carboxylic acids the presence of carboxylic C=O stretch shows the peak at 1710cm⁻¹. Eventually, this peak disappeared after the NHS/DCC carbodiimide reaction. A new peak of C=O antisymmetric and symmetric stretch and carbonyl (ester) stretch appeared at 1730, 1780 and 1800cm⁻¹ respectively when carboxylic acids end groups were converted. The FTIR spectra of the final product, HB-PNIPAM-van, shows that all these peaks were diminished when vancomycin was attached. The full spectra also show the large broad peak of phenolic (O-H) obtained from vancomycin at 3300cm⁻¹. The changes in the IR spectra of linear analogous polymer were similarly observed at all steps.

2.4.3 Size Exclusion Chromatography (SEC) analysis

Over the past few decades, the controlled radical polymerisation (CRP) technique has been employed to synthesise various types of complex polymer architectures, such as star polymers and highly branched polymers. SEC analysis is one of the techniques that provides the average molar masses and also dispersity (\bar{D}) and has the advantage that various detectors can be used, which in this case included UV absorption (295nm), reflective index (RI) and viscometry [148]. The signal is proportional to the amount of polymer sample eluting from the column and the time of elution is related to their hydrodynamic radius (R_H). Early applications of SEC used only a single detector, such as RI or UV to provide comparative molecular weight by reference to a calibration curve generated from a series of standard polymers of known molecular weight. However, the accuracy of this approach depends on the polymer composition and differences in chemical structure between the samples and the standards. A UV detector can assess the distribution of chromophores in the polymers but a RI detector measures the change in refractive index of any sample without regard to chromophores. It provides comparable information on the concentration of the analyte, which is considered an advantage over a UV detector. However, samples containing mixed components may display a wide range of refractive index some of which could be close to that of the solvent phase making them undetectable. Consequently, the use of a single detector has limitations and it is ideally employed as part of a multi-detection system, comprising a RI detector with a viscometer or light scattering detector. A viscometric detector provides a response due to the viscosity of the polymer solution compared to solvent alone and the molecular weight data can be obtained by reference to a universal calibration curve using the relationship shown in equation (1) [147]. The intrinsic viscosity $[\eta]$ of the polymer samples can also be used to derive the hydrodynamic radius (R_H) using the Stokes Einstein equation (3), which is sensitive to the type of solvent [149]. However, the analysis of amphiphilic polymers requires careful consideration in types of stationary and mobile phase to prevent adsorption. There are several kinds of common eluents used in SEC, such as dimethylformamide (DMF) and tetrahydrofuran (THF).

In order to choose the solvents used for analysing polymers by SEC, a range of factors have to be considered. The polymers used in this study contained different types of functionalities, namely pyrrole, carboxylic acid and vancomycin, for which a change in eluent might normally be needed. However, it was found that all types of polymers despite the different end groups were soluble in methanol. The use of methanol as the mobile phase for SEC was

rare but Swift et al. [150] recently described its use with and a new stationary phase, PolarGel. This product is marketed for use with polar solvents but an unexpected finding was that it was not susceptible to absorption. A series of linear PNIPAMs were prepared and analysed by SEC, with viscometric detection in THF to obtain absolute molar mass, and DOSY NMR in deuterated methanol to obtain intrinsic viscosities. Then, both values were used to calibrate a SEC-methanol system [150]. To analyse the samples in this work, the polymers were prepared in methanol at 1mg/ml concentration and analysed using refractive index (RI) and viscometric detectors. The molecular weight was obtained via a universal calibration curve, which is shown in figure 2.11. Excluded polymers passed through the columns with a retention time of 13.97 minutes, and toluene flow rate markers eluted at 33 minutes. Figure 2.12 shows the examples of molar mass distribution of L-PNIPAM-van and HB-PNIPAM-van by methanol SEC.

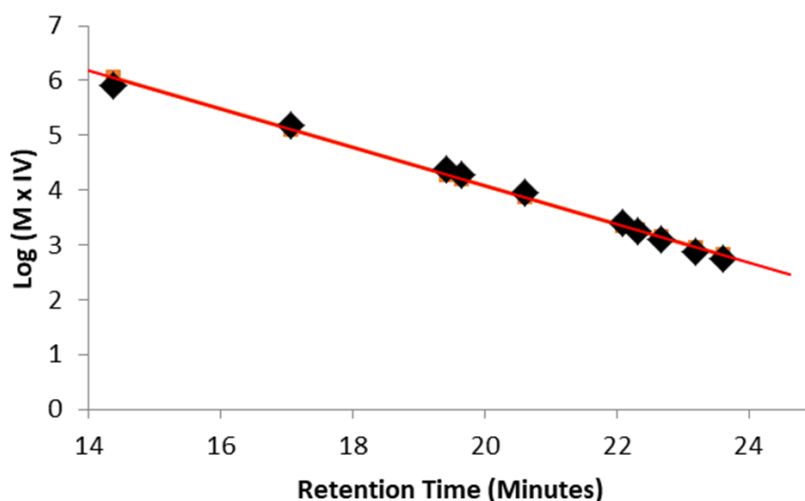


Figure 2.11 The universal calibration curve of methanol-SEC generated by retention time of series of PNIPAM standard polymer (provided by Dr T Swift and published in 2017; [150])

The universal calibration procedure uses the observation that SEC separates polymer by hydrodynamic volume (V_H) defined by the Flory-Fox equation.

$$\Phi[\eta]M = V_H$$

$[\eta]$ = intrinsic viscosity

M = molecular weight

Φ = a universal constant

For different polymers of the same V_H in the same solvent,

$$[\eta]_1 M_1 = [\eta]_2 M_2 \quad (1)$$

$[\eta]$ = intrinsic viscosity of standard polymers

M_1 = molar mass of standard polymers

$[\eta]$ = intrinsic viscosity of unknown

M_2 = molar mass of unknown

Thus, M_2 can be calculated by using $[\eta]M_1$ from calibration curve and $[\eta]_2$ from capillary viscometry or diffusion-ordered NMR spectroscopy (DOSY NMR) shown in equation (2).

$$M_2 = \frac{[\eta]_1 M_1}{[\eta]_2} \quad (2)$$

The intrinsic viscosity $[\eta]$ of the polymer samples can also be used to derive the hydrodynamic radius (R_H) or hydrodynamic volume (V_H) using the Stokes Einstein equation shown in equation (3).

$$R_H = \frac{k_B T}{6\pi\eta D} \quad (3)$$

K_B = Boltzmann constant

T = temperature

η = solution viscosity

D = diffusion coefficient

The calibration curve used in this work was provided by Dr. T Swift following a procedure designed to determine $[\eta]$ and M of specially prepared PNIPAM standard. According to Gaborieaa et al, the universal calibration procedure is valid for branched polymers [151].

Table 2.2 summarises the number-average molar mass (M_n), the weight-average molar mass (M_w), dispersity (\mathfrak{D}) and the Mark-Howink-Sakurada exponent α values of linear and highly branched polymer with different chain ends. The data include the normal dispersity variable $\mathfrak{D}_1 = M_w/M_n$. However, these non-Gaussian distributions are not well described by \mathfrak{D}_1 . Given the bimodal distribution we consider that the use of both \mathfrak{D}_1 and \mathfrak{D}_2 ($\mathfrak{D}_2 = M_z/M_w$) gives a fuller description. \mathfrak{D}_1 is affected by the lower molar mass tail, while \mathfrak{D}_2 shows the variation indicating the broadness of the higher molar mass component. As shown in Table 2.1, both

types of polymers were considered as high molecular weight which were greater than 10^5 g/mol. Changes in $\mathcal{D}_{(w/n)}$ were found during the different stages, which reflect some chain-chain coupling and the removal of low molar mass fraction during ultrafiltration.

Table 2.2 Molar mass and dispersity of the synthesised PNIPAMs from methanol SEC

Type of polymer	M_n (kgmol^{-1})	M_w (kgmol^{-1})	M_z (kgmol^{-1})	$\mathcal{D}_{(w/n)}$	$\mathcal{D}_{(z/w)}$	α
HB-PNIPAM-pyrrole	550	3,020	5,990	5.4	1.98	0.26
HB-PNIPAM-COOH	226	3,900	7,400	17.4	1.87	0.23
HB-PNIPAM-van	2,000	6,970	10,550	3.48	1.52	0.31
L-PNIPAM-co-VBA	555	661	730	1.19	1.10	0.68
L-PNIPAM-van	640	850	990	1.33	1.16	0.51

M_n = the number-average molar mass; M_w = weight-average molar mass, M_z = z-average molar mass, \mathcal{D} = dispersity

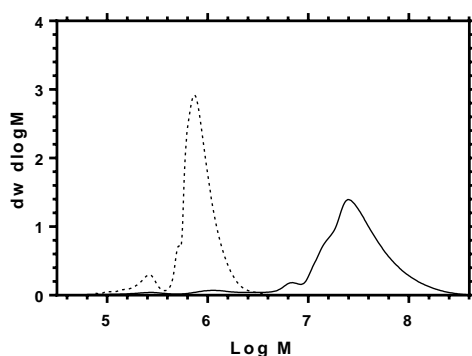


Figure 2.12 Molar mass distributions of HB-PNIPAM-van (—) and L-PNIPAM-van (--) from determined by methanol SEC

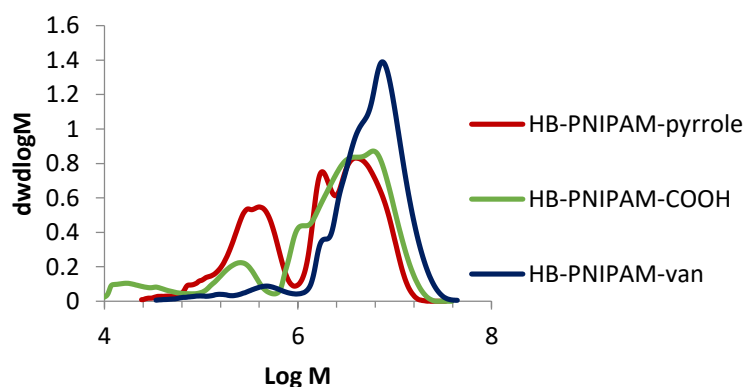


Figure 2.13 Molar mass distributions of HB-PNIPAM with different type of chain ends

Figure 2.13 shows that the low molar mass fraction (10^5 - 10^6) was eliminated during chain end modification from pyrrole to vancomycin due to the use of ultrafiltration to remove the lower molecular weight fraction in the purification process leading to the changes in $\mathfrak{D}_{(w/n)}$ because $\mathfrak{D}_{(w/n)}$ is affected by the lower molar mass tail, while $\mathfrak{D}_{(z/w)}$ shows the variation indicating the broadness of the higher molar mass component [150].

SEC analysis also provided the exponent α value calculated by Mark-Houwink-Sakurada (MHS) equation, shown in Equation 4.

$$[\eta] = KM^\alpha \quad (4)$$

$[\eta]$ = intrinsic viscosity

K and α = constants for polymer/solvent pair

M = molecular weight

Intrinsic viscosity $[\eta]$ is a useful property in characterising polymers in dilute solutions and recently it has received considerable attention for determining the topological structure of polymers and the molecular weight, especially of highly branched polymers. The $[\eta]$ is defined by

$$[\eta] = \lim_{\phi \rightarrow 0} \frac{(\eta - \eta_0)}{\eta_0 \phi}$$

η = viscosity of solution

η_0 = viscosity of solute alone

ϕ = volume fraction of the solute in solution

The $[\eta]$ is the ratio of a specific viscosity to the concentration of the polymer extrapolated zero concentration. It is related to molar mass by MHS equation (4).

$$[\eta] = KM^\alpha \quad (4)$$

$$\ln[\eta] = \ln k + \alpha \ln M \quad (5)$$

The α is a parameter that defines the effect of molar mass on the intrinsic viscosity and relates to the space occupied by the polymer coils. It can be obtained from a MHS plot from equation (5) and used to describe the conformation of the polymers. A large α value results from large effects of molar mass on $[\eta]$. Generally, linear polymers tend to have $0.5 > \alpha > 1$

with polymer/solution and the lower limit for α is 0.5 in a theta solvent (a solution in a state of incipient precipitation) and 1 in good solvents. On the other hand, for more compact structures, such as branched polymers, the molar mass affects $[\eta]$ to a lesser degree and α is lower than 0.5 because as concentration of HB polymers increases; their viscosity increases less than linear version [152]. From Table 2.1, the architecture of the highly branched polymer can be indicated by the low value of α , which is 0.31, while α of L-PNIPAM-van was 0.51. Lu et al. revealed that α of a linear polymer follows the Mark-Houwink-Sakarada equation relationship. They found that the exponent α of highly branched polymers reduced with decreasing in molecular weight, which is consistent with a reduction in the intrinsic viscosity $[\eta]$. However, at the same molecular weight, an increase in degree of branching also led to a decrease in the intrinsic viscosity originating from increased degree of branching [152]. Generally, for a linear polymer the lower limit for α is 0.5 in a Theta solvent but branched polymers attain lower α [150].

Reporting the size of polymers is also as important as the molar mass distributions for several applications such as biomedical applications especially for a study of antimicrobial activity of materials. Therefore, hydrodynamic radii of the vancomycin functionalised polymers are characterised. The number average R_H (R_{Hn}) can be also obtained from methanol SEC using equation (6) and (7).

$$[\eta] = \frac{2.5NV_H}{M} \quad (6)$$

$$V_H = \frac{4}{3}\pi R_H^3 \quad (7)$$

Distributions of R_H of HB-PNIPAM-van and L-PNIPAM-van in figure 2.14 shows that HB-PNIPAM-van, although it has a much higher molar mass, exhibit similar distributions of R_H to the linear polymer.

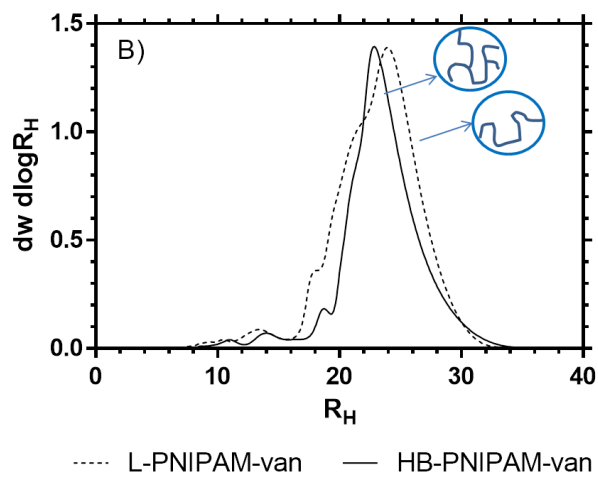


Figure 2.14 Hydrodynamic radii distributions of L-PNIPAM-van (--) and HB-PNIPAM-van (—) determined by methanol SEC.

2.4.4 Low critical solution temperature and cloud point of the polymers

The phase transition temperature (LCST) of a polymer is a crucial key characteristic of interest, because the temperature used for further applications, such as response to a stimulus, directly affects the polymer's behaviour [153, 154]. In this work, HB-PNIPAM and L-PNIPAM with vancomycin end groups were synthesised and their properties compared in terms of interaction with bacteria. Thus, the influence of end group modification of highly branched and linear analogue polymers on their properties, especially LCST, was investigated. It is well-known the change in hydrophobicity and shape of the PNIPAM polymer results in a change in the phase transition behaviour of the polymers [137, 153]. PNIPAM is an amphiphilic polymer which is soluble in water below the critical temperature and turns insoluble when its temperature rises above its LCST, resulting in phase separation which is driven by hydrophobic interactions and hydrogen bonding interactions between polymer chains [155-157].

There are several parameters that play a significant role in the phase behaviour of PNIPAM in aqueous solutions, which have brought about extensive studies and controversial discussion relating to the structure of the polymer, end group functionalities, the ionic kosmotropes of solute and types of comonomers [17, 105, 154, 158-162]. Previous studies showed that various polymer architectures, such as block copolymers, graft copolymers and dendrimers, directly affect the critical solution behaviour [98]. Li et al. also found that the LCST of poly(*N*-(4-vinylbenzyl)-*N,N*-diethylamine) (PEVA) could be increased by copolymerising with PNIPAM. Also, various morphologies of such a copolymer could be obtained by adjusting the mixture of solvents. However, in this study, only polymer structures and types of chain end functionalities will be demonstrated [154].

There are several steps in the chain end modifications carried out in this work to obtain highly branched and linear polymers with vancomycin end group, e.g. from pyrrole group to carboxylic acid and vancomycin chain ends. Therefore, it is interesting to investigate the effect of different types of polymer chain ends and polymer architecture on the phase transition temperature of the polymers in aqueous solution so that both polymer properties can be compared and made further use of.

2.4.4.1 LCST and aggregation behaviour of L-PNIPAM and HB-PNIPAM polymers with different chain ends.

In this research, two techniques were used for determining the phase transition temperature of polymers, namely microDSC and turbidimetry. Firstly, the LCST of the polymers were determined by microDSC and are shown in Table 2.3. The LCST is given as the temperature corresponding to peak maxima on heating, which can be seen in Figure 2.15.

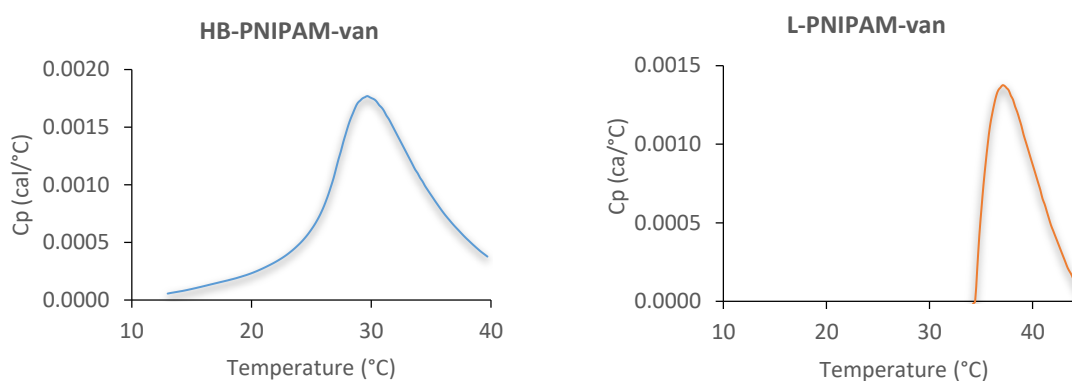


Figure 2.15 Example endothermic curves of HB-PNIPAM-van and L-PNIPAM-van from microDSC

Table 2.3: LCST of HB-PNIPAM and L-PNIPAM analogues with different end groups, determined by microDSC and example of thermogram obtained from microDSC

Types of polymers	LCST (°C) measured by microDSC
HB-PNIPAM-pyrrole	18
HB-PNIPAM-COOH	22
HB-PNIPAM-van	31
L-P(NIPAM-co-VBA)	33
L-PNIPAM-van	37

As shown in Table 2.3, the LCST for pyrrole terminated highly branched polymers was 18°C. This value increased to 22°C when the chain ends were modified to carboxylic acid. When vancomycin was attached it was 31°C, indicating the increased hydrophilic nature of polymer. The linear analogous has an LCST of 33°C which increased to 36°C when vancomycin was attached. In the case of the highly branched polymer, there was a significant increase in LCST when the polymer chain ends were modified from pyrrole to carboxylic

acid and vancomycin. This could be explained by the increase in hydrophilicity of the polymers. The presence of hydrophobic aryl units and pyrrole groups decrease solvation of the polymer. However, these hydrophobic effects (due to pyrrole end groups and styryl branching units) were partially balanced by the presence of carboxylic acid groups after chain end modification. Chung et al. suggested that the effect of hydrophobic groups on the LCST of PNIPAM was particularly significant when such groups were situated at free chain termini. Thus, the LCST of HB-PNIPAM-pyrrole was much lower than typical PNIPAM, which is about 32°C [163].

However, the HB-PNIPAM-pyrrole is still able to dissolve in water at low temperatures because the ratio of amide groups originating from NIPAM to pyrrole, stemming from RAFT monomer, is 25:1 (mol/mol). Therefore, it was expected that the solubility of HB-PNIPAM-pyrrole resulted from hydrogen bonds between amide groups of NIPAM and water molecules. The LCST was increased from 18°C to 22°C when pyrrole chain ends were converted to carboxylic acid. This was due to the change in chain end functionality from hydrophobic to hydrophilic. It could be explained by the fact that in solution, there were more hydrogen bond interactions between HB-PNIPAM-COOH and water molecules compared with that in HB-PNIPAM-pyrrole, and this led to a rise in the LCST of the polymer.

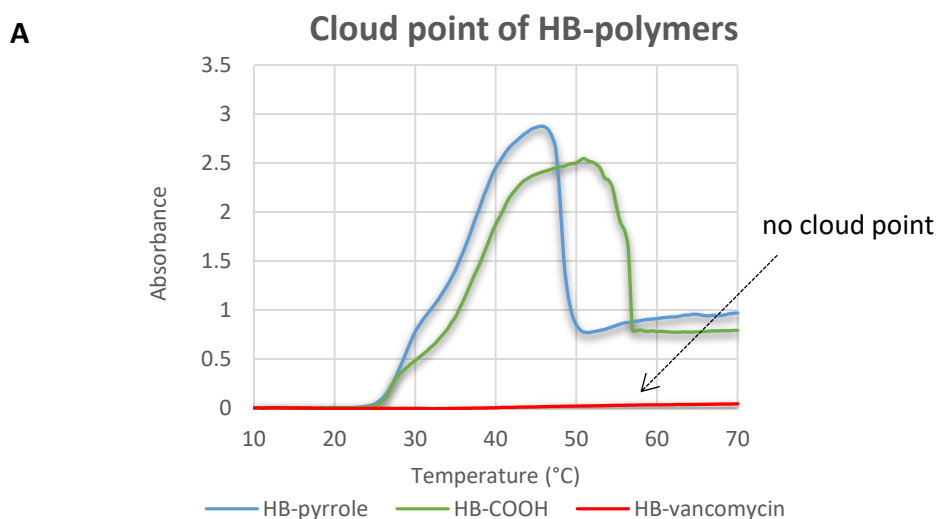
With HB-PNIPAM-van, there was also a significant increase in LCST from 22 to 31°C when the carboxylic acid end groups were modified to be vancomycin. Moreover, it was noticed that a thermogram of HB-PNIPAM-van determined by microDSC at the same concentration gave a very broad peak making the LCST difficult to determine and this was different from other types of polymers. The behaviour can be explained by the structure of the vancomycin molecule. Vancomycin consists of several amide linkages and one carboxyl group, which are all able to form hydrogen bonds with water molecules. Thus it was reasonable to expect that modification of HB-PNIPAM chain ends with vancomycin should raise the LCST of the polymer above that of the unmodified version [17]. Additionally, it was observed that it was easier for HB-PNIPAM-van to dissolve in water at room temperature compared with HB-PNIPAM-pyrrole and HB-PNIPAM-COOH. Nakayama and Okano suggested that terminal groups of thermo-responsive polymeric micelles synthesised from poly(*N*-isopropyl acrylamide-co-*N,N*-dimethyl acrylamide) (PID) and poly(benzyl methacrylate (PBzMA) affected the LCST of the polymer. The LCST of such a polymeric micelle was decreased when the chain ends were phenyl groups compared with hydroxylated PID/PBzMA [153]. Recently, work by our group showed that chain end modification using the arginine-glycine-

aspartic acid (RGD) peptide provided a stable colloid of sub-micron particles in solution above its LCST. RGD could stabilise aggregates of hyper branched polymers due to the high polar property of such a peptide [98].

From comparisons of three different types of functionalities – those of pyrrole, carboxylic and vancomycin end groups, used in this work – it is obvious that the pyrrole group has less hydrophilic properties than carboxylic acid and vancomycin, respectively. Therefore, it was reasonable that attachment of vancomycin to HB-PNIPAM could raise the LCST to be much higher than unmodified polymers.

MicroDSC is not the only method to determine the LCST of thermo-responsive polymers. The technique of turbidity measurement is another popular way to investigate phase transition temperatures of smart polymers. Generally, the turbidity technique is used for measuring cloud points based on UV-Vis spectrophotometer in the range of 200-800nm and at low polymer concentrations (0.5-1% w/v). The turbidity of a thermo-responsive polymer solution is caused by the presence of aggregates when the temperature of the polymer solution rises above its LCST, i.e. it appears cloudy. The cloud point determined by turbidimetry was defined as the onset temperature that corresponds to the absorbance value at which there is the first sign of opaqueness occurring [111].

In this study, the cloud points of all polymers were determined from absorbance at 550nm using a UV-Vis spectrometry with the range of temperature of 10-70°C. The temperature cycle (heating and cooling) was set in the temperature range at 1°C/min. The cloud points of HB and linear analogue versions are shown in Figure 2.16.



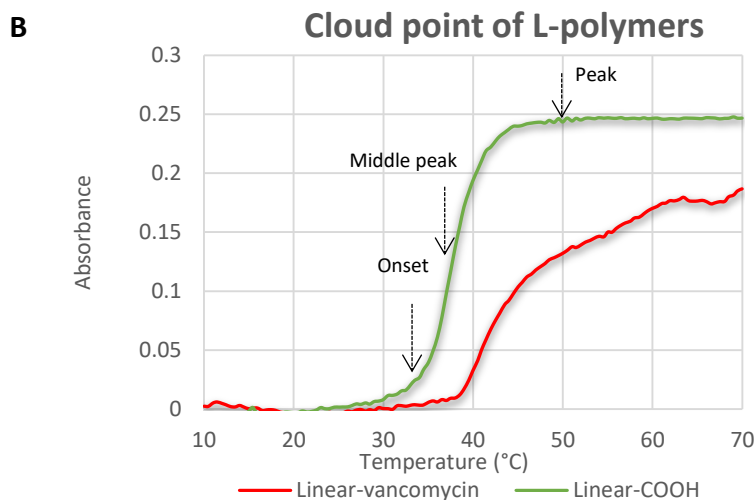


Figure 2.16 Cloud point of HB-PNIPAM (A) and linear analogue PNIPAM (B) with different chain ends measured by turbidimetry

Table 2.4: Summary of cloud points of various polymers measured by turbidimetry

Types of polymer	Onset	Middle peak	Peak
L-P(NIPAM-coVBA)	33	38	48
L-PNIPAM-vancomycin	37	46	62
HB-PNIPAM-pyrrole	25	35	46
HB-PNIPAM-COOH	27	38	50
HB-PNIPAM-vancomycin	None	None	None

As can be seen from Figure 2.16, L-P(NIPAM-co-VBA) provided a sharp peak of phase transition temperature that was similarly to ordinary PNIPAM and its LCST obviously increased when the vancomycin was attached as polarity of end groups was increased. In all cases the cloud points of the various polymers increased with functionalisation of the chain ends, but with the exception of the vancomycin HB-PNIPAM. In this case no cloud point could be determined even when the polymer concentration was increased to 15mg/ml. Moreover, the absorbance values of HB-PNIPAM-pyrrole and HB-PNIPAM-COOH solution did not remain stable, and decreased after a certain temperature. This is due to the polymer aggregates precipitating from solution and settling down to the bottom of the cuvette, so the solution becomes more transparent and the absorbance decreases.

As previously reported, turbidimetry could provide cloud points of HB-PNIPAM-pyrrole and HB-PNIPAM-COOH but a cloud point was not obtained when the vancomycin derivative of HB-PNIPAM was examined. Also, it was obvious that linear and highly branched polymers functionalised with vancomycin at the chain ends exhibited significantly different aggregation behaviours in solution upon heating, which can be seen in figure 2.17.

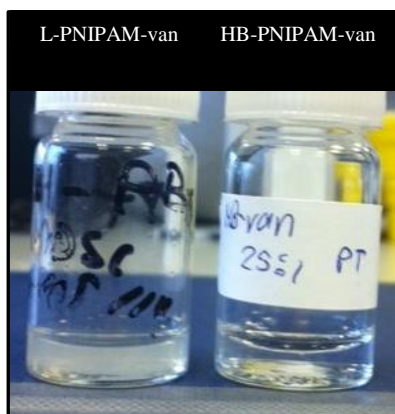


Figure 2.17 L-PNIPAM-van (left) and HB-PNIPAM-van (right) in deionised water at 37°C

Figure 2.17 shows the differences in phase transition behaviour between L-PNIPAM-van and HB-PNIPAM-van in deionised water above the LCSTs. The samples were prepared at 5mg/ml and incubated at 37°C for 30 minutes. It was found that the solution of L-PNIPAM-van turned cloudy due to the precipitation of the polymer, whereas there was no change in opacity of the HB-PNIPAM-van mixture at 37°C.

It is interesting that the calorimetry technique detected the LCST of all polymer types including HB-PNIPAM-van, whereas turbidimetry did not. While turbidimetry is a versatile technique that can be used for measuring the behaviour of thermo-responsive polymer solutions over a range of temperatures, microDSC provides the LCST from endothermic and exothermic transition peaks upon heating and cooling at the microscopic level and from our data is clearly the more appropriate method [111, 164, 165].

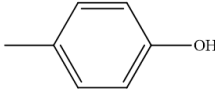
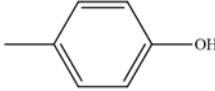
Calorimetry provides information on the heat released from the dehydration process between water molecules and the polymers. Endothermic peaks obtained from the thermogram describe coil-to-globule transition, while exothermic peaks describe globule-to-coil transition temperature data. Therefore, during the heating process, the phase transition of the polymer could have occurred from open-coiled to globular state but the turbidity of the solution might not change due to a stable colloid structure, which leads to failure to produce macroscopic aggregates and an optical density change. Such behaviours have been studied by Zhou Y. et

al.[166] and a fuller consideration of the conformations of the polymers in aqueous solution is given in section 7.1.

The aggregates of highly branched PNIPAM could be defined as protein-like polymers which consist of a hydrophobic core and hydrophilic shell. The increase in temperature above the LCST of the polymer results in the breaking of hydrogen bonding between the water molecule and PNIPAM, leading to the exclusion of water from polymer molecules. The densely packed core of PNIPAM stems from the hydrophobic interaction, which is the result of intramolecular hydrogen bonds between amide and carbonyl groups, while the shell structure surrounding the hydrophobic core originates from highly polar end groups of vancomycin, which maintain a provide colloidal stability in dispersion. It is suggested that vancomycin chain ends stabilise the polymer collapse by electrostatic repulsion leading to non-aggregation of polymer above its LCST.

HB-PNIPAM-van consists of five ionisable groups from vancomycin that affect the charge of the molecule at different pHs. Firstly, there is the carboxyl group, which has a pK_a of 2.2, which means that above pH 2.18 most of the carboxylic acid will be dissociated and in the form of negative carboxylate. Secondly, there is also a secondary amine with a pK_a 8.8, which also means that below pH 8.8 it will be positively charged form and finally, there are three phenol groups with high pK_a , of 9.6, 10.4 and 12. Therefore, the charge of HB-PNIPAM-van depends on the pH of the solution. The primary amine was removed during the reaction of vancomycin with the polymer, thus it could affect the overall charge of the polymer. To confirm the effect of vancomycin chain ends on colloidal stability of the HB polymer in solution, HB-PNIPAM-van solutions were prepared at 0.5% w/v concentration (5mgml^{-1}) in deionised water at pH 2 and 7.6, which was the solution pH without any addition of acid. The opacity of the polymer solutions was investigated above the LCST (40°C). The results are shown in table 2.5.

Table 2.5 The effect of ionisable groups from vancomycin on the colloidal stability of HB-PNIPAM-van in solution above the LCST

pH of solution	pKa = 2.2	pKa = 8.8	pKa = 10-12	Opacity (at 40°C)
pH = 2	-COOH	$\text{---NH}_2^+\text{---CH}_3$		Cloudy
pH = 7.6	-COO ⁻	$\text{---NH}_2^+\text{---CH}_3$		Clear

The data in table 2.5, suggests that the charge on HB-PNIPAM-van end groups results from the carboxylate anions and that electrostatic repulsion from these prevents aggregation above the LCST mainly. The protonated secondary amine group did not provide sufficient electrostatic colloidal stability to the polymer above the LCST to maintain solution and so the polymer precipitated. At pH 7.6, carboxylic acid groups on HB-PNIPAM vancomycin ends were fully deprotonated, which would lead to a negative charge repulsion between the carboxyls and the secondary amine groups on vancomycin were protonated, which would result in positive charge and balance the net charge of the globules. However, it should be only partially protonated, which would not fully balance the total net charge on the polymer surface because the pH of the solution was close to its pKa [167]. To further explore the effect of electrostatic repulsion between polymer molecules, the charge of the polymers was measured. The charges of both linear and HB-polymer with vancomycin chain ends were determined by zeta potential values using ZetaPALS.

2.4.5 Electrostatic charge of HB-PNIPAM-van and L-PNIPAM-van

The stability of particles in suspension can be inferred from the magnitude of the zeta potential. This can be determined from the electrophoretic mobility, which is the ratio between particle velocity and the applied field. The data can be then converted to zeta potential using the Henry equation as follow:

$$UE = \frac{2\varepsilon z f(ka)}{3\eta}$$

Z = zeta potential

UE = electrophoretic mobility

ε = dielectric constant

f(ka) = Henry function; (f(ka) = 1.5 for aqueous suspensions in Smoluchowski approximation)

η = viscosity of solution

If the particles contain high negative or positive charges, which denote a high zeta potential value, they tend not to aggregate in suspension because of electrostatic repulsions between each other. On the other hand, if the zeta potential of the particles is low, they are more likely to aggregate in aqueous suspension due to van der Waals attraction [168]. Particles with a zeta potential between +30 mV and -30 mV are usually considered as unstable while particles with a high absolute zeta potential of more than +30 mV or -30 mV are classified as stable colloids in suspension. However, it should be noted that zeta potential is also influenced by pH due to protonation-deprotonation of surface functional groups, conductivity of the medium or presence of electrolytes such as anionic molecules. Tauer et al. suggested that the electrostatic charge of the precipitated particle of PNIPAM is associated with the phase transition behaviour of the polymer [157]. In order to determine the charge of HB-PNIPAM-van and L-PNIPAM-van, zeta potential measurement was performed. Samples were prepared at 0.1% w/v concentration (1mg/ml) in ultrapure H₂O. 15 μ l of sample was added to 1485 μ l of 1mmol KCl solution. Measurements were made at 25°C by Brookhaven Instrument Coporation ZetaPALS analyser. These studies were carried out at the pH of solution without any addition of acid or base (pH 7.6). The results for both polymers are shown in Figure 2.18.

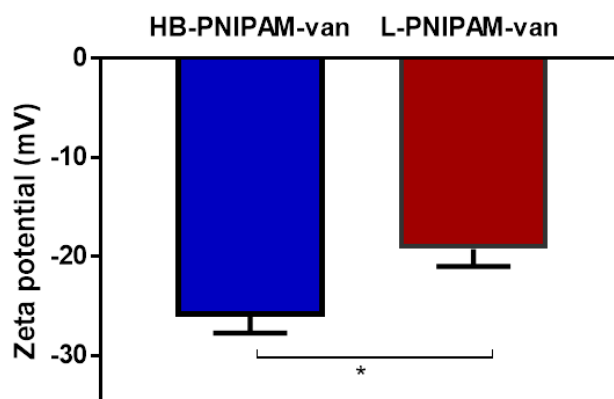


Figure 2.18 Zeta potential values of HB-PNIPAM-van and L-PNIPAM-van at 25°C. The pH of the solution was 7.6. The degree of significance is defined by P value from unpaired t-test: * when $P \leq 0.05$

From zeta potential measurement, at pH 7.6 in deionised water, the charges of both linear and highly branched PNIPAM functionalised with vancomycin were negative owing to the carboxyl groups in the vancomycin. The measured zeta potential values for HB-PNIPAM-van were close to -30 mV which is generally considered to be moderately stable dispersions, whereas the zeta potential of L-PNIPAM-van was significantly lower (-19 mV), indicating instability in the surface charge. This indicates that when the temperature was increased the coil-to-globule transition of L-PNIPAM-van formed chain-folded structures in which some of the vancomycin pendant groups were shielded within the globule resulting in less ionised groups and stabilised aggregates of the linear polymer. Therefore, the coil-to-globule transition produced a cloud point. Since the turbidity of the HB-PNIPAM-van solution hardly changed when the temperature was raised, it is thought that due to the highly branched nature of HB-PNIPAM, the polar chain ends were not shielded within the collapsed polymer structure and remain at the surface during heating so contributing to colloidal stability in dispersion. Perhaps more importantly though, they would still be functional in terms of their binding property [167]. Therefore, when the temperature was increased above its LCST, the carboxylate of vancomycin and some unmodified carboxylic acid residues would stabilise the collapse of the polymer in dispersions by providing electrostatic repulsion between particles and so reduce the aggregation of the polymer [139]. This would result in no detectable cloud point by turbidimetry measurement above its LCST.

There are several studies showing that the phase transition behaviour of PNIPAM depends on the polymer architecture. This includes the type of co-monomers that lead to highly branched polymers or block copolymers, and also the nature of the chain ends which influence the charge density of the particles and hydrophilicity of the polymer [169]. Balamuragan et al. reported a broad range of transition temperature of a PNIPAM brush grafted onto the surface of gold particles. They indicated that the phase transition temperature of PNIPAM occurred over a wide temperature range from 10-40°C because the outer segments of the polymer brush remained in the open-coiled state until it reached its LCST, whereas the inner segment of PNIPAM close to the surface of the particle at lower temperatures and became densely packed [170]. Lou et al. also showed the effect of core-shell formation on phase transition behaviour of micelles comprising hyper branched polyester with PNIPAM brushes. They showed that strong interchain repulsion between brushes can cause a broad phase transition of the polymer, which was associated with the broad peak of the polymer's LCST [171]. Our findings are consistent with this concept with the vancomycin functionalised chain ends influencing the aggregation behaviour of the polymer. Recently further support for a core-shell morphology has been provided by Plenderleith et al. who studied the effect of degree of branching of HB-PNIPAM on its transition behaviour. They found that HB-PNIPAM polymer with acid ends has biphasic morphology, which means that it has a collapsed inner core and more open outer shell in aqueous environments. Moreover, they suggested that HB-PNIPAM-COOH with a high degree of branching did not exhibit a cloud point at its LCST because electrostatic repulsion originating from carboxyl end groups prevented aggregation of the polymer [137]. Moreover, Rimmer et al suggested that HB-PNIPAM with RGD end groups forms colloiddally stable dispersions above its LCST thanks to RGD-end groups located at the surface of the particle. Similarly, there is electrostatic repulsion between chains that have vancomycin end groups. Therefore, the undetectable cloud point of HB-PNIPAM-van is explained by the effect of a core-shell structure to the polymer (see Figure 2.18).

The cloud point of linear PNIPAM-van was detected using both microDSC and turbidimetry. In this case, during the heating process, the increase in absorbance above the LCST could be attributed to the polymer architecture. In these linear polymers a high fraction of vancomycin became trapped inside the polymer globule. These trapped vancomycin groups do not provide electrostatic repulsion and do not contribute to the colloidal stability of the globules. This then results in precipitation. Schematics of both L-PNIPAM-van and HB-PNIPAM-van behaviour in deionised water at 37°C are shown in Figure 2.19.

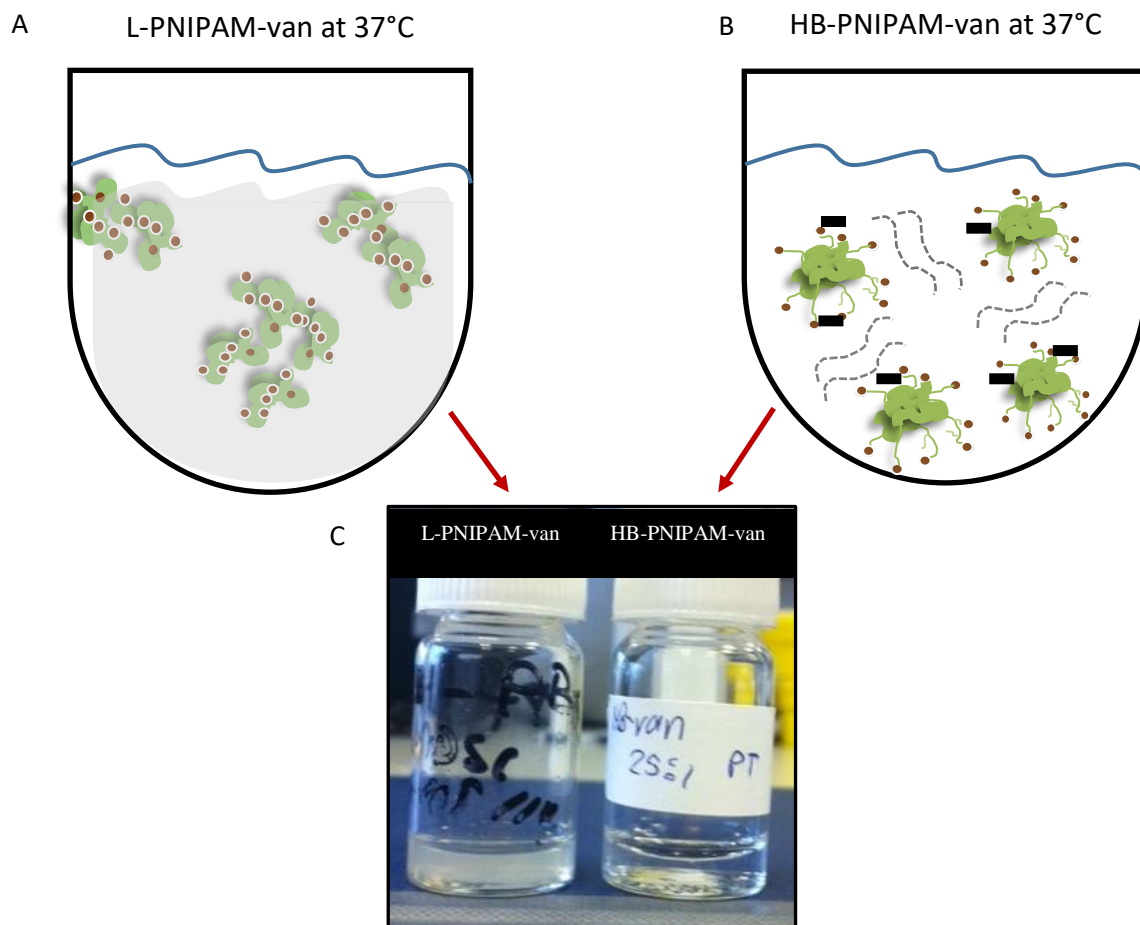


Figure 2.19 Schematic diagram representing the behaviour of (A) L-PNIPAM-van and (B) HB-PNIPAM-van in water above their LCSTs. L-PNIPAM-van precipitates from solution above its LCST whereas that does not occur with HB-PNIPAM-van. (C) shows an image of L-PNIPAM-van and HB-PNIPAM-van at 37 °C in deionised water.

In summary, according to the LCST determination of L-PNIPAM and HB-PNIPAM with different kinds of chain ends using microDSC and cloud point measurement, it can be concluded that the hydrophobicity of polymer-chain ends and polymer structures plays a crucial role in determining the LCST of thermo-responsive PNIPAM. The addition of RAFT agents or vinyl benzoic acid to PNIPAM results in a decrease in the LCST of compared to the linear homopolymer of PNIPAM. This is due to the hydrophobic influence of the aryl group on the LCST. However, with chain end modification from pyrrole to carboxylic acid, the LCST of HB-PNIPAM-COOH was increased because of the hydrophilic effect of carboxyl chain ends. Again, a stable colloid of HB-PNIPAM-van was obtained due to highly polar molecules at the chain ends of the highly branched structure. This prevents a cloud point being detected. However, microDSC could identify the LCST of HB-PNIPAM-van because it

monitors the amount of heat consumption and heat released during phase transition, whereas turbidimetry can only record macroscopic aggregate formation.

The above findings were obtained when the polymers were dissolved in water. However, phosphate-buffered saline (PBS) (pH 7.4) is the most commonly used solvent in biological work. To investigate a biological sample *in vitro*, it is necessary to maintain the conditions that would apply in the natural environment such as at physiological pH and osmolality. PBS is a water-based balanced salt solution consisting of sodium and potassium dihydrogen phosphates and sodium and potassium chlorides giving a pH 7.4 and 137 mM sodium chloride. However, for more than a century, it has been known that the solubility of proteins in aqueous solution is affected by the presence and concentration of salt [172]. This is known as the Hofmeister effect, or salting-out effect and it applies to other polymers as well. It was reported that salt in buffer solutions has a notable influence on the LCST of PNIPAM owing to interruption of the interaction between the polymer and water, and also a change in the structure of water surrounding the hydrated polymer by anionic salts [173, 174]. It was interesting, therefore, to investigate the phase transition behaviour of both polymers in this PBS. The polymer was prepared at 5mg/ml and the conditions set for microDSC and turbidity measurement were similar to those employed in the water-based experiments. It was found that the cloud point of HB-PNIPAM-van in PBS could be detected at 40°C (onset) by turbidimetry (Figure 2.20).

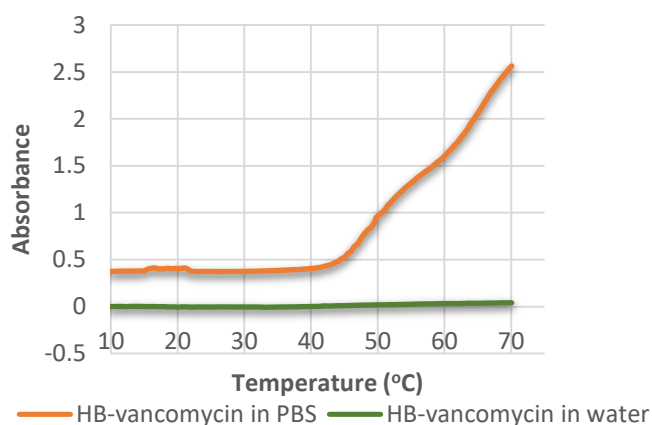


Figure 2.20 Comparison of the cloud points of HB-PNIPAM-van in water and in PBS showing the effect of salt on the behaviour of aggregates

To observe the effect of salt on the phase separation of L-PNIPAM-van and HB-PNIPAM-van, the LCSTs of both polymers were measured in PBS and in water by microDSC and turbidimetry. The results are shown in Table 2.6.

Table 2.6: Summary of phase transitions of polymers in PBS and in water measured by turbidimetry and microDSC

Type of polymer	Cloud point measured by turbidimetry (°C, onset)	
	In PBS	In water
L-PNIPAM-van	34	37
HB-PNIPAM-van	40	-
Type of polymer	LCST measured by microDSC (°C)	
	In PBS	In water
L-PNIPAM-van	32	35
HB-PNIPAM-van	28	33

From table 2.6, it is evident that there was no cloud point of HB-PNIPAM-van detected in water, but a cloud point could be detected (40°C) in PBS. A small decrease in phase transition temperature of L-PNIPAM-van was observed in PBS buffer compared with water.

The effects of salt on phase transition temperatures of thermo-responsive polymers have been extensively studied, especially the temperature-induced aggregation behaviour of PNIPAM [175]. The LCST of PNIPAM was shown to reduce with increasing concentration of sodium chloride [176]. According to the Hofmeister effect, it was suggested that inorganic ions in solution can either disorder or promote the water structuring in the aqueous system [177]. Eeckman et al. showed that the addition of salt results in a reduction in the LCST of PNIPAM and the kind of salt, salt concentration, electron valence and size of salt anions also play crucial roles in the phase transition temperature of PNIPAM [178]. Geever et al. studied the effect of salts in pH buffers on the phase transition temperature of polyvinyl pyrrolidinone (PVNP)-PNIPAM random copolymer, since the LCST is a most important factor for such a material used in controlled drug delivery system. They reported that the presence of salts incorporated in the PBS decreased the LCST of the PVNP-PNIPAM copolymer to below 37°C, leading to it becoming less soluble in aqueous solution due to a salting-out effect [173]. It is not only anionic salts that cause a change in phase transition behaviour of thermo-responsive polymers; cationic salts do as well. However, the effects of anions on the phase

separation behaviour of PNIPAM are more pronounced, especially for divalent ion (SO_4^-), because anions are more polarisable, thus their hydration is typically stronger when it is compared with cations [179, 180].

It is interesting how the presence of salt ions in HB-PNIPAM-van solution have a notable effect on the cloud point of the polymer. From Figure 2.20, it appears that the presence of inorganic salts in PBS could affect the stabilisation of HB-PNIPAM-van collapse/aggregates in solution, leading to a change from transparent to cloudy.

The mechanisms behind the effect of a specific salt on HB-PNIPAM-van solutions are complicated, primarily because there are a great many kinds of intermolecular interactions that are relevant to these processes: i.e., polymer and water, ion and water, and ion to polymer molecule interactions. Therefore, when salt is added not only is there a reduction in the number of hydrogen bonds between polymer and water, but also the interactions between cations of electrolytes and negatively charged polymers come into play. It is obvious that the nature of polymers plays a role in this system, such as the negative charging of HB-PNIPAM-van [180]. Zhang et al. suggested that there were three mechanisms involved in the phase separation of PNIPAM in the presence of salt ions in aqueous solution: i) destabilisation of hydrogen bonding between amide groups of PNIPAM and water molecule by anions; ii) the surface tension effects originating from the hydration of hydrophobic segments of PNIPAM; and, iii) the interaction of anions on the polymer molecule [175, 179]. The first and second situations lead to a decrease in LCST (salting-out) while the third one results in salting-in effect. In this work, not only did the first two mechanisms occur, but the interaction between cations and the negative charge of vancomycin located outside of the core-shell of HB-PNIPAM-van was also involved. It is believed that the phase separation of HB-PNIPAM-van in PBS is strongly relevant to the disappearance of electrostatic repulsion originating from the vancomycin end groups. The presence of cations in the polymer solution could shield negative charges stemming from the carboxylate group of vancomycin, which stabilise the collapse of HB-PNIPAM-van in solution above its LCST. Thus, when the temperature rose above its LCST, there was no effect of electrostatic repulsion preventing the polymer from precipitation, resulting in the detectable cloud point of HB-PNIPAM-van by turbidimetry [177].

These studies show that the presence of salt in both HB-PNIPAM-van and L-PNIPAM-van solution can induce a significant decrease in the LCST of the polymers and also causes

precipitation as detected by turbidimetry, because the presence of salts in the polymer solution cause a change in the orientation of water molecules in the hydration shells surrounding the polymer by inducing water molecules to form a rigid structure around the inorganic ions, so allowing an enhanced hydrophobic nature of the polymer. Additionally, cationic salt can reduce the effect of electrostatic repulsion between HB-PNIPAM-van molecules by shielding negatively charges on vancomycin, resulting in the collapse of the polymer in the solution [173, 176, 178].

In summary, it can be confirmed that the effect of chain end modifications on the LCST of the amphiphilic polymers, PNIPAM, is directly correlated to the hydrophobicity and hydrophilicity of the polymers and polymer architecture. The phase transition temperature could be triggered by not only a variety of polymer end groups, but also polymer architecture. In order to investigate the phase transition behaviour of thermo-responsive polymers like HB-PNIPAM, appropriate analytical methods need to be employed. This work has shown that it is more appropriate to use microcalorimetry to determine the LCST of HB-PNIPAM-van because of the complexities of the core-shell structure of the polymer. The negative charge of both linear and highly branched polymers functionalised with vancomycin at the chain ends is likely to result from the carboxylate groups in vancomycin.

2.4.6 Development of assay for quantifying amount of vancomycin in polymers

2.4.6.1 Vancomycin-copper(II) complex

In order to compare the properties between HB-PNIPAM-van and L-PNIPAM-van, especially in terms of their interaction with bacteria, it is necessary to know whether any differences in their behaviour could be due to differences in the amount of vancomycin functionalisation in each type of polymer. Vancomycin can be used not only as a glycopeptide antibiotic, but also as a chiral selector for the separation of anionic compounds due to its unique combination of structural characteristics that can form hydrogen bonding or dipole-dipole interaction with chiral analytes. As it consists of five ionisable groups in its structure, namely carboxylic acid group, phenolic, primary amine and especially secondary amine moieties vancomycin is positively charged under its pI of 7.2 [181]. Previously, several studies proved that vancomycin shows dominant enantioselectivity by forming a complex between copper(II) ions and the secondary amine of *N*-methyl leucine of vancomycin, the deprotonated nitrogen atom of amide groups, and the oxygen at asparagine. The remaining

position is occupied by water. This results in a violet compound when at 1:1 equivalent molarity at pH 7.4. Thus, vancomycin-copper complexing was tried as a method to determine the amount of vancomycin in the polymers [181, 182].

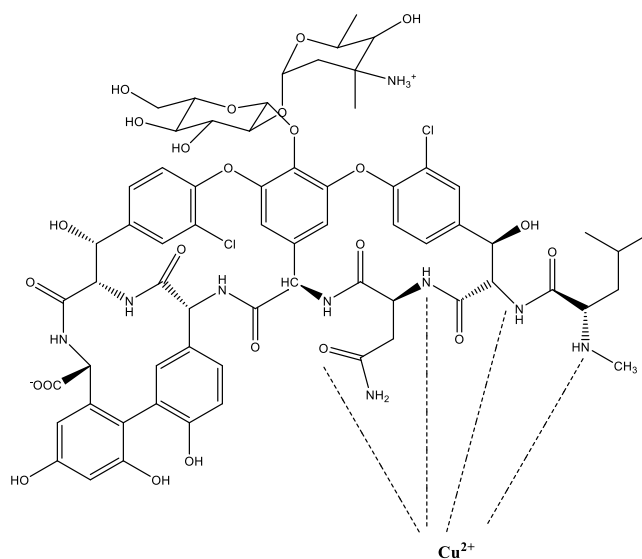


Figure 2.21 Chemical structure of vancomycin coordinating with copper (II) ion. Dashed lines show the coordination of copper (II) with the secondary amine of N-methyl leucine of vancomycin, the deprotonated nitrogen atom of amide groups and the oxygen at asparagine.

Materials

Copper (II) nitrate trihydrate ((Cu(NO₃)₂·3H₂O) (Sigma Aldrich, 99%) and Copper(II) sulphate pentahydrate (CuSO₄·5H₂O) (Sigma Aldrich, 98%) and Copper(II) chloride (CuCl₂) (Sigma Aldrich, 97%) was used as received. Sodium hydroxide (Sigma Aldrich, 97%) and Sodium bicarbonate (Sigma Aldrich) were used as received. Vancomycin hydrochloride hydrate (Sigma Aldrich) was used as received. Citric acid monohydrate (Sigma Aldrich), Trisodium citrate dehydrate (Sigma Aldrich) were used as purchased.

Methods

The vancomycin-copper(II) complex was prepared by mixing 0.05M of vancomycin solution with 0.05M of copper(II) nitrate trihydrate solution in deionised water. The pH of the mixture was adjusted by titration to 7.4 using dilute sodium hydroxide (0.001M). The absorbance of the violet mixture was scanned over the wavelength range 300-800nm to obtain the optimum excitation wavelength. Then, the calibration plot was created by varying the concentration of vancomycin solution from 0-0.05M. 100ul of each mixture was pipetted into 96 well plates and the absorbance was measured at 570nm using a UV-Vis spectroscope.

Polymer samples were prepared by dissolving in deionised water and then assayed by mixing with 0.05M of copper(II) nitrate trihydrate solution. The pH of the mixture was adjusted as previously described.

Results and discussions

On initial mixing of the vancomycin solution with copper(II) nitrate trihydrate, the colour of the mixture was as shown in Figure 2.22 (left), which was light blue from copper(II). The colour started changing from light blue to deep violet when dilute sodium hydroxide was added however, when the pH reached 7.4, the solution turned to violet permanently, as shown in Figure 2.22 (right).

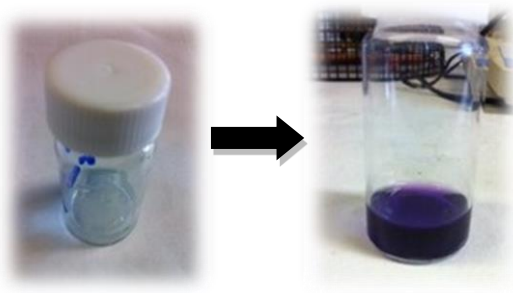


Figure 2.22 Images of the mixture of vancomycin and copper(II) solution: (left) the mixture before adjusting pH with diluted base solution; (right) the mixture of vancomycin-copper(II) complex at pH 7.4. The absorbance of the violet solution was measured at 300-800nm, as shown in Figure 2.23.

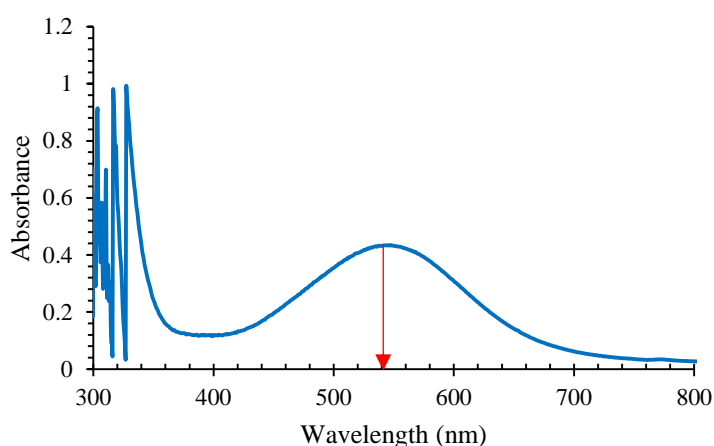


Figure 2.23 The absorbance spectra of vancomycin-copper(II) complex

It was found that the maximum excitation wavelength of the violet complex was 570nm, which was similar to that reported by previous workers [181].

However, in the case of L-PNIPAM-van and HB-PNIPAM-van, the result showed that when vancomycin was linked to the polymers it did not form a complex with copper(II) ions. Raising the pH by adding a small amount of dilute sodium hydroxide (0.001M NaOH) to the polymer mixtures resulted in a light green cloudy solution, which can be seen in Figure 2.24 (B). This is because the amino group on the sugar involved in copper(II) coordination was used to react with the polymers. Thus, the absence of the key amine group on vancomycin-linked polymer resulted in failure of copper (II) to bind to either L-PNIPAM-van or HB-PNIPAM-van. Addition of hydroxide resulted in the precipitation of $\text{Cu}(\text{OH})_2$ because the copper had not complexed with the vancomycin in the polymer. This notion is supported by the observations of Brzezowska et al [179] who reported that the modification of N-terminal structure of teicoplanin, a member of the group of glycopeptide antibiotics with a similar structure to vancomycin, significantly decreases the binding affinity of teicoplanin toward copper (II)

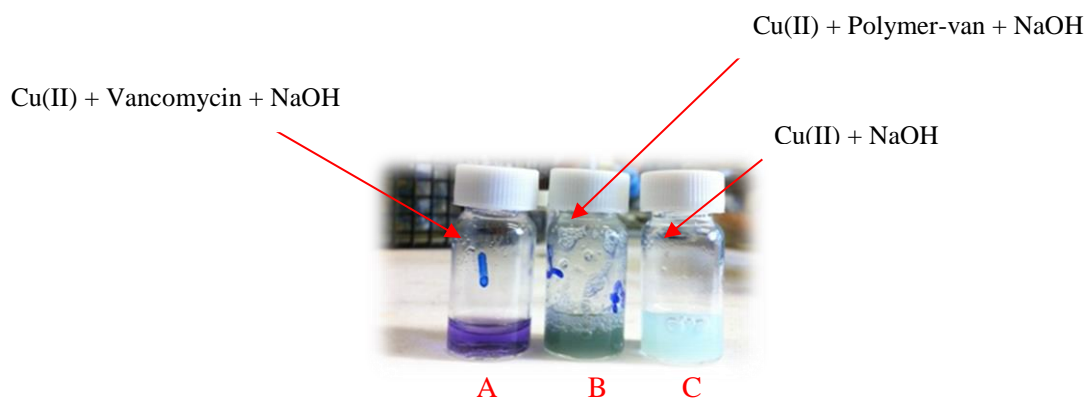
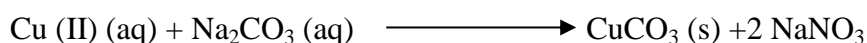
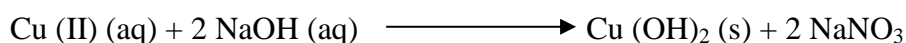


Figure 2.24 Three different types of samples with copper(II) nitrate solution (A) copper(II)-vancomycin solution at pH 7.4 (B) the mixture of copper(II) and HB-PNIPAM-van at pH 7.4; (C) the mixture of copper (II) nitrate at pH 7.4



Although this explanation seems the most likely, it is also possible that the amount of vancomycin bound to both the linear and HB-polymers was below the detection limit of the method. Vila et al. found that the quantitation limit for vancomycin coordinated with copper(II) using a flow injection technique was around 0.25 mmol/dm^3 .

Nonetheless, while there was no doubt that the polymers had vancomycin linked to them (from ^1H NMR spectra of the polymers) the quantity could not be determined using that method or copper(II) complexing. However, quantification of vancomycin chain ends of both kinds of polymers remained an important goal therefore, an alternative technique was developed.

2.4.6.2 Enzyme-linked immunosorbent assay (ELISA) to quantify vancomycin

A “sandwich” enzyme-linked immunosorbent assay (multi-layered ELISA) is a commonly used method for quantifying a concentration of antigens in unknown samples. The sensitivity of the technique can be increased depending on the number of layers of antibodies used in the system. There are different types of ELISA, namely direct ELISA, indirect ELISA and multi-layered ELISA. It depends on the underlying layer of capture, primary and detection antibodies [183].

The multi-layered ELISA technique was thought to be a possible method for determining the amount of vancomycin in a functionalised polymer. There are several factors that influence antibody-antigen reactions in ELISAs and these are classified into two groups, namely factors influencing the equilibrium constant, such as temperature, pH and ionic strength, and other factors not affecting the equilibrium of reaction, such as concentration of antigens and antibodies and incubation time. In order to quantify the amount of vancomycin in each polymer, a standard curve needed to be established and the various reaction parameters optimised.

Materials

Vancomycin-hydrochloride, 3,3',5,5'-tetramethylbenzidine (TMB), phosphate-citrate buffer tablets (pH 5.0), phosphate buffer tablets (pH 7.4), and sulphuric acid (98%) were all obtained from Sigma-Aldrich and used as received. Hydrogen peroxide was used as received. Mouse monoclonal and rabbit polyclonal antibodies to vancomycin, sheep polyclonal antibodies and goat anti-rabbit IgG conjugated to horse radish peroxidase (HRP) were obtained from Abcam Plc, (Cambridge UK) and diluted for use as shown below.

Optimisation of the ELISA

Methods

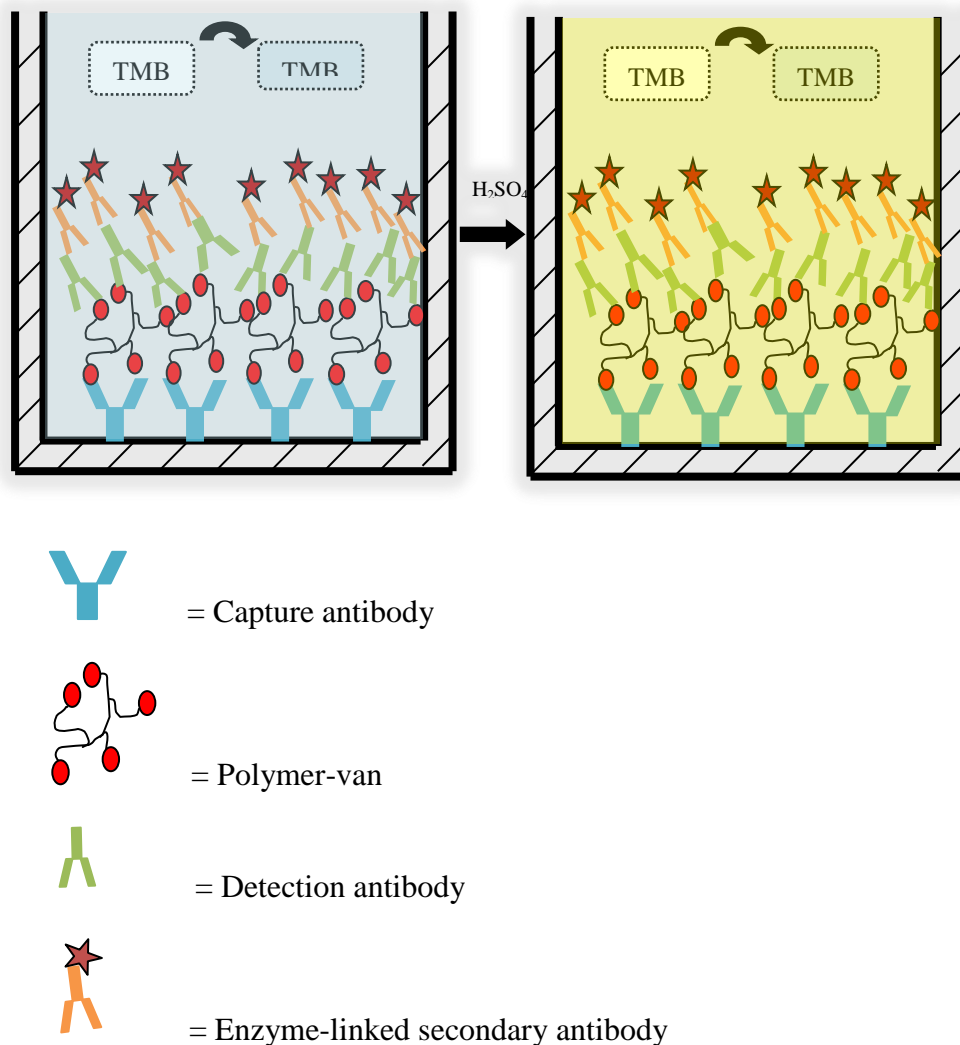


Figure 2.25 The design of the multi-layered ELISA used in this study

To prepare a microplate for standard curves and polymer samples, each plate was coated with 100 μ l of the capture antibody in carbonated buffer (pH 9.5), called a coating buffer, then the microplate was incubated at 4°C overnight. After that, the plate was washed with 200 μ l of PBS-Tween four times, followed by blocking wells with 200 μ l of PBS-5% BSA, and the plate was then incubated at 4°C overnight. The next step was the addition of vancomycin and polymer samples. A dilution series of vancomycin hydrate hydrochloride in PBS-1% BSA was established over the concentration range 0 - 2.5mg/ml and incubated at 4°C overnight for 24 hours. Then the plate was washed with PBS-Tween four times and 100 μ l of the detection

antibody in PBS-1%BSA was added. The plate was incubated at room temperature for two hours. Before adding the HRP-conjugated antibodies, again each well was washed with 200µl of PBS-Tween four times. A HRP-conjugated secondary antibody solution was prepared in PBS-1%BSA and added into each well. The microplate was incubated at room temperature for 90 minutes. In order to measure the absorbance, one tablet of TMB substrate was dissolved in 25ml of citrate buffer and 10µl of hydrogen peroxide (30%v/v). 100µl of TMB solution was added. The reaction time between TMB and IgG conjugate was 15 minutes. 100µl of sulphuric acid (10% v/v) was added to stop the reaction. The absorbance was measured at 450nm using a microplate reader.

Results and discussion

To quantify the amount of vancomycin contained in polymers by ELISA, the protocol needed to be optimised. There were several variables to be considered namely the assay plate, coating buffer, capture antibody, blocking buffer, washing step, detection antibody and enzyme conjugated antibody.

Antibodies

For a sandwich ELISA, there are two different antibodies used in assays, which are primary antibodies (the capture antibodies) and secondary antibodies (the detection antibodies). An essential requirement is both antibodies should react with different epitopes on the unknown samples. In addition, the primary antibody should not provide steric hindrance to the secondary antibody leading to a decrease in signal. To choose the capture and detection antibodies for a sandwich ELISA, it is also important that both antibodies are produced from different kinds of animal so that matched pairs can be avoided. Concentrations of each antibody are also a most important parameter that needs to be optimised.

Blocking buffer

The non-specific binding of protein or antibodies to wells can cause a high background signal. Thus, to prevent non-specifically bound reactants, an optimal blocking buffer is commonly used, which are most commonly skimmed milk or bovine serum albumin (BSA). In order to choose a type of blocking agent for each ELISA application, cross reactivity needed to be examined. The addition of a non-ionic detergent (Tween-20) to the blocking buffer is also commonly done to reduce the hydrophobic interaction between antibodies and any blocking agent consisting of protein. The typical concentration of Tween-20 is about

0.05% (v/v). In order to obtain successful blocking, the appropriate blocking buffer volume is essential.

Washing step

Efficient washing of the plate after the addition of the capture antibodies, blocking agent, detection antibodies and enzyme conjugated is a crucial step leading to low signal to noise ratio. Washing should take place approximately 4-6 times for each step. The most common buffer used for washing the plate is phosphate-buffered saline consisting of 0.05% (v/v) Tween-20.

Considering all the factors mentioned above, the ELISA protocol for quantifying the amount of vancomycin contained in the polymers for our study was optimised as follows. For the first model, which we named “ELISA Model 1”, rabbit anti-vancomycin was used as the capture antibody. Sheep anti-vancomycin was chosen as the second antibody, and finally HRP-conjugated rabbit anti-sheep IgG was used as the detecting layer. TMB was used as the enzyme substrate. The absorbance was measured at 450nm. The conditions used are shown in Table 2.7.

Table 2.7: The conditions of each parameter for ELISA Model 1

Dilution of capture antibody (Rabbit anti-vancomycin)	Dilution of detection antibody (Sheep anti-vancomycin)	Conjugated - HRP
1:1,000	1:3,000	1:5,000
1:1,000	1:5,000	1:5,000
1:1,000	1:8,000	1:5,000

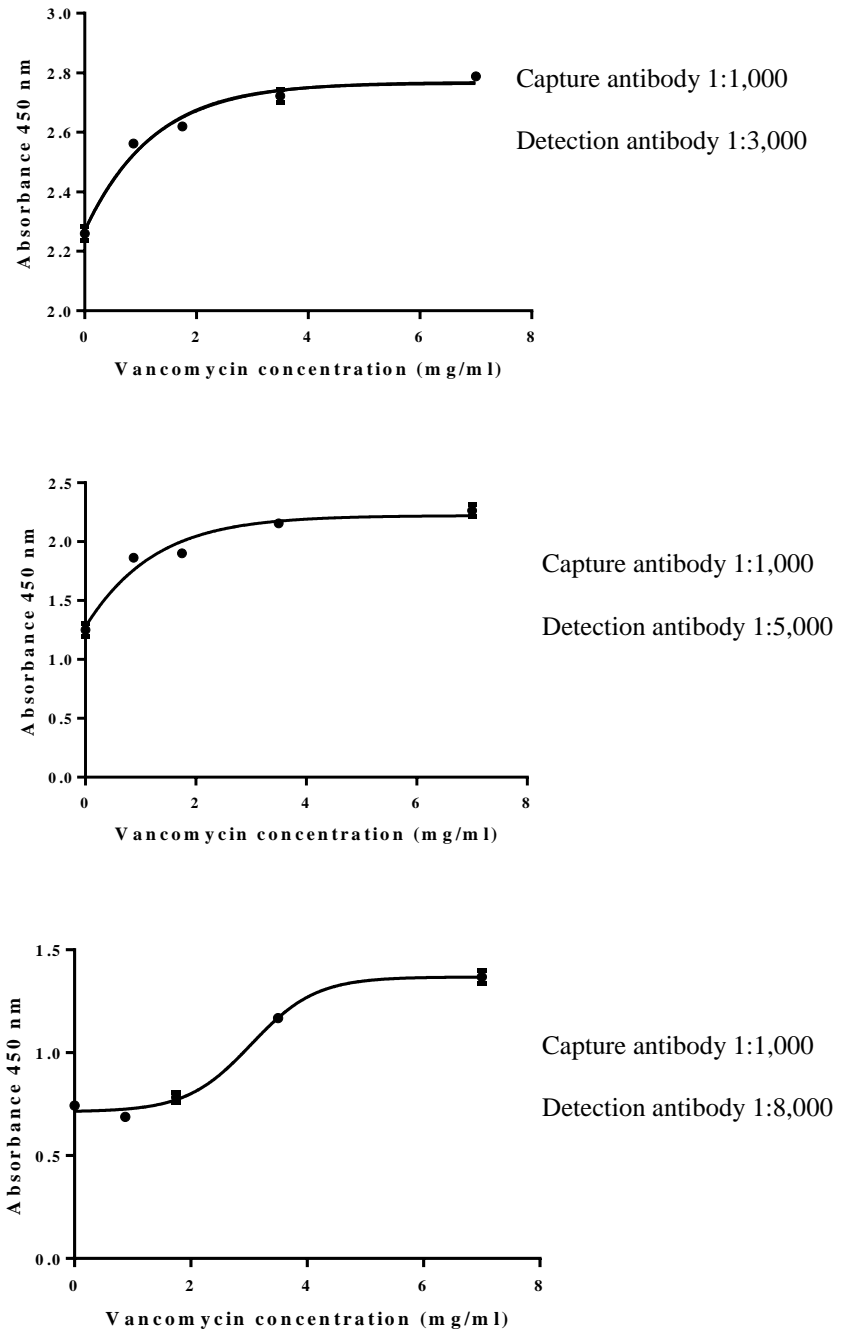


Figure 2.26 Standard curves of ELISA Model 1 (A-C). The curves were fitted by 4-parameter logistic fit (4PL) of the data points. (A) Dilution of capture antibody was 1:1,000 and dilution of detection antibody was 1: 3,000. (B) Dilution of capture antibody was 1:1,000 and dilution of detection antibody was 1: 5,500. (D) Dilution of capture antibody was 1:1,000 and dilution of detection antibody was 1: 8,000.

From the data shown in Figure 2.26, it was found that the negative control (0mg of vancomycin) was too high when 1: 1,000 dilution of the capture antibody and 1: 3,000

dilution of the primary antibody were used. High levels of antibodies used can cause non-specific binding and high background results in the negative controls, which is reasonably common in sandwich ELISAs [183]. Indeed, a decrease in the concentration of the primary detecting antibody from 1: 1,000 to 1: 8,000 resulted in a significant decrease in background colour obtained.

The main factors affecting multi-layer ELISA are not only the concentrations of antibodies, but also type of antibodies. Not all kinds of antibodies can work successfully with the ELISA technique [184]. Each antibody must be evaluated specifically for individual applications. Therefore, the properties of the antibodies were considered. There are several properties of antibodies that have effect on the specificity of the binding of antigen to antibody, such as purity and clonality. The sheep anti-vancomycin antibody employed was a polyclonal type but also whole anti-serum rather than a purified IgG fraction and this can lead to non-specific binding. Therefore, other types of antibody were substituted.

Mouse monoclonal anti-vancomycin was used as the capture antibody. Rabbit polyclonal anti-vancomycin was used as the primary detecting antibody following by HRP-conjugated goat anti-rabbit IgG. TMB was used as substrate again measured at 450nm. A monoclonal antibody was chosen to be used as the capture antibody thanks to the high specificity to its antigen, and less background due to less cross-reaction with other proteins. Therefore, another ELISA model, referred to as “ELISA Model 2”, was developed. The dilution of each antibody is shown in Table 2.8.

Table 2.8: The dilution of each antibody used in ELISA Model 2

Dilution of capture antibody (Mouse anti-vancomycin)	Dilution of detection antibody (Rabbit anti-vancomycin)	HRP
1:100	1:5,000	1:5,000
	1:10,000	
	1:15,000	
1:250	1:5,000	1:5,000
	1:10,000	
	1:15,000	
1:500	1:5,000	1:5,000
	1:10,000	
	1:15,000	

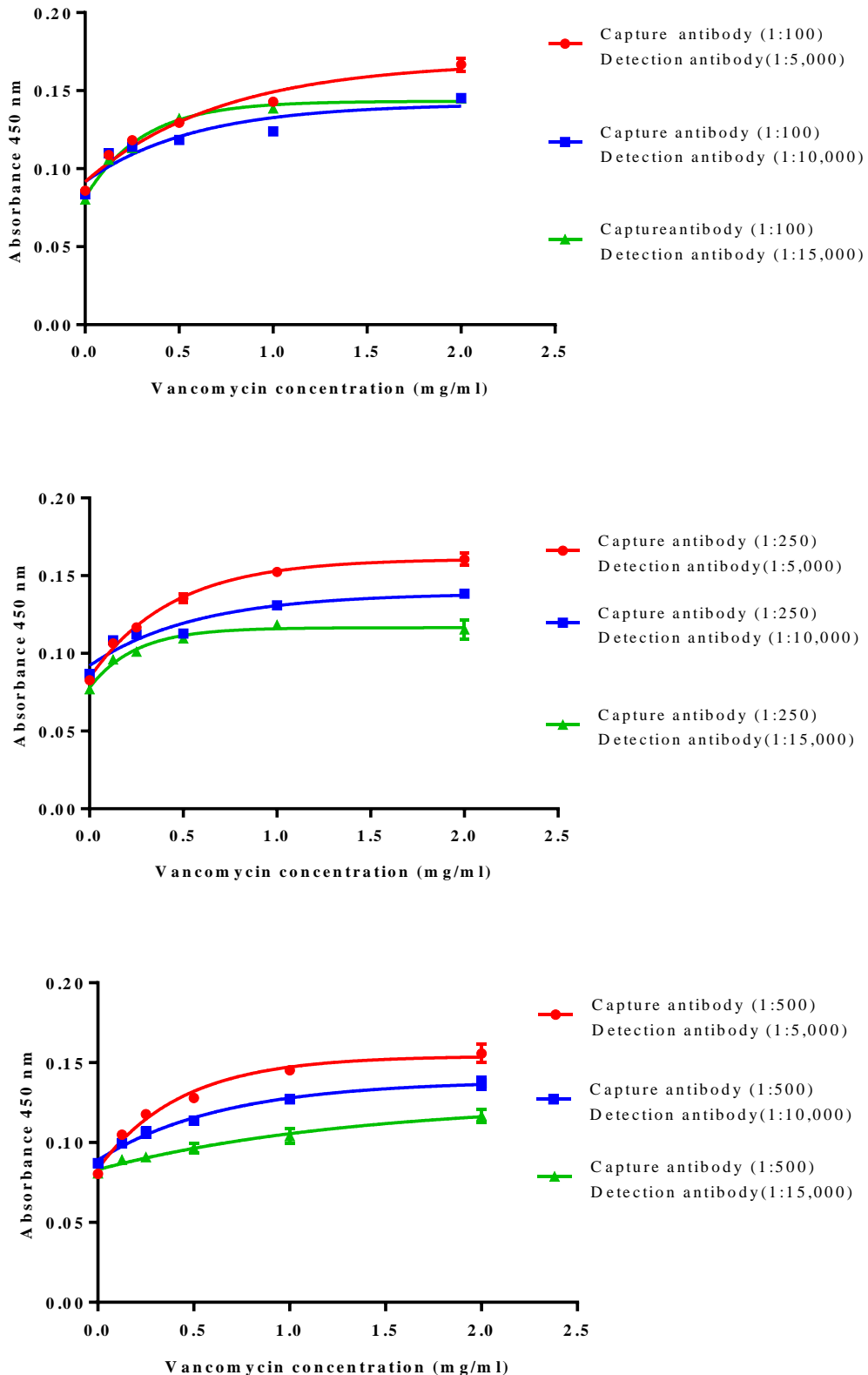


Figure 2.27 The standard curve ELISA using monoclonal mouse anti-vancomycin as the capture and rabbit anti-vancomycin as the detector at various dilutions. The curves were fitted by 4-parameter logistic fit (4PL) of the data points.

A 1:500 dilution of mouse anti-vancomycin was chosen as the capture antibody and a 1:5,000 dilution of rabbit anti-vancomycin was used as the detector antibody for quantifying vancomycin on the polymers. The final protocol is summarised in Table 2.9.

Table 2.9: The conditions of the next-developed sandwich ELISA used for measurement of vancomycin in L-PNIPAM-van and HB-PNIPAM-van

Capture antibody	Mouse monoclonal anti-vancomycin (1:500)
Blocking agents	5% w/v BSA in PBS-Tween-20
Detector antibody	Rabbit polyclonal anti-vancomycin (1:5,000)
Enzyme conjugated	Goat anti rabbit IgG-HRP (1:5,000)
Substrates	TMB/H ₂ O ₂

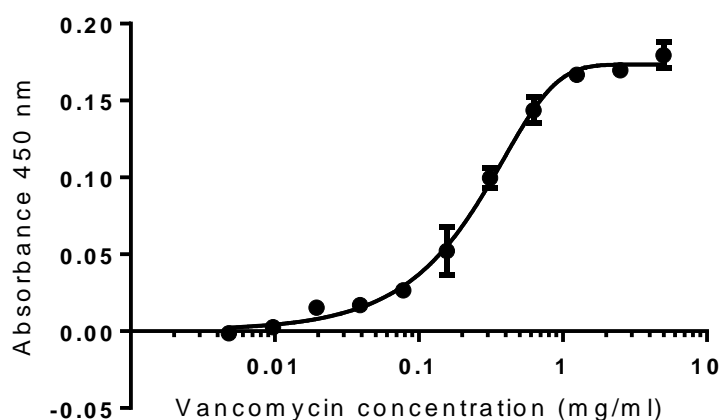


Figure 2.28 Standard curve of vancomycin and quantification of the amount of vancomycin in L-PNIPAM-van and HB-PNIPAM-van. The curve was fitted by sigmoidal, 4-parameter logistic fit (4PL) of the data points. X is log(concentration)

To quantify the amount of vancomycin by ELISA, we exploited the effect of salt on the solution behaviour of HB-PIPAM-van to precipitate it away from small molecular material, including any un-bound. To do this, the polymers were dissolved in PBS, and then heated above their LCSTs. The precipitates were separated from the bulk fluid by centrifugation and then re-dissolved at room temperature. The process was repeated until it was certain that there was no free vancomycin. The resultant final preparations were then checked for free

vancomycin by mass spectrometry and biological assay. The molecular formula for vancomycin is $C_{66}H_{75}C_{12}N_9O_{24}$ and the molecular weight is 1449 g/mol. There was no peak at m/z 1450, (associated with the protonated vancomycin ion, (M+H)), found in the polymer after purification by centrifugation in PBS. The biological assay involved spotting the re-dissolved polymers and supernatants from 1st, 2nd and 3rd precipitations directly onto BHI agar that had been pre-coated with *S. aureus*. After incubation overnight at 37°C, the presence of any inhibition of growth could be seen as an area of clearing in the bacterial 'lawn'.

It was found that supernatant of the polymers obtained from the first and second washing still had antimicrobial activity, whereas the supernatant and the polymer from the third precipitation did not. An example of the biological assay is shown in figure 2.29. The findings were expanded upon and confirmed using minimal inhibitory concentration testing which is reported in Chapter 3.

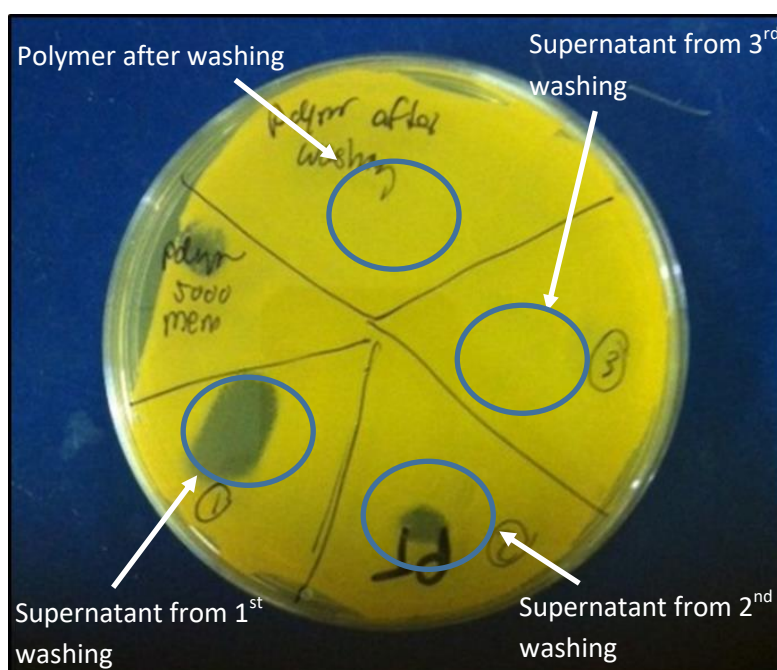


Figure 2.29 The rapid test of bactericidal activity of polymers before and after washing by heating vancomycin-functionalised polymer in PBS and the supernatants obtained by centrifugation from each precipitation step were spotted onto lawns of *S. aureus*. Blue circles indicate areas of sample application.

When all polymer samples were purified as described above, an ELISA was carried out in order to determine the amount of vancomycin in the polymers.

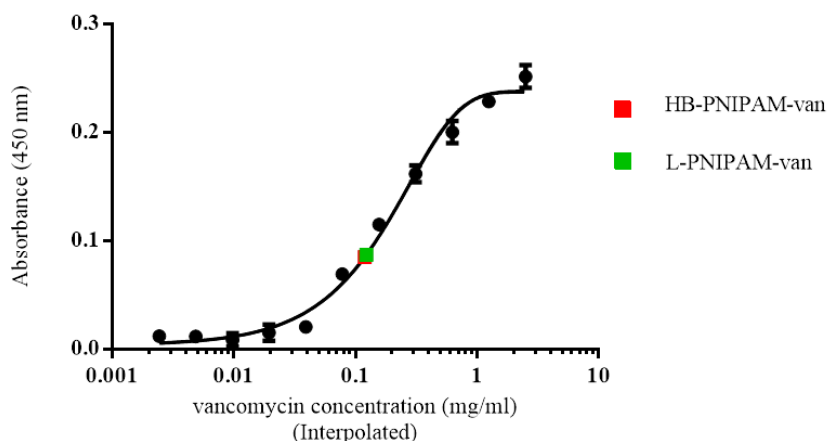


Figure 2.30 Standard curve of an ELISA of vancomycin and the amount of vancomycin (per mg of polymer) contained in HB-PNIPAM-van (■) and L-PNIPAM-van (■)

Table 2.10 Summary of the determination of the amount of vancomycin in the polymers from ELISA and ¹HNMR

Type of polymer	Loading of vancomycin ^a (mg/mg of polymer)	% Vancomycin functionality ^b
HB-PNIPAM-van	0.025	3
L-PNIPAM-van	0.028	2.6

^aLoading of vancomycin (per mg of polymer) from ELISA

^b% Vancomycin functionality estimated from ¹HNMR in D₂O by rise of peak at 5.2-5.6 ppm (1H integral per vancomycin) compared to the isopropyl peak (1H integral per backbone unit)

Figure 2.30 shows a representation of the vancomycin standard plot. The vancomycin concentrations were varied from 0-2.5mg/ml in 1%BSA (w/v) -PBS-Tween-20 using 1:2 dilutions. The result indicates that the vancomycin contained in L-PNIPAM-van and in the HB-PNIPAM-van was at very similar levels i.e. 0.028 mg and 0.025 mg (per mg of polymer), respectively. These data are based on repeat experiments but using only a single concentration of polymer for the assay. For a more accurate determination of the amount of vancomycin present, a dilution series of each polymer should be assayed, which was not done. However, despite this weakness, the finding that L-PNIPAM-van and HB-PNIPAM-van polymers contained equivalent amounts of vancomycin was confirmed by other methods, namely the binding of vancomycin groups to its D-Ala-D-Ala dipeptide target, the details of which are included in Chapter 6 and by estimation from ¹HNMR. The %vancomycin

functionality estimated from ^1H NMR showed it to be very similar to the %vancomycin loading value obtained from ELISA (2.5% in HB-PNIPAM-van and 2.8% in L-PNIPAM-van). The ELISA method may give an underestimate of the amount of vancomycin present on the polymer because it relies on antibody being able to access all of the vancomycin groups on the polymer molecules. It is possible though that some groups may be inaccessible, however, the polymers were in the open coil morphology in the ELISA method we used so the vancomycin in the outer shell of the HB-PNIPAM should be accessible to antibody. It is acknowledged, however, that vancomycin groups in the inner core may not be accessible to antibody, although these would not be accessible to bacteria either, so the amount detected could be considered to be that which are functionally binding groups on the polymer. Interestingly though, the percentage vancomycin content detected by ELISA was very similar to that detected by NMR suggesting that the amount estimated by ELISA is not a significant underestimate.

2.5 Conclusions

HB-PNIPAM-van was successfully synthesised by SCVP-RAFT polymerisation using 4-vinylbenzyl pyrrolocarbodithioate as a RAFT monomer to provide branching points. The polymer chain ends were functionalised with vancomycin antibiotics to result in targeting *S. aureus*. The linear analogue version was synthesised with the same amount of vancomycin and the same fraction of repeating units using vinyl benzoic acid as a comonomer to place aryl groups into the polymer and produce an equivalent monomer composition to the branched analogue. A HB-polymer and a linear polymer with different end groups, namely, carboxylic acids and vancomycin, were characterised using several techniques. The results from micro calorimetry and turbidimetry showed that linear and highly branched polymers with vancomycin chain ends behaved differently above their LCST due to their architecture. This observation could be explained by HB-PNIPAM-van having a core-shell structure. The densely packed core originates from desolvated PNIPAM and the outer shell stems from solvated polymer that is swollen with water with the charged vancomycin probably adding to the osmotic component of the swelling by partial penetration of the end groups into the shell. The particles in nanoscale dispersion were stabilised by electrostatic repulsion above the LCST, resulting in an undetectable cloud point by turbidimetry. However, the LCST of the L-PNIPAM-van could be detected by both techniques because, above its LCST, vancomycin would be shielded inside the globule, leading to aggregation of the polymer. Thus, it could be concluded that the polymer architecture and the nature of the end groups play a significant role in the phase transition behaviour of polymers. In this work, an alternative sandwich ELISA was developed to determine the amount of vancomycin in both linear and highly branched polymer. This method proved to be reproducible and can be routinely used for the assay of vancomycin in these types of the polymers. From these results, it could be concluded that both linear and highly branched polymers functionalised with vancomycin by the above protocol contain the same amount of vancomycin which is useful for comparison of their behaviour in further experiments. Purification of the polymer is a most crucial step because any trace of free vancomycin and small polymers molecules with vancomycin will confound the measurement of the polymer functionalisation.

Chapter 3 : Determination of the killing capability of polymers functionalised with vancomycin

3.1 Introduction

S. aureus is considered to be one of the major causes of severe infection leading to bacteraemia and sepsis with potentially fatal outcome [4, 5, 7, 52, 185, 186]. From 1942 to the early 1950s, the β -lactam antibiotic benzylpenicillin, was used for treatment of *S. aureus* infection. However, by the late 1950s, resistant *S. aureus* strains were discovered due to the expression of a β -lactamase enzyme. In 1959, methicillin had been developed which protected the sensitive β -lactam bond from β -lactamases in resistant strains. Unfortunately, methicillin-resistant *S. aureus* (MRSA) occurred as soon as it was applied clinically. With the emergence of MRSA since the 1980s, glycopeptide antibiotics were employed as ‘last resort’ antibiotics and are still used today. Vancomycin was the first member of the group to be used clinically for treating MRSA infection [62, 187, 188] but the emergence of vancomycin-resistant enterococci in the middle of the 1980s and subsequent transfer of that property to MRSA strains has heightened awareness of the antibiotic-resistance problem. Now many strains of *S. aureus* are showing decreased sensitivity to vancomycin and in the last decade, the clinical and laboratories standards institute (CLSI) showed the minimum inhibitory concentration (MICs) of resistance, intermediate and susceptible *S. aureus* strains for vancomycin have changed from ≥ 16 to ≥ 32 $\mu\text{g/ml}$, from $\leq 4-8$ $\mu\text{g/ml}$ to $\leq 6-8$ $\mu\text{g/ml}$ and from ≤ 2 $\mu\text{g/ml}$ to ≤ 4 $\mu\text{g/ml}$ respectively [189]. It is obvious that the increase in antibiotic-resistance of *S. aureus* has focussed attention on the need for new strategies to tackle this problem. Such strategies include the introduction of novel antimicrobial agents, improved early detection of infection and improved antibiotic stewardship across the world.

Here, we have focussed on the idea of improving detection of infection and have used vancomycin-functionalised PNIPAMs as responsive binding moieties for *S. aureus*. While we have already described that the highly branched PNIPAM functionalised with vancomycin (HB-PNIPAM-van) can bind *S. aureus* resulting in altered LCST and consequent coil-to-globule transition and desolvation and that this could be useful for detection of infection, it is essential that use of this ‘detector’ would not lead to selection of yet more vancomycin resistance. Also, features of bacteria themselves could influence their interaction with the polymers and so we have extended the range of strains of *S. aureus* studied and explored their relative sensitivity to vancomycin.

There are several techniques used for measuring antimicrobial effect. The most common is determination of the MIC, which is the lowest concentration of active agent that inhibits the growth of the test organism. MICs are routinely determined by broth microdilution (BMD) or break-point in agar. The BMD method was chosen as the most appropriate for the form of the drug i.e. polymer-conjugated vancomycin –because it provides actual MICs rather than sensitivity to a pre-determined break point [189].

3.2 Materials

Vancomycin hydrochloride hydrate (Sigma Aldrich), Brain heart infusion broth (BHI; Sigma Aldrich), Brain heart infusion agar (Sigma Aldrich) were used as purchased. Four strains of *S. aureus* were used; NCTC 6571 (Oxford), S235, Newman and L9879. Two versions of PNIPAM were tested; L-PNIPAM-van, 25:1 HB-PNIPAM-van.

3.3 Methods

3.3.1 Determination of Minimum Inhibitory Concentration (MIC)

All bacterial strains were cultured in BHI broth and incubated overnight at 37°C. Vancomycin hydrochloride hydrate was dissolved in BHI broth and filter sterilised (0.22 µm). Twelve two-fold serial dilutions of vancomycin were prepared in 96 well plates with control wells containing BHI broth but no drug. Suspensions of each bacterial strain in BHI were adjusted to an optical density of 0.1 (600nm) and 100µl of each added to the wells containing the vancomycin. The plates were then incubated at 37°C overnight and the MIC determined by observing the lowest concentration where there is no bacterial growth. Each MIC test was conducted on two separate occasions. Figure 3.1 shows the layout of the wells with the relevant vancomycin concentrations. The 96 well plates were designed as figure 3.1. The concentrations of vancomycin ranged from 1250 µg/ml – 1.2µg/ml.

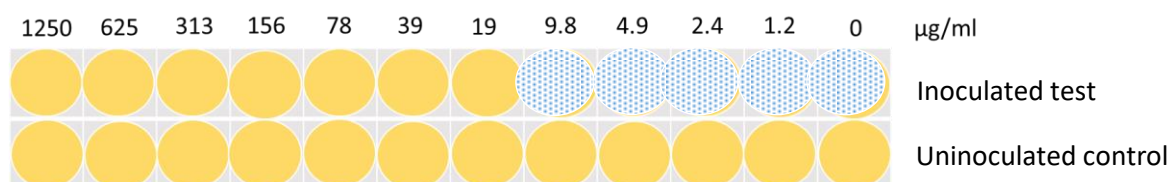


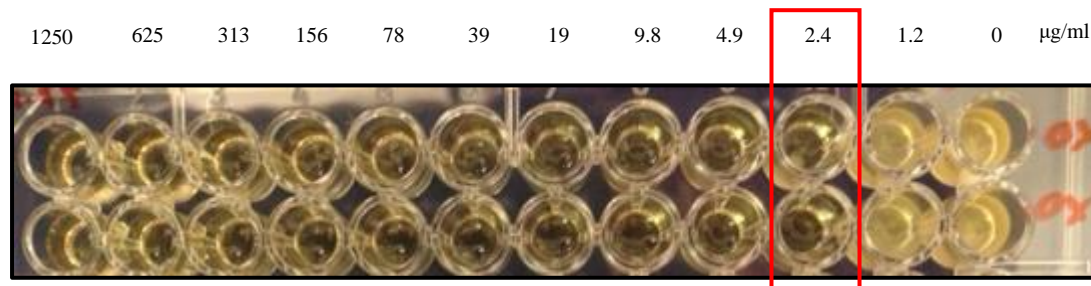
Figure 3.1 Schematic showing the layout of the 96 well plates with the range of the concentration of vancomycin. In this example the MIC for the strain is 19 µg/ml

3.4 Results and Discussion

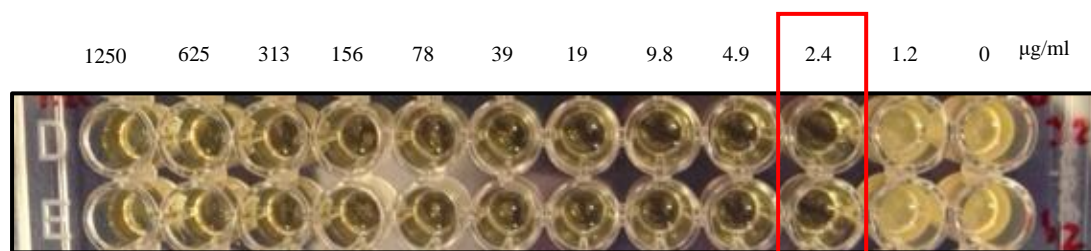
The minimum inhibitory concentrations (MIC) of vancomycin of the four strains of *S. aureus* employed are shown in Figure 3.2. Strain L9879 was the most sensitive (MIC 1.2 µg/ml), the sensitivity reference strain NCTC 6571 (Oxford) and the clinical isolate, S235 had an MIC of 2.4 µg/ml, while strain Newman was slightly more resistant (MIC 4.9 µg/ml) (Figure 3.2). The MICs of two vancomycin-functionalised polymers, were tested with the four *S. aureus* strains; L-PNIPAM-van, HB-PNIPAM-van. In contrast to the free vancomycin, no polymer demonstrated any inhibitory activity towards any of the strains up to a concentration of 1250 µg/ml (figure 3.3).

MIC of vancomycin of four *S. aureus* strains

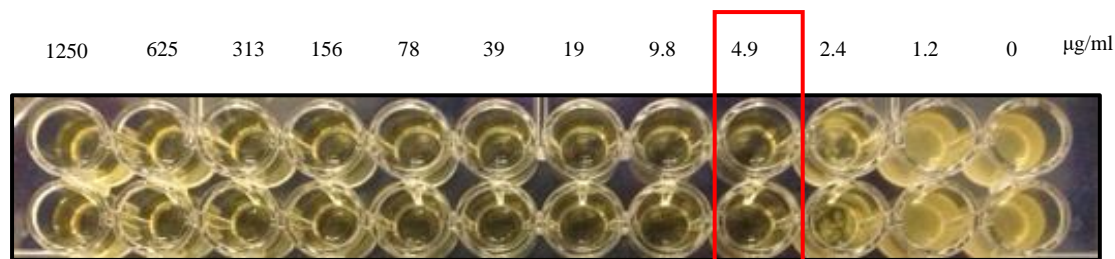
Oxford (NCTC 6571)



S235



Newman (Du5883)



L9879

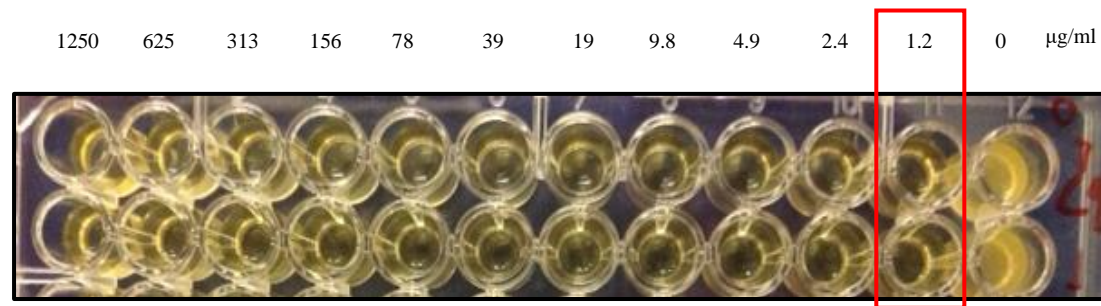


Figure 3.2 MICs of vancomycin of four strains of *S. aureus*. The lowest concentrations of vancomycin required to inhibit the visible growth of bacteria are the concentration between the last wells in which there is no bacterial growth and the first well showing growth (cloudy) after overnight incubation.

Table 3.1 MICs of vancomycin on the four strains of *S. aureus*

Types of strains	MICs (µg/ml)
Oxford (NCTC6571)	2.4
S235	2.4
Newman (Du5883)	4.9
L9879	1.2

MICs of the two different types of polymers functionalised with vancomycin

We then tested the linear and hyperbranched polymers functionalised with vancomycin, which had been purified by repeated precipitation (as described above), for inhibitory activity. The results are shown in Figure 3.3. Unlike free vancomycin, neither L-PNIPAM-van nor HB-PNIPAM-van had antimicrobial activity against any of the *S. aureus* strains and this was true for all batches of the polymers tested.

L-PNIPAM-van with Oxford (NCTC 6571) strain

1250 625 313 156 78 39 19 9.8 4.9 2.4 1.2 0 µg/ml



25:1 HB-PNIPAM-van with Oxford (NCTC 6571) strain

1250 625 313 156 78 39 19 9.8 4.9 2.4 1.2 0 µg/ml



Figure 3.3 Example images of antimicrobial activity testing of L-PNIPAM-van and HB-PNIPAM-van with Oxford (NCTC 6571) strain which show that neither polymers had any detectable inhibitory activity toward *S. aureus*

Krishnamurthy et al. synthesised bifunctional polymer with vancomycin and fluorescein in order to bind to *S. aureus*. They showed that the bifunctional polymer could recognise the Gram-positive bacterial surface and also provide specific binding by anti-fluorescein antibodies used for promoting phagocytosis of opsonised bacteria. Interestingly, they concluded that for bacteria to be bound to the polymer through vancomycin it is not necessary for the polymer molecule to diffuse through the peptidoglycan of bacterial cell wall [25, 36]. This confirms the work reported here and is consistent with our interpretation that HB-PNIPAM-van binds to bacteria and forms a polymer-bacteria complex but without killing

the organism. This can be explained by consideration of the bacterial cell wall structure. The peptidoglycan of bacterial cell walls comprises glycan chains with four appended amino acid peptides that are cross-linked to an adjacent peptide of a glycan chain. That cross-linking is mediated by cleavage of the terminal two amino acids, D-Ala-D-Ala, and the linking of the penultimate amino acid to the adjacent chain, usually via diaminopimelic acid or lysine residues [10]. Much of this cross-linking is thought to occur near the cytoplasmic membrane at the growing points [39]. The resultant cross-linked peptidoglycan is a three dimensional structure with pores and these pores provide an element of sieving since there is a size exclusion limit [190]. The diffusion ability of molecules mainly depends on shapes, relative sizes and the types of molecules [25, 191]. However, the bacterial cell walls are not uniform and pore sizes can be changed depending on several factors such as ionic environment. Additionally, the nature of solute, charge and hydrophobicity, and chemical reaction between matrix and solvent also have an effect on diffusion of molecules [192]. Scherrer et al. studied the sieving properties of the *Bacillus megaterium* cell wall using various types and sizes of hydrophilic molecules. They concluded that the cell walls of *B. megaterium* selectively allowed molecules, of M_n 70-120 kDa and a hydrodynamic radius of approximately 8.3 nm to pass through. However, this size range is not necessarily applicable to all Gram-positive bacterial cell walls since they demonstrate diversity in architecture and degree of cross-linking [191]. The staphylococcal cell wall is considered to be one a highly cross-linked type with about 80-90%, cross-linking while other species are about 50-55% cross-linked [190, 193]. From this it can be assumed that for molecules to penetrate into the *S. aureus* cell wall they would need to be smaller than 70kDa. However, that conclusion is only valid for linear polymers. Branched polymers are more compact and much higher molar masses can be attained with hydrodynamic radii in the 5 to 10 nm range. Lienkamp et al. also showed that antimicrobial activity depends on molecular weight of polymeric antimicrobials. They synthesised doubly-selective synthetic mimics of antimicrobial peptides (SMAMPs) that were able to differentiate between *E. coli* (Gram-negative) and *S. aureus* (Gram-positive) bacteria respectively and showed that SMAMPs with a molecular weight of 3000 g/mol could penetrate into the *S. aureus* cell wall and kill the cell, while SMAMPs of 50000 g/mol remained outside the peptidoglycan layer of *S. aureus* with concomitant loss of antimicrobial activity. They reported that the higher molecular weight the greater the hydrodynamic volume of the SMAMP [194]. Reporting the size of polymers is also important for a study of antimicrobial activity of materials. Therefore, hydrodynamic radii of the vancomycin

functionalised polymers are characterised. The number average R_H (R_{Hn}) can be also obtained from methanol SEC.

Here we have shown that both the L-PNIPAM-van and the HB-PNIPAM-van did not have antimicrobial activity against *S. aureus* but that the HB-PNIPAM-van still bound to bacteria and formed bacteria-polymer complexes. The result from methanol SEC of our L-PNIPAM-van and HB-PNIPAM-van clearly showed that the average molar mass and hydrodynamic radii of HB-PNIPAM-van was much higher than that of the SMAMP. Considering that the average molar mass of HB-PNIPAM-van and L-PNIPAM-van was about 2000 kg/mol and 640 kg/mol respectively (table 2.2) these are an order of magnitude larger than the SMAMPs of 5000 g/mol used in the study by Lienkamp et al.[194]. Moreover, the peak number average hydrodynamic radii of HB-PNIPAM-van and L-PNIPAM-van obtained from methanol SEC (Fig2.14) were approximately 20nm, which was greater than the exclusion size of *S. auerus* peptidoglycan (~8nm) reported by Lienkamp et al (2009). Particle sizes were also measured using a Brookhaven Instruments 90Plus particle size analyser, which provides both average diameter with the dispersity index and the size distribution. The average diameter of HB-PNIPAM-van was found to be 321 ± 4.4 nm while the mean diameter of L-PNIPAM-van was 380 ± 93 nm. The dispersity index of HB-PNIPAM-van and L-PNIPAM-van were 0.19 ± 0.01 and 0.44 ± 0.02 , respectively. The intensity distribution is shown in appendix 3. The large mean diameter of the polymer obtained from this technique is thought to indicate considerable aggregation of both polymers in dispersion at that temperature. Moreover, a high dispersity was observed for the L-PNIPAM-van, which coupled with a lower average zeta potential indicates a less stable colloidal dispersion in suspension. This is likely to be due to the polymer architecture.

There are several factors that can influence the quality of dynamic light scattering (DLS) data including long distance electrostatic interactions between the particles, the sample concentration, viscosity effects and multiple scattering. Even though, the method can be used to analyse samples consisting of a broad range of distribution of species, it is less reliable when used for non-rigid molecules, like our highly solvated coils of PNIPAM. Also, although the Stokes-Einstein equation provides hydrodynamic diameter values from the DLS measurement, it is only accurate when single scattering events are measured (i.e. that each photon detected has been scattered by the sample only once). If the polymer is highly solvated or contains large particles, it may significantly affect the precision of DLS analysis. Moreover, DLS at a fixed angle can only provide accurate results for single scattered light

and certain particles. Different sizes of particles scatter different intensities, which depend on the scattering angle. Thus, multiangle DLS at several scattering angles is recommended in order to provide the highest quality measurements. However, such an instrument was not available to us at the time this work was undertaken. More investigation using other techniques is required to determine the hydrodynamic radius of our polymers such as diffusion-ordered NMR spectroscopy (DOSY NMR). Swift et al. found that DOSY NMR provided a similar number average (R_{Hn}) of PNIPAM using the Stokes Einstein equation to the value determined from methanol SEC when the polymers were analysed in deuterated methanol [150]. Based on these results, we suggest that the vancomycin at the chain ends of HB-PNIPAM-van bind only to the D-Ala-D-Ala peptides available near the surface of the peptidoglycan and is not be able to diffuse through the *S. aureus* cell wall. Moreover, Demchick et al. studied the permeability of isolated saccule of the Gram-positive bacillus, *Bacillus subtilis*, using the fluorescein-labelled dextran. They found that, after an incubation time of 24h, only molecules with a mean radius 2-2.8 nm could penetrate the peptidoglycan, which corresponded to a linear polymer M_n of 24kDa. They concluded that any large globular molecules (>50 kDa) could not pass through their prepared cell walls [195]. Nonetheless, our hypothesis that actual penetration of the peptidoglycan by our L- and HB-PNIPAM-van polymers is not required for binding is supported by the report of Krishnamurthy et al. who found that a bifunctional polyacrylamide with vancomycin and fluorescein (pA-V-F), which had a particle size of about 100 nm and a molecular weight was 136 kDa, could interact with D-Ala-D-Ala of peptidoglycan of Gram-positive bacteria but did not diffuse through that layer. They confirmed that such a polymer was too large to pass to the membrane surface and did not act as a lytic antibiotic [25]. These data and our data seem to suggest that the HB-PNIPAM-van interacts with a proportion of the D-Ala-D-Ala peptide located towards the surface of the bacterium, as illustrated in Figure 3.4.

A schematic summarising how HB-PNIPAM-van could be interacting with the cell wall of *S. aureus* is showed in figure 3.4 below.

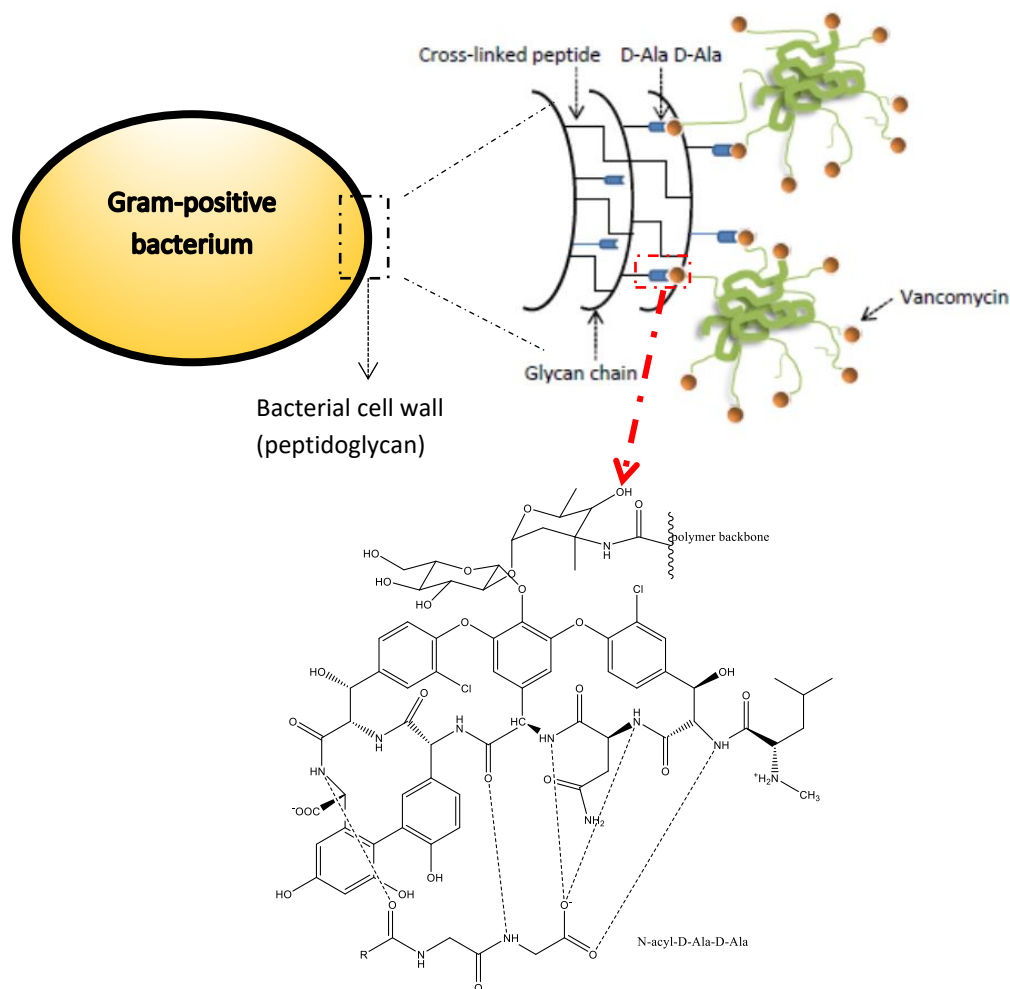


Figure 3.4 A model explaining how HB-PNIPAM with vancomycin chain ends could interact with D-Ala-D-Ala peptides in the cell wall without influencing the integrity of the cell wall (not to scale)

3.5 Conclusions

In conclusion, we have shown that purification by repeated salt and heat precipitation results in highly purified vancomycin functionalised L-PNIPAM and HB-PNIPAM. Our data show that these polymers do not kill *S. aureus* because they are too large, in terms of M_n and hydrodynamic radii, to penetrate sufficiently into the cell wall to bind to enough uncross-linked D-Ala-D-Ala residues to disrupt the integrity of the peptidoglycan wall. Further work is required to obtain definitive particle size data but all indications are that the polymers are too large to penetrate through bacterial peptidoglycan. We conclude, therefore, that the binding interaction involves only surface-located D-Ala-D-Ala on the bacterial cell wall. This is most likely to be concentrated near cell division sites.

Chapter 4 : The effect of hydrophobicity and electrostatic charge of bacteria on binding ability of the polymers

4.1 Introduction

Over the last decade, several studies have focused on the development of polymeric materials that can either detect or capture microorganisms for diagnostic purposes [26]. One of the major reasons for the interest in synthetic polymers is that they not only are able to interact with microorganisms but also have desirable functionalities that can be designed [34, 35].

The binding of microorganisms to their targets is a complex process. There are a variety of factors that influence the system, such as hydrophobicity of the bacterial cell surface and its targets or electrostatic interaction between bacteria and receptors [192]. The hydrophobicity of various strains of *S. aureus* has been considered an important property that plays a crucial role in the interaction between the bacteria and targets, such as host tissues or medical devices [47, 48] and Rosenberg *et al.* showed that the hydrophobic nature of bacteria plays a crucial role in the attachment of bacteria to living and non-living target surfaces [192, 196]. Jonsson and Wadstrom showed that strains of *S. aureus* with high levels of surface protein A exhibit better interaction with the hydrophobic-interaction chromatography matrix, Octyl Sepharose and it is thought that this feature also influences its ability to adhere to other surfaces, including mammalian targets [197]. However, given the apparent importance of PNIPAM desolvation in the response to bacterial interaction, we wished to explore whether electrostatic charge and hydrophobicity influence the interaction between *S. aureus* and vancomycin-functionalised PNIPAM polymers.

4.2 Hydrophobicity test of *S. aureus* strains

It is well known that there is variation in the hydrophobicity of *S. aureus* strains and this can affect their behaviour in terms of adherence to surfaces and other binding properties [192]. This variation in hydrophobicity depends on the presence and amount of certain molecules on the bacterial cell surface, for example for *S. aureus* the structure and amount of protein A and IsdA [46, 198]. Given that our results in chapter 2 (section 2.4.4) showed that the change in hydrophobicity of the polymer chain end significantly affects the phase transition temperatures and solubility of our PNIPAM polymers, it seemed possible that the hydrophobicity/hydrophilicity of a strain may influence its binding of our vancomycin-functionalised polymers. We therefore compared the hydrophobicity of strains of *S. aureus* and correlated that with their ability to form aggregates with the vancomycin-functionalised polymers.

The method of assessing bacterial hydrophobicity used in this work was based on their partition between the non-polar solvent, hexadecane, and an aqueous phase, (phosphate-urea-magnesium buffer; PUM). The degree of hydrophobicity correlates with the degree of partition into the hydrophobic solvent.

4.2.1 Materials

Hexadecane (Sigma Aldrich) was used as purchased. $\text{KH}_2\text{PO}_4 \cdot 3\text{H}_2\text{O}$ (Sigma Aldrich), KH_2PO_4 (Sigma Aldrich), $\text{MgSO}_4 \cdot 7\text{H}_2\text{O}$ (Sigma Aldrich), urea (Sigma Aldrich) were used as received.

4.2.2 Methods

Phosphate-urea-magnesium buffer (PUM buffer) was prepared by dissolving 7.26 g of $\text{KH}_2\text{PO}_4 \cdot 3\text{H}_2\text{O}$, 19.7 g of K_2HPO_4 , 0.2 g of $\text{MgSO}_4 \cdot 7\text{H}_2\text{O}$ and 1.8 g of urea in 1 dm³ of deionised water. *S. aureus* NCTC 6571 (Oxford), S235, L9879 and Newman were grown overnight in BHI broth at 37°C. The cells were harvested by centrifugation and washed with PBS three times. After that, the bacterial strains were resuspended in PUM buffer to 10⁸ cells/ml. The hydrophobicity of each strain was determined using the method of Rosenberg et al. [199]. Briefly 200 µl of n-hexadecane was added to 3 ml of each bacterial suspension, vortex mixed for 2 minutes, and then left for 15 minutes at room temperature to allow the two solvents phases to separate. The aqueous phase, which was the lower layer, was carefully collected and its optical

density (OD) measured at 540 nm using a spectrophotometer. The % hydrophobicity was calculated by equation 4.1.

$$\%hydrophobicity = \frac{Initial\ OD - Final\ OD}{Initial\ OD} \times 100 \quad eq.4.1$$

Initial OD = Absorbance values of aqueous bacterial suspension before adding n-hexadecane

Final OD = Absorbance values of aqueous phase (bacterial suspension) after mixing with n-hexadecane

S. aureus strains considered highly hydrophobic show values $\geq 50\%$. The values between 20%-50% are considered to be moderately hydrophobic and hydrophilic strains have values less than 20%.

4.2.3 Results and discussion

The % hydrophobicity of the four strains of *S. aureus* obtained by the hexadecane partition method are shown in figure 4.1.

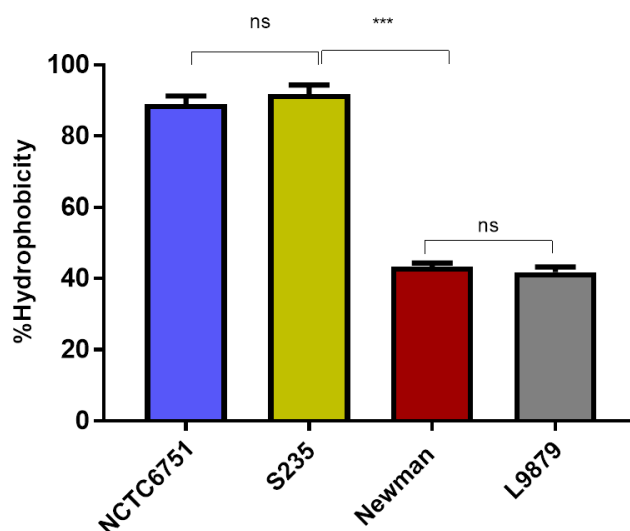


Figure 4.1 %Hydrophobicity of four strains of *S. aureus*, namely Oxford (NTC6571), S235, Newman and L9897. The significance between differences in zeta potential were tested using one way ANOVA incorporating Tukey's multiple comparison statistical test. The degree of significance is defined by *P* value: *** $P \leq 0.001$, ns = not significant, $P > 0.05$

Figure 4.1 shows that the % hydrophobicity of the NTC6571 (Oxford) and S235 strains was $89\% \pm 3.2$ and $91\% \pm 3.7$ respectively, which indicates that they are hydrophobic strains, whereas the % hydrophobicity of the L9879 and Newman strains was $41\% \pm 2.1$ and $43\% \pm 1.4$ respectively, indicating that they were only moderately hydrophobic strains.

Wilkinson et al. showed that *S. aureus* is typically hydrophobic and its level of hydrophobicity increases in stationary-phase cultures compared with exponential-phase cultures [192]. The cultures used here were in stationary phase. As mentioned above, there are several factors that influence the hydrophobicity-hydrophilicity of *S. aureus*. Rosenberg et al. revealed that hydrophobicity of *S. aureus* correlated with presence of protein A on the cell surface and Reifsteck et al. suggested that fibronectin-binding proteins, as well as protein A play a primary role in the total cell surface hydrophobicity of staphylococci. However, capsulation also affects hydrophobicity as this is a relatively hydrophilic layer on the cell wall [192, 196].

4.3 Assessment of polymer binding to bacteria

Having determined the relative hydrophobicity of four strains of *S. aureus*, we now wanted to see if there was any correlation between that property and their ability to interact with the vancomycin-functionalised polymers.

4.3.1 Materials

UltraPure™ Ethidium bromide (EtBr) (Thermo Fisher) was used as received. Alexa Fluor® 488 (abcam) was used as purchased. DMSO (Sigma Aldrich) was used as received.

4.3.2 Methods

Bacteria preparation

Four strains of *S. aureus* were employed, namely Oxford (NCTC 6751), S235, L9879 and Newman. These were cultured in BHI broth at 37°C overnight, washed in PBS and resuspended in appropriate buffer to obtain the desired concentration (cells/ml).

Bacterial counting

1 μl of bacterial suspension was diluted with PBS (49 μl) and 5 μl of this suspension was added to a Helber counting chamber to count the total number of bacteria present. Equation 4.2 was used to calculate the number of bacteria per millilitre.

$$\frac{X}{80} \times 400 \times 50 \times 100 \times df = \text{the number of bacteria in ml eq. 4.2}$$

X = the number of bacteria counted in one small square of the chamber

df = dilution factor (usually 1:50)

The volume of bacterial suspension to provide the required number of bacteria per well was calculated using equation 4.3 To visualise the bacteria in the mat/button experiments, they were suspended in PBS/Ethidium bromide.

$$\frac{\text{Desired number of bacteria } \left(\frac{\text{cfu}}{\text{ml}}\right)}{\text{Original number of bacteria / ml } \left(\frac{\text{cfu}}{\text{ml}}\right)} \times V = \text{the volume of bacteria in suspension } (\mu\text{l}) \text{ eq. 4.3}$$

$$V = \text{total volume per well } (\mu\text{l})$$

Mat/button aggregation – rapid method for assessing bacterial binding to PNIPAM-van polymers

5mg of L-PNIPAM-van and HB-PNIPAM-van was dissolved in 1ml of PBS. The concentration of each strain *S. aureus* was prepared at 1×10^8 cells/ml. HB-PNIPAM-van and L-PNIPAM-van solutions were incubated with each strain individually in PBS at 37°C for 24 hours in round-bottomed 96 well plates. In this method non-aggregated bacteria settle to the bottom of the well rolling down the sides to collect as a tight button. Aggregated bacteria, however, settle as a thin mat and are unable to roll down to form a button. The controls of the experiment were HB-PNIPAM-van, L-PNIPAM-van, and *S. aureus* alone and prepared under the same conditions. After 24 hours, the samples were viewed under UV light. The binding ability of the polymers was extrapolated from their ability to form a mat of polymer-bacteria complex compared with the controls.

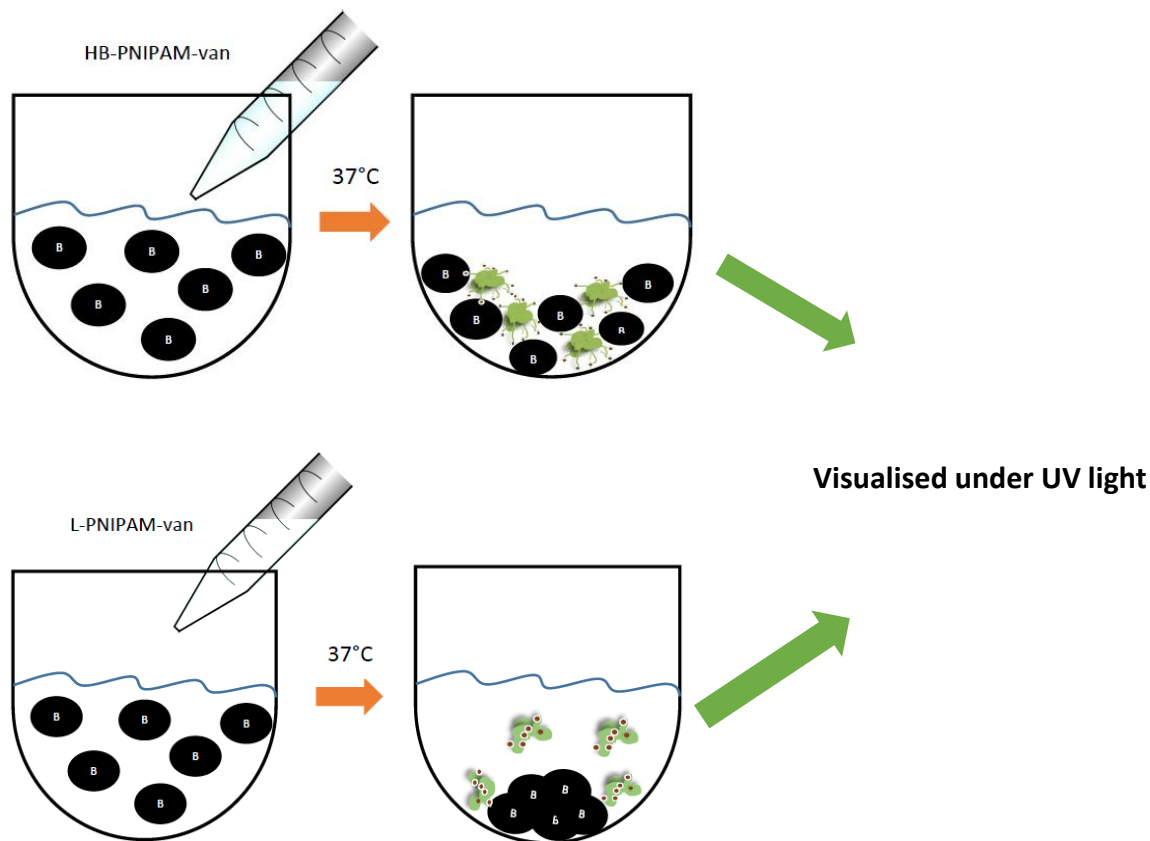


Figure 4.2 The scheme of rapid Mat/button assay for HB-PNIPAM-van and L-PNIPAM-van

4.3.3 Results and discussion

4.3.3.1 Aggregation assay (mat-button) comparing HB-PNIPAM-van and Linear PNIPAM -van using *S. aureus* Oxford (NCTC6751)

Highly branched and linear polymers were incubated in PBS without bacteria as controls (Fig 4.3 J, K). HB-PNIPAM-van and L-PNIPAM-van (samples were incubated with 1×10^8 cfu/ml of the *S. aureus* Oxford (NCTC6751) in PBS (Fig 4.3 B, E, H and A, D, G respectively)). Bacteria alone are shown in fig 4.3 C, F, I. After 2, 4 and 24 hours of incubation to allow the bacteria to attach to the polymer modified with antibiotics, the samples were visualised under UV light, and images were captured. The bright area shows the location of non-aggregated bacteria.

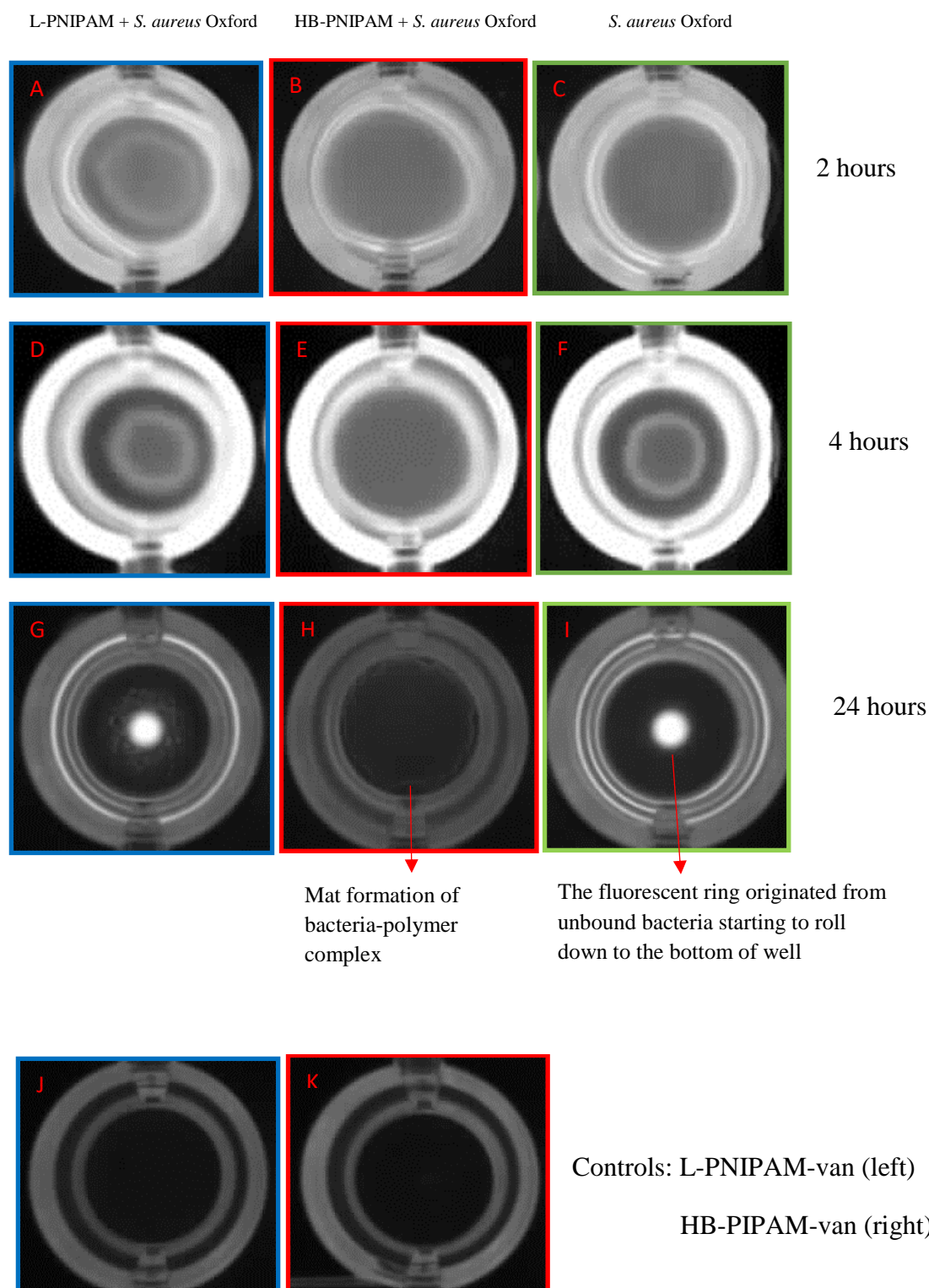


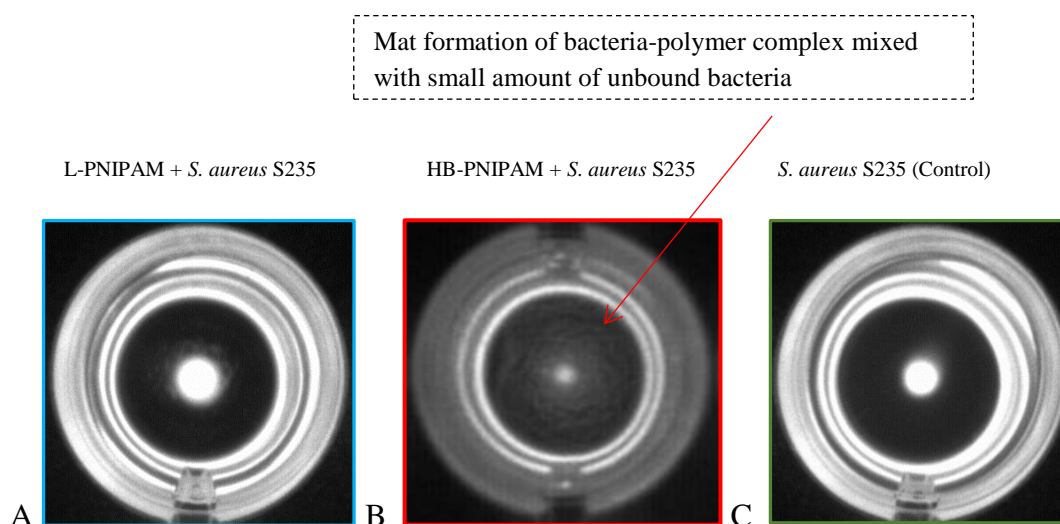
Figure 4.3 Images captured under UV light of HB-PNIPAM-van and L-PNIPAM-van incubated with *S. aureus* (1×10^8 cfu/ml) for 2, 4 and 24 h (panels A-K). A central 'button' of cells represents no aggregation in L-PNIPAM-van (Fig 4.3I), whereas panel H shows a mat of aggregated bacteria and HB-PNIPAM-van (arrow). L-PNIPAM-van incubated with *S. aureus* Oxford (NCTC6751) (1×10^8 cfu/ml) for 2, 4 and 24 hours imaged under UV-light (A,

D and G respectively). Control L-PNIPAM-van in PBS (J). HB-PNIPAM-van incubated with *S. aureus* Oxford (NCTC6751) (1×10^8 cfu/ml) for 2, 4 and 24 h images under UV-light (B, E and H respectively). Control HB-PNIPAM-van in PBS (K). *S. aureus* Oxford (NCTC6751) (1×10^8 cfu/ml) in PBS at 2, 4 and 24 hours (C, F and I respectively)

After incubation for 2 h, it was observed that the mat was formed in HB-PNIPAM-van whereas there was a bright ring in L-PNIPAM-van, which indicated that bacteria had started to collect at the bottom of the well. Further incubation until 24h showed the collection of bacteria more clearly (Fig 4.3 G v. H) with a clear mat forming in the HB-PNIPAM-van but a button in the presence of L-PNIPAM-van, which appeared similar to the controls.

4.3.3.2 Aggregation assay (mat-button method) comparing HB-PNIPAM-van and Linear PNIPAM -van in the presence of other strains of *S. aureus*

The previous results showed that the complete aggregation of bacteria-polymer complex was fully formed after 24 hours' incubation, therefore, in order to investigate the aggregation of other strains, namely S235, L9879 and Newman, a 24 h incubation period was used.



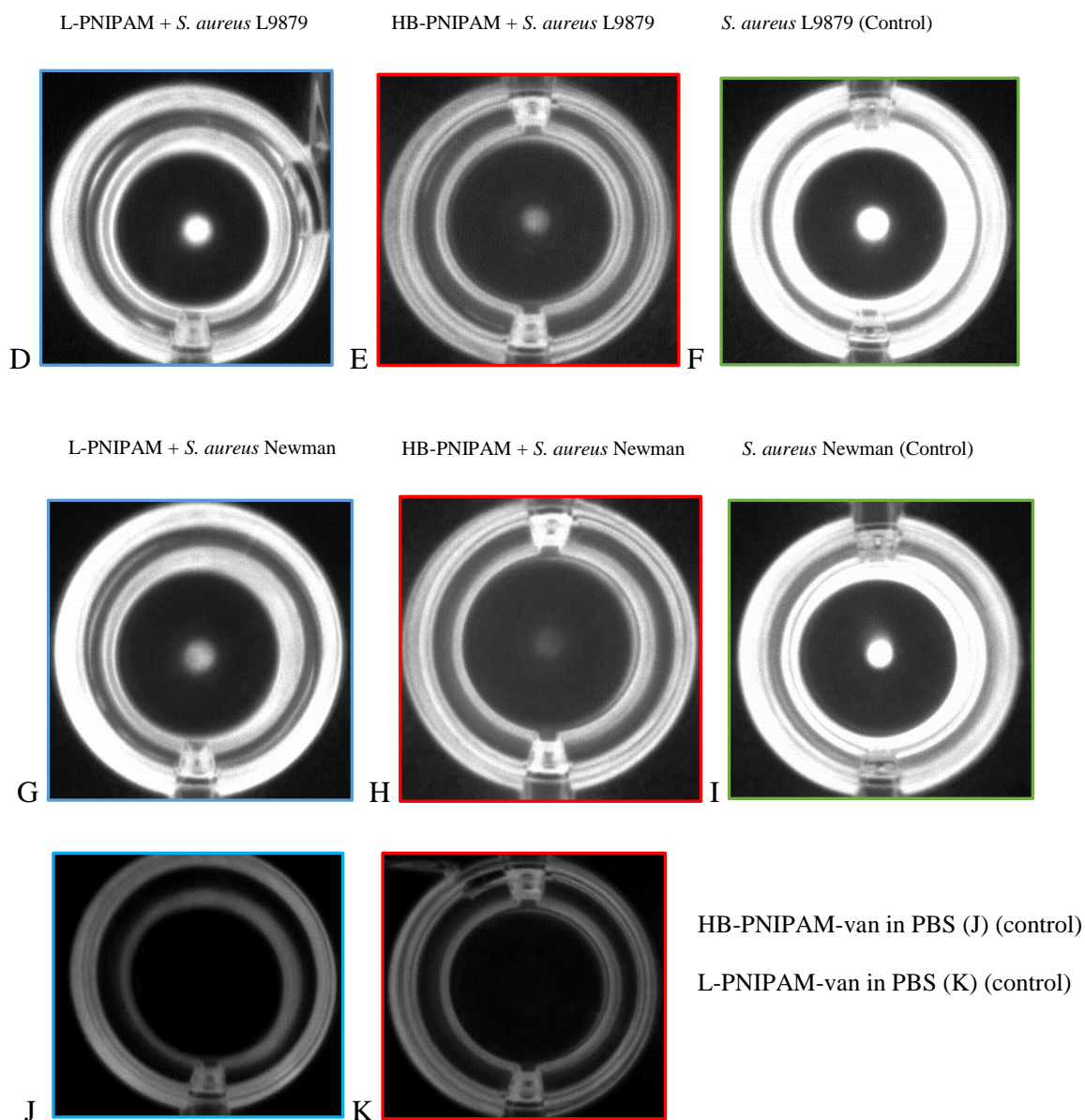


Figure 4.4 Images captured under UV light of HB-PNIPAM-van and L-PNIPAM-van incubated with *S. aureus* S235, L9879 and Newman (1×10^8 cfu/ml) for 24 h (panels A, B, D, E, G and H) L-PNIPAM -van incubated with *S. aureus* S235 (A), HB-PNIPAM-van incubated with *S. aureus* S235 (B), Control *S. aureus* S235 in PBS (C). L-PNIPAM -van incubated with *S. aureus* L9879 (D), HB-PNIPAM-van incubated with *S. aureus* L9879 (E), Control *S. aureus* L9879 in PBS (F), L-PNIPAM -van incubated with *S. aureus* Newman (G), HB-PNIPAM-van incubated with *S. aureus* Newman (H), Control HB-PNIPAM-van in PBS (J), Control L-PNIPAM-van in PBS (K), L-PNIPAM-van fails to bind to *S. aureus* S235, L9879 and Newman as the tight buttons of non-aggregated cells show in the centre of (A), (D) and (G). A slightly smaller button mixing with some aggregates was observed in HB-PNIPAM-van incubated with *S. aureus* S235 (fig 4.4B)

Linear-PNIPAM-van and HB-PNIPAM-van were prepared using similar chemical synthetic processes and with equivalent amount of vancomycin loading. Summary of results for both polymers can be seen in table 4.1.

Table 4.1 Summary of molar mass averages, vancomycin content, degree of functionality and LCST of L-PNIPAM-van and HB-PNIPAM-van

Polymer	M_n^a (kg/mol)	$D_{(w/n)}^a$	Loading of vancomycin ^b (mg per mg of polymer)	% vancomycin functionality ^c	LCST ^d (°C)
L-PNIPAM-van	640	1.33	0.028	2.6	37
HB-PNIPAM-van	2,000	3.48	0.025	3	33

^a Data calculated from methanol SEC

^b Loading of vancomycin (per mg of polymer) determined by ELISA

^c Percentage vancomycin functionality estimated by rise of peak at 5.2-5.6 ppm (1H integrals per vancomycin) compared to the isopropyl peak (1H integrals per backbone unit) from ¹HNMR of purified products in D₂O

^d LCST determined by microDSC

The *S. aureus* laboratory strain Oxford (NCTC6751) is employed as a standard for in vitro antibiotic sensitivity assays and was used here initially as a representative of the species. HB-PNIPAM-van was efficiently bound to this strain (fig 4.3), as it formed a mat of bacteria-polymer complex, whereas the linear analogue version L-PNIPAM-van did not but instead a button was formed, which was similar to the control of bacteria alone in PBS.

For the similarly hydrophobic strain, S235, which is a clinical isolate obtained from the Royal Hallamshire hospital, HB-PNIPAM-van could also bind to the bacteria showing mat formation in the assay. However, small amounts of unbound bacteria still appeared as tiny buttons, but the amount of unbound bacteria was much smaller than that of the control. Again with the linear polymer, a button of unbound bacteria was formed.

The L9879 and Newman strains were more hydrophilic than the other two strains. L9879 is a clinical isolate from the RHH diagnostic laboratory and strain Newman is a widely used strain in research labs. The former has a truncated protein A (I. Douglas, personal communication) while the latter does not retain the fibronectin-binding proteins on its cell surface [200]. It was found that HB-PNIPAM-van failed to form a mat (aggregate) with either strain and buttons were clearly visible. However, compared with the control and the L-PNIPAM-van polymer, the buttons were less distinct and slightly smaller. It could be speculated that HB-PNIPAM-van was able to bind to small amounts of bacteria but was not efficient enough to cause aggregation of bacteria compared with the Oxford (NCTC6751) and S235 strains. L-PNIPAM-van again failed to bind to either the L9879 or Newman strains as shown by button formation in the assay. There was no visible change in wells containing L-PNIPAM-van and HB-PNIPAM-van polymers alone after incubation.

To confirm that the mats seen in the above assay represent the formation of aggregates, confocal microscopy was used to examine them further.

Confocal microscopy is a versatile technique that is widely used in the fields of biomedical and material sciences. It has the advantages over traditional light microscopy of higher resolution and the ability to visualise both the lateral and axial directions as well as generating three-dimensional images. This technique can also be used to image living or fixed cells that are labelled with fluorescent dyes.

4.3.3.3 Confocal imaging of all samples

In order to view samples by confocal microscopy, bacteria were labelled with Alexa Fluor® 488 fluorescent dye. *S. aureus* NCTC6571 (Oxford), S235, L9879, Newman were studied and *P. aeruginosa* was used as a control Gram-negative species. All strains were subcultured overnight, then, the cells were harvested by centrifugation and washed with PBS three times. 1mg of Alexa Fluor® 488 was dissolved in 1 ml of DMSO. 10 ml of Alexa Fluor® 488 solutions was added into 10^8 cfu of bacteria in 1 ml of carbonate buffer pH 8.5. The mixtures were incubated with shaking at 4°C for 2 hours. Afterwards, bacteria were washed with PBS three times in order to remove unbound dye. HB-PNIPAM-van and L-PNIPAM-van samples were incubated with fluorescent *S. aureus* (10^8 cfu/ml) in PBS at 37°C overnight. The controls were *S.*

aureus without polymer and the polymers were added to *P. aeruginosa*, which should not bind vancomycin.

After incubating for 24 h to allow the bacteria to attach to the vancomycin-functionalised polymers, the samples were visualised by confocal microscopy. Representative images are shown in figures 4.5 – 4.8. In figure 4.5, *P. aeruginosa*, the Gram-negative control species, was seen not to aggregate with either of the PNIPAM-van polymers, whereas *S. aureus* Oxford (NCTC6751) aggregated with the HB-PNIPAM-van (fig. 4.5F) but not the linear analogous version (fig 4.5E). This finding conformed the specificity of binding of the vancomycin-moiety on the HB-PNIPAM-van by the observation that *P. aeruginosa* did not aggregate. The control (fig 4.6D) also showed no aggregates.

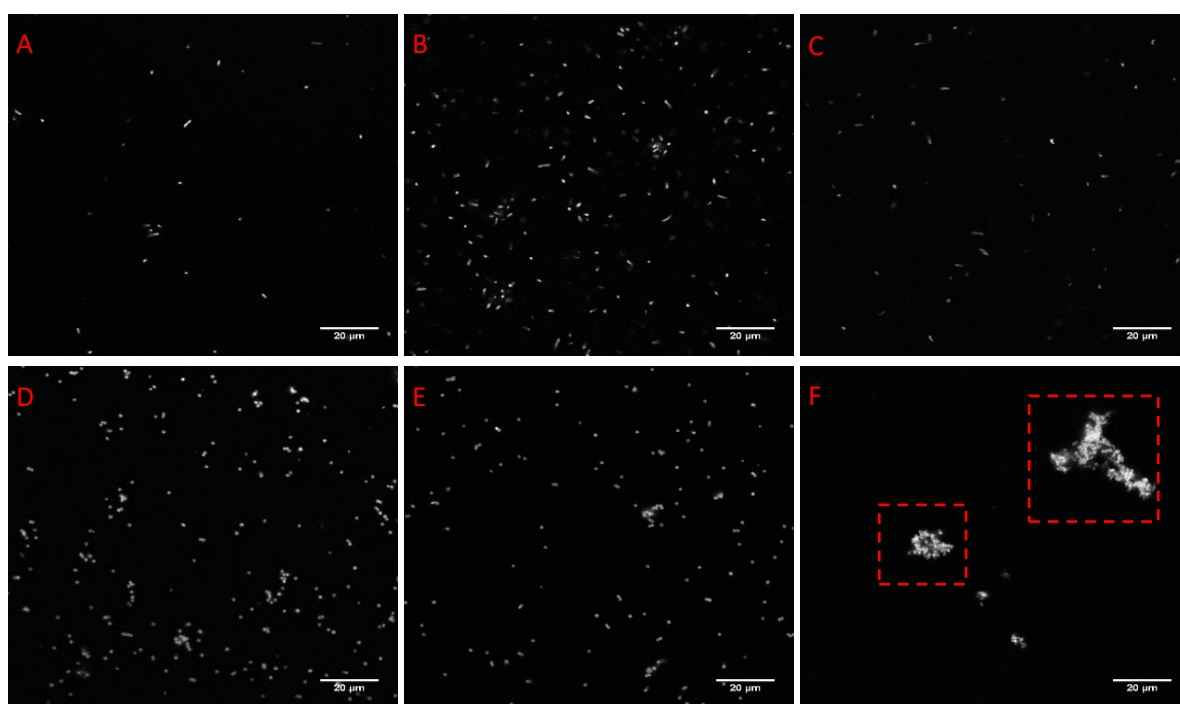


Figure 4.5 Confocal images of *P. aeruginosa* and *S. aureus* Oxford (NCTC6751) (both 1×10^8 cfu/ml) incubated for 24 h at 37 °C. *P. aeruginosa* in PBS (A). L-PNIPAM-van incubated with *P. aeruginosa* (10^8 cfu/ml) in PBS (B). HB-PNIPAM-van incubated with *P. aeruginosa* (10^8 cfu/ml) in PBS (C). *S. aureus* Oxford (NCTC6751) (10^8 cfu/ml) in PBS (D). L-PNIPAM-van incubated with *S. aureus* Oxford (NCTC6751) (10^8 cfu/ml) in PBS (E). HB-PNIPAM-van incubated with *S. aureus* (10^8 cfu/ml) in PBS (F). These assays were conducted at 37°C.

In figures 4.5 and 4.8, the white spots/or green spots showed the location of bacteria. It was observed that large clumps of *S. aureus* Oxford (NCTC6571) and S235 cells were formed with HB-PNIPAM-van whereas no clusters of bacteria were found in the presence of L-PNIPAM-van or in the PBS control.

S. aureus strain Newman did not form a proper mat with HB-PNIPAM-van and this corresponded with the confocal microscope images (figure 4.8) that show only small clumps of fluorescent *S. aureus* Newman. This also occurred when *S. aureus* strain L9879 was incubated with HB-PNIPAM-van (figure 4.7). Both the mat/button assay and the confocal microscope images demonstrate that HB-PNIAM-van is capable of binding to *S. aureus* strains Oxford (NCTC6751) and S235 at 37°C, above its LCST. Although strains L9879 and Newman did develop small aggregates of cells when incubated with HB-PNIPAM-van, they were considerably smaller than that seen with strains Oxford (NCTC6751) and S235. Also, L-PNIPAM-van was unable to bind to any strain of *S. aureus* above the LCST of the polymer suggesting that the polymer architecture plays a significant role in the accessibility of its binding ligand to its target. The binding of four strains of *S. aureus* to both types of polymers are summarised in table 4.2.

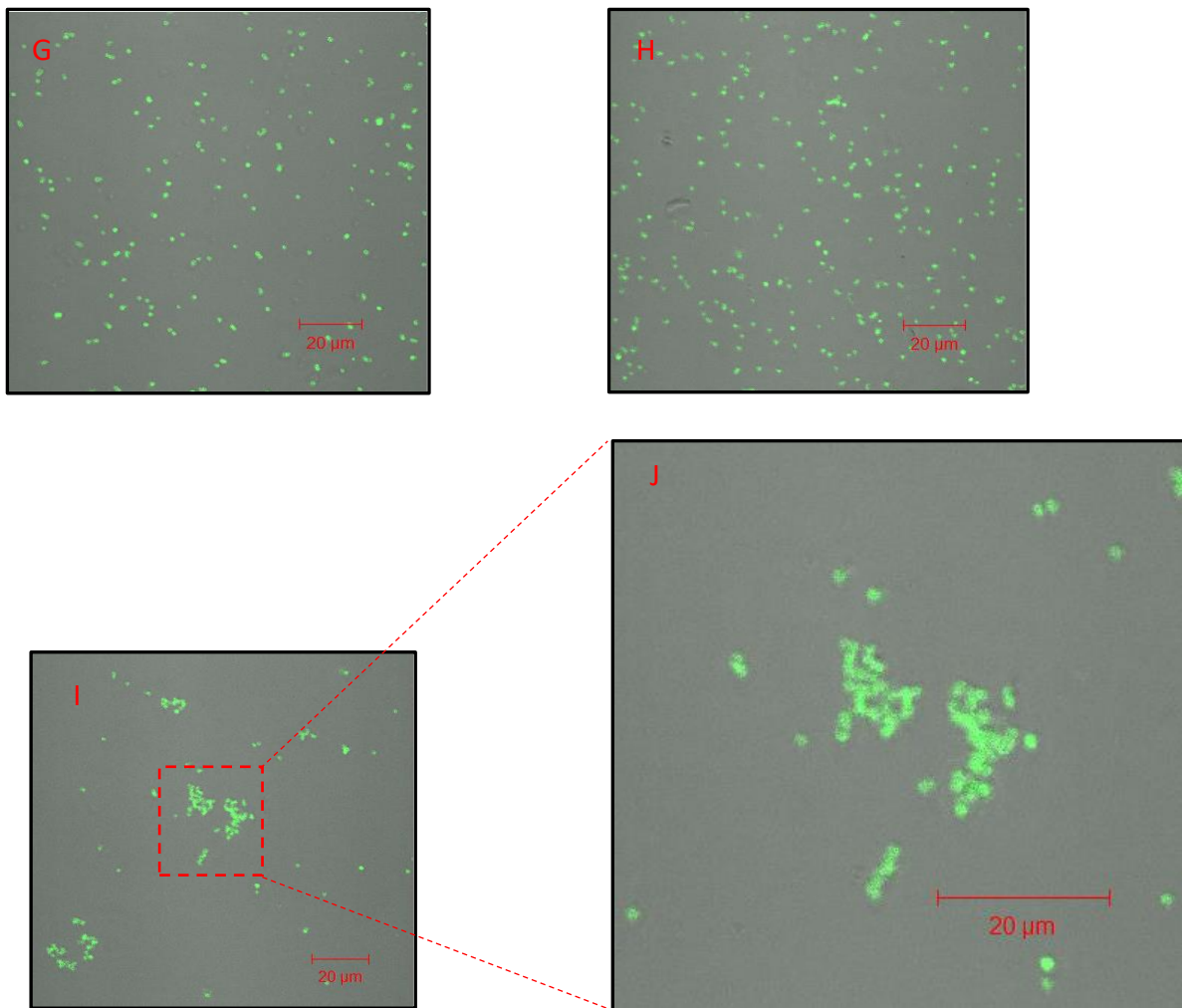


Figure 4.6 Confocal images of *S. aureus* strain S235 (1×10^8 cfu/ml) incubated at 37°C for 24 h in (G) PBS; (H) L-PNIPAM-van; (I) HB-PNIPAM-van. (J) Zoom in of HB-PNIPAM-van incubated with *S. aureus* S235.

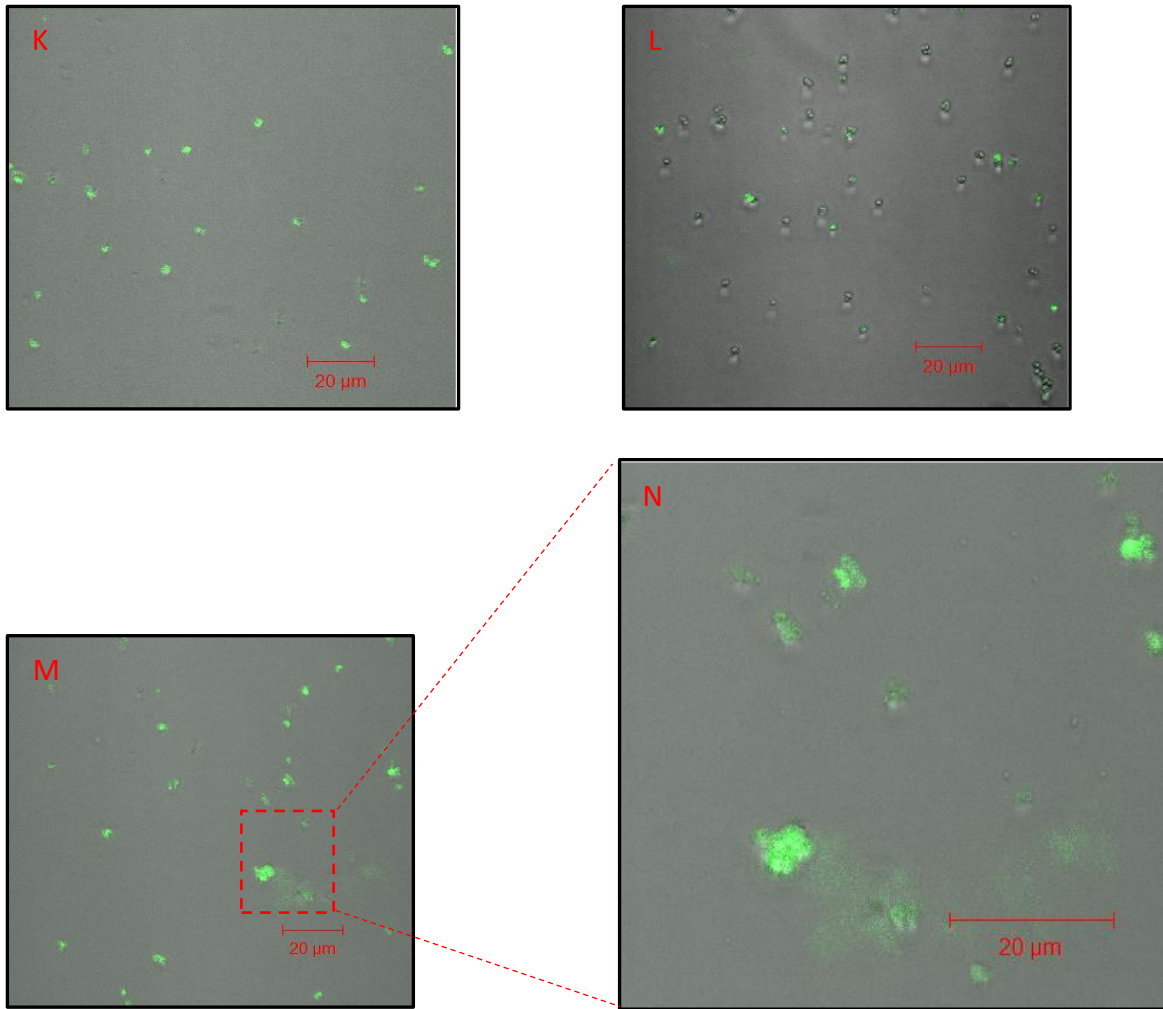


Figure 4.7 Confocal images of HB-PNIPAM-van and L-PNIPAM-van incubated with *S. aureus* Newman (10^8 cfu/ml) in PBS at 37°C for 24 h in (K) PBS; (L) L-PNIPAM-van; (M) HB-PNIPAM-van . (N) Zoom in of HB-PNIPAM-van incubated with *S. aureus* Newman.

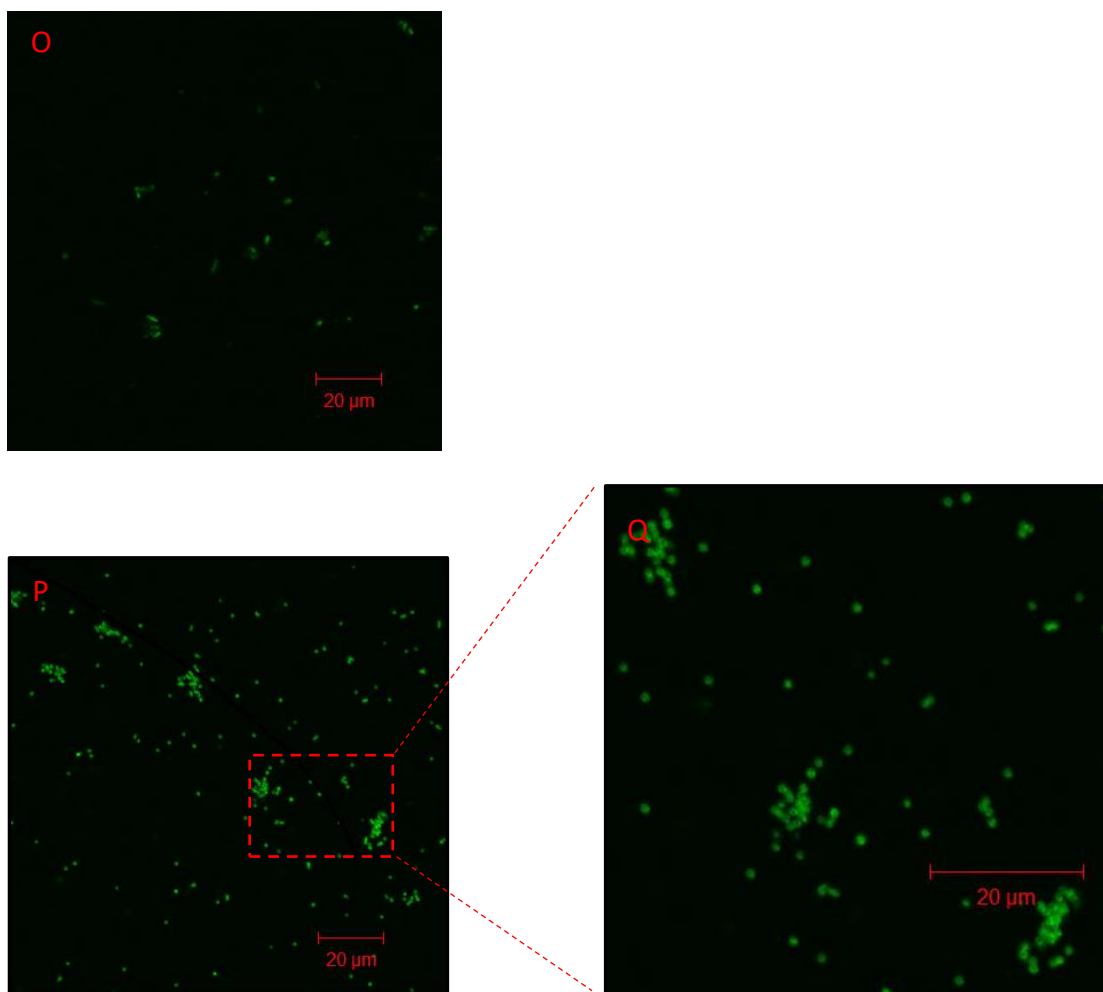


Figure 4.8 Confocal images of HB-PNIPAM-van and L-PNIPAM-van incubated with *S. aureus* L9879 (10^8 cfu/ml) in PBS at 37°C for 24 h with (O) L-PNIPAM-van, (P) HB-PNIPAM. (Q) Zoom in of HB-PNIPAM incubated with *S. aureus* L9879.

Another aspect to be considered is the interaction between the polymers and the bacteria at temperatures below their LCST, when both polymers would be in the solvated form. To investigate this, mat/button assays were carried out at room temperature in PBS. Figure 4.9 (A-H) shows the results of this study.

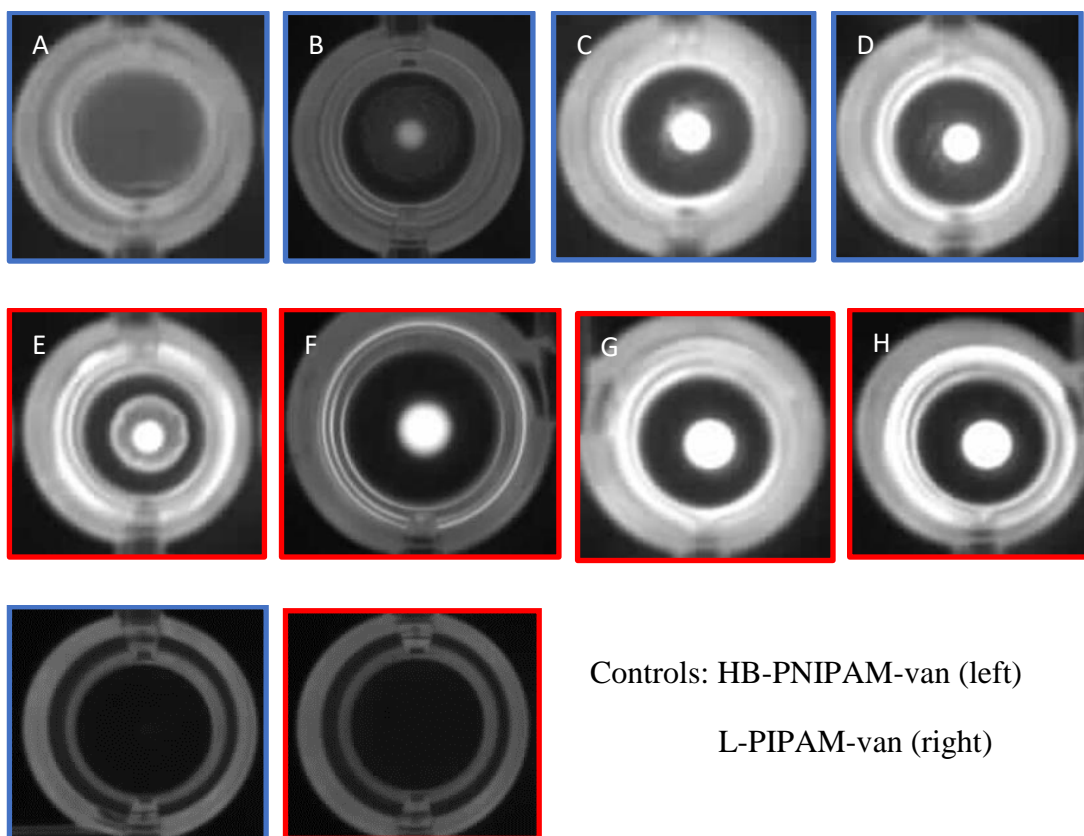


Figure 4.9 Images of *S. aureus* strains (1×10^8 cfu/ml) incubated with HB-PNIPAM-van and L-PNIPAM-van for 24 hours in PBS at room temperature (22°C). HB-PNIPAM-van incubated with *S. aureus* (Oxford) (A). HB-PNIPAM-van incubated with *S. aureus* (S235) (B). HB-PNIPAM-van incubated with *S. aureus* (Newman) (C). HB-PNIPAM-van incubated with *S. aureus* (L9879) (D). L-PNIPAM-van incubated with *S. aureus* (Oxford) (E). L-PNIPAM-van incubated with *S. aureus* (S235) (F). L-PNIPAM-van incubated with *S. aureus* (Newman) (G). L-PNIPAM-van incubated with *S. aureus* (L9879) (H).

A summary of the results of these aggregation assays comparing HB-PNIPAM-van and L-PNIPAM-van with four *S. aureus* strains below and above the LCST is shown below in table 4.2.

Table 4.2 Summary of results of binding of four *S. aureus* strains to HB-PNIPAM-van and L-PNIPAM-van at below and above the LCST of the polymers

Samples	Oxford		S235		Newman		L9879	
	22°C	37°C	22°C	37°C	22°C	37°C	22°C	37°C
HB-PNIPAM-van	++	++	+	+	-	-	-	-
L-PNIPAM-van	+	-	-	-	-	-	-	-

(++ represents complete mat formation, + represents a mixture of aggregated and non-aggregated bacteria; – represents unbound bacteria)

To determine the mechanism of phase change of PNIPAM-vancomycin with *S. aureus*, it is necessary to understand the basic mechanism of free vancomycin interactions with the bacterial cell wall. As described earlier, the *S. aureus* cell wall consists of highly cross-linked peptidoglycan, which is a cross-linked structure of strands of alternating *N*-acetylglucosamine (NAG) and *N*-acetylmuramic acid (NAM) and tetrapeptide chains (L-Alanine-D-Glutamic acid-L-Lysine- D-Alanine) that are cross linked from the lysine component to adjacent chains by pentapeptide glycine bridges [187, 201]. However, during synthesis of new peptidoglycan units the initial NAM-NAG-peptide complex that is transported across the cell membrane has a pentapeptide rather than a tetrapeptide. The pentapeptide terminates in D-Alanine-D-Alanine and the ultimate D-Alanine is cleaved during the transpeptidation cross-linking process. Vancomycin binds to D-Alanine-D-Alanine and so hinders the cross-linking reaction resulting in a weakened cell wall and subsequent osmotic lysis. Vancomycin binds to *N*-Acetyl-D-Alanine-D-Alanine through 5 hydrogen bonding interactions [55, 56, 202], shown as dashed lines in figure 4.10.

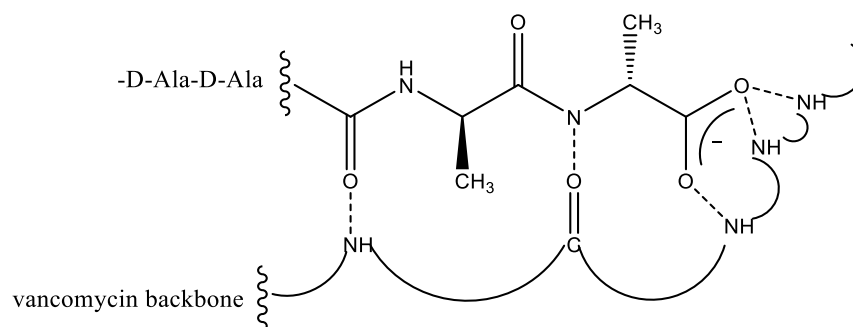


Figure 4.10 Binding of vancomycin to Alanine-D-Alanine of bacteria cell wall

However, there are several factors that influence vancomycin activity. The diffusion rate of vancomycin to the division septum in bacteria, which is the main location for the uncross-linked D-Alanine-D-Alanine residues, plays a crucial role in determining the efficiency of vancomycin killing [188, 203]. During the early stage of the synthesis of the septum, there are fewer cross-linked D-Ala-D-Ala moieties which results in a high rate of binding of vancomycin. However, when growth is slow or stopped and new cell wall is not being synthesised many more D-Ala-D-Ala moieties have had chance to be cross-linked and so there is less opportunity for vancomycin binding [62]. In addition, the interference by any process that competes with the hydrogen bond interaction between vancomycin and D-Ala-D-Ala residues of the peptidoglycan is another factor that influences the binding activity [10]. In the case of polymers functionalised with vancomycin in the presence of bacteria, the binding of the vancomycin pendant is illustrated in Figure 4.11 and further explained below.

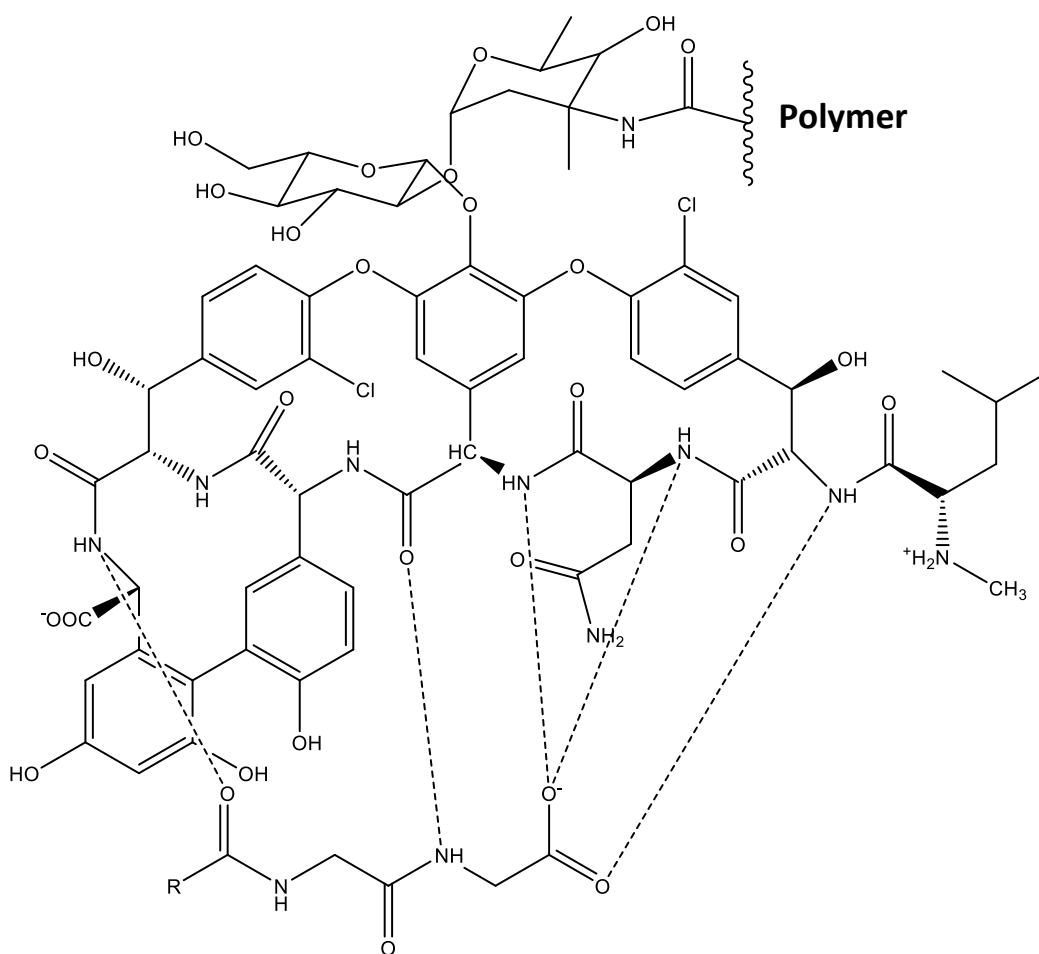


Figure 4.11 The interaction of polymer modified with vancomycin to D-Ala-D-Ala in Gram-positive *S. aureus* cell wall peptidoglycan

HB-PNIPAM-van can bind to *S. aureus* Oxford (NCTC6751) below and above its LCST resulting in an aggregate of polymer-bacteria complex. Interestingly, when L-PNIPAM-van was incubated with *S. aureus* Oxford at 22°C (below LCST of the polymer) a small mat formed but with a significant accompanying button but there was no sign of mat formation when the L-PNIPAM-van was incubated with bacteria above its LCST (Fig 4.9E). This finding could be explained by the accessible functionality and polymer conformations. Several studies have shown that a flexible polymer backbone with multivalent ligands has greater potency in biological activity because it can adopt a more extended conformation to bind to recognition targets. At 22°C both polymers with vancomycin ends are in the fully-open coil conformation, thus, vancomycin binding sites must be accessible for binding to its target. Binding of bacteria to vancomycin on both HB-PNIPAM-van and L-PNIPAM-van should induce phase transition of the polymers leading to the aggregate formation [17]. However, in

the case of the L-PNIPAM-van, formation of a much smaller mat occurred and with a considerable button. This would be consistent with a degree of initial polymer binding to the bacteria via the vancomycin pendant groups but this would be followed by desolvation of the linear polymer and conformational change such that the rest of the pendant vancomycin groups would be shielded within the globule. However, the different-length spacers and binding positions of vancomycin in L-PNIPAM-van and HB-PNIPAM-van may have an effect on ligand-receptor accessibility and extent of cell interactions [144]. Even when the L-PNIPAM-van polymer is in the fully solvated conformation, and vancomycin pendants on the L-PNIPAM-van that are located along the polymer backbone would be expected to bind to bacteria, one or more of the vancomycin groups of its nearest neighbour polymer chains may not be able to orient itself properly to bind to other bacteria cells. We suggest, therefore, that this results in less cross-linking between polymer-vancomycin bound to one bacterial cell also binding to other bacterial cells. In contrast, complete bacteria-polymer complex formation was found with HB-PNIPAM-van. It was likely due to accessible functionality between ligands and receptors. Vancomycin groups on HB-PNIPAM-van are located at the terminal chain segments of on average approximately 25 repeat units, and because more bacteria are bound within the complex, it is possible that there is longer spacer length compared to L-PNIPAM-van, and this affects the accessibility of vancomycin to interact with bacteria. Work by Pasparakis et al [144] indicated that the position of glucose functionality in copolymers of PNIPAM and 2-(dimethylamino)ethyl methacrylate affected the accessibility of ligands on bacterial cells. In their work two types of polymers were prepared, and glucose residues were incorporated via either the anomeric carbon or the 2-amino position of glucosamine. They found that the latter copolymer formed larger aggregates of polymer-bacteria complex compared to the aggregates formed by the former. It was likely due to not only the different molar mass between the copolymers, but also the difference in attachment position of the binding sites and spacer length in both copolymers. This is consistent with the findings of our study in that the much smaller aggregate (mat) formation of *S. aureus* Oxford (NCTC6751) with L-PNIPAM-van occurred below its LCST, which indicates that a change in polymer behaviour is associated with a change in polymer architecture from linear to branched while the chemical composition was kept constant.

Considering the formation of the bacteria-polymer complex (mat) when HB-PNIPAM-van was incubated with Oxford (NCTC6751) and S235 bacteria above its LCST (at 37°C), it is possible that there are a number of influences on this complex formation. These include binding of bacteria to vancomycin ends induced coil-to-globule transition of the polymer, a role for hydrophobic interactions and also a role for cooperativity in multivalent interactions. *S. aureus*, similar to many bacteria, is relatively hydrophobic. Binding of bacterial cells to the polymer chain ends through vancomycin molecules may trigger a chain of events that leads to desolvation of the outer segments of the HB-PNIPAM-van, which creates more hydrophobic-interactive environment for bacteria [17, 204]. This is consistent with the work described in chapter 6 using the ligand, D-Ala-D-Ala. Moreover, the cross-linking network between vancomycin groups on the polymer and cell-surface receptor (D-Ala-D-Ala) on bacteria could also be explained by chelate effect and ligand-induced-receptor clustering, which contribute to in multivalent interaction reported by Bertozzi and Keissling [205]. Cooperativity is a phenomenon in the system that consists of multiple molecules in which the strength of the interaction between ligands and receptors is higher than individual pairwise interaction. Vancomycin groups on the polymer interacting with D-Ala-D-Ala in the bacterial cell walls are considered as multivalent ligands and receptors respectively. They are able to form five hydrogen bonds to each other called multivalent interactions [75]. Thus, binding of vancomycin chain ends to D-Ala-D-Ala on bacterial cell surface could cause bacterial clustering that leads to aggregate formation [144]. In the case of L-PNIPAM-van, no aggregation occurs when the polymer was incubated with bacteria above its LCST because the organisation of binding sites is one of the factors that is involved in the multivalent binding mechanism, especially chelate effect. Above the LCST, the pendant ligands of L-PNIPAM-van became shielded inside the globule, rendering them unavailable for interacting with bacteria. An increase in activity of multipoint interaction can occur if the display of binding groups is favourably oriented. This notion suggests that the polymer architecture plays a vital role in the outcome of polymer binding. Moreover, the results from chapter 2, which highlight the effect of polymer architecture on the LCST, showed that the collapsed state of HB-PNIPAM-van above the LCST still consists of multiple-binding sites being available, whereas vancomycin on the linear analogue would be shielded within the collapsed form of the polymer. Thus, above the LCST, the aggregated mats are still formed when HB-PNIPAM-van

was incubated with *S. aureus* Oxford and S235 because the vancomycin end groups do not penetrate into the collapsed coils and these groups still remain at the surface, even after the coil-to globule transition, resulting in cross-linking between polymer-bound to bacteria and other bacterial cells. Thus, if HB-PNIPAM-van can bind to more than one bacterial cell thanks to multiple binding sites, it is likely that a network of bacteria-polymer is formed. Furthermore, the same shielding behaviour that resulted in the formation of L-PNIPAM-van aggregates, which provided a cloud point as detected by turbidimetry, also prevented binding of pendant vancomycin to the bacteria. Similarly, at 37°C, it seems likely that in the globules of HB-PNIPAM-van, the vancomycin was located at the interface of the polymer and provided electrostatic colloidal stability so that they were still available for accessing D-Ala-D-Ala moieties in the bacterial cell wall. Assuming that these suggestions are true, then aggregation of *S. aureus* into large bacteria-polymer complexes is due, not only to binding of the bacteria to the pendant vancomycin groups of the HB polymer, but also the consequent phase transition of the polymer which induces a more hydrophobic-interactive environment for the bacteria [206]. From the results in this work, a model for formation of bacteria-polymer aggregates (mat) with HB-PNIPAM-van is shown in figure 4.12 and the interaction with L-PNIPAM-van in figure 4.13. A composite of supporting evidence is also shown in figure 4.14.

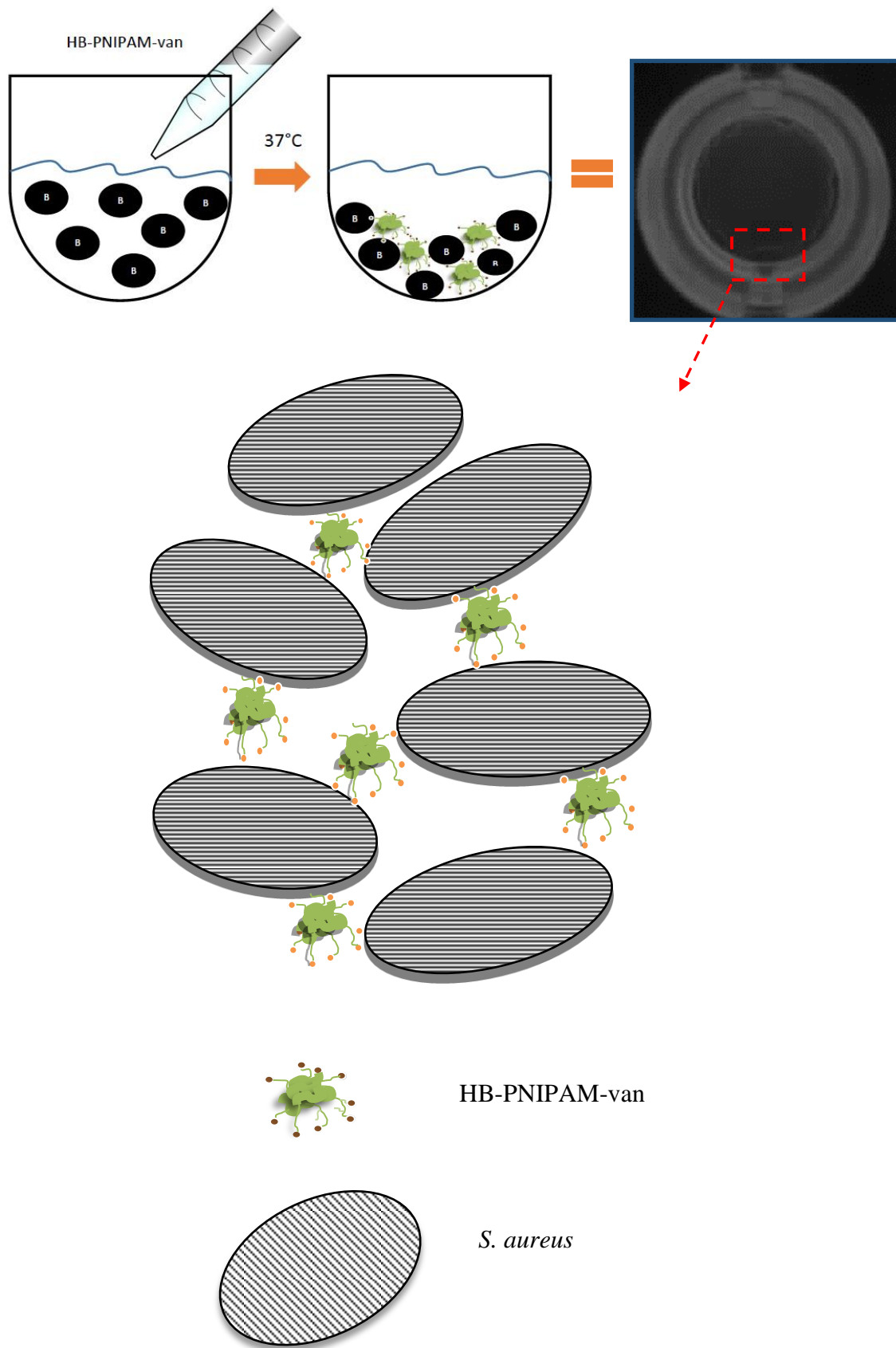


Figure 4.12 Schematic representation of the mat formation of bacteria-HB-PNIPAM-van polymer complex

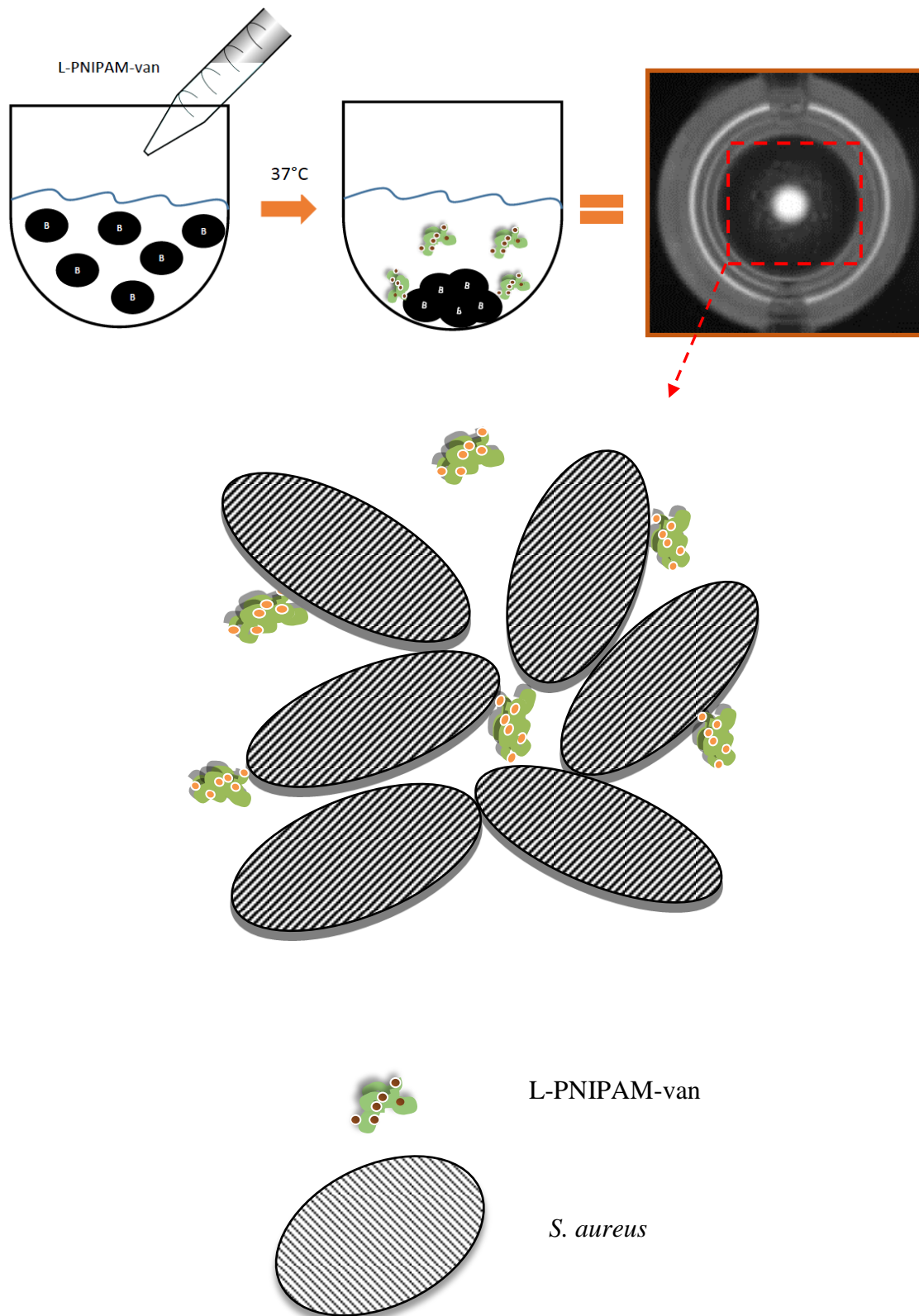


Figure 4.13 Schematic representation of the mat formation of Bacteria-L-PNIPAM-van complex

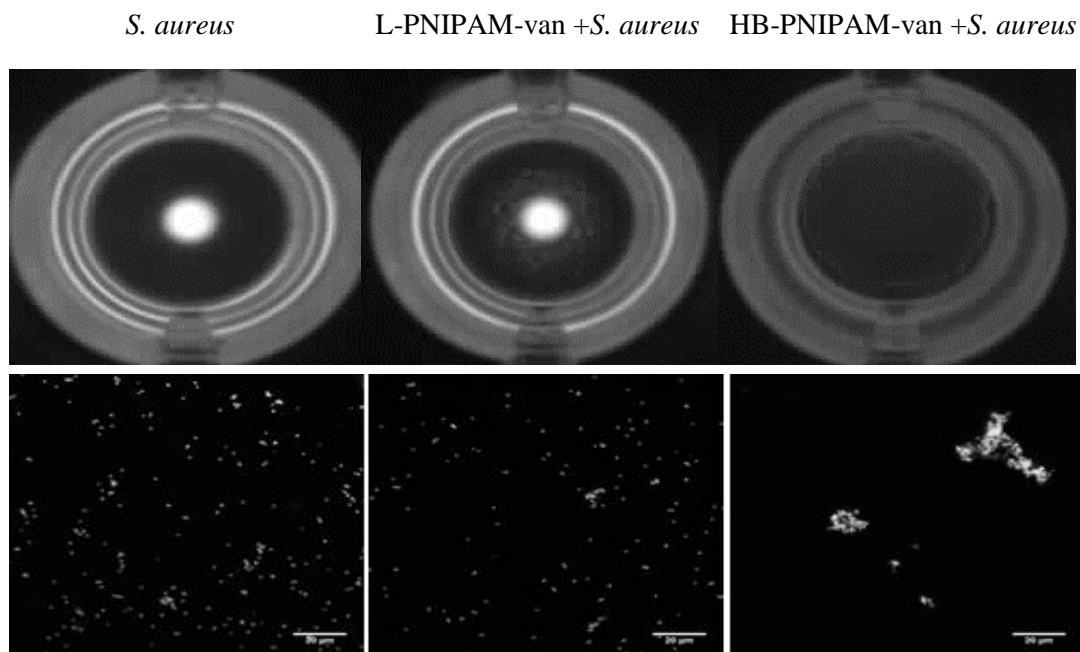


Figure 4.14 Images of the mat/button assay and confocal microscopy of HB-PNIPAM-van and L-PNIPAM-van incubated with *S. aureus* Oxford (NCTC6751) in PBS for 24 h (composite of sections of figs 4.4 & 4.8)

In summary, polymer architecture and the accessibility of functional groups have a significant effect on its ability to interact with its ligand (i.e. HB-PNIPAM-van vs. L-PNIPAM-van). Also, it is noteworthy that only the *S. aureus* Oxford (NCTC6571) and S235 strains formed a mat of bacteria-polymer complex with HB-PNIPAM-van, resulting in large clusters of bacteria, whereas no aggregates were formed with the *S. aureus* Newman and L98789 strains. This is most likely to be due to factors other than the availability of D-Ala-D-Ala in the cell wall such as electrostatic charge and hydrophobicity. We have investigated hydrophobicity and seen a relationship between that character and polymer interaction so we then investigated a possible role for surface charge.

4.4 Bacterial surface charge

According to the core-shell structure hypothesis of HB-PNIPAM-van in solution, the result in Chapter 2 indicates that the aggregates of HB-PNIPAM-van are stabilised in solution by electrostatic repulsion, which then fails to aggregate with some bacterial strains above its LCST. Consequently, it is important to investigate whether the negative charge on the vancomycin HB-PNIPAM end groups might cause a decrease in the binding ability of the polymer to the hydrophilic strains of *S. aureus*, due to charge repulsion interactions. There are several studies that have shown the effect of the *S. aureus* surface charge on the interaction with their targets [207]. Collins et al. found that the modification of negative charges on the WTAs by introducing positive charges along them had a great influence on the interaction between the bacteria and other molecules [42]. In addition, it was reported that positively charged polymer was able to bind to a range of bacterial species through electrostatic interactions with their negatively charged cell walls [207]. Therefore, the lower efficiency of the HB-PNIPAM-van with respect to the interaction with the hydrophilic *S. aureus* Newman and L9879 strains could possibly be influenced by the degree of bacterial cell surface charge. Surface charge can be measured using electrophoretic mobility as a function of ionic strength (zeta potential measurement) [208] and so in this study, the electrophoretic mobility of the bacterial cells and the polymers in suspension was assessed. Bacterial surface charge is affected by the pH and ionic strength of the aqueous suspending medium. The charge on the bacterial cell surface stems from dissociation of phosphate, carboxyl and hydroxyl groups at different pH values and the absorption of ions in the solution [168, 209].

Furthermore, Wilson et al. showed that the electrostatic charge of bacteria, has an influence on the polarity of those bacteria and their degree of hydrophilicity [208]. Therefore, the charges of the four strains of *S. aureus* studied above could be a contributing factor to its binding to the PNIPAM-van polymers. Consequently, the aim of this part of the study was to investigate whether bacterial cell surface charge of *S. aureus* strains was correlated with the levels of hydrophobicity of the strains and/or with their binding to the PNIPAM-van polymers.

4.4.1 Materials

Potassium chloride (Sigma Aldrich), Dipotassium phosphate (K_2HPO_4) (Sigma Aldrich), monopotassium phosphate (KH_2PO_4) (Sigma Aldrich), Magnesium phosphate pentahydrate ($MgSO_4 \cdot 7H_2O$), (Sigma Aldrich) were used as received. Urea was also used as purchased.

4.4.2 Methods

Four strains of *S. aureus*, namely NCTC6751 (Oxford), S235, Newman and L9879 were subcultured in BHI broth at 37°C overnight. The cells were harvested by centrifugation and washed with 0.1M KCl pH7 twice. Bacteria were suspended in either 0.1M phosphate buffer pH 7, PBS pH 7.4 and PUM buffer pH7 to evaluate the effect of buffer on the bacterial behaviour. Bacterial suspensions in the three buffer solutions were adjusted to OD 1 (600 nm). For zeta potential measurement 50 µl of stock bacterial suspension was added to 1500 µl of each of the buffers and the mixtures were vortexed before transferring to cuvettes. Zeta potentials were determined using a ZetaPALS analyser (Brookhaven Instrument Corporation). Measurements were carried out in triplicate for each sample. The parameters used in this study are shown below (Table 4.3).

Table 4.3 Parameters for determination of zeta potential

No. cycles	20
No. runs	5
Temperature (°C)	20
Liquid	Water
pH	7

4.4.3 Results and discussion

The zeta potential (Z_p) values of the four *S. aureus* stains, in each type of buffer are shown in figure 4. 15.

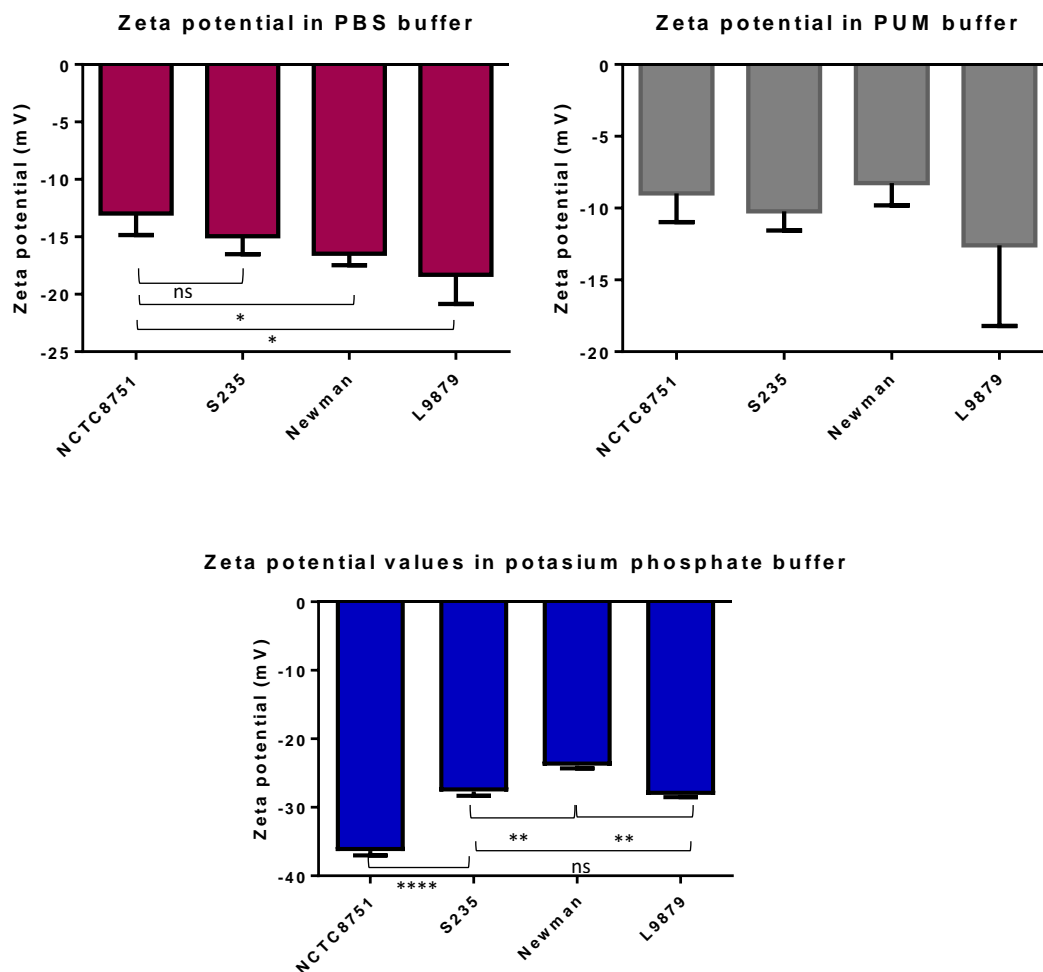


Figure 4.15 Bar charts showing the zeta potential values of four strains of *S. aureus* suspended in three different buffers. The ionic strengths of PBS, PUM buffer and potassium phosphate buffer was 0.164 M, 0.602 M and 0.12 M respectively. The significance between differences in zeta potential were tested using one way ANOVA incorporating Tukey's multiple comparison statistical test. The degree of significance is defined by *P* value as follows: **** $P \leq 0.0001$, ** $P \leq 0.01$, ns = not significant, $P > 0.05$

Several methods have been used to characterise the electrostatic properties of the bacterial cell surface but the most commonly used method is the electrophoretic mobility measurement, from which the zeta potential value of the bacterial cell surface can be calculated. The charge group of the bacterial cell wall responds strongly to changes in pH and ionic strength. It can be dissociated or associated depending on environmental changes. Thus, three buffers with different ionic strengths were chosen as described above. PBS is a common buffer used in biological studies. It maintains not only the osmolality of the bacterial cells but also the pH at

7.4, which is the pH of blood. Thus, it is interesting to investigate the electric properties of each strain in PBS. PUM was also chosen to study the electrophoretic properties of the bacteria because it was used in the hydrophobicity tests and potassium phosphate buffer was used because it is a low ionic strength and is often used for electrophoretic mobility studies. [209]. Soni et al. used the zeta potential measurement to investigate the influence of culture conditions and live and dead bacterial cells on electrophoretic properties of several species. They found that the zeta potential values varied depending on the richness of the culture media and the viability of the cells [210]. It was important for us to use constant culture conditions and that they were the same as those used for the hydrophobicity and polymer interaction studies. Note that in figure 4.15-4.16, the zeta potential values were obtained from the ZetaPALS program, and they were calculated from electrophoretic mobility of each sample using the Smoluchowski equation, which can be seen in equation 4.3.

From figure 4.15, in PBS buffer, strain L9879 shows the highest Z_p of -18.3 ± 2.5 , while the lowest was shown by NCTC 6751(Oxford) (-13.0 ± 1.9). The result indicates that in PBS buffer, the bacterial cell wall of the L9879 strain has the highest negatively charged wall. Interestingly, when all strains were prepared in phosphate buffer pH7, NCTC6751 shows the highest zeta potential values followed by the L9879, S235 and Newman strains and these were much higher than seen in PBS.; Similar differences were also seen in PUM but with the other strains being more similar to NCTC 6751(Oxford), although the standard errors were higher. The Zeta potential results showed that all of the bacterial strains had net negative charges and the Z_p values decreased as the ionic strength of the buffer increased, which can be observed in the summary figure 4.16.

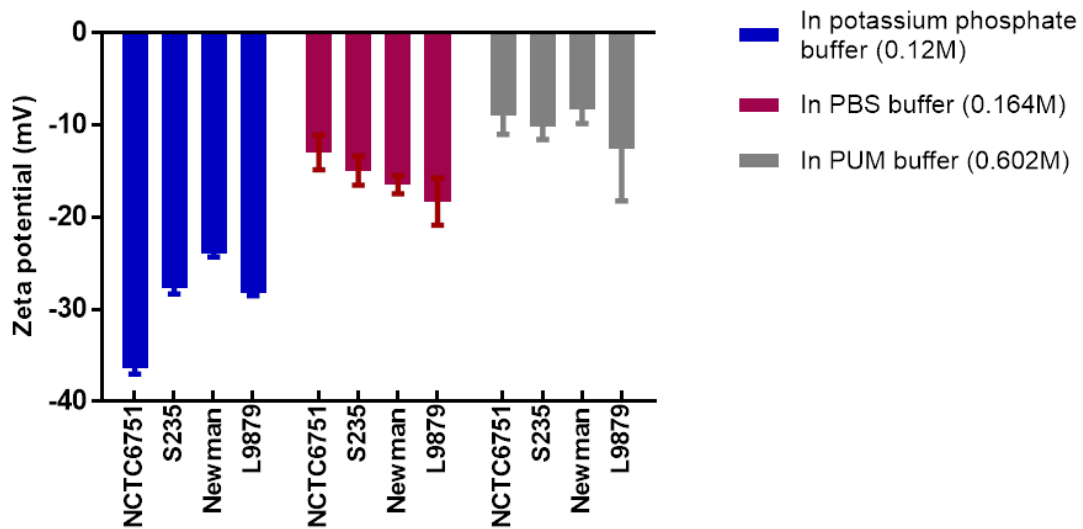


Figure 4.16 Summary of zeta potential values of all stains used in this study in potassium phosphate buffer (0.12M), PBS (0.164M) and PUM buffer (0.602M)

The zeta potential of a particle is considered as the voltage at the shear plane that is a distance between the surface of colloid particles and the solvent far away from the electric double layer; it can be determined by the electrophoretic mobility and obtained using the Henry equation [208], as shown in equation 4.2.

$$UE = \frac{2\varepsilon z f(ka)}{3\eta} \quad eq. 4.2$$

Z = zeta potential

UE = electrophoretic mobility

ε = dielectric constant

η = viscosity

However, for large particles like bacteria, the Smoluchowski equation is usually used which is shown below (equation 4.3) [208]; and a simple model of the measurement of zeta potential is shown in figure 4.17.

$$z = \frac{\eta}{\epsilon} UE \quad \text{eq.4.3}$$

Z = zeta potential

UE = electrophoretic mobility

ϵ = dielectric constant

η = viscosity

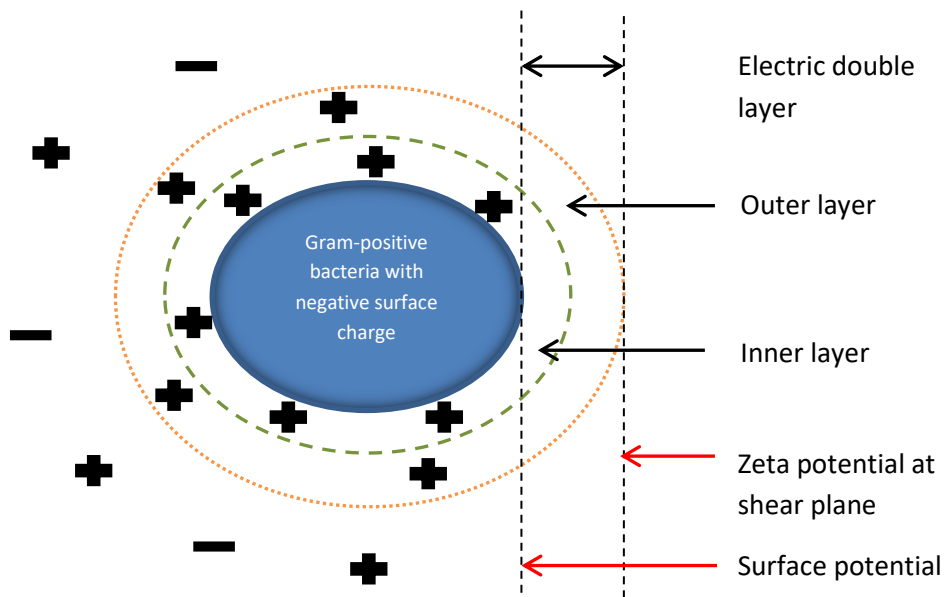


Figure 4.17 Cross-sectional representation of a bacterial cell illustrating the various layers of ions surrounding the cell surface

The electrophoretic mobility can be obtained by measuring the velocity of the bacteria that moves toward the opposite electrode when a potential is applied using Laser Doppler velocimetry (LDV). The LDV technique is used in a wide variety of studies from engineering, such as the supersonic flows in jet engines, to biological studies. Generally, the charge on the particle surface is balanced by oppositely charged ions in the solution. However, the counter charge in the surrounding solution diffuses in different layers of colloidal solution systems. The charge of the particle cell surface can have an effect on the distribution of ions around the interfacial region, and it can cause the formation of an electrical double layer around the cells if the concentration of counter ions next to the cell surface increases. The electrical potential decreases exponentially as the distance from the bacterial cell to outside the electric double

layer increases [211]. The electrical double layer consists of an inner region and outer region. Ions in solution are firmly bound to the inner region, whose boundary is called the Stern layer, whereas there is less binding between ions and the outer layer, with its boundary is referred to as the shear plane. However, there are stable regions between the ions and particles within the outer layer. Under an applied electric field, when the particles start moving, ions bound to particles in the inner region travel with the particles whereas the ions in outer region do not. At this boundary region, called the slipping plane or shear plane, the zeta potential occurs and a charge density can be assumed. In a real system, the surface potential of the particles cannot be measured directly. Only the electrostatic mobility can be determined; thus, the zeta potential can be inferred. Therefore, it is essential to understand that the zeta potential value corresponds to the charge density at the shear plane while the surface potential is the surface charge density at the inner layer [168, 211-213].

The stability of particles in suspension can be indicated by the magnitude of the zeta potential. If the particles contain a high amount of negative or positive charges, which denotes a high value of the zeta potential, they tend not to aggregate in suspension because of electrostatic repulsions between each other. On the other hand, if the zeta potential of the particles is low, they are likely to aggregate in aqueous suspension due to van der Waals attraction. Particles with a zeta potential between +30 mV and -30 mV are usually considered as unstable while particles with a high absolute zeta potential of more than +30 mV or -30 mV are classified as stable colloids in suspension [168].

Characterisation of the bacterial cell surface charge is complicated compared with an inert colloidal particle due to the complex cell wall composition, the hydrophobicity and environmental effects on bacterial behaviour, such as the pH of the solution and ionic strength values [168, 214]. Normally, it is understood that Gram-positive bacteria possess a net negative surface charge because of phosphoryl groups in the WTAs and for Gram-negative bacteria the carboxyl groups of lipopolysaccharide. It was reported that both groups particularly influence the cell surface charge of bacteria at physiological pH [168, 210].

From Figure 4.16, it is seen that the ionic strength of the buffer influences Z_p for all strains. Z_p decreased in all types of strain when the ionic strength of the buffer was

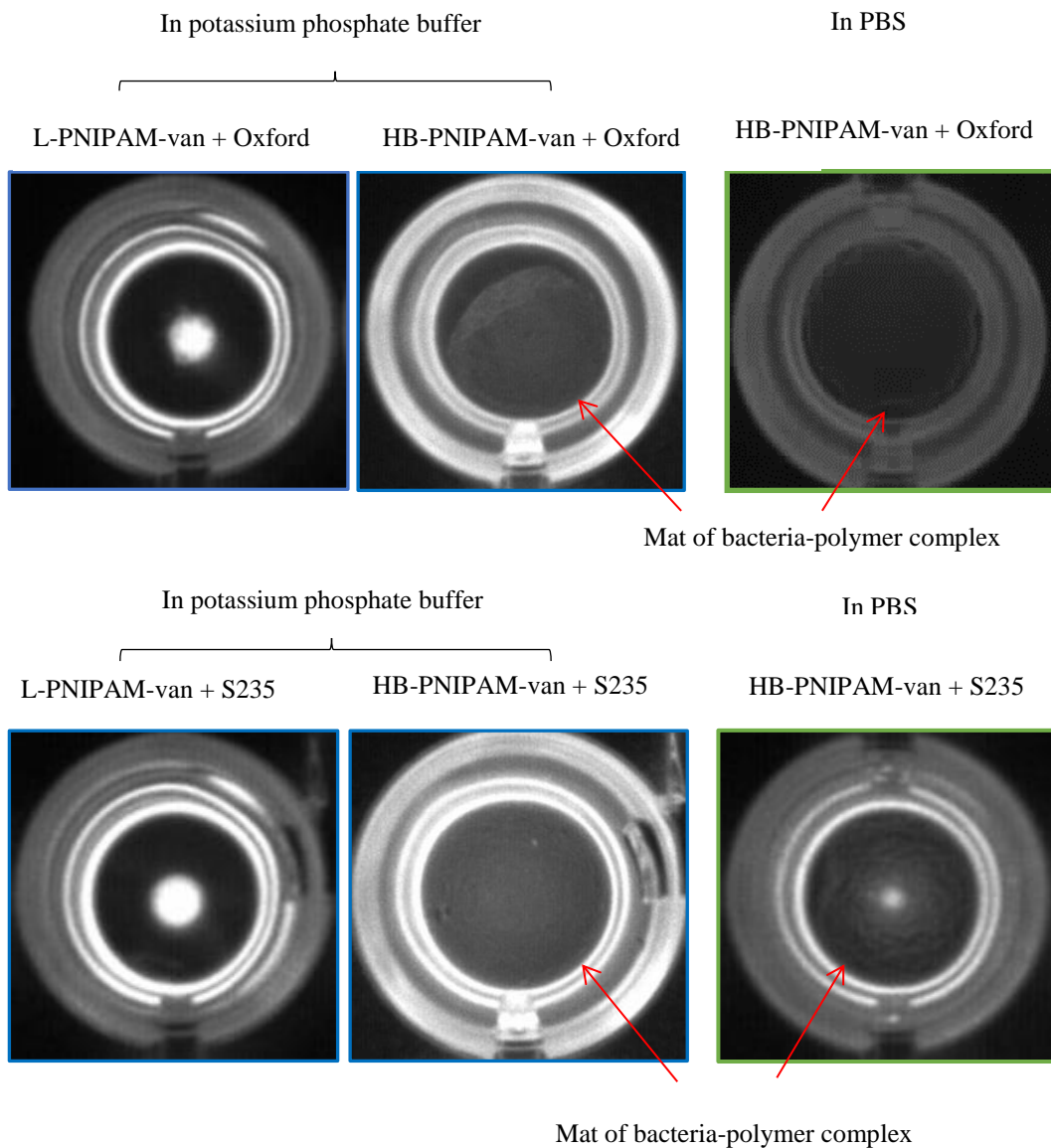
increased. Carneiro et al. showed that the increase in ionic strength of the polysaccharide solutions resulted in a decrease in the zeta potential values [215]. To evaluate the effect of ionic strength on zeta potential of polysaccharide solution, they used different concentrations of sodium chloride to vary the ionic strength of the solution. They found that increasing the sodium chloride concentration results in a reduction of the Z-average value. In addition, the distribution of charge groups inside the bacterial cell wall affects the electric double layer interaction between the bacterial cells and the surface of its target at different ionic strengths [209, 215, 216]. Therefore, non-statistically significant differences between the electrophoretic behaviours of strains in PUM buffer could be due to the high ionic strength of the solution compared to other buffers used in this study. PUM was chosen to study the electrophoretic properties of the bacteria because it was used in the bacteria hydrophobicity tests. However, the results indicated that PUM buffer is not appropriate for measuring electrophoretic mobility because of its high salt concentration. However, it was interesting that Oxford (NCTC6751) showed the highest zeta potential value in potassium phosphate buffer followed by the S235, L9879 and Newman strains, while the trend was the opposite for PBS buffer. Therefore, it is important to investigate whether charge on the bacterial cell surface or hydrophobicity of the bacteria affect the binding ability of bacteria on the polymer functionalised with vancomycin using a rapid aggregation assay (Mat/button assay). The hypothesis was that if the bacterial surface charge plays an important role in the binding of bacteria to the polymer-van, mat formation of the Oxford (NCTC6751)-polymer complex should not appear in potassium phosphate buffer due to the electrostatic repulsion between the bacteria and the polymer.

Aggregation assay of *S. aureus* with HB-PNIPAM-van and L-PNIPAM-van in potassium phosphate buffer

HB-PNIPAM-van and L-PNIPAM-van were incubated with Oxford (NCTC6751), S235, Newman and L9879 in a 96-well plate (U-bottom) at 37°C for 24 hours. Potassium phosphate pH7 buffer was used instead of PBS to investigate the effect of the charge of each strain on its binding ability to both types of polymers. The aggregation assay was conducted as previously described. All strains were labelled with EtBR to enable visualisation under UV light. The zeta potential results of each

strain in potassium phosphate buffer showed that Oxford (NCTC6751) is the highest negatively charged cell surface followed by S235, Newman and L9879.

The hypothesis was that if the charge of the bacterial cell surface affects the interaction with the polymers, HB-PNIPAM-van should be unable to bind to Oxford (NCTC6751) due to its highly negative charged surface, whereas the polymer should bind to the Newman and L9879 strains. The results from the Mat/button assay of both polymers for all strains in potassium phosphate buffer pH7 are shown in figure 4.18.



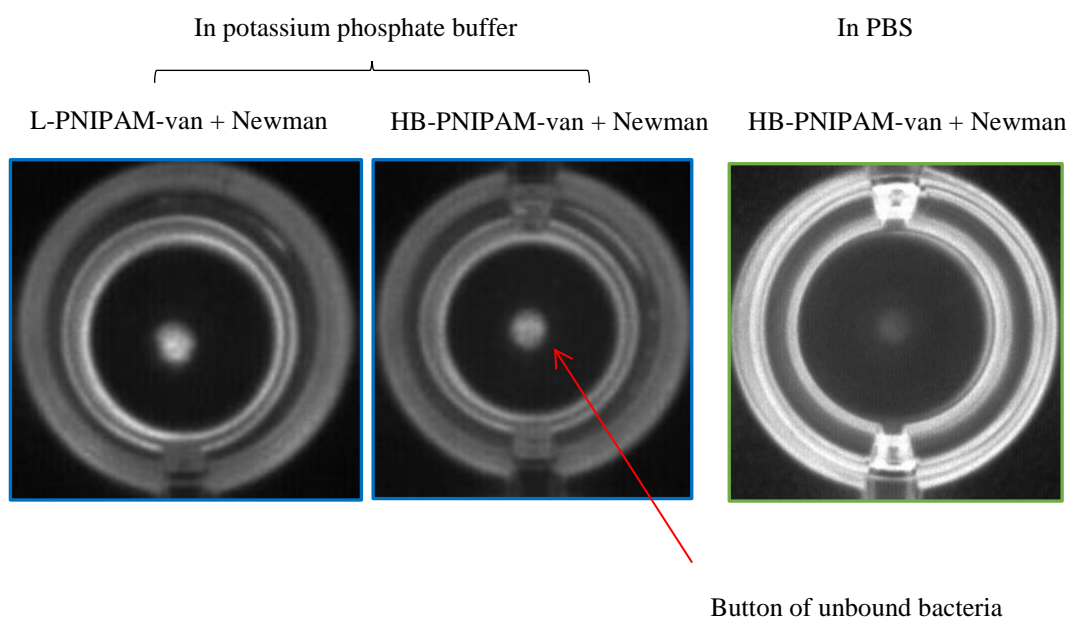
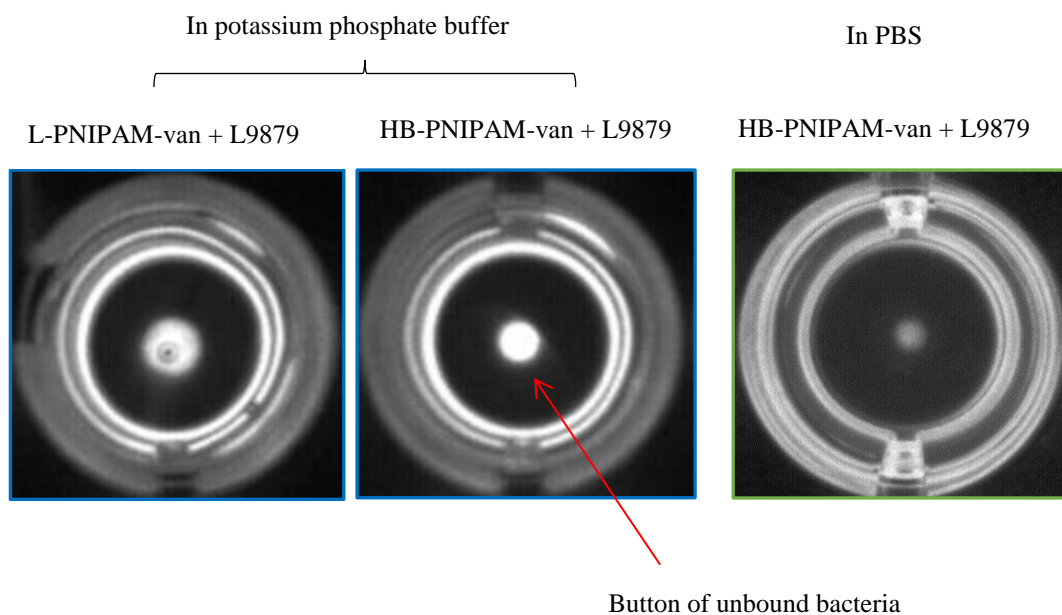


Figure 4.18 Images of aggregation assays of HB-PNIPAM-van and L-PNIPAM-van incubated with Oxford (NCTC6751), S235, L9879 and Newman strain labelled with Et/Br in potassium phosphate buffer (navy line) and in PBS (green line) at 37°C for 24 hours.

From Figure 4.18, it can be seen that only HB-PNIPAM-van was able to cause mat formation with strains Oxford (NCTC6751) and S235 in potassium phosphate buffer whereas there was no aggregation of strains L9879 and Newman with the polymer.

The hypothesis that at pH 7, HB-PNIPAM-van has a negative charge and should repel the highly negatively charged bacteria, resulting in less binding of bacteria to the polymer-vancomycin. This hypothesis was consistent with the bacterial behaviour in PBS in so far as only strains Oxford (NCTC6751) and S235 bound polymer and these showed significantly lower surface negative charges than the other two strains ($p < 0.005$). This might suggest then that there was less charge repulsion between HB-PNIPAM-van and strains Oxford (NCTC6751) and S235.

However, in potassium phosphate buffer, the results do not agree with this hypothesis. The hypothesis was that if charge on the bacterial cell wall affects the binding ability of polymer-van to bacteria, a mat should be seen with the Newman strain plus HB-PNIPAM-van while binding of Oxford (NCTC6751) with the polymer should not occur because this strain had the highest negative charge in potassium phosphate buffer. Interestingly, the result revealed that HB-PNIPAM-van still formed a mat of bacteria-polymer complex with the Oxford (NCTC6751) and S235 strains, (Figure 4.18), whereas the bacteria-polymer complex was not formed in the polymer with the L9879 and Newman strains.

There are several factors playing a role in the binding of bacteria to the polymer with vancomycin ends. These include polymer architecture, accessibility of functional groups and the properties of bacterial surface such as hydrophobicity and surface charge of bacteria [144, 217]. Bacterial surface charge is mostly responsible for the initial adhesion of bacteria to surfaces including biomaterials [208, 218]. However, whether bacterial surface charges affects the binding ability of PNIPAM polymers with vancomycin ends resulting in the cross-linking network of bacteria-polymer complex has not been studied before. The results show that there is no relationship between the bacterial surface charge of the four strains tested and the binding ability of HB-PNIPAM-van to them with subsequent aggregate formation. Indeed mat formation of bacteria-polymer complex appeared when HB-PNIPAM-van bound to two hydrophobic strains, Oxford (NCTC6751) and S235, but failed to do so with the two hydrophilic strains, L9879 and Newman, even though Oxford (NCTC6751) and S235 had higher negative charge compared to the latter.

Initial attachment between bacteria in aqueous solution and a material surface depends on the fluid interface, the characteristics of bacteria and the specificities of

substratum. After initial attachment of bacteria to a surface, specific intermolecular interactions, such as hydrophobic interaction or ligand-receptor interaction, occurs. Gristina et al. suggested that an initial repulsion occurs between the negatively charged material surface and negatively charged bacteria but the degree of hydrophobicity of bacteria also plays a role in positioning bacteria at the primary minimum where attractive hydrophobic interactions overcome repulsion. The repulsion force can be overcome by hydrophobic interactions at the distance of approximately 8-10nm. When bacteria are proximate to the surface, short-range interactions, such as hydrogen or covalent bonding, can occur [48, 49].

Interaction between vancomycin and the bacterial cell wall involves five hydrogen bonds between three amide NH groups of vancomycin and carboxylate anion of C-terminal D-Ala-Ala, while the two hydrogen bonds result from the carboxyl group of residue 4 and the backbone amide group of residue 7 of vancomycin (Fig1.5A). Kamaromi et al reported that the length of hydrogen bonds between vancomycin and D-Ala-D-Ala is approximately 2.3 to 3 Å, which is slightly higher than the usual values because this binding mode involves five hydrogen bonds. Therefore, a slight increase in the distance is more energetically favoured for this formation of the complex [219].

A likely explanation for the behaviour of *S. aureus* with HB-PNIPAM-van is that initially the negatively charged bacterial cell surface may tend to repel the negative charge on the polymer due to the carboxylate group on vancomycin. However, once hydrogen bonds between vancomycin and D-Ala-D-Ala are formed, the binding is promoted by hydrophobic interactions originating from Ala methyl groups in their contacts with the aromatic rings of vancomycin [61]. A biphasic structure of HB-PNIPAM-van with a globular desolvated core and binding sites located at the polymer/aqueous interface could favourably contribute to ligand binding because multipoint binding involves conformational entropy. It is suggested that the flexibility of vancomycin groups attached to terminal chain segments of on average approximately 25 repeating units can reach at least the outer regions of surface-located D-Ala-D-Ala on the bacterial cell wall. Moreover, with the larger size of bacteria compared to polymer molecule and Brownian motion of bacteria in suspension, hydrophobic interactions are exerted and enable the polymer to become closer to the bacterial cell surface and then specific short-range interactions occurs,

which are mainly hydrogen bonds between vancomycin and D-Ala-D-Ala [49]. These ideas are shown in figure 4.19.

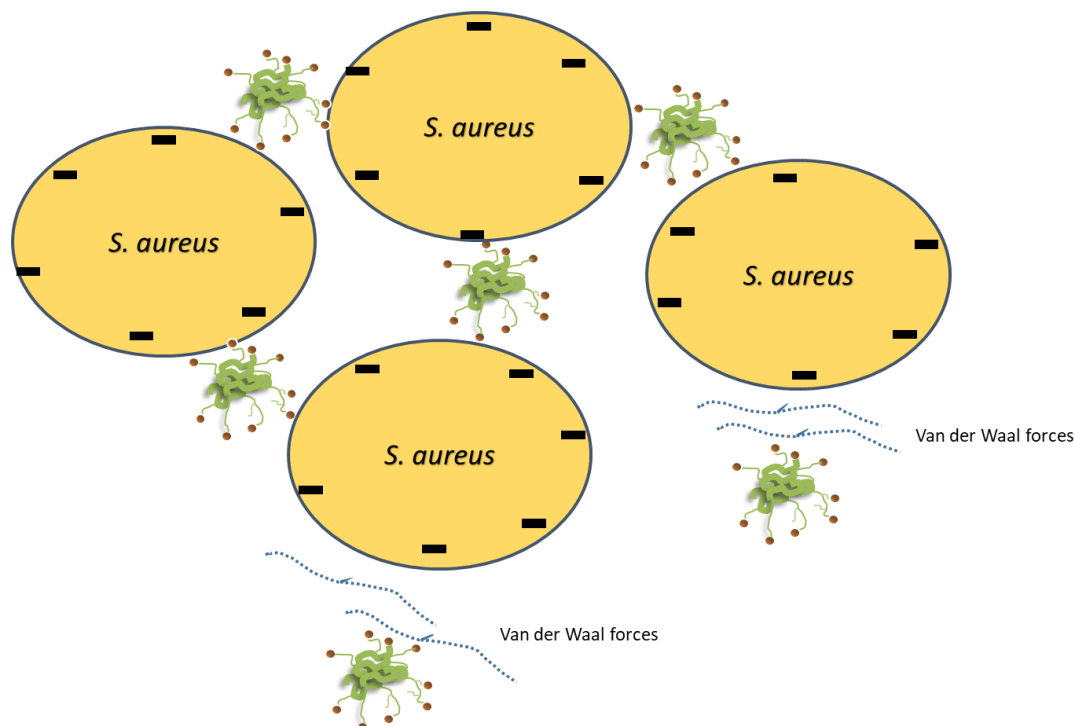


Figure 4.19 Schematic diagram presenting the interactions that occur between bacteria and HB-PNIPAM-van polymer. The initial repelling interaction between the negatively charged bacteria and the polymer are overcome at short distance about 1nm [49]. Hydrogen bonding occurs between the vancomycin groups at the chain ends of the polymers and D-Ala-D-Ala in the bacterial cell wall. This scheme is not to scale. (Bacteria ~800 nm, polymer ~30 nm)

In summary, there was no relationship between the charge of the bacterial cell surface and the binding capability of the PNIPAM-van polymers. The binding of Oxford (NCTC6751) and S235 *S. aureus* to HB-PNIPAM-van, which resulted in the aggregation of bacteria and mat formation of the bacteria-polymer complex, could however be at least partially attributed to the effects of hydrophobicity (see Section 4.3.3 above).

Another factor that might explain the variable behaviour of strains with the vancomycin-functionalised polymers is the number of D-Ala-D-Ala binding sites on the bacterial cell surface. We therefore, undertook to determine the degree of availability of D-Ala-D-Ala binding sites on the surface of each strain.

4.5 Comparison of D-Ala-D-Ala binding sites on *S. aureus* strains using fluorescent vancomycin

4.5.1 Materials and Methods

S. aureus, Oxford (NCTC6751) and L9879, were subcultured in BHI broth at 37°C overnight. The cells were harvested by centrifugation, washed and resuspended in PBS to an O.D 0.5 (600nm). Fluorescent vancomycin (Vancomycin BODIPY®FL) (2µg/ml) was added to the bacterial suspensions and mixed by vortexing. The samples were incubated for 15 minutes then washed twice with PBS to remove unbound fluorescent vancomycin. 100µl of each of these bacterial suspensions was placed in black 96-well plates and the fluorescence intensity measured at 493 nm_{ext} and 530 nm_{emm}.

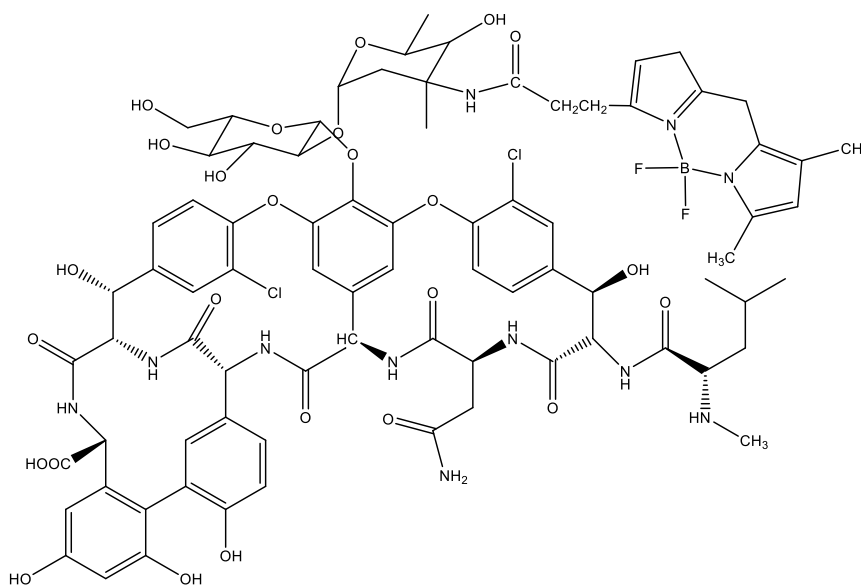


Figure 4.20 Chemical structure of fluorescent vancomycin (BODIPY®FL) (MW = 1723 g/mol)

4.5.2 Results and discussion

It is possible that the efficiency of the interaction between bacteria and the PNIPAM-van polymers could be affected by the amount or density of available D-Ala -D-Ala binding sites on the surface of each strain. The rationale for the assay method employed to measure D-Ala-D-Ala was that the amount of fluorescent vancomycin that binds to the bacterial cell surface would indicate the amount of D-Ala-D-Ala that was available.

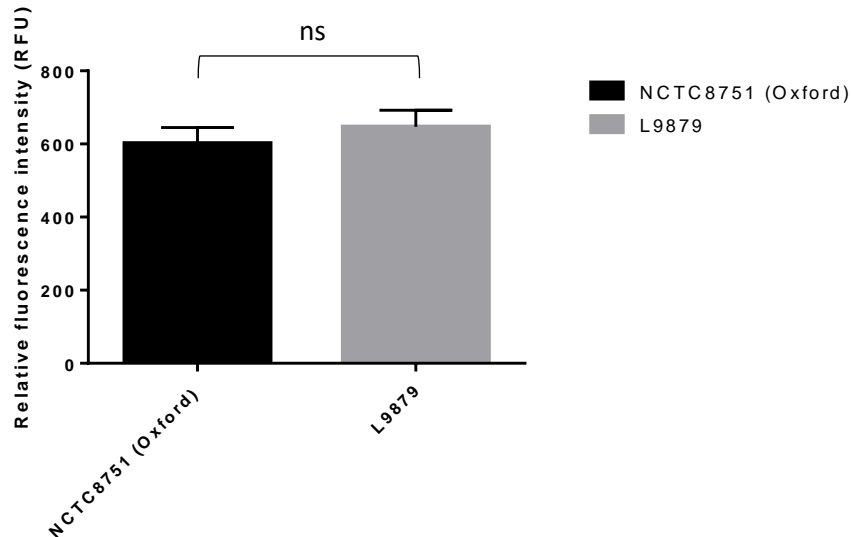


Figure 4.21 Relative fluorescence intensity of bound fluorescent vancomycin to two *S. aureus* strains. The significance between differences in relative fluorescence intensity of bound fluorescent vancomycin was tested using t-test. The degree of significance is defined by P value as follows: **** when $P \leq 0.0001$, *** when $P \leq 0.001$, ** when $P \leq 0.01$, * when $P \leq 0.05$ and no significant when $P > 0.05$

No significant difference was found in the level of vancomycin binding between the two strains ($p = 0.1064$) and by extension we surmise that there was no clear difference in the opportunity of the PNIPAM-van to bind to each strain through D-Ala-D-Ala binding sites. The cells used were in the same phase of growth (i.e. stationary phase) as in the other assays and the method used here was a rapid technique rather than an in depth analysis of the *S. aureus* bacterial cell wall. In future work it would be useful to compare fluorescent vancomycin binding to cells at different stages of the growth cycle, which would have different amounts of D-Ala-D-Ala available.

4.6 Conclusions

In summary, it can be concluded that HB-PNIPAM-van binds specifically to *S. aureus* resulting in the formation of aggregates (a mat) of bacteria-polymer complex, whereas L-PNIPAM-van fails to form such aggregates under these conditions. The hydrophobicity of bacteria appears to have a significant effect on the binding of the bacteria to HB-PNIPAM-van and subsequent aggregate formation, whereas the electrical charge on the bacterial cell surface did not play a significant role in the interaction between HB-PNIPAM-van and *S. aureus*. Moreover, differences in the behaviour of different strains of *S. aureus* with the PNIPAM-van polymers could not be explained on the basis of them having differing levels of D-Ala-D-Ala available for vancomycin binding.

Chapter 5 : Development of a reporter system for Gram-positive bacteria based on L-PNIPAM and HB-PNIPAM modified with vancomycin using Nile red dye as a probe

5.1 Introduction

The results from chapter 4 show that highly branched PNIPAM functionalised with vancomycin at the chain ends undergoes a phase transition on interaction with bacteria (aggregate formation). However, aggregate formation is not a useful test for application to biomedical and clinical situations and so a solvatochromic dye was used to exploit the desolvation state of the HB-PNIPAM on phase transition in the presence of bacteria. Nile red was chosen as a potential reporter of the micro-environment of the polymers. Moreover, we considered that Nile red could be used to investigate behavioural differences between the linear and HB polymers and also determine the sensitivity of the polymer at different bacterial concentrations.

Nile red is a solvatochromic dye that responds to changes in environmental polarity [140, 142, 220-222]. For example, in non-polar solvents such as dioxane, Nile red assumes a highly fluorescent pink colour, while in polar solvents, such as methanol, the dye is blue with a low fluorescence due to the bathochromic shift [223, 224]. The change in the fluorescence and colour of the Nile red in polar and non-polar solvents is shown in figure 5.1.



Figure 5.1 Nile red solution in various types of solvents (n-hexane, acetone)

Previously, Plenderleith et al. suggested that Nile red could detect the desolvation state of various HB-PNIPAM polymers with different degrees of branching and at different temperatures [137]. The hypothesis to be tested was that Nile red may be a useful probe for detecting a conformational change in L-PNIPAM-van and HB-PNIPAM on contact with

bacteria. We reasoned that the binding of HB-PNIPAM-van to *S. aureus* should be detected by an increase in fluorescence intensity and a wavelength shift due to the change in hydrophobicity of the environment experienced by Nile red. In terms of L-PNIPAM-van, we expected no significant changes in the Nile red fluorescence intensity or wavelength with bacteria because the polymer would have less binding ability to its targets above its LCST.

5.2 Materials

Nile red (Sigma Aldrich) and PBS tablets were used as received. Dimethyl sulfoxide anhydrous (DMSO, >99.99%) (Sigma Aldrich) was used as purchased.

5.3 Methods

5.3.1 Bacteria preparation

In this study, the standard laboratory strain of *S. aureus* Oxford (NCTC 6751) was used as a representative Gram-positive strain. Bacteria were cultured and prepared in suspension as described in chapter 4. Also, the concentrations of bacteria (10^5 - 10^8 cfu/ml) were prepared as described in chapter 4.

5.3.2 Mat/button aggregation – rapid method for assessing bacterial binding to PNIPAM-van polymers

Solutions of the L-PNIPAM-van and HB-PNIPAM-van polymers were prepared in PBS at 5mg/ml. HB-PNIPAM-van and L-PNIPAM-van solutions (100 μ l) were incubated with *S. aureus* at 1×10^5 , 1×10^6 , 1×10^7 , 1×10^8 cfu/ml in PBS at 37°C in round-bottomed 96-well plates. The controls were HB-PNIPAM-van, L-PNIPAM-van, and *S. aureus* alone in PBS. The samples were viewed and images were captured under UV light during the incubation period at 2, 4 and 24 h.

5.3.3 Addition of Nile red to polymer incubated with bacteria

All polymer samples and bacterial suspensions were prepared as previously described. However, in this part of the work a black flat-bottomed 96-well plate was used instead of a round-bottomed 96-well plate to measure the fluorescence intensity. Nile red stock solution was prepared by adding 0.01M of Nile red in DMSO to 1 ml of PBS. After 2 hours of incubation, the Nile red solution (100 μ l) was added directly to all of the samples, and the fluorescence intensity was measured using a micro plate reader

(Tecan Spectrophotometer, infinite M200 at 2 h, 4 h and 24 h incubation. The excitation wavelength was 550 nm and emission wavelength was 600-700 nm. The results were analysed via Tecan Magellan software.

5.4 Results and discussion

5.4.1 Aggregation assay of HB-PNIPAM-van and L-PNIPAM-van incubated with *S. aureus* at various bacterial concentrations and incubation times

The HB-PNIPAM-van and L-PNIPAM-van were incubated with varying concentrations of bacteria and for varying times because previous experiments showed that the incubation time had a significant effect on the formation of polymer-bacterial complexes.

The images in Figure 5.2 show that at 2 hours initial settling of bacteria had begun which then increased by 4h and then in some wells a tight button of cells was visible after 24h. A fluorescent ring appeared in the L-PNIPAM-van after 2h which then progressed to a button by 24h. This was in contrast to the HB-PNIPAM-containing wells where a mat was visible at all-time points. However, this was only obvious with 10^8 cfu/ml although a very small button was visible in the wells containing 10^7 cfu/ml. The latter number of bacteria was the lowest that could be used in the mat/button technique because it relies on being able to see the collection of bacteria. Below that number there were just too few bacteria to visualise.

However, in general, a bacterial concentration above 10^5 cfu/ml is considered to represent an infection rather than mere colonisation. Thus, we attempted to develop an alternative method that could probe the binding of the bacteria to the polymers with higher sensitivity compared to the mat/button assay.

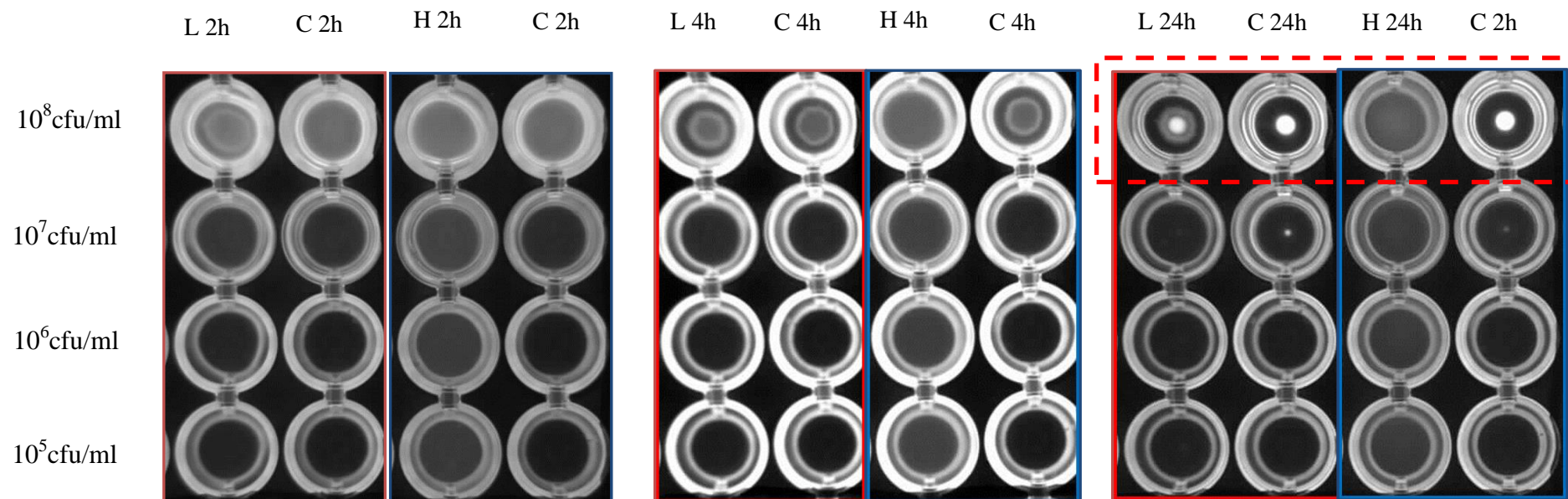
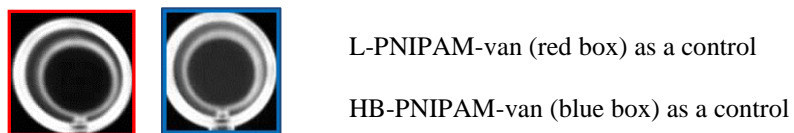


Figure 5.2 Mat/button assay of *S. aureus* Oxford (NCTC6751) with PNIPAM-van polymers for varying times and with varying number of bacteria. Bacteria were stained with ethidium bromide and the plates were viewed under UV-light.

L = Linear-PNIPAM-van; H = highly branched PNIPAM-van and C = bacterial suspension controls. Wells were incubated for 2h, 4h or 24h at 37°C.



5.4.2 Development of a detection system for the binding of *S. aureus* to HB-PNIPAM-van and L-PNIPAM-van at various bacterial concentrations with Nile red as a probe

The HB-polymers-bacteria complex seen in Figure 5.2 (mat formation) appeared to represent a phase transition from a hydrophilic, expanded state to a more hydrophobic, collapsed state. The aim of this part of the study was to develop a detection system for this phase transition phenomenon and we reasoned that the addition of a solvatochromic dye that could detect the change in the solvation of the micro-environment might provide the way forward. We chose Nile red since it could indicate the solvency of the PNIPAM segments as a change in its optical properties and which could be easily measured [225]. Moreover, a system in which a Nile red solution is added to a mixture of bacteria and polymer is simple, involving a small number of operational steps. Therefore, it could be a simple, sensitive and inexpensive technique to probe the interaction between the bacteria and the polymer, and future incorporation of Nile red into the polymer backbone might be useful for addition to a smart bandage. Nile red dye has been used as a fluorescent probe in a wide range of applications, such as a probe for the determination of lipids in algae and for the differentiation of normal cells and cells that accumulated phospholipids in lysosomes because its colour and fluorescence intensity change in response to the hydrophobicity of its local environment [226].

Results and discussion

To test whether a solvatochromic dye could be used as a reporter for changes in the solvation of the microenvironment of the polymer after binding to the bacteria, polymer samples were prepared as previously described for the mat/button assay and Nile red in DMSO/PBS was added directly to this and incubated with 10^8 cfu/ml bacteria for 2 h at 37°C. The fluorescence intensity was measured. The excitation wavelength was 550 nm and emission wavelength was 640 nm. The measurements were repeated at 4 hours and 24 hours. The representative relative fluorescence intensity of all samples are shown in figure 5.3.

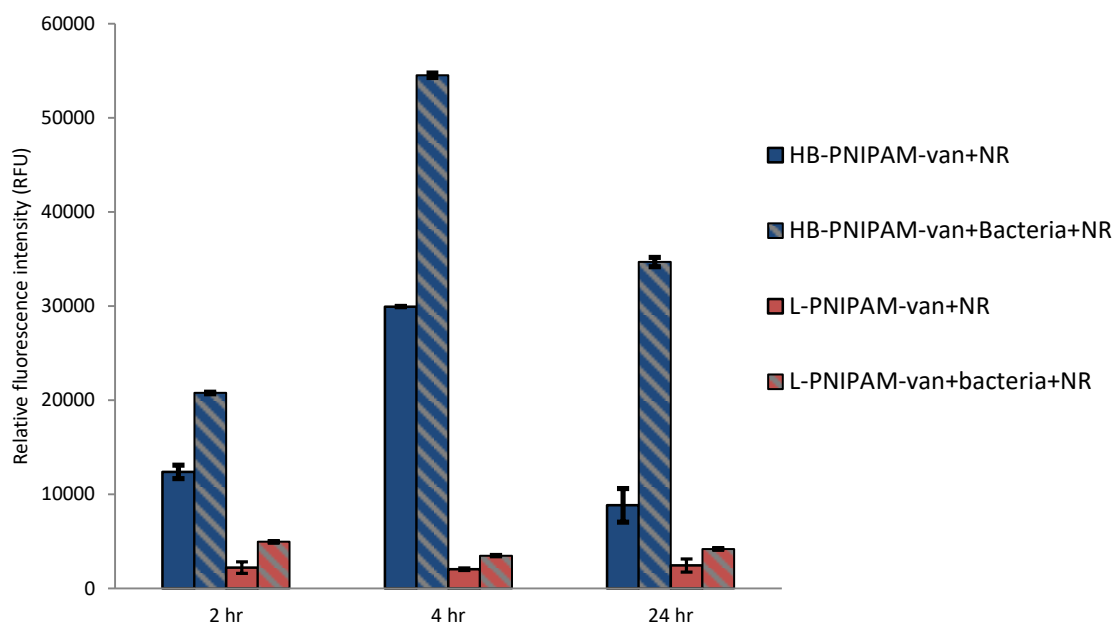


Figure 5.3 Bar chart showing relative fluorescent intensity of HB-PNIPAM-van and L-PNIPAM-van with Nile red solution incubated with 10^8 cfu/ml *S. aureus* at 37°C for 2, 4 and 24 hours Data are from three independent experiments performed in duplicate with the fluorescence of the controls (bacteria alone) subtracted

Figure 5.3 shows that a significant increase in the fluorescence intensity in the HB-PNIPAM-van system on binding to the bacteria occurred at each time point. A much smaller change in the fluorescence and intensity of the fluorescence of L-PNIPAM-van mixed with *S. aureus* was seen compared with that observed with HB-PNIPAM-van at every time point All these showed greater fluorescence than a control of HB-PNIPAM-van alone. It is suggested that this relative increase in fluorescence indicates the change in solvation of the polymer in the presence of bacteria, which was greatest with the HB-PNIPAM-van. However, the above data were generated from a single concentration of bacteria (10^8 cfu/ml) but our aim was to try to detect a more clinically relevant number of bacteria i.e. 10^5 cfu/ml. Consequently varying numbers of bacteria (10^5 - 10^8 cfu/ml) were incubated with polymer plus Nile red at 37°C for 2 h and the fluorescence intensity measured (550 nm excitation) after 2, 4 and 24 hours Representative fluorescence spectra of all samples are shown in figures 5.4-5.6 over a range of 600-700 nm_{em} with a maximum peak at 640 nm.

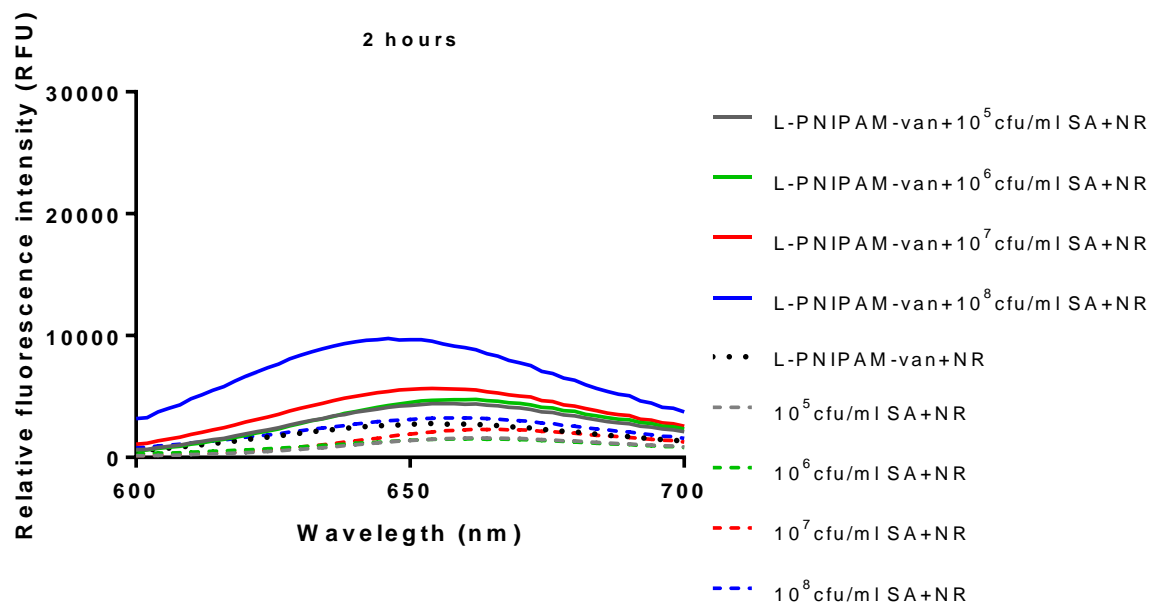
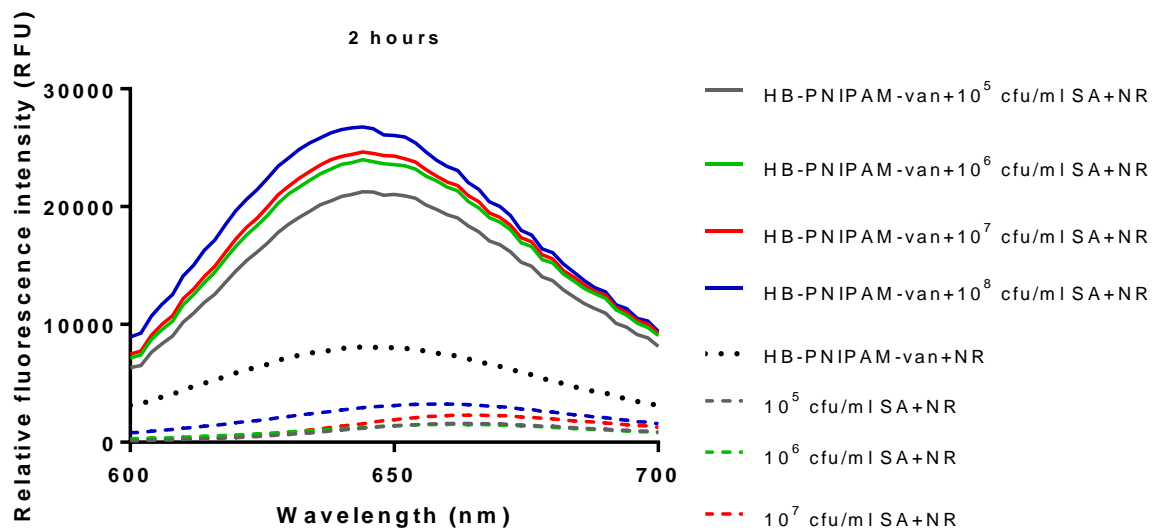


Figure 5.4 Fluorescence intensity of HB-PNIPAM-van and L-PNIPAM-van solutions incubated with 10^5 - 10^8 cells/ml *S. aureus* and Nile red at 37°C at 2 h

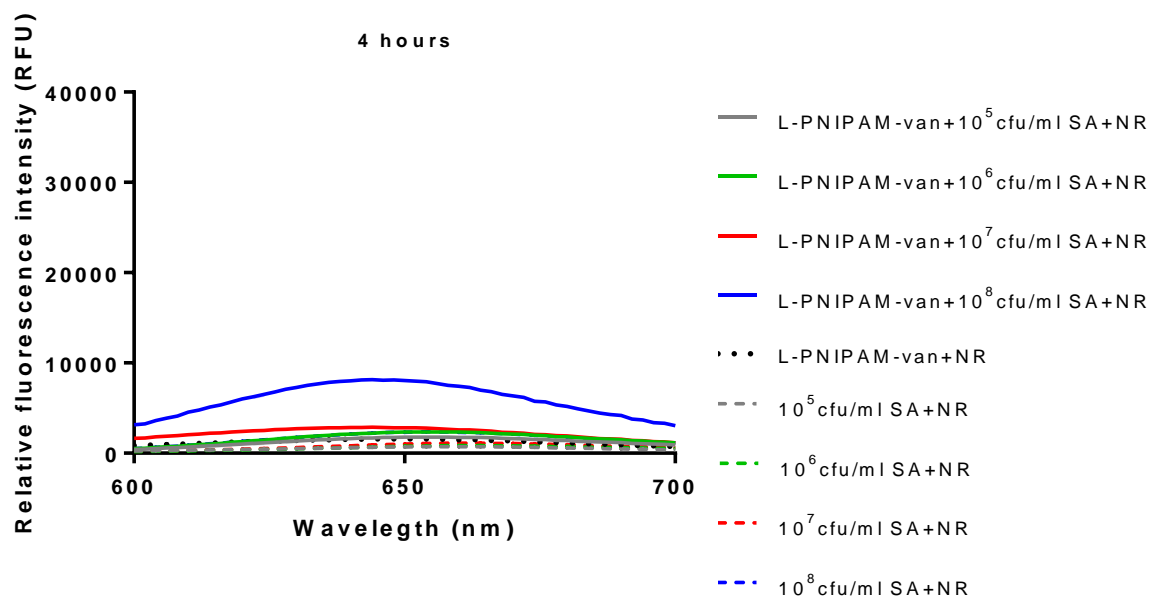
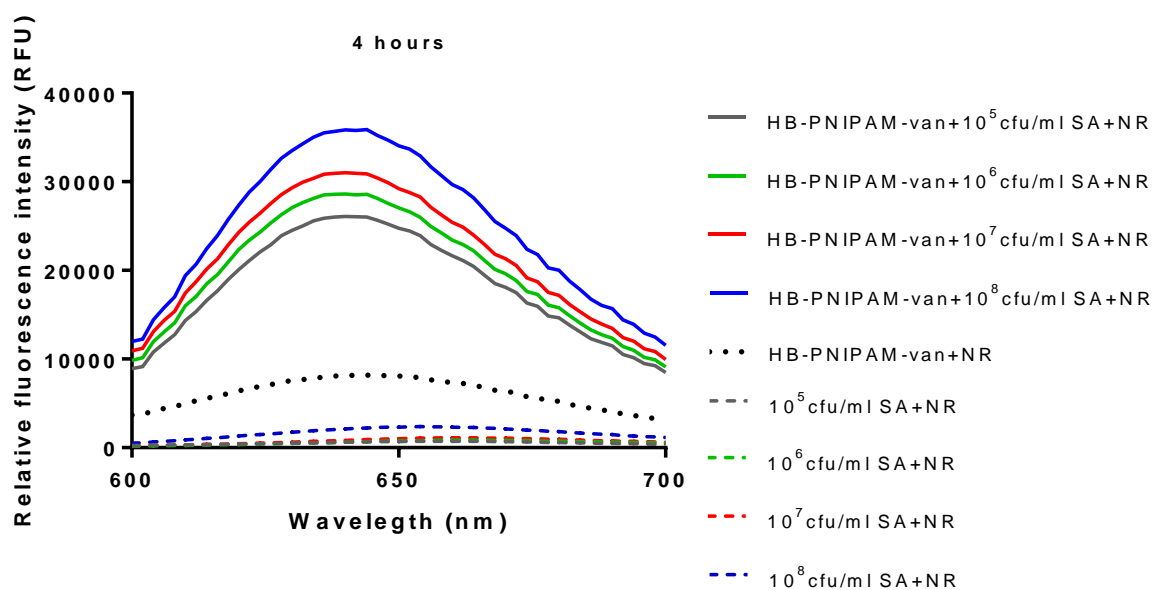


Figure 5.5 Fluorescence intensity of HB-PNIPAM-van and L-PNIPAM-van solutions incubated with 10^5 - 10^8 cells/ml *S. aureus* and Nile red at 37°C at 4 h

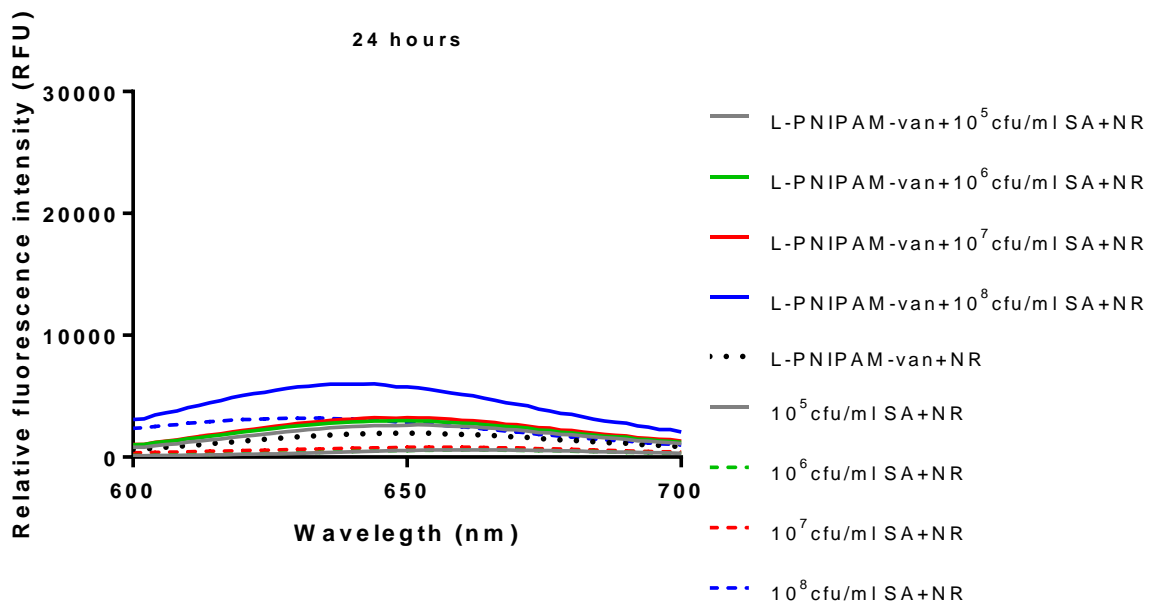
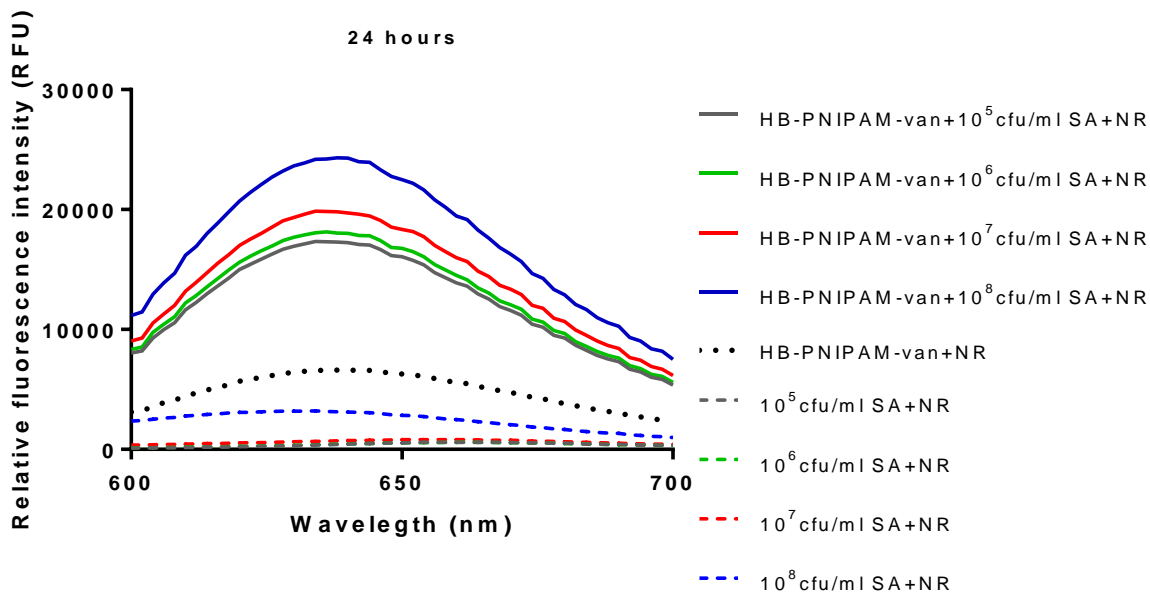
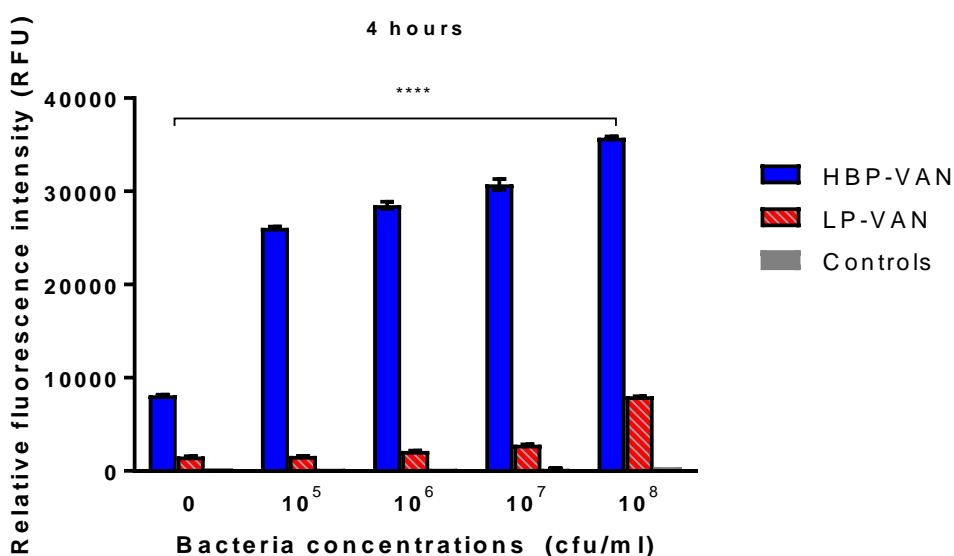
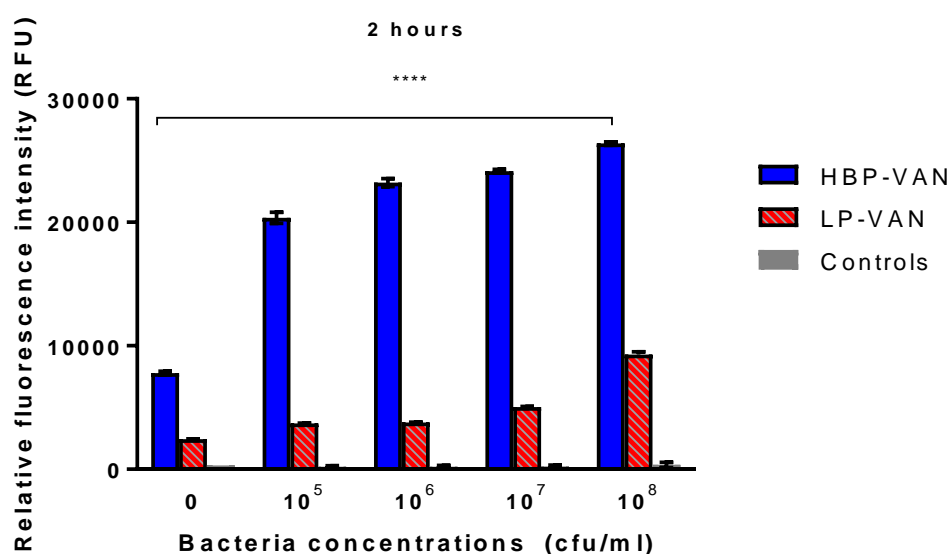


Figure 5.6 Fluorescence intensity of HB-PNIPAM-van and L-PNIPAM-van solutions incubated with 10^5 - 10^8 cells/ml *S. aureus* and Nile red at 37°C at 24 h

The fluorescence intensity measurements of the polymers incubated with *S. aureus* at different bacterial concentrations with Nile red show that, at the same bacterial concentration at all-time points, the fluorescence intensity of HB and the linear polymer decreased in the

order $10^6 < 10^7 < 10^8$ cfu/ml at all times but there was no significant difference between the polymer with 10^5 and with 10^6 cfu/ml of bacteria. A significant increase in the fluorescence intensity was found with HB-PNIPAM-van plus Nile red incubated with 10^8 cfu/ml *S. aureus* compared with other bacteria concentrations. Also, a comparison of the maximum fluorescence peaks achieved with highly branched versus linear-PNIPAM-van showed that more fluorescence occurred with the HB-PNIPAM-van at all times.

The fluorescence intensity values of the HB-PNIPAM-van and L-PNIPAM-van in the presence of bacteria are re-worked as a bar chart to make comparison easier and this is shown in figure 5.7. The values of the controls (polymer alone and bacteria alone), were subtracted.



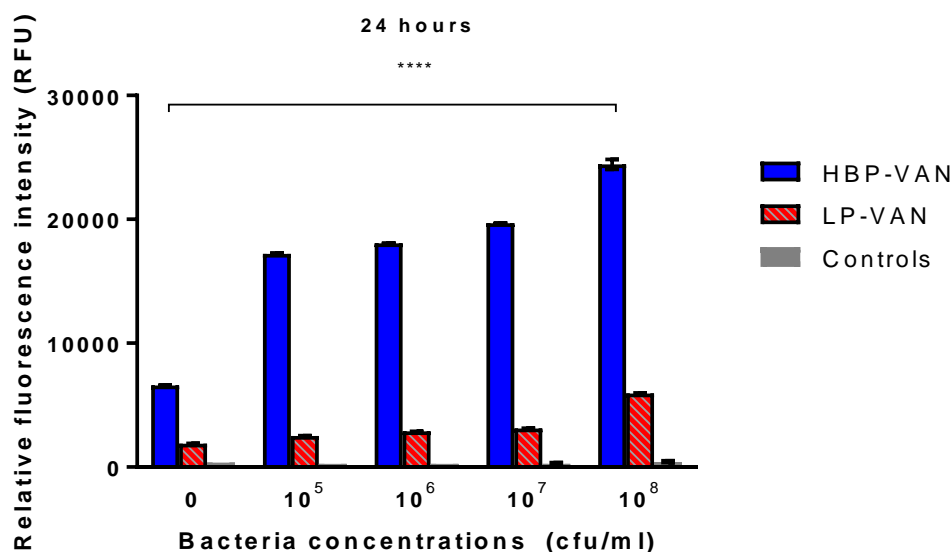


Figure 5.7 Fluorescence intensity of L-PNIPAM-van and HB-PNIPAM-van with increasing number of bacterial cells (10^5 - 10^8 cfu/ml) at 2, 4 and 24 hours using Nile red as probe with excitation at 550 nm and emission at 640 nm. The degree of significance is defined by *P* value: **** when $P \leq 0.0001$.

We found that, at any given bacterial load, the fluorescence intensity of the Nile red with HB-PNIPAM-van was much greater than with the L-PNIPAM-van or the controls. Moreover, the fluorescence intensity associated with both polymers decreased as the number of bacteria decreased ($10^5 < 10^6 < 10^7 < 10^8$ cfu/ml) for all incubation times. However, no obvious change in the fluorescence intensity was evident for either type of polymer using 10^5 - 10^6 cfu/ml. This suggests that the lower number of bacteria did not induce sufficient conformational change of the HB-PNIPAM-van polymer to be detectable with Nile red in this system.

A slight increase in the fluorescence intensity of the L-PNIPAM-van polymer was evident when it was incubated with bacteria at any concentration tested, but it was still very low compared with HB-PNIPAM-van. This phenomenon could be explained by the effect of the polymer structure on availability of vancomycin for binding to the target. The turbidimetric data also indicated that vancomycin did not stabilise the collapsed form of L-PNIPAM-van at 37°C, leading to a detectable cloud point. This is thought to be due to the collapsed form of the linear polymer shielding most of the vancomycin inside the globules, resulting in less available ligands for binding to the bacteria and a low hydrophobic concentration of segments that protected the Nile red from quenching in the fluorescence spectrum.

In the absence of the bacteria, the Nile red molecules partitioned into a solvated highly branched structure, but fluorescence quenching was decreased because the partly hydrated core of the highly branched segments due to hydrophobic aryl branching unit provided a less polar environment for the Nile red than the open coiled form of the linear polymer. Thus, a comparison of two polymer types alone in PBS showed that HB-PNIPAM-van had a higher intensity than the linear polymer. In the presence of bacteria, the increase in fluorescence intensity was due to bacterial binding to HB-PNIPAM-van leading to the desolvation of the polymer, which changed the micro-environment of the Nile red from polar to non-polar.

The LCST measurements described in chapter 2 indicated that both polymer types are in a semi-collapsed form at 37°C. At the LCST of such a thermo-responsive polymer, the cleavage of the hydrogen bonds between water molecules and the amide groups of the PNIPAM segment occur, causing the release of water molecules from the polymer chain. This state is the desolvated state in which the polarity of the polymer is decreased and hydrophobic interactions originating from isopropyl groups behave as a domain [223]. Moreover, the desolvated state causes a decrease in the free energy of hydration that results in a coil-to-globule transition of the polymer [131]. The collapse of the linear polymer may cause the shielding of the polymer chain ends, resulting in less efficient access to the binding sites and smaller or less aggregation of bacteria. However, the desolvation of the polymer did not shield the polymer-chain ends in highly branched structures within the globules, which is consistent with a core-shell structure of the globules. The binding sites are still located at the interface of the globules and stabilised in solution by hydrogen bonding, which can be observed as the lack of cloud point above the LCST reported in chapter 4. Therefore, the binding sites of the HB-PNIPAM-van can still bind to the target. Obviously, the core shell structure of vancomycin functional HB-PNIPAM plays a crucial role in the ability of the polymers to bind to the target. In contrast, a significant change in fluorescence intensity was not observed for the linear PNIPAM-van, which implied that the functional groups on the polymers were not available to access their targets at any bacterial concentration because the chain ends were shielded in a collapsed globule and so insufficient end groups were available to bind to the bacteria and cross-link them.

The results of these experiments suggest that the chain ends of HB-polymers (vancomycin) were not shielded in the polymer coils and could bind to *S. aureus*, leading to a significant increase in the fluorescence intensity, which is consistent with the hypothesis of desolvation of the HB-PNIPAM upon binding to the bacteria.

Solvatochromic dyes, especially nile red, are extensively used as hydrophobic detectors in a wide range of applications because of their visible optical changes, which can be used to characterise structures in a micro-heterogeneous system and are sensitive to changes in solution dynamics such as the polarity of a solvent and interactions between molecules in solution [140-142, 222, 224, 227, 228]. Stuart et al. chose nile red as a probe to investigate the aggregation behaviour of a surfactant in different types of solvents. They showed that the fluorescence intensity of nile red in methanol was much higher than the fluorescence of Nile red in *t*-butanol and water, respectively. The emission maximum of nile red in methanol decreased when the solvent polarity increased. They found that a conformational change of a surfactant in different solvent types could be detected by nile red. They concluded that Nile red could be used to measure the polarity of a surfactant in a ternary solvent system [229]. Additionally, Cartwright chose two different negative and positive types of solvatochromic dyes as molecular probes for detecting homeopathic potency due to several advantages of solvatochromic dyes, such as the simplicity of operation and their ability to provide specific information [224]. Lobnik et al. also exploited nile red as a polarity-sensitive probe for investigating a sol-gel system by dropping nile red into various types of sol-gel systems so that the micro-polarity could be investigated. They found that the intensity and the position of the absorption peak changed considerably as the polarity of the sol-gel system changed. They suggested that nile red is a viable detector of the polarity inside the ormosil cage which is modified siloxanes representing hybrid system between hydrophilic and hydrophobic properties of sol-gels precursors [225]. Previous workers showed that nile red can also be used to detect conformational changes in proteins. For example, nile red was used for detecting changes in structure of the calmodulin in the presence of calcium ions. Binding of the calmodulin protein to calcium ions induces an α -helical configuration, resulting in the exposure of hydrophobic domains that leads to the enhancement of, and a shift in, the fluorescence intensity of nile red [142].

It was initially expected that a solvatochromic shift would occur when the HB-PNIPAM-van bound to the bacteria because of the solvatochromic properties of nile red in environments of different polarity. The maximum nile red peak of the polymer incubated with the bacteria should be shifted from a higher to a lower wavelength if the binding of the HB-PNIPAM-van to *S. aureus* caused a coil-to-globule transition of the polymer because such binding should directly change the nile red environment from hydrophilic to hydrophobic. However, the hypsochromic shift of nile red in the mixture of HB-PNIPAM-van polymers incubated with bacteria could not be clearly observed but a considerable change in the fluorescence intensity

was observed. The small hypsochromic shift is a consequence of the heterogeneous distribution of the Nile red portioned within the domains of the HB-PNIPAM-van polymer. The data suggest a core-shell structure in the absence of binding consisting of a desolvated inner core and solvated outer domain. Nile red then partitions between these two domains. Binding of chain end ligand to its receptor causes desolvation of the shell domain but this effects only a fraction the portioned Nile red and the effect on the overall spectrum is small. However, the fluorescence emission spectrum is also affected by desolvation. Desolvation inhibits quenching of fluorescence because water is prevented from interacting with the dye. Therefore, the fluorescence intensity increases as the bound domains desolvate. The schematic in Figure 5.8 illustrates this explanation.

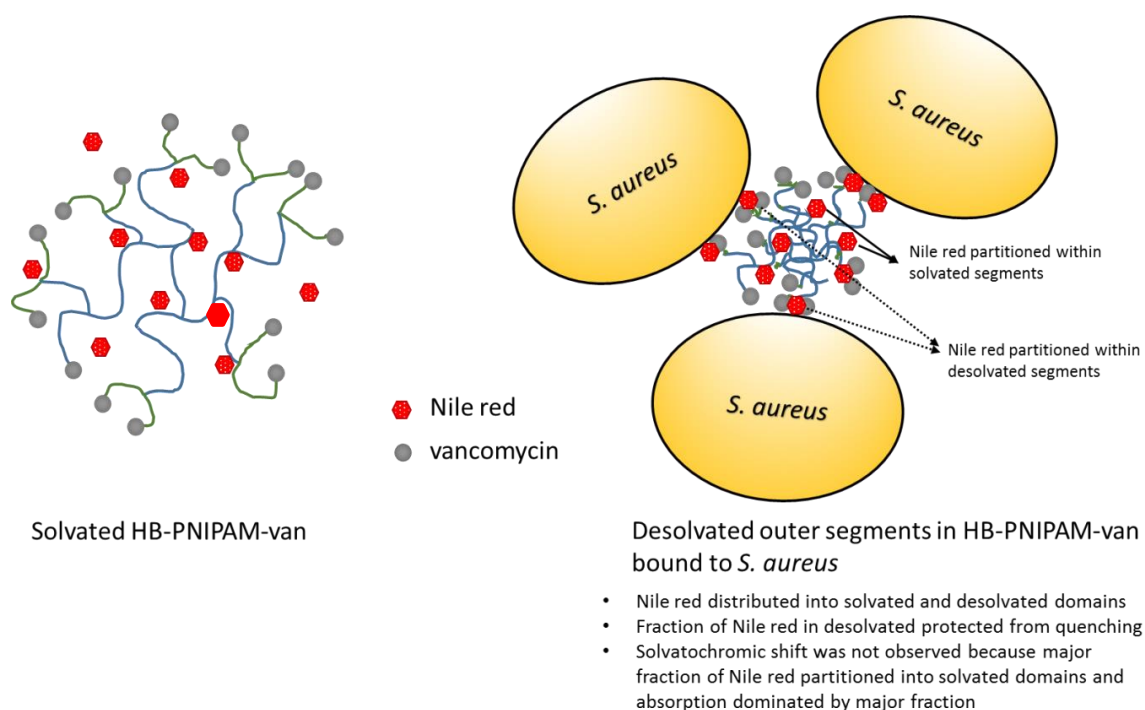


Figure 5.8 A Schematic diagram showing non-homogeneous response of HB-PNIPAM-van on binding to bacteria (via its binding site D-Ala-D-Ala) in presence of Nile red

It was previously assumed that the binding of *S. aureus* to HB-PNIPAM-van resulted in a homogeneously desolvated state. However, the current results show that only segments of the polymer bound to bacteria collapsed and this is illustrated in Figure 5.8. These observations are best compared in the absence of bacteria because the Nile red is localised homogeneously through the polymer segments but when the polymer binds to bacteria, a fraction of the polymer segments become desolvated, and the Nile red is partitioned between the solvated and the desolvated domains. Because the Nile red responses in the polymer-bacterial system

are sensitive at the segment length scale, the binding of vancomycin at the chain ends of the HB polymer at a low bacterial concentration would not have a significant effect on the Nile red molecules partitioned in the open coil segments. Therefore, these observations could also explain why the change in the environment of the outer domains due to the binding of vancomycin to the bacteria at 10^5 - 10^6 cfu/ml would not be sufficient for the Nile red to respond to the system. With HB-PNIPAM-van and bacteria at 10^8 cfu/ml, however, Nile red could detect a significant change in the hydrophobicity of its environment via a fluorescence increase, presumably because sufficient bacteria are bound to vancomycin end groups to induce the polymer to assume the collapsed form. Furthermore, partitioning of the Nile red molecules that are in the desolvated segments, which are close to bound vancomycin could decrease the quenching of the fluorescence, resulting in detectable changes in intensity. However, as Nile red is partitioned between the solvated domain (i.e., the highly branched structure) and the desolvated parts in which only the outer segments are bound to the bacteria, it is reasonable to suggest that insufficient Nile red is contained in the desolvated segments to produce a solvatochromic shift in the adsorption spectrum. These data indicate that most of the Nile red molecules are not present in the outer segment. The calorimetric results in chapter 6 also suggest that binding of polymer chain ends with a D-Ala-D-Ala dipeptide would not affect the entire polymer segment. Only a non-homogenous response of HB-PNIPAM-van binding to the chain ends occurs [204]. Plenderleith et al. also used Nile red to detect the relative polarity changes produced as the degrees of branching change in HB-PNIPAM at different temperatures. Their results suggested that the Nile red shows a marked decrease in the peak emission wavelength if the degree of branching of HB-PNIPAM is low, (i.e., 65:1, 75:1 and 85:1 repeating units per branching point) in a temperature range of 10-45°C. However, only small changes in the fluorescence spectra of 25:1 and 15:1 repeating units per branching point were noted compared with the low degree of HB-PNIPAM [137]. Their results support the model shown in figure 5.8, which explains how Nile red detected the desolvation of HB-PNIPAM-van interaction with *S. aureus* by an increase in the fluorescence intensity but not a change in wavelength.

5.5 Conclusions

In summary, binding of bacteria to highly branched PNIPAM functionalised with vancomycin induced a coil-to-globule transition on a segment length scale and formation of a crosslinked polymer-bacteria complex. This was not the case with a linear analogue of the PNIPAM-van probably because of shielding of the vancomycin substituted chain ends. The HB-PNIPAM-van phase transition with bacteria was detectable by the addition of Nile red. However, a hypsochromic shift of Nile red in this system could not be observed due to the non-homogeneous response of HB-PNIPAM-van to binding of bacteria. Also a decrease in the concentration of bacteria present plays a significant role in the amount of HB-polymer that changes phase, and this results in a detection limit for Nile red as a 'diagnostic' probe.

Chapter 6 : Comparison of the interactions of HB-PNIPAM-van and L-PNIPAM-van with D-Ala-D-Ala peptide: Investigation of enthalpy change and LCST of the polymers

6.1 Introduction

It is known that changing the environment of HB-PNIPAM-van, (e.g. by cationic or anionic salts, chain end modification, polymer architecture) have a marked influence on the phase transition of the polymer in solution and the results shown in Chapters 2-5 revealed that the polymer architecture significantly influences PNIPAM-van interaction with *S. aureus* [17, 132, 137, 157, 159, 161, 173, 230].

L-PNIPAM-van and HB-PNIPAM-van, and the results (shown in Chapters 2-5) revealed that the polymer architecture significantly influences their interaction with *S. aureus*

In terms of the differences observed so far in the interaction of the L-PNIPAM-van and the HB-PNIPAM-van with bacteria, it is important that we determine whether these differences are due to impaired access of L-PNIPAM-van to D-Ala-D-Ala dipeptides in the bacterial cell wall, or to differences in the response of the polymer to D-Ala-D-Ala binding itself. Consequently, studying interaction with isolated D-Ala-D-Ala dipeptide provides a good model system that avoids the possible influence of other constituents of the bacterial cell wall [202, 231].

The antibiotic-peptide interaction is an extensively used model for examining molecular recognition processes by various techniques. Copper et al. studied the interaction of vancomycin with dipeptide (N-Acetyl-D-Ala-D-Ala) using isothermal titration microcalorimetric (ITC) technique and showed that the enthalpy (ΔH) exhibited some dependence on the concentration of vancomycin due to aggregation/dimerization of antibiotics even at low concentration (0.004-1mM) [232]. Therefore, the D-Ala-D-Ala peptide provides a simple model for studying the accessibility of a small target like D-Ala-D-Ala peptide to vancomycin pendant groups on both HB-PNIPAM-van and L-PNIPAM-van polymers and that this interaction lends itself to study of the enthalpy changes and the LCST of the polymers.

In this work, the interaction between polymers functionalised with vancomycin and D-Ala-D-Ala peptides was examined using Micro Differential Scanning Calorimetry (microDSC). This technique can be used not only for determining the LCST of thermo-responsive polymers, but

also for investigating the enthalpy change of the polymer during the binding process. This is due to the fact that microDSC can measure the specific heat capacity (C_p) of polymers required to break hydrogen bonds between water and the polymer molecules during the phase transition process [105, 233, 234].

The hypothesis to be tested in this part of the work was that binding D-Ala-D-Ala dipeptides to the polymer chain ends would disrupt the hydration of the polymer owing to the reduced amount of water molecules involved, so that a decrease in enthalpy and LCST could be observed during the binding process. Our rationale for these experiments was that we expected both HB-PNIPAM-van and L-PNIPAM-van to bind to the D-Ala-D-Ala dipeptide target, and that the energy transfer required to transition the polymer from opened coil to a collapsed globule state would be lower when the peptide was bound to the vancomycin end groups, because binding would perturb the solvation of the polymer chain ends, leading to a decrease in the LCST of the polymers. We envisaged that both linear and highly branched versions of the polymer would behave the same because of the small size of the dipeptide vancomycin ligand and the possibility, therefore, of penetration of this peptide into regions of the polymer where the vancomycin would not be available to larger targets (i.e. whole bacteria).

6.2 Materials and Method

D-Ala-D-Ala dipeptide (Sigma Aldrich) and phosphate-buffered saline (Sigma Aldrich) were used as received.

5mg of all the types of polymers, namely HB-PNIPAM-van, L-PNIPAM-van, L-PNIPAM-COOH, HB-PNIPAM-pyrrole and HB-PNIPAM-COOH, were dissolved in 1ml of PBS. D-Ala-D-Ala peptide powder was dissolved in PBS to obtain a 1mg/ml stock solution, which was aliquoted and stored at -20°C . A range of peptide concentrations was prepared as shown in Table 6.1. The unmodified polymers (HB-PNIPAM-pyrrole, HB-PNIPAM-COOH and L-PNIPAM-COOH) were used as controls for the vancomycin-functionalised versions.

Table 6.1: The concentrations of the polymers (obtained from ELISA) and peptide used for measuring enthalpy change and LCST by microDSC

Polymer concentration (mg/ml)	D-Ala-D-Ala concentration ($\mu\text{g/ml}$)
5	0
5	0.1
5	0.2
5	0.4
5	0.5
5	0.6
5	0.7

Concentration of vancomycin attached to L-PNIPAM-van ^a (mM)	Concentration of dipeptide (mM)	Ratio of dipeptide to vancomycin
0.19	0	0
0.19	0.347	1.809
0.19	0.694	3.618
0.19	1.389	7.242
0.19	1.734	9.041
0.19	2.081	10.850
0.19	2.428	12.660

Concentration of vancomycin attached to HB-PNIPAM-van ^a (mM)	Concentration of dipeptide (mM)	Ratio of dipeptide to vancomycin
0.17	0	0
0.17	0.347	2.027
0.17	0.694	4.054
0.17	1.389	8.113
0.17	1.734	10.129
0.17	2.081	12.155
0.17	2.428	14.182

^a The concentration of vancomycin attached to the polymers calculated from ELISA (Molecular weight of vancomycin is 1458 g/mol)

The samples were prepared by vortex mixing the polymer solution with peptide solutions. The samples were degassed using a ThermoVac before use. For measuring enthalpy change using microDSC, temperature cycles were set from 10 to 40°C at a heating and cooling rate of 1°C/min. The energy used for collapsing polymers was calculated by integrating the areas under the thermogram curves.

6.3 Results and Discussion

MicroDSC was used to examine the energy required to drive transition of the linear and highly branched versions of the PNIPAM-van from coil to globule state in the presence or absence of D-Ala-D-Ala. The microDSC technique provides not only the phase transition temperatures of polymers, but also accurate amounts of heat capacity (C_p) consumed for the phase transition from liquid (solution) to solid (gel) or heat release during reversible phase change from the gel-sol state. Enthalpy changes for the sol-gel transition can be calculated from the thermogram measurement. Results obtained from instruments are a recorder output of heat capacity as a function of temperature in which the area under curve between experimental temperature limit describes the enthalpy change [159, 234, 235].

$$C_p = \left(\frac{dq}{dT}\right)_P = \left(\frac{\partial H}{\partial T}\right)_P \quad \text{Equation 6.1}$$

$$\Delta H = \int_{T_1}^{T_2} \left(\frac{\partial H}{\partial T}\right)_P dT = \int_{T_1}^{T_2} C_p dT$$

C_p	=	heat capacity
H	=	enthalpy of system
P	=	pressure
T	=	temperature

MicroDSC works on null balance concept, in which an unknown quantity is balanced by a known quantity that is varied until response of two is equal to zero. The instrument consists of two sample holders, which are the reference and sample holder. Energy is provided to each chamber independently, and the temperatures of each are detected as varying thermal

behaviour of samples change. For instance, when a phase transition of a polymer has occurred, the polymer will absorb additional associated heat. Thus, the power supply must generate additional energy to the sample so that its temperature is equal to the reference. When the phase transition is accomplished, the temperature of the polymer sample will increase and so electrical power is no longer needed to supply additional heat. Therefore, the varying electrical input shows a record of the phase transition behaviour of the polymer. Other workers have used this method to study thermo-responsive polymer phase transition [165]. Also, microcalorimetry has been used to study bacterial cell metabolic activity in relation to antibiotic sensitivity [236].

The results of our microDSC work are expressed as endothermic curves that correspond to the specific heat capacity (C_p) consumed by breaking H-bonds between polymer and water molecules versus temperature. The smaller the peak area, the lower the energy consumption during the desolvation process of the polymers. The example thermogram of L-PNIPAM-van in presence of dipeptide is shown below. From the thermogram, it can be seen that the magnitude of endothermic curve was clearly reduced when 100 μ g of peptide was added, compared with the control, which was polymer-van alone in PBS.

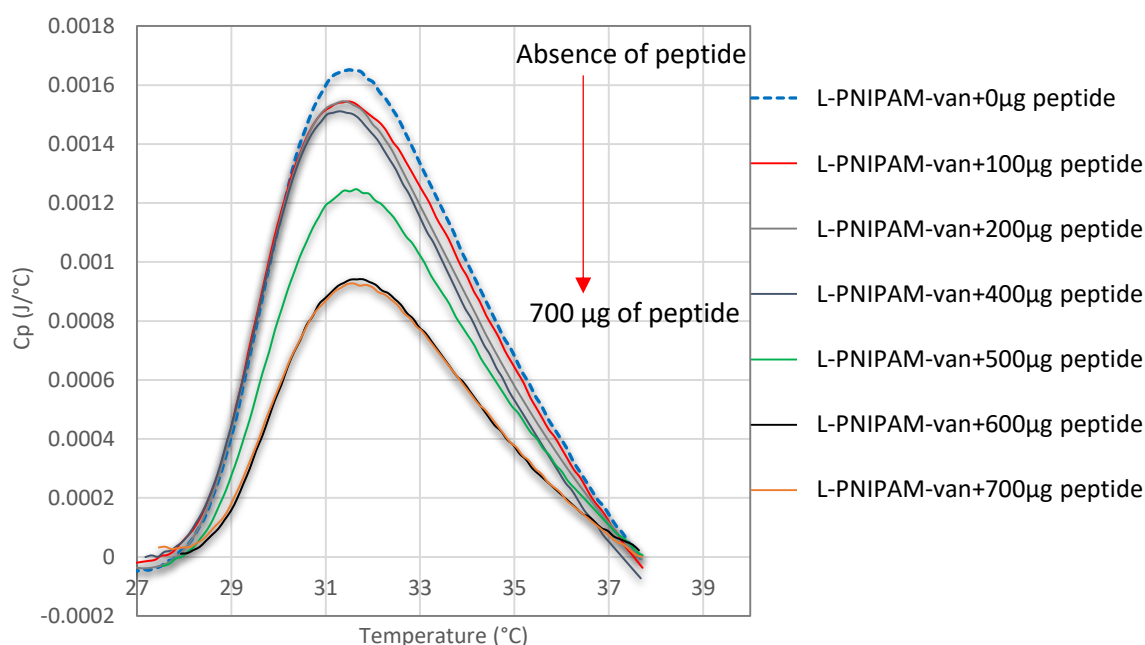


Figure 6.1 The microDSC curve of L-PNIPAM-van solution with various concentrations of D-Ala-D-Ala peptide on heating from 10 to 40 $^{\circ}$ C with the same heating rate of 1 $^{\circ}$ C/min.

From Figure 6.1, it can be seen that an increase in peptide concentration from 100 to 400 μg slightly reduced the energy needed to collapse L-PNIPAM-van from opened coiled to globule state. Then there was a more dramatic decrease in energy consumed during the phase transition of the polymer when the amount of peptide was increased up to 600 $\mu\text{g}/\text{ml}$ and reached a plateau at 700 $\mu\text{g}/\text{ml}$. Unfunctionalised L-PNIPAM-COOH was used as a control in order to confirm the specific binding between vancomycin on the polymer and D-Ala-D-Ala peptide sequences. The control polymers did not undergo a decrease in enthalpy at transition in the presence of the peptide (700 μg), which shows a decrease in enthalpy of about 0.3-4%. However, the phase transition temperature at peak maximum of the polymer in the presence of different concentrations of dipeptide appears at a similar position, which is about 32°C. There was no change in LCST of the polymer observed. This result evidently confirms an accessibility of vancomycin functionality on the L-PNIPAM-van polymers to bind to a small target like the D-Ala-D-Ala dipeptide. In the case of HB-PNIPAM-van, the results showed the same pattern as the linear version, (Figure 6.2), that is that the energy transfer required to pass HB-PNIPAM-van through opened coil to collapsed globule transition was reduced as the concentrations of the peptide sequences increased. The percentage of enthalpy decrease of both polymers with an increase in concentration of D-Ala-D-Ala peptide ($\mu\text{g}/\text{ml}$) is shown in Figure 6.2.

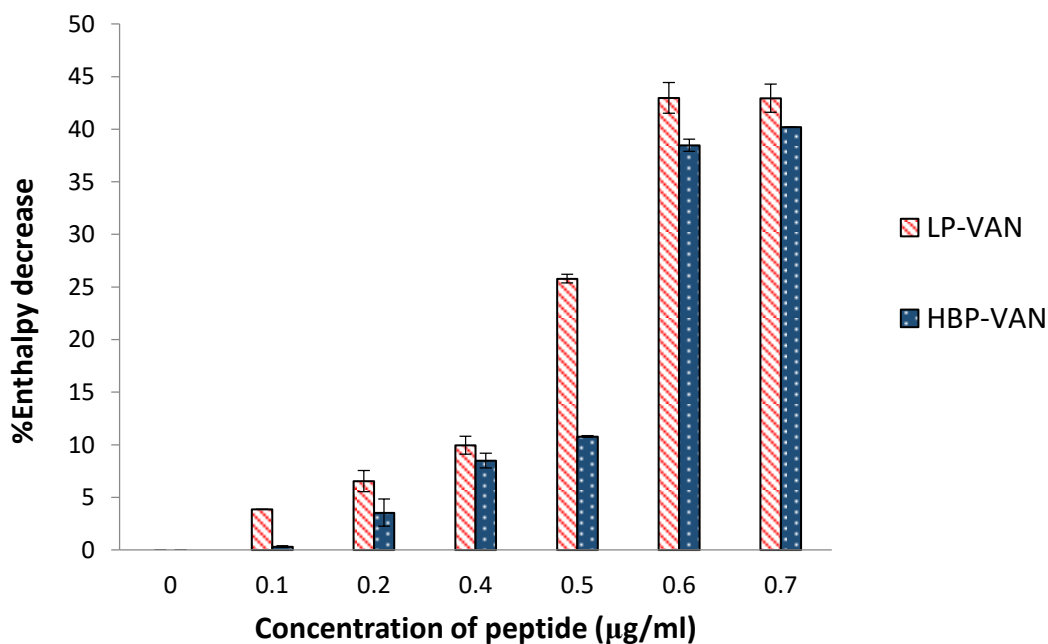


Figure 6.2 The percentage enthalpy decrease of L-PNIPAM-van and HB-PNIPAM-van in the presence of D-Ala-D-Ala peptides at various concentrations.

The percentage decreases in enthalpy for each polymer at each peptide concentration were obtained by comparison with that found with the polymers in the absence of peptide. Figure 8.2 shows that there were continuous decreases in heat used to transition both the L-PNIPAM-van and the HB-PNIPAM-van through open coiled to collapsed states when peptide concentrations were increased from 100 μ g/ml to 500 μ g/ml. Also, in both cases a significant 'step' decrease in enthalpy occurred when the peptide concentration was increased to 600 μ g/ml and a plateau was reached when the peptide concentration reached 700 μ g/ml. Unfunctionalised HB-PNIPAM with the peptide, used as a control, did not show the difference in enthalpy required to pass the polymer through to the collapsed state. These data could be explained by the equilibrium binding process between vancomycin and peptide sequences leading to abrupt conformational changes of HB-PNIPAM-van polymer. It resulted in much lower energy consumption in switching the polymer conformation from coil to globule state in the presence of peptide.

Indeed, comparison between the interactions of vancomycin in the L-PNIPAM-van and in the HB-PNIPAM-van with D-Ala-D-Ala peptide in terms of the enthalpy change can also be shown in relation to the ratio of peptide concentration (M) to concentration of vancomycin (M) on the polymer. These data are shown in Table 6.2. The concentration of vancomycin on each polymer was obtained from ELISA results (Chapter 2, section 2.3.4); which were 0.1918mM and 0.1712mM attached to L-PNIPAM-van and HB-PNIPAM-van respectively. The results of these experiments are shown in Figures 6.3 and 6.4. Figures 6.3 and 6.4 show the percentage of enthalpy change of L-PNIPAM-van and HB-PNIPAM-van observed in the presence of peptide compared to the absence of peptide.

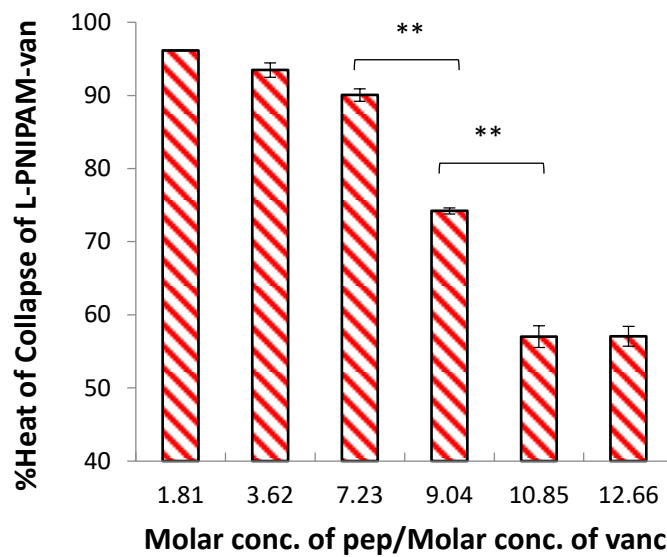


Figure 6.3 Changes in enthalpy of L-PNIPAM-van compared with the ratio of peptide: vancomycin. The significance between differences in zeta potential were tested using one way ANOVA incorporating Tukey's multiple comparison statistical test. The degree of significance is defined by P value: ** $P \leq 0.01$

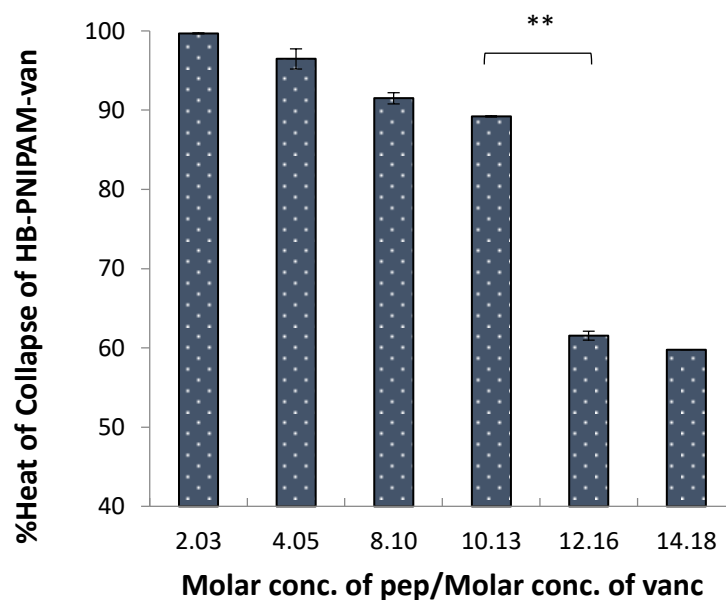


Figure 6.4 Changes in enthalpy of HB-PNIPAM-van as the ratio of peptide: vancomycin increase. The significance between differences in zeta potential were tested using one way ANOVA incorporating Tukey's multiple comparison statistical test. The degree of significance is defined by P value: ** $P \leq 0.01$

The heat consumed to pass both polymers from open to collapsed form in the absence of the peptide was considered to be 100%. There was a gradual decrease in the enthalpy change when both L-PNIPAM-van and HB-PNIPAM-van were incubated with increasing concentration of the D-Ala-D-Ala peptide. When the ratio of peptide concentration to vancomycin concentration was 12.16 for HB-PNIPAM-van and 10.85 for L-PNIPAM-van, there was a dramatic decrease in percentage of heat consumption (from 100% to ~ 60%) required to drive the polymers through to the collapsed state. Unfunctionalised polymers, HB-PNIPAM with pyrrole chain ends and L-PNIPAM-COOH, were used as controls. The result shows that a sudden step change in enthalpy reduction occurs when the ratio of peptide to vancomycin on both types of polymers is about 10:1. These data indicate the crucial number of interactions required to cause abrupt collapse of most polymer chain ends. Moreover, a significant change in enthalpy used for passing through coil to globule transition of both polymers could not be observed at lower ratios. This could be because there were not a sufficient proportional of chain ends occupied by peptide to cause detectable changes. Interestingly, such a step change is similar for both linear and highly branched polymers which could infer that both polymers contain the same amount of vancomycin binding sites. Burova et al. studied the effects of conformations of copolymer of PNIPAM with polyacrylic acids (PAA) on the binding ability of low molecular weight ionic ligands. They found that the enthalpy of collapse of the polymer decreased when the concentrations of ligands was increased [231].

There are several techniques that researchers have been used for studying the model of binding to antibiotics. Molinari et al. used the D-Ala-D-Ala dipeptide to study how the structure of vancomycin interacted with the D-Ala-D-Ala dipeptide in solution using NMR. They found that the complex of vancomycin with dipeptide resulted in observable proton chemical shifts of amide groups, which indicate strong hydrogen bonding at these positions. Moreover, they suggested that the binding of vancomycin and such a dipeptide did not cause a crucial conformational change in vancomycin antibiotic because the hydrogen atom of the secondary amine presenting on the *N*-methyl leucine of vancomycin retained the same conformation compared with the absence of dipeptide [59]. Calorimetry techniques have been used for studying non covalent interaction between peptides and antibiotics. McPhail and Copper exploited the microcalorimetry technique to study the dimerisation of vancomycin in the presence of its specific binding ligand, *N*-Acetyl-D-Ala-D-Ala. They found that vancomycin dimerisation was enhanced in the presence of such a peptide and affected the

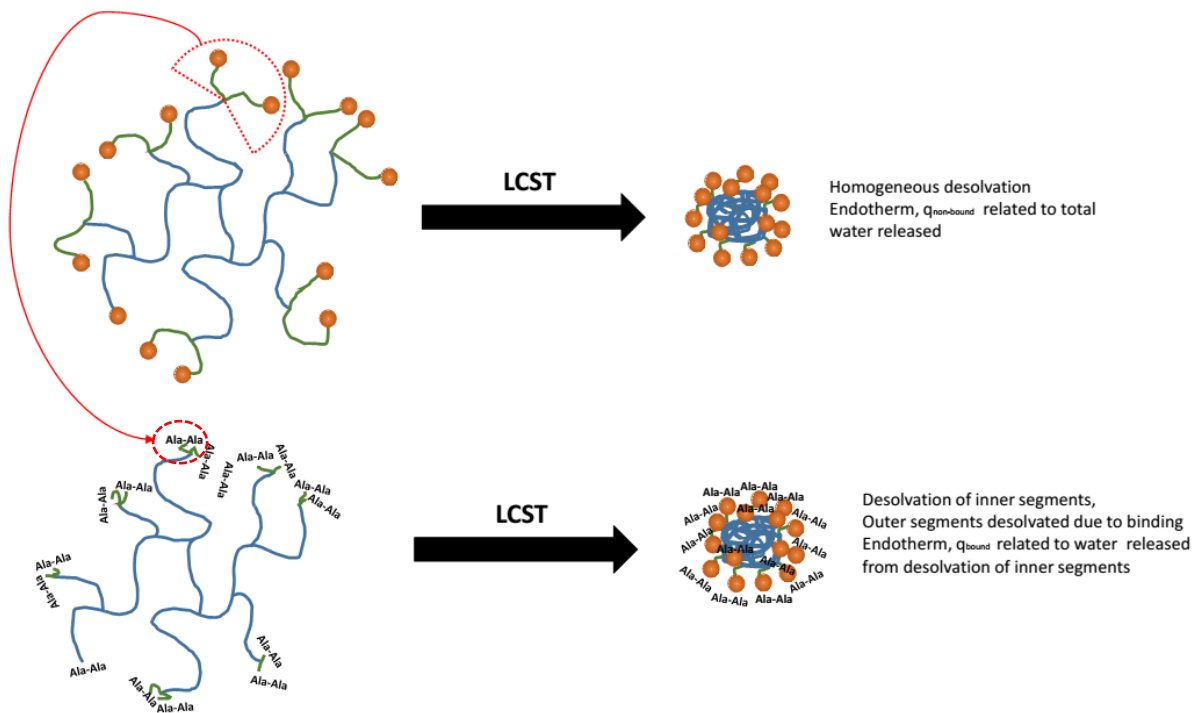
enthalpies of ligand binding [237]. Here we used microDSC to investigate the binding of D-Ala-D-Ala to the polymers and showed not only that a decrease in the magnitude of endotherm and a change in the phase transition peak occurred but also that the dipeptide could provide information on the accessibility of vancomycin on L-PNIPAM-van and HB-PNIPM-van by the target ligand (D-Ala-D-Ala).

The data from figure 6.3-6.4 can be interpreted as being evidence of D-Ala-D-Ala dipeptide binding to the vancomycin pendant of both linear and highly branched polymers and that this event significantly perturbed the solvated state of the polymers, leading from an open coiled to a collapsed state. This is illustrated by the decrease in magnitude of the endothermic peak and area under the curve of the thermogram. However, we found that there was no change in phase transition temperature of the polymers (LCST, temperature at which the peak is maximum; 31.34 °C) in the presence of the dipeptide. The decrease in peak maxima of endotherm without an observable change in phase transition peak suggests that the binding of vancomycin end groups of both polymers to the D-Ala-D-Ala dipeptide affected only the desolvation of polymer segments, rather than the whole polymer chain. The binding of vancomycin located at the outer regions of the polymer coils reduced the solvation of chain end segments, but the distant regions from the end groups remain unaffected [204]. The phase transition of the inner regions of HB structure would be dominated by the segment crowding effects [137]. This heterogeneous desolvation is also supported by the results from Chapter 5. The data from Chapter 5 revealed that the binding of vancomycin end groups of highly branched polymers to *S. aureus* provided only desolvation of the outer segment, which was detected by an increase in fluorescence intensity of the solvatochromic dye, Nile red. However, some of the Nile red, which was not present in these desolvated segments, was quenched, resulting in no detectable shift in the spectrum. This situation could also support the explanation of heterogeneous desolvation in this study. The schematic diagram is shown in Figure 6.5.

From Figure 6.5 (A) and (B), whole HB-PNIPAM-van segments are fully opened in the absence of the peptide. When the temperature is increased above its LCST all water molecules are released from the polymer chains, resulting in homogenous desolvation. On the other hand, in the presence of D-Ala-D-Ala peptides, the binding of small peptides to chain ends of HB-PNIPAM-van causes the collapse of only the chain end regions, which are represented by green lines. Therefore, once the temperature has risen to its LCST less energy is required for releasing water molecules left surrounding the inner segments, which are

represented by blue lines. Even though we expected that the addition of peptide to the vancomycin derivative polymers might cause a decrease in their LCST owing to desolvation, in fact the addition of D-Ala-D-Ala peptide did not shift the peak transition of either linear or HB functionalised polymers. This was due to highly polar vancomycin end groups of the HB-PNIPAM-van and therefore the ability to partially penetrate the polymer coils, resulting in osmotic pressure, which swells the outer segments of the branches below the LCST. Thus, when vancomycin on the polymer is bound to D-Ala-D-Ala peptides, such osmotic-driven swelling does not take place because the chain ends become less polar and desolvated, which we consider then leads to desolvation of the outer domains. Therefore, when the polymer-dipeptide complex was heated and started passing through the LCST, a smaller endotherm was found because there was less water involved in the solvation of the remaining parts.

HB-PNIPAM-van



L-PNIPAM-van

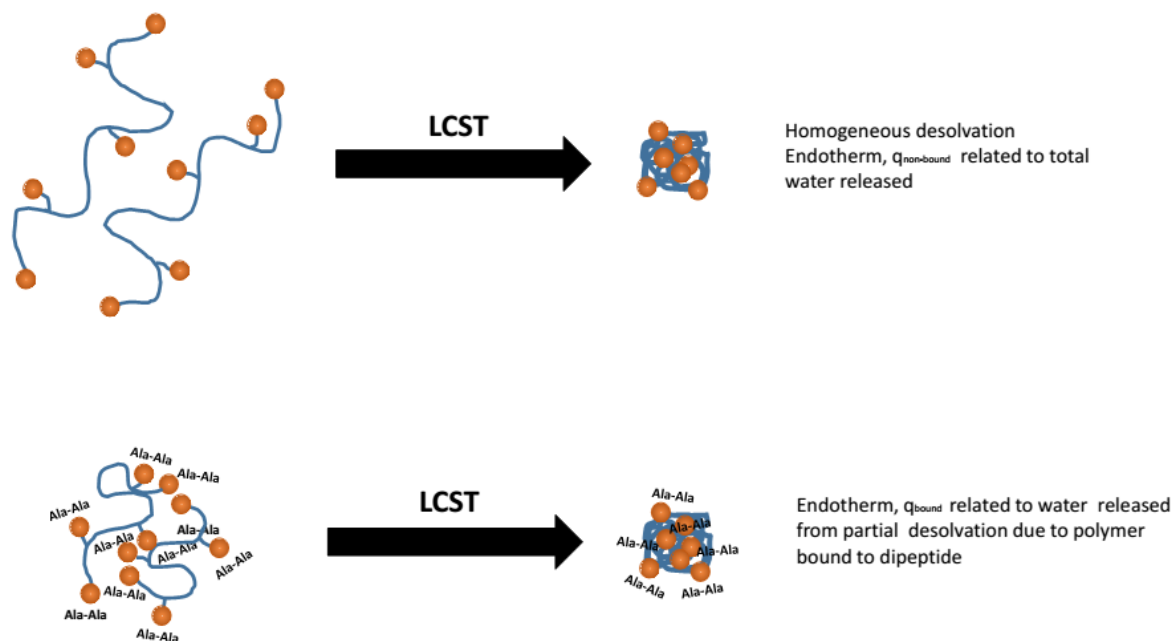


Figure 6.5 A schematic diagram showing a non-homogenous response of HB-PNIPAM-van to binding to the D-Ala-D-Ala dipeptide and relation to the LCST.

The core-shell morphology of HB-PNIPAM with polar end groups also was studied by Plenderleith et al. using calorimetry. They found that HB-PNIPAM with carboxyl end groups showed a biphasic core-shell structure. They revealed that above the coil-to-globule transition temperature of HB-PNIPAM-COOH, the inner parts of the polymer are in a desolvated state at all temperatures studied, while outer regions remain as solvated coils and these then pass through to a collapsed state as the temperature is raised. They concluded that polar end groups of HB-PNIPAM, in that case carboxylic acids, were located at the outer-shell of the globule at the LCST of the polymer [137]. Even though this model has been studied only in HB-PNIPAM with carboxylic acid end groups, vancomycin is also hydrophilic and larger than carboxylic acid group. Therefore, it is likely that core-shell formation of HB-PNIPAM-van above its LCST is a result of the effect of polar end groups in a similar way to HB-PNIPAM-COOH. Luo et al. have also reported double phase transitions of a PNIPAM brush at the surface of a hydrophobic core, which was the hyperbranched polyester Boltorn H40. The phase transition behaviour of that polymer was investigated using laser light scattering and microDSC. They found that the polymer displayed double phase changes in aqueous solution due to the micelles' structure, the first phase change of which occurred over a wide

temperature range because of the n-cluster-induced desolvation of the inner segments which are close to the hydrophobic core; the second transition, which originated from the outer segments of the PNIPAM brush, took place later. The double phase transition leads to a broad peak of LCST which can be shown by microDSC [171]. The notion of a heterogeneous response of HB-PNIPAM-van when bound to its target is also supported by results shown in Chapter 5. The addition of Nile red to the HB-PNIPAM-van-bacteria complex provided an increase in fluorescence intensity, but there was no solvatochromic shift because the Nile red molecules were distributed into both solvated and desolvated domains. The binding of vancomycin on the highly branched polymer to *S. aureus* only collapsed the outer domains while most of the Nile red partitioning within solvated domains was quenched and not affected by the change in desolvation of the outer domains, and this is why there was only a small detectable wavelength shift of Nile red. It is clear that the effect of binding of vancomycin pendant groups of HB-PNIPAM-van to targets induced the collapse of the outer region of HB-polymer, leading to a heterogeneous desolvation, which was detected by the decrease in magnitude of the endothermic peak shown in the microDSC thermogram.

In the mixture of L-PNIPAM-van with D-Ala-D-Ala, again, the phase transition temperature maintains the same position in both systems, which was about 32°C. However, a step decrease in the endotherm was observed when the concentration of peptide was increased, which could be explained by a schematic diagram in figure 6.5(B). In the absence of peptide, L-PNIPAM-van chains are in an open state. When the temperature is risen up above its LCST, hydrogen bonds between the polymer and water molecules are broken that lead to a release of water from polymer chains, resulting in homogenous desolvation. On the contrary, in the presence of D-Ala-D-Ala, these data indicated that as the polymer bound to dipeptides hydration was disrupted so that the amount of water involved was decreased, leading to less enthalpy being consumed in the desolvation process. A decrease in the magnitude of the endotherm detected by microDSC without a substantial shift in the transition peak temperature suggested that the binding of small dipeptides to vancomycin attached to the linear polymer could cause only partial desolvation of the chain end segments rather than the whole chain. The results reported here show that the D-Ala-D-Ala peptide binds to vancomycin end groups on both the L-PNIPAM-van and the HB-PNIPAM-van. However, there are differences in the behaviour of these polymers with bacteria not apparently reflected by the polymers' interaction with isolated D-Ala-D-Ala peptide. These differences appear, therefore, to be due to differences in the accessibility of the vancomycin binding sites by D-

Ala-D-Ala in the bacterial cell wall. The binding of bacteria to HB-PNIPAM-van leading to bacteria-polymer aggregation could be considered as a property called cooperativity. Cooperativity is considered to occur where there is more than one type of molecule present and where one of them is multivalent, and this results in the strength of interaction between them being much higher than two molecules acting as a simple pair. Hydrophobic interaction exhibits cooperativity, while some other types of intermolecular interactions, such as van der Waals interaction, do not [238]. Cooperative binding underlies a wide range of biochemical systems particularly where there are multiple structures, such as dimer, dendrimers and polymers. Binding of bacteria to vancomycin end groups on the highly branched polymer resulting in aggregates of bacteria-polymer complex could be explained by one of the mechanisms responsible for cooperativity, namely ligand-induced-protein clustering reported by Bertozzi and Keissling. This is because the HB polymer with vancomycin pendants displays multivalent ligands and can occupy multiple binding sites on the bacterial cell walls. Thus, the presence of aggregates of bacteria-polymer complex could be due to the ability of multivalent ligands to cluster their receptors in cooperativity [205] (Fig. 4.12). Binding of multivalent groups on the HB-PNIPAM-van to *S. aureus* can cause not only desolvation of the polymer, which creates a more hydrophobic-interactive environment to the bacteria but also clustering of the bacterial cells resulting in the mat of aggregates. In the case of L-PNIPAM-van, no aggregation occurs when the polymer was incubated with bacteria above its LCST because the organisation of binding sites is one of the factors that is involved in the multivalent binding mechanism. Above the LCST, the pendant ligands of L-PNIPAM-van became shielded inside the globule, rendering them unavailable for interacting with bacteria. An increase in activity of multipoint interaction can occur if the display of binding groups is favourably oriented. However, as mentioned above the effect of cooperative binding between multivalent ligands and their targets can display a wide range of different effects depending on their binding mechanisms. In the case of ligand-induced-protein clustering, the activity seen is due to the ability of multivalent derivatives to form clusters with their targets. Since the D-Ala-D-Ala were individual moieties in solution that contain only binding site, thus the polymers with vancomycin are not able to cluster them and form cross-linking networks. However, the D-Ala-D-Ala on the bacterial cell surface is anchored so binding networks of these could be formed.

6.4 Conclusions

We sought to confirm that vancomycin end groups of both linear and highly branched polymers were still functional and able to bind to their targets. The data presented here indicate that as the vancomycin residues on the chain ends of the polymers bind to D-Ala-D-Ala peptide, hydration was disrupted so that the amount of water involved was decreased, resulting in less energy consumed in the heat-driven desolvation process of the polymers. However, the results showed that binding of D-Ala-D-Ala peptides only decreased the energy used for passing the polymers through from solvated to desolvated states because only polymer chain end segments, which are located near to vancomycin residues were affected. The binding of vancomycin end groups to the D-Ala-D-Ala peptide did not influence the inner region, which is called a non-homogenous response. Thus, the binding of peptide sequences to the polymer modified with vancomycin only reduced the amount of water molecules around the chain end region of polymer coils, resulting in heterogeneous desolvation. Therefore, when the polymer bound to the dipeptide was heated, only a reduction in magnitude of the endothermic peaks was observed.

Interestingly, the data suggested that there was no evident difference in behaviour between L-PNIPAM-van and HB-PNIPAM-van in terms of their interaction with small molecules such as D-Ala-D-Ala. Moreover, it provides strong support for the differences in binding behaviour to *S. aureus* shown in Chapter 4 not being due to differences in the degree of vancomycin substitution between the two types of polymers. Instead it is due to the polymer architecture.

Chapter 7 : Summary, and Conclusions

7.1 Summary and Conclusions

In this work, I have focused on a comparison of behaviours of linear and highly branched analogous PNIPAM functionalised with vancomycin at the chain ends. The vancomycin acts as responsive binding sites for Gram-positive bacteria, such as *S. aureus* and has potential application for the detection of infection. A range of techniques were used to show that polymer architectures play a crucial role in their ability to bind to their targets. HB-PNIPAM-van was successfully synthesised via self-condensing vinyl polymerisation (SCVP)-reversible addition-fragmentation chain transfer (RAFT) polymerisation using 4-vinylbenzyl-1-pyrrole carbodithioate as the chain transfer monomer. The linear analogous polymer was carefully synthesised by copolymerising NIPAM with vinyl benzoic acid to provide a similar fraction of repeating units, because HB-PNIPAM consists of aryl branching points. The end groups of the polymers were modified from pyrrole to carboxylic acids and vancomycin. The functionalities of both polymers were investigated using FTIR spectroscopy at each step of chain end modification. It was found that C=O stretching of carboxylic acids ends disappeared after succinimide/DCC reaction and new peaks originating from C=O antisymmetric and symmetric stretch and carbonyl stretch appeared. All these peaks diminished when vancomycin was attached. Methanol-based SEC analysis was used to determine the molar mass average of both polymers using three different types of detectors and the results show that the molecular weight of L-PNIPAM-van and HB-PNIPAM-van were higher than 10^5 g/mol. Highly branched architecture was indicated by a α value from the Houwink Sakurada equation. Values of α were less than 0.5 for HB-PNIPAM-van and about 0.5 for the linear copolymer, as expected. Nonetheless, the highly branched polymer could be indicated from the critical solution behaviour.

In this study, microDSC and turbidimetry techniques were used to determine the phase transition temperature of the polymers. The results from microDSC showed that the LCST of HB-PNIPAM was increased at each step of chain end modification and also with linear polymer when vancomycin was attached thanks to the change in the nature of polar end groups. Interestingly, the cloud point of HB-PNIPAM-van could not be observed by turbidimetry, whereas it could for the linear analogous version.

Generally, colloidal stability of PNIPAM in a dilute solution is attained by inclusion of a negatively or positively charged comonomer. This leads to the formation of stable aggregates above the LCST due to electrostatic intermolecular interaction between the polymer strands. Aseyev et al reported that PNIPAM can form mesoglobules in a dilute solution at temperatures above the LCST [239]. Mesoglobules are the stable collections of equally-sized spherical globules of polymer chains in aqueous solution without immediate precipitation upon heating. The intermolecular aggregation will not continue when a certain size aggregates are formed. There are two main factors affecting the size of such mesoglobules, which are polymer concentration and heating rate. The size of mesoglobules increases with increasing concentration of the polymer. Additionally, a high heating rate (non-equilibrium heating) passing through the polymer's LCST results in small sized particles compared to those formed when the rate of heating is slow (equilibrium heating). This is because at slow heating rates the polymer chains tend to associate with each other before they collapse which leads to larger sizes of mesoglobules. Moreover, colloidal stability of PNIPAM is affected by the presence of salt in in the solute.

Considering the conformation of L-PNIPAM-van in aqueous solution at 37°C, which is the phase separation boundary for L-PNIPAM-van, polymer coils pass from an extended solvated form to a collapsed conformation. The phase transition is mainly driven by hydrophobic interaction and intermolecular interaction between the polymer chains. L-PNIPAM-van consists of vancomycin pendant groups along the polymer backbone and since these are charged moieties, they should contribute to the formation of stable mesoglobules in aqueous solution. Consequently, it would be expected that when L-PNIPAM-van reaches its phase transition temperature the hydrophobic backbone passes from solvated coils to desolvated collapsed globules. Some vancomycin groups become trapped within the globules, while those that are not trapped turn outside toward water molecules, so stable aggregates should be formed. However, in our bacteria binding experiments the polymer concentration (5mg/ml) used was high (concentration of a typical dilute solution is 0.1-1mg/ml), thus, the size of the mesoglobules of L-PNIPAM-van in aqueous solution would be expected to be larger than those formed in a dilute solution. In addition, the polymer would gradually precipitate upon heating leading to a cloudy solution due to the strong tendency of macromolecules to aggregate. This is shown in Chapter 2, Fig 2.17. While this principle would similarly contribute to the behaviour of HB-PNIPAM-van, in fact the polymer did not precipitate macroscopically at any temperature and so did not form a cloudy solution. However, the

polymer did go through a phase transition since its collapse was detectable by microDSC. (Fig 2.15). This behavior can be explained by the ‘core-shell’ concept of HB-PNIPAM-van. In the case of the highly branched structure, when above the LCST, vancomycin groups are located at the outer edges of globules and provide electrostatic colloidal stability. On the other hand, some of vancomycin on the linear analogous polymers becomes trapped within the globule above its LCST, and so are not available to stabilise the collapse, resulting in large aggregates of L-PNIPAM-van in solution that are detectable using turbidimetry.

Quantification of vancomycin substitution in L-PNIPAM-van and HB-PNIPAM-van was carried out using multi-layered ELISA. The results show that both polymers contained the same amount of vancomycin and while these data were generated from a single concentration of polymer, support from other findings confirmed the similarity of vancomycin loading. It was important to determine whether these functionalised polymers had antimicrobial activity and so this was assessed against a common pathogen, *S. aureus*. Neither the L-PNIPAM-van nor the HB-PNIPAM-van demonstrated antimicrobial activity and this is thought to be due to the fact that the large polymer chains were unlikely to penetrate deep within the peptidoglycan structure of the bacterial cell wall to access the target a large number of D-Ala-D-Ala groups near the cell membrane but rather the vancomycin groups bind only to surface located Ala-Ala peptides.

L-PNIPAM-van and HB-PNIPAM-van were further assessed in terms of the polymer binding to bacteria. It was found that HB-PNIPAM-van binds specifically to *S. aureus* at 37°C, resulting in the formation of a mat of bacteria-polymer complex and the aggregation of bacteria, whereas L-PNIPAM-van fails to bind and form a mat under these conditions. This is suggested to be because binding of the pendent vancomycin triggers a chain of events that leads to desolvation of the polymer resulting in shielding of the vancomycin end groups. In contrast, as a result of the core-shell conformation of HB-PNIPAM-van, vancomycin did not penetrate into the globule and thus vancomycin binding sites were still available for interaction with the targets. A cross-linking of bacteria-polymer complex and an aggregation of bacteria in the presence of HB-PNIPAM-van visualised under UV light and by confocal microscopy suggested that this was due not only to the consequence of the phase transition of the polymer, but also to binding of bacteria to multiple-chain ends of the HB-PNIPAM-van. This in turn provided a more hydrophobic interactive environment for the bacteria and lead to a cross-linked network of bacteria and polymer. It is evident that the core-shell formation of

HB-PNIPAM-van plays a crucial role in both the behaviour of the polymer in solution, and the accessibility of the binding sites to their targets.

We also found that the hydrophobicity of bacteria has a significant effect on the binding of the bacteria to HB-PNIPAM-van. The Mat/button assay and confocal microscopy results showed that HB-PNIPAM-van was able to bind to *S. aureus* Oxford (NCTC6751) and S235, which are hydrophobic strains, whereas it was much less efficient in aggregating the L9879 and the Newman strains, which are more hydrophilic. Despite this, and recognising that the binding of microorganisms to various compounds and substrates is a complex process, it seemed possible that interaction between bacteria and polymers could be influenced by the surface charge on the bacteria. Investigation of bacterial cell surface charge showed that all four strains tested had net negative charges and the Zeta potential values decreased as the ionic strength of the buffer increased. However, HB-PNIPAM-van caused mat formation with the Oxford (NCTC6751) and S235 strains, even though they showed the highest negative charge in the potassium phosphate buffer, indicating that there is no relationship between the charge of the bacterial cell surface and the binding capability of the polymer and that variations in polymer-bacteria aggregation observed were most likely due to hydrophobicity/hydrophilicity of the bacteria. The higher the hydrophobicity, the greater the binding to HB-PNIPAM-van.

The amount of D-Ala-D-Ala binding sites available on the bacterial cell wall was considered to be another factor that might play a role in the polymer-bacteria interaction. However, determination of D-Ala-D-Ala binding sites on each strain, as determined by probing with fluorescent vancomycin, showed that polymer binding to different bacteria could not be explained by this parameter.

The relationship between formation of bacterial aggregates by the polymers and the phase change in the polymer was further examined in terms of the solvation changes in the polymers on interaction of their vancomycin chain ends with its target. For this we employed the fluorescent solvatochromic dye, Nile red and found that the HB-PNIPAM-van showed a significant increase in fluorescence intensity in the presence of bacteria. The phase transition of the polymers was detected by a change in the fluorescence intensity of the dye, not by a hypochromic shift in the absorption spectrum. The lack of a hypochromic shift could be explained by a non-homogenous response of the polymer bound to the bacteria. It could be speculated that the presence of Nile red in the polymer-bacteria system is sensitive at the

segment length scale and binding of vancomycin end groups of the HB-polymer to the target provided only desolvated outer segments. A large fraction of the inner segment would not be affected. Also, the results indicated that the majority of Nile red was not present in the desolvated domains and so a solvatochromic shift could not be observed. The increase in fluorescence intensity, on the other hand, was thought to be due to a fraction of the Nile red present in the desolvated state being protected from quenching. Compared with the linear analogous polymer, the fluorescence intensity of Nile red with HB-PNIPAM-van incubated with bacteria at any given bacterial load was much higher than with the L-PNIPAM-van. We also found that a decrease in concentration of bacteria plays an important role in the amount of HB-PNIPAM-van that changes during the phase transition. This leads to a detection limit for Nile red that can be used as a form of infection diagnosis.

Finally, we also extended the comparison of both polymers in terms of their interaction with the D-Ala-D-Ala peptide. The data indicated that the difference in binding behaviour between linear and highly branched polymers functionalised with vancomycin is due to the polymer architecture and not to a difference in the degree of vancomycin substitution. The magnitude of the endothermic curves was significantly decreased when dipeptide interacted with the pendent vancomycin on both polymers. These data strongly indicate that the binding of vancomycin end groups to the Ala-Ala dipeptide affected the solvation of the outer segment rather than the whole polymer coil. Desolvation of the bound region reduced the amount of water involved in the coil-to-globule transition, thus, when the polymer dipeptide complex was heated up, a lesser endothermic peak was observed. These results could also support the heterogeneous desolvation of chain end segments bound to bacteria detected by the addition of Nile red.

In conclusion, the highly branched PNIPAM has advantages over the linear analogous version in several aspects, in particular the accessibility of ligands to their targets above its LCST. The HB-PNIPAM functionalised with vancomycin chain ends would appear to be a novel material that could be used for detecting *S. aureus* for diagnostic purposes.

Chapter 8: Future Work

There are several features of this study that are worthy of further exploration.

The SEC analysis of highly branched polymers is more complicated than that of linear polymers. The different types of chain end functionalities obtained from each modification directly affect the solubility and require different types of eluents than those used in standard SEC. Moreover, a significant difference in the chemical structure of the polymer standards and the samples could lead to different behaviour in solution and inaccurate results. Therefore, the data could be improved by using DOSY NMR to determine the average molar mass and the hydrodynamic radius of highly branched polymers compared with SEC analysis.

Following on from Chapter 5, incorporation of solvatochromic dyes into the polymer backbone by copolymerising NIPAM with Nile red acrylate could increase the sensitivity of the detection system for a wide range of bacterial concentrations, and also when the polymer conformation of local segments change due to binding to bacteria. Another consideration is the location of dye on the structure. Different types of branched polymers, with various degrees of linear extended branches incorporated with the solvatochromic dye at different locations, should be considered, so that when the polymer chain ends bind to their targets, the dye may be sufficiently sensitive to the change in polymer conformation to allow easy detection.

Finally, using bacteria instead of the D-Ala-D-Ala peptide to investigate the change in the phase transition temperature of vancomycin derivatised polymers by microDSC could provide clearer and useful information. This would require the equipment to be available for use with bacteria. Also, high resolution ^1H NMR spectrometry (500 MHz) would be a technique that would help investigate the conformational changes of the polymers in the presence of target molecules (D-Ala-D-Ala) by monitoring the chemical shift and the resonance peak of the amide proton, methylene proton and methyne proton. The change in phase transition temperature of the polymer with vancomycin chain ends bound to dipeptide might be able to be detected by a down shift of the amide proton and the sharper peaks of protons from side chains due to the increase in mobility of the polymers as temperature is increased.

References

- [1] Hurley JC. Comparison of mortality associated with methicillin-susceptible and methicillin-resistant *Staphylococcus aureus* bacteremia: An ecological analysis. *Clinical Infectious Diseases*. 2003;37:866-68.
- [2] Kasten KR, Makley AT, Kagan RJ. Update on the critical care management of severe burns. *Journal of intensive care medicine*.2011;26:223-36.
- [3] Golabi M, Kuralay F, Jager EWH, Beni V, Turner APF. Electrochemical bacterial detection using poly(3-aminophenylboronic acid)-based imprinted polymer. *Biosensors & bioelectronics*. 2016;93:87-93.
- [4] Church D, Elsayed S, Reid O, Winston B, Lindsay R. Burn wound infections. *Clinical Microbiology Reviews*. 2006;19:403-34.
- [5] Lowy FD. *Staphylococcus aureus* infections. *The New England Journal of Medicine*. 1998;339:520-32.
- [6] Rybak JM, Barber KE, Rybak MJ. Current and prospective treatments for multidrug-resistant gram-positive infections. *Expert opinion on pharmacotherapy*.2013;14:1919-32.
- [7] Whitehouse JD, Friedman D, Kirkland KB, Richardson WJ, Sexton DJ. The impact of surgical-site infections following orthopedic surgery at a community hospital and a university hospital: Adverse quality of life, excess length of stay, and extra cost. *Infection Control and Hospital Epidemiology*. 2002;23:183-9.
- [8] Mi L, Xue H, Li Y, Jiang S. A Thermoresponsive Antimicrobial Wound Dressing Hydrogel Based on a Cationic Betaine Ester. *Advanced Functional Materials*.2011;21:4028-34.
- [9] Tan SP, McLoughlin P, O'Sullivan L, Prieto ML, Gardiner GE, Lawlor PG, et al. Development of a novel antimicrobial seaweed extract-based hydrogel wound dressing. *International journal of pharmaceutics*.2013;456:10-20.
- [10] Howden BP, Davies JK, Johnson PDR, Stinear TP, Grayson ML. Reduced Vancomycin Susceptibility in *Staphylococcus aureus*, Including Vancomycin-Intermediate and Heterogeneous Vancomycin-Intermediate Strains: Resistance Mechanisms, Laboratory Detection, and Clinical Implications. *Clinical Microbiology Reviews*. 2010;23:99-139.
- [11] Kobayashi J, Okano T. Thermoresponsive thin hydrogel-grafted surfaces for biomedical applications. *Reactive & Functional Polymers*.2013;73:939-44.

- [12] Gandhi A, Paul A, Sen SO, Sen KK. Studies on thermoresponsive polymers: Phase behaviour, drug delivery and biomedical applications. *Asian Journal of Pharmaceutical Sciences*. 2015;10:99-107.
- [13] de las Heras Alarcon C, Pennadam S, Alexander C. Stimuli responsive polymers for biomedical applications. *Chemical Society Reviews*. 2005;34:276-85.
- [14] Liu Y, Meng S, Mu L, Jin G, Zhong W, Kong J. Novel renewable immunosensors based on temperature-sensitive PNIPAAm bioconjugates. *Biosensors & Bioelectronics*. 2008;24:710-5.
- [15] Lam SJ, O'Brien-Simpson NM, Pantarat N, Sulistio A, Wong EHH, Chen Y-Y, et al. Combating multidrug-resistant Gram-negative bacteria with structurally nanoengineered antimicrobial peptide polymers. *Nature Microbiology*. 2016;1.
- [16] Shepherd J, Sarker P, Rimmer S, Swanson L, MacNeil S, Douglas I. Hyperbranched poly(NIPAM) polymers modified with antibiotics for the reduction of bacterial burden in infected human tissue engineered skin. *Biomaterials*. 2011;32:258-67.
- [17] Shepherd J, Sarker P, Swindells K, Douglas I, MacNeil S, Swanson L, et al. Binding Bacteria to Highly Branched Poly(N-isopropyl acrylamide) Modified with Vancomycin Induces the Coil-to-Globule Transition. *Journal of the American Chemical Society*. 2010;132:1736-40.
- [18] Mi FL, Wu YB, Shyu SS, Schoung JY, Huang YB, Tsai YH, et al. Control of wound infections using a bilayer chitosan wound dressing with sustainable antibiotic delivery. *Journal of Biomedical Materials Research*. 2002;59:438-49.
- [19] Wasiak J, Cleland H, Campbell F, Spinks A. Dressings for superficial and partial thickness burns. *Cochrane Database of Systematic Reviews*. 2013, Issue3. Art No:CD002106
- [20] Su C-H, Chang S-C, Yan J-J, Tseng S-H, Chien L-J, Fang C-T. Excess Mortality and Long-Term Disability from Healthcare-Associated Staphylococcus aureus Infections: A Population-Based Matched Cohort Study. *Plos One*. 8.2013;8:e71055
- [21] Weiss A, Friendly D, Eglin K, Chang M, Gold B. Bacterial periobital and orbital cellulitis in childhood. *Ophthalmology*. 1983;90:195-203.
- [22] Dover JE, Hwang GM, Mullen EH, Prorok BC, Suh S-J. Recent advances in peptide probe-based biosensors for detection of infectious agents. *Journal of Microbiological Methods*. 2009;78:10-9.
- [23] Amin R, Elfeky SA. Fluorescent sensor for bacterial recognition. *Spectrochimica Acta Part a-Molecular and Biomolecular Spectroscopy*. 2013;108:338-41.

- [24] Magennis EP, Fernandez-Trillo F, Sui C, Spain SG, Bradshaw DJ, Churchley D, et al. Bacteria-instructed synthesis of polymers for self-selective microbial binding and labelling. *Nature Materials*. 2014;13:748-55.
- [25] Krishnamurthy VM, Quinton LJ, Estroff LA, Metallo SJ, Isaacs JM, Mizgerd JP, et al. Promotion of opsonization by antibodies and phagocytosis of Gram-positive bacteria by a bifunctional polyacrylamide. *Biomaterials*. 2006;27:3663-74.
- [26] Pasparakis G, Alexander C. Synthetic polymers for capture and detection of microorganisms. *Analyst*. 2007;132:1075-82.
- [27] Silbert L, Ben Shlush I, Israel E, Porgador A, Kolusheva S, Jelinek R. Rapid chromatic detection of bacteria by use of a new biomimetic polymer sensor. *Applied and Environmental Microbiology*. 2006;72:7339-44.
- [28] dos Santos Pires AC, Ferreira Soares NdF, Mendes da Silva LH, de Andrade NJ, Araujo Silveira MF, de Carvalho AF. Polydiacetylene as a Biosensor: Fundamentals and Applications in the Food Industry. *Food and Bioprocess Technology*. 2010;3:172-81.
- [29] Sun XL, Cui WX, Haller C, Chaikof EL. Site-specific multivalent carbohydrate labeling of quantum dots and magnetic beads. *Chembiochem*. 2004;5:1593-6.
- [30] Xue C, Velayudham S, Johnson S, Saha R, Smith A, Brewer W, et al. Highly Water-Soluble, Fluorescent, Conjugated Fluorene-Based Glycopolymers with Poly(ethylene glycol)-Tethered Spacers for Sensitive Detection of Escherichia coli. *Chemistry-a European Journal*. 2009;15:2289-95.
- [31] Jelinek R, Kolusheva S. Carbohydrate biosensors. *Chemical Reviews*. 2004;104:5987-6015.
- [32] Disney MD, Zheng J, Swager TM, Seeberger PH. Detection of bacteria with carbohydrate-functionalized fluorescent polymers. *Journal of the American Chemical Society*. 2004;126:13343-6.
- [33] Kim BS, Hong DJ, Bae J, Lee M. Controlled self-assembly of carbohydrate conjugate rod-coil amphiphiles for supramolecular multivalent ligands. *Journal of the American Chemical Society*. 2005;127:16333-7.
- [34] Xue X, Pan J, Xie H, Wang J, Zhang S. Specific recognition of staphylococcus aureus by staphylococcus aureus protein A-imprinted polymers. *Reactive & Functional Polymers*. 2009;69:159-64.
- [35] Tokonami S, Nakadoi Y, Nakata H, Takami S, Kadoma T, Shiigi H, et al. Recognition of gram-negative and gram-positive bacteria with a functionalized conducting polymer film. *Research on Chemical Intermediates*. 2014;40:2327-35.

- [36] Arimoto H, Nishimura K, Kinumi T, Hayakawa I, Uemura D. Multi-valent polymer of vancomycin: enhanced antibacterial activity against VRE. *Chemical Communications*. 1999;1361-2.
- [37] Li Y, Hu X, Tian S, Li Y, Zhang G, Zhang G, et al. Polyion complex micellar nanoparticles for integrated fluorometric detection and bacteria inhibition in aqueous media. *Biomaterials*. 2014;35:1618-26.
- [38] Ogston A. Micrococcus Poisoning. *Journal of anatomy and physiology*. 1882;17:24-58.
- [39] Silhavy TJ, Kahne D, Walker S. *The Bacterial Cell Envelope*. Cold Spring Harbor Perspectives in Biology. 2010;2.a000414
- [40] Krishna S, Miller LS. Host-pathogen interactions between the skin and *Staphylococcus aureus*. *Current Opinion in Microbiology*. 2012;15:28-35.
- [41] Casewell MW, Hill RLR. THE carrier state-methicilin-resistant *Staphylococcus aureus*. *Journal of Antimicrobial Chemotherapy*. 1986;18:1-12.
- [42] Collins LV, Kristian SA, Weidenmaier C, Faigle M, van Kessel KPM, van Strijp JAG, et al. *Staphylococcus aureus* strains lacking D-alanine modifications of teichoic acids are highly susceptible to human neutrophil killing and are virulence attenuated in mice. *Journal of Infectious Diseases*. 2002;186:214-9.
- [43] Weidenmaier C, Goerke C, Wolz C. *Staphylococcus aureus* determinants for nasal colonization. *Trends in Microbiology*. 2012;20:243-50.
- [44] Gordon RJ, Lowy FD. Pathogenesis of methicillin-resistant *Staphylococcus aureus* infection. *Clinical Infectious Diseases*. 2008;46:S350-S9.
- [45] Patti JM, Allen BL, McGavin MJ, Hook M. MSCRAMM-mediated adherence of microorganisms to host tissue. *Annual Review of Microbiology*. 1994;48:585-617.
- [46] DeDent AC, McAdow M, Schneewind O. Distribution of protein A on the surface of *Staphylococcus aureus*. *Journal of Bacteriology*. 2007;189:4473-84.
- [47] Beck G, Puchelle E, Plotkowski C, Peslin R. Effect of growth on surface-charge and hydrophobicity of *Staphylococcus aureus*. *Annales De L Institut Pasteur-Microbiologie*. 1988;139:655-64.
- [48] Harris LG, Foster SJ, Richards RG. An introduction to *Staphylococcus aureus*, and techniques for identifying and quantifying *S. aureus* adhesins in relation to adhesion to biomaterials: Review. *European Cells & Materials*. 2002;4:39-60.
- [49] Gristina AG. Biomaterial-centered infection-microbial adhesion versus tissue integration. *Science*. 1987;237:1588-95.

- [50] O'Riordan K, Lee JC. *Staphylococcus aureus* capsular polysaccharides. *Clinical Microbiology Reviews*. 2004;17:218-34.
- [51] Brackman G, De Meyer L, Nelis HJ, Coenye T. Biofilm inhibitory and eradicating activity of wound care products against *Staphylococcus aureus* and *Staphylococcus epidermidis* biofilms in an in vitro chronic wound model. *Journal of Applied Microbiology*. 2013;114:1833-42.
- [52] Tong SYC, Chen LF, Fowler VG, Jr. Colonization, pathogenicity, host susceptibility, and therapeutics for *Staphylococcus aureus*: what is the clinical relevance? *Seminars in Immunopathology*. 2012;34:185-200.
- [53] Dinges MM, Orwin PM, Schlievert PM. Exotoxins of *Staphylococcus aureus*. *Clinical Microbiology Reviews*. 2000;13:16-34.
- [54] Weidenmaier C, McLoughlin RM, Lee JC. The Zwitterionic Cell Wall Teichoic Acid of *Staphylococcus aureus* Provokes Skin Abscesses in Mice by a Novel CD4+T-Cell-Dependent Mechanism. *Plos One*. 2010;5:e13227.
- [55] Butler MS, Hansford KA, Blaskovich MA, Halai R, Cooper MA. Glycopeptide antibiotics: Back to the future. *Journal of Antibiotics*. 2014;67:631-44.
- [56] Van Bambeke F, Van Laethem Y, Courvalin P, Tulkens PM. Glycopeptide antibiotics from conventional molecules to new derivatives. *Drugs*. 2004;64:913-36.
- [57] Stapleton PD, Taylor PW. Methicillin resistance in *Staphylococcus aureus*: Mechanisms and modulation. *Science Progress*. 2002;85:57-72.
- [58] Harris CM, Harris TM. Structure of the glycopeptide antibiotic vancomycin-evidence for and an asparagine residue in the peptide. *Journal of the American Chemical Society*. 1982;104:4293-5.
- [59] Molinari H, Pastore A, Lian LY, Hawkes GE, Sales K. Structure of vancomycin and a vancomycin D-Ala-D-Ala complex in solution. *Biochemistry*. 1990;29:2271-7.
- [60] Cooper MA, Williams DH. Binding of glycopeptide antibiotics to a model of a vancomycin-resistant bacterium. *Chemistry & Biology*. 1999;6:891-9.
- [61] Williams DH, Bardsley B. The vancomycin group of antibiotics and the fight against resistant bacteria. *Angewandte Chemie-International Edition*. 1999;38:1173-93.
- [62] Pereira PM, Filipe SR, Tomasz A, Pinho MG. Fluorescence ratio imaging microscopy shows decreased access of vancomycin to cell wall synthetic sites in vancomycin-resistant *Staphylococcus aureus*. *Antimicrobial Agents and Chemotherapy*. 2007;51:3627-33.
- [63] Pootoolal J, Neu J, Wright GD. Glycopeptide antibiotic resistance. *Annual Review of Pharmacology and Toxicology*. 2002;42:381-408.

- [64] Reynolds PE. Structure, biochemistry and mechanism of action of glycopeptide antibiotics. *European Journal of Clinical Microbiology & Infectious Diseases*. 1989;8:943-50.
- [65] Beauregard DA, Williams DH, Gwynn MN, Knowles DJC. Dimerisation and membrane anchors in extracellular targeting of vancomycin group antibiotics. *Antimicrobial Agents and Chemotherapy*. 1995;39:781-5.
- [66] Mackay JP, Gerhard U, Beauregard DA, Maplestone RA, Williams DH. Dissection of the contributions toward dimerisation of glycopeptide antibiotics. *Journal of the American Chemical Society*. 1994;116:4573-80.
- [67] Malabarba A, Nicas TI, Thompson RC. Structural modifications of glycopeptide antibiotics. *Medicinal Research Reviews*. 1997;17:69-137.
- [68] Sun BY, Chen Z, Eggert US, Shaw SJ, LaTour JV, Kahne D. Hybrid glycopeptide antibiotics. *Journal of the American Chemical Society*. 2001;123:12722-3.
- [69] Kaplan J, Korty BD, Axelsen PH, Loll PJ. The role of sugar residues in molecular recognition by vancomycin. *Journal of Medicinal Chemistry*. 2001;44:1837-40.
- [70] Williams DH, Waltho JP. Molecular-basis of the activity of antibiotics of the vancomycin group. *Biochemical Pharmacology*. 1988;37:133-41.
- [71] Peschel A, Vuong C, Otto M, Gotz F. The D-alanine residues of *Staphylococcus aureus* teichoic acids alter the susceptibility to vancomycin and the activity of autolytic enzymes. *Antimicrobial Agents and Chemotherapy*. 2000;44:2845-7.
- [72] Sieradzki K, Tomasz A. Alterations of cell wall structure and metabolism accompany reduced susceptibility to vancomycin in an isogenic series of clinical isolates of *Staphylococcus aureus*. *Journal of Bacteriology*. 2003;185:7103-10.
- [73] Oh JK, Drumright R, Siegwart DJ, Matyjaszewski K. The development of microgels/nanogels for drug delivery applications. *Progress in Polymer Science*. 2008;33:448-77.
- [74] Hoffman AS. Applications of thermally reversible polymers and hydrogels in therapeutics and diagnostics. *Journal of Controlled Release*. 1987;6:297-306.
- [75] Langer R. Perspectives: Drug delivery - Drugs on target. *Science*. 2001;293:58-9.
- [76] Peppas NA, Hilt JZ, Khademhosseini A, Langer R. Hydrogels in biology and medicine: From molecular principles to bionanotechnology. *Advanced Materials*. 2006;18:1345-60.
- [77] Cunliffe D, Alarcon CD, Peters V, Smith JR, Alexander C. Thermoresponsive surface-grafted poly(N-isopropylacrylamide) copolymers: Effect of phase transitions on protein and bacterial attachment. *Langmuir*. 2003;19:2888-99.

- [78] Sun S, Wu P. Infrared Spectroscopic Insight into Hydration Behavior of Poly(N-vinylcaprolactam) in Water. *Journal of Physical Chemistry B*. 2011;115:11609-18.
- [79] Vasilevskaya VV, Khalatur PG, Khokhlov AR. Conformational polymorphism of amphiphilic polymers in a poor solvent. *Macromolecules*. 2003;36:10103-11.
- [80] Ramos J, Imaz A, Forcada J. Temperature-sensitive nanogels: poly(N-vinylcaprolactam) versus poly(N-isopropylacrylamide). *Polymer Chemistry*. 2012;3:852-6.
- [81] Meeussen F, Nies E, Berghmans H, Verbrugghe S, Goethals E, Du Prez F. Phase behaviour of poly(N-vinyl caprolactam) in water. *Polymer*. 2000;41:8597-602.
- [82] Arndt KF, Schmidt T, Reichelt R. Thermo-sensitive poly(methyl vinyl ether) micro-gel formed by high energy radiation. *Polymer*. 2001;42:6785-91.
- [83] Suzuki M, Hirasa O. An approach to artificial muscle using polymer gels formed by microphase separation. *Advances in Polymer Science*. 1993;110:241-61.
- [84] Chhabra H, Gupta P, Verma PJ, Jadhav S, Bellare JR. Gelatin-PMVE/MA composite scaffold promotes expansion of embryonic stem cells. *Materials Science & Engineering C-Materials for Biological Applications*. 2014;37:184-94.
- [85] Calo E, de Barros JMS, Fernandez-Gutierrez M, San Roman J, Ballamy L, Khutoryanskiy VV. Antimicrobial hydrogels based on autoclaved poly(vinyl alcohol) and poly(methyl vinyl ether-alt-maleic anhydride) mixtures for wound care applications. *Rsc Advances*. 2016;6:55211-9.
- [86] Teichmann J, Nitschke M, Pette D, Valtink M, Gramm S, Haertel FV, et al. Thermo-responsive cell culture carriers based on poly(vinyl methyl ether)-the effect of biomolecular ligands to balance cell adhesion and stimulated detachment. *Science and Technology of Advanced Materials*. 2015;16:045003.
- [87] Bo J, Wang L, Li W, Zhang X, Zhang A. Comb-like polymers pendanted with elastin-like peptides showing sharp and tunable thermoresponsiveness through dynamic covalent chemistry. *Journal of Polymer Science Part a-Polymer Chemistry*. 2016;54:3379-87.
- [88] Betre H, Setton LA, Meyer DE, Chilkoti A. Characterization of a genetically engineered elastin-like polypeptide for cartilaginous tissue repair. *Biomacromolecules*. 2002;3:910-6.
- [89] Hocine S, Li M-H. Thermoresponsive self-assembled polymer colloids in water. *Soft Matter*. 2013;9:5839-61.
- [90] Chilkoti A, Dreher MR, Meyer DE, Raucher D. Targeted drug delivery by thermally responsive polymers. *Advanced Drug Delivery Reviews*. 2002;54:613-30.

- [91] Dreher MR, Simnick AJ, Fischer K, Smith RJ, Patel A, Schmidt M, et al. Temperature triggered self-assembly of polypeptides into multivalent spherical micelles. *Journal of the American Chemical Society*. 2008;130:687-94.
- [92] Dzwolak W, Muraki T, Kato M, Taniguchi Y. Chain-length dependence of alpha-helix to beta-sheet transition in polylysine: Model of protein aggregation studied by temperature-tuned FTIR spectroscopy. *Biopolymers*. 2004;73:463-9.
- [93] Gasperini L, Mano JF, Reis RL. Natural polymers for the microencapsulation of cells. *Journal of the Royal Society Interface*. 2014;11:20140817.
- [94] MacNeil S. Biomaterials for tissue engineering of skin. *Materials Today*. 2008;11:26-35.
- [95] Van den Bulcke AI, Bogdanov B, De Rooze N, Schacht EH, Cornelissen M, Berghmans H. Structural and rheological properties of methacrylamide modified gelatin hydrogels. *Biomacromolecules*. 2000;1:31-8.
- [96] Muraoka T, Sadhukhan N, Ui M, Kawasaki S, Flazemi E, Adachi K, et al. Thermal-aggregation suppression of proteins by a structured PEG analogue: Importance of denaturation temperature for effective aggregation suppression. *Biochemical Engineering Journal*. 2014;86:41-8.
- [97] Chen YJ, Huang LW, Chiu HC, Lin SC. Temperature-responsive polymer-assisted protein refolding. *Enzyme and Microbial Technology*. 2003;32:120-30.
- [98] Rimmer S, Carter S, Rutkaite R, Haycock JW, Swanson L. Highly branched poly-(N-isopropylacrylamide)s with arginine-glycine-aspartic acid (RGD)- or COOH-chain ends that form sub-micron stimulus-responsive particles above the critical solution temperature. *Soft Matter*. 2007;3:971-3.
- [99] Lam CN, Kim M, Thomas CS, Chang D, Sanoja GE, Okwara CU, et al. The Nature of Protein Interactions Governing Globular Protein-Polymer Block Copolymer Self-Assembly. *Biomacromolecules*. 2014;15:1248-58.
- [100] Winter GD. Formation of scab and rate of epithelization of superficial wounds in skin of young domestic pig. *Nature*. 1962;193:293-4.
- [101] Svensjo T, Pomahac B, Yao F, Slama J, Eriksson E. Accelerated healing of full-thickness skin wounds in a wet environment. *Plastic and Reconstructive Surgery*. 2000;106:602-12.
- [102] James C, Johnson AL, Jenkins ATA. Antimicrobial surface grafted thermally responsive PNIPAM-co-ALA nano-gels. *Chemical Communications*. 2011;47:12777-9.

- [103] Dong LC, Hoffman AS. Thermally reversible hydrogels-swelling characteristics and activities of copoly(N-isopropylacrylamide) gels containing immobilised asparaginase. American Chemical Society Symposium Series. 1987;350:236-44.
- [104] Rimmer S, Soutar I, Swanson L. Switching the conformational behaviour of poly(N-isopropyl acrylamide). Polymer International. 2009;58:273-8.
- [105] Chee C-K, Hunt BJ, Rimmer S, Rutkaite R, Soutar I, Swanson L. Manipulating the thermoresponsive behaviour of poly(N-isopropylacrylamide) 3. On the conformational behaviour of N-isopropylacrylamide graft copolymers. Soft Matter. 2009;5:3701-12.
- [106] Yoshida R, Uchida K, Kaneko Y, Sakai K, Kikuchi A, Sakurai Y, et al. COMB-TYPE GRAFTED HYDROGELS WITH RAPID DE-SWELLING RESPONSE TO TEMPERATURE-CHANGES. Nature. 1995;374:240-2.
- [107] Chang K, Rubright NC, Lowery PD, Taite LJ. Structural optimization of highly branched thermally responsive polymers as a means of controlling transition temperature. Journal of Polymer Science Part a-Polymer Chemistry.2013;51:2068-78.
- [108] Chetty A, Kovacs J, Sulyok Z, Meszaros A, Fekete J, Domjan A, et al. A versatile characterization of poly(N-isopropylacrylamide-co-N,N'-methylene-bis-acrylamide) hydrogels for composition, mechanical strength, and rheology. Express Polymer Letters.2013;7:95-105.
- [109] Chee CK, Rimmer S, Soutar I, Swanson L. Fluorescence investigations of the conformational behaviour of poly(N-vinylcaprolactam). Reactive & Functional Polymers. 2006;66:1-11.
- [110] Ringsdorf H, Venzmer J, Winnik FM. Fluorescence studies of hydrophobicity modified poly(N-isopropylacrylamides). Macromolecules. 1991;24:1678-86.
- [111] Constantin M, Cristea M, Ascenzi P, Fundueanu G. Lower critical solution temperature versus volume phase transition temperature in thermoresponsive drug delivery systems. Express Polymer Letters. 2011;5:839-48.
- [112] Oh SY, Bae YC. Role of intermolecular interactions for upper and lower critical solution temperature behaviors in polymer solutions: Molecular simulations and thermodynamic modeling. Polymer.2012;53:3772-9.
- [113] Bergbreiter DE, Mijalis AJ, Fu H. Polymer Inverse Temperature-Dependent Solubility: A Visual Demonstration of the Importance of $T \Delta S$ in the Gibbs Equation. Journal of Chemical Education.2012;89:675-7.

- [114] Hamcerencu M, Desbrieres J, Khoukh A, Popa M, Riess G. Thermodynamic investigation of thermoresponsive xanthan-poly (N-isopropylacrylamide) hydrogels. *Polymer International*.2012;60:1527-34.
- [115] Alfurhood JA, Bachler PR, Sumerlin BS. Hyperbranched polymers via RAFT self-condensing vinyl polymerization. *Polymer Chemistry*. 2016;7:3361-9.
- [116] Charleux B, Faust R. Synthesis of branched polymers by cationic polymerization. *Branched Polymers I*. 1999;142:1-69.
- [117] Ishizu K, Ohta Y, Kawauchi S. Kinetics of hyperbranched polystyrenes by free radical polymerization of photofunctional inimer. *Macromolecules*. 2002;35:3781-4.
- [118] Matyjaszewski K. Controlled radical polymerization. *Current Opinion in Solid State & Materials Science*. 1996;1:769-76.
- [119] Chiefari J, Chong YK, Ercole F, Krstina J, Jeffery J, Le TPT, et al. Living free-radical polymerization by reversible addition-fragmentation chain transfer: The RAFT process. *Macromolecules*. 1998;31:5559-62.
- [120] Willcock H, O'Reilly RK. End group removal and modification of RAFT polymers. *Polymer Chemistry*.2010;1:149-57.
- [121] Moad G, Chong YK, Postma A, Rizzardo E, Thang SH. Advances in RAFT polymerization: the synthesis of polymers with defined end-groups. *Polymer*. 2005;46:8458-68.
- [122] York AW, Kirkland SE, McCormick CL. Advances in the synthesis of amphiphilic block copolymers via RAFT polymerization: Stimuli-responsive drug and gene delivery. *Advanced Drug Delivery Reviews*. 2008;60:1018-36.
- [123] Moad G, Rizzardo E, Thang SH. Radical addition-fragmentation chemistry in polymer synthesis. *Polymer*. 2008;49:1079-131.
- [124] Favier A, Charreyre M-T. Experimental requirements for an efficient control of free-radical polymerizations via the reversible addition-fragmentation chain transfer (RAFT) process. *Macromolecular Rapid Communications*. 2006;27:653-92.
- [125] Moad G, Rizzardo E, Thang SH. End-functional polymers, thiocarbonylthio group removal/transformation and reversible addition-fragmentation-chain transfer (RAFT) polymerization. *Polymer International*.2011;60:9-25.
- [126] Goto A, Sato K, Tsujii Y, Fukuda T, Moad G, Rizzardo E, et al. Mechanism and kinetics of RAFT-based living radical polymerizations of styrene and methyl methacrylate. *Macromolecules*. 2001;34:402-8.

- [127] Monteiro MJ. Design strategies for controlling the molecular weight and rate using reversible addition-fragmentation chain transfer mediated living radical polymerization. *Journal of Polymer Science Part a-Polymer Chemistry*. 2005;43:3189-204.
- [128] Favier A, Charreyre MT, Pichot C. A detailed kinetic study of the RAFT polymerization of a bi-substituted acrylamide derivative: influence of experimental parameters. *Polymer*. 2004;45:8661-74.
- [129] Carter SR, England RM, Hunt BJ, Rimmer S. Functional graft Poly(N-isopropyl acrylamide)s using reversible addition-fragmentation chain transfer (RAFT) polymerisation. *Macromolecular Bioscience*. 2007;7:975-86.
- [130] Plummer R, Goh YK, Whittaker AK, Monteiro MJ. Effect of impurities in cumyl dithiobenzoate on RAFT-mediated polymerizations. *Macromolecules*. 2005;38:5352-5.
- [131] Kamath G, Deshmukh SA, Baker GA, Mancini DC, Sankaranarayanan SKRS. Thermodynamic considerations for solubility and conformational transitions of poly-N-isopropyl-acrylamide. *Physical Chemistry Chemical Physics*. 2013;15:12667-73.
- [132] Rimmer S, Macneil S, Swanson L, Douglas CWI. Method for removing bacteria from medium, involves providing stimuli-responsive polymer capable of binding bacteria, applying functionalized polymer to medium and removing polymer-bound bacteria from medium. University of Sheffield.
- [133] Reddy TT, Kano A, Maruyama A, Hadano M, Takahara A. Synthesis and Characterization of Semi-Interpenetrating Polymer Networks Based on Polyurethane and N-isopropylacrylamide for Wound Dressing. *Journal of Biomedical Materials Research Part B-Applied Biomaterials*. 2009;88B:32-40.
- [134] England RM, Rimmer S. Hyper/highly-branched polymers by radical polymerisations. *Polymer Chemistry*. 2010;1:1533-44.
- [135] Vogt AP, Gondi SR, Sumerlin BS. Hyperbranched polymers via RAFT copolymerization of an acryloyl trithiocarbonate. *Australian Journal of Chemistry*. 2007;60:396-9.
- [136] Vogt AP, Sumerlin BS. Tuning the Temperature Response of Branched Poly(N-isopropylacrylamide) Prepared by RAFT Polymerization. *Macromolecules*. 2008;41:7368-73.
- [137] Plenderleith R, Swift T, Rimmer S. Highly-branched poly(N-isopropyl acrylamide)s with core-shell morphology below the lower critical solution temperature. *Rsc Advances*. 2014;4:50932-7.
- [138] Wang C, Liu M, Yuan L, Wang L, Sun D, Wang Z, et al. Calorimetric and spectroscopic studies on temperature- and pH-dependent interactions of stimuli-responsive

poly (N-isopropylacrylamide) with piceatannol. *Journal of Chemical Thermodynamics*. 2016;98:186-92.

[139] Hopkins S, Carter SR, Haycock JW, Fullwood NJ, MacNeil S, Rimmer S. Sub-micron poly(N-isopropylacrylamide) particles as temperature responsive vehicles for the detachment and delivery of human cells. *Soft Matter*. 2009;5:4928-37.

[140] Golini CM, Williams BW, Foresman JB. Further solvatochromic, thermochromic, and theoretical studies on Nile Red. *Journal of Fluorescence*. 1998;8:395-404.

[141] Jose J, Burgess K. Syntheses and properties of water-soluble Nile Red derivatives. *Journal of Organic Chemistry*. 2006;71:7835-9.

[142] Sackett DL, Wolff J. Nile red as a polarity-sensitive fluorescent-probe of hydrophobic protein surfaces. *Analytical Biochemistry*. 1987;167:228-34.

[143] Briggs MSJ, Bruce I, Miller JN, Moody CJ, Simmonds AC, Swann E. Synthesis of functionalised fluorescent dyes and their coupling to amines and amino acids. *Journal of the Chemical Society-Perkin Transactions 1*. 1997;0:1051-8.

[144] Pasparakis G, Cockayne A, Alexander C. Control of bacterial aggregation by thermoresponsive glycopolymers. *Journal of the American Chemical Society*. 2007;129:11014-5.

[145] Lapworth JW, Hatton PV, Rimmer S. Thermally responsive gels formed from highly branched poly(N-isopropyl acrylamide)s with either carboxylic acid or trihistidine end groups. *Royal Society of Chemistry Advances*. 2013;3:18107-14.

[146] Frechet JMJ, Hawker CJ. Hyperbranched polyphenylene and hyperbranched polyesters: New soluble, three-dimensional, reactive polymers. *Reactive & Functional Polymers*. 1995;26:127-36.

[147] Moad G, Rizzardo E, Thang SH. End-functional polymers, thiocarbonylthio group removal/transformation and reversible addition-fragmentation-chain transfer (RAFT) polymerization. *Polymer International*. 2011;60:9-25.

[148] Vancoillie G, Vergaelen M, Hoogenboom R. Ultra-high performance size-exclusion chromatography in polar solvents. *Journal of Chromatography A*. 2016;1478:43-9.

[149] Meunier DM, Lyons JW, Kiefer JJ, Niu QJ, DeLong LM, Li Y, et al. Determination of Particle Size Distributions, Molecular Weight Distributions, Swelling, Conformation, and Morphology of Dilute Suspensions of Cross-Linked Polymeric Nanoparticles via Size-Exclusion Chromatography/Differential Viscometry. *Macromolecules*. 2014;47:6715-29.

- [150] Swift T, Hoskins R, Telford R, Plenderleith R, Pownall D, Rimmer S. Analysis using size exclusion chromatography of poly(N-isopropyl acrylamide) using methanol as an eluent. *Journal of Chromatography A*. 2017;1508:16-23.
- [151] Gaborieau M, Nicolas J, Save M, Charleux B, Vairon JP, Gilbert RG, et al. Separation of complex branched polymers by size-exclusion chromatography probed with multiple detection. *Journal of Chromatography A*. 2008;1190:215-23.
- [152] Lu YY, Shi TF, An LJ, Wang ZG. Intrinsic viscosity of polymers: From linear chains to dendrimers. *Europhysics Letters*. 2012;97.
- [153] Nakayama M, Okano T. Polymer terminal group effects on properties of thermoresponsive polymeric micelles with controlled outer-shell chain lengths. *Biomacromolecules*. 2005;6:2320-7.
- [154] Li ST, Su Y, Dan MH, Zhang WQ. Thermo-responsive ABA triblock copolymer of PVEA-b-PNIPAM-b-PVEA showing solvent-tunable LCST in a methanol-water mixture. *Polymer Chemistry*. 2014;5:1219-28.
- [155] Durand A, Hourdet D. Thermoassociative graft copolymers based on poly(N-isopropylacrylamide): Relation between the chemical structure and the rheological properties. *Macromolecular Chemistry and Physics*. 2000;201:858-68.
- [156] Chee CK, Rimmer S, Shaw DA, Soutar I, Swanson L. Manipulating the thermoresponsive behavior of poly(N-isopropylacrylamide). 1. On the conformational behavior of a series of N-isopropylacrylamide - Styrene statistical copolymers. *Macromolecules*. 2001;34:7544-9.
- [157] Tauer K, Gau D, Schulze S, Voelkel A, Dimova R. Thermal property changes of poly(N-isopropylacrylamide) microgel particles and block copolymers. *Colloid and Polymer Science*. 2009;287:299-312.
- [158] Schild HG, Muthukumar M, Tirrell DA. Cononsolvency in mixed aqueous-solution of poly(N-isopropylacrylamide). *Macromolecules*. 1991;24:948-52.
- [159] Schild HG, Tirrell DA. Interaction of poly(N-isopropylacrylamide) with sodium normal-alkylsulfates in aqueous-solution. *Langmuir*. 1991;7:665-71.
- [160] Chee CK, Rimmer S, Soutar I, Swanson L. Fluorescence investigations of the thermally induced conformational transition of poly(N-isopropylacrylamide). *Polymer*. 2001;42:5079-87.
- [161] Swift T, Lapworth J, Swindells K, Swanson L, Rimmer S. pH responsive highly branched poly(N-isopropylacrylamide) with trihistidine or acid chain ends. *Royal Society of Chemistry Advances*. 2016;6:71345-50.

- [162] Furyk S, Zhang YJ, Ortiz-Acosta D, Cremer PS, Bergbreiter DE. Effects of end group polarity and molecular weight on the lower critical solution temperature of poly(N-isopropylacrylamide). *Journal of Polymer Science Part a-Polymer Chemistry*. 2006;44:1492-501.
- [163] Chung JE, Yokoyama M, Suzuki K, Aoyagi T, Sakurai Y, Okano T. Reversibly thermo-responsive alkyl-terminated poly(N-isopropylacrylamide) core-shell micellar structures. *Colloids and Surfaces B-Biointerfaces*. 1997;9:37-48.
- [164] Hofmann C, Schonhoff M. Do additives shift the LCST of poly (N-isopropylacrylamide) by solvent quality changes or by direct interactions? *Colloid and Polymer Science*. 2009;287:1369-76.
- [165] Hirun N, Bao H, Li L, Deen GR, Tantishaiyakul V. Micro-DSC, rheological and NMR investigations of the gelation of gallic acid and xyloglucan. *Soft Matter*. 2012;8:7258-68.
- [166] Zhou Y, Jiang K, Song Q, Liu S. Thermo-induced formation of unimolecular and multimolecular micelles from novel double hydrophilic multiblock copolymers of N,N-dimethylacrylamide and N-isopropylacrylamide. *Langmuir*. 2007;23:13076-84.
- [167] Sarker P, Shepherd J, Swindells K, Douglas I, MacNeil S, Swanson L, et al. Highly Branched Polymers with Polymyxin End Groups Responsive to *Pseudomonas aeruginosa*. *Biomacromolecules*. 2011;12:1-5.
- [168] Klodzinska E, Szumski M, Dziubakiewicz E, Hryniewicz K, Skwarek E, Janusz W, et al. Effect of zeta potential value on bacterial behavior during electrophoretic separation. *Electrophoresis*. 2010;31:1590-6.
- [169] Yusa S, Sakakibara AK, Yamamoto T, Morishima Y. Reversible pH-induced formation and disruption of unimolecular micelles of an amphiphilic polyelectrolyte. *Macromolecules*. 2002;35:5243-9.
- [170] Balamurugan S, Mendez S, Balamurugan SS, O'Brien MJ, Lopez GP. Thermal response of poly(N-isopropylacrylamide) brushes probed by surface plasmon resonance. *Langmuir*. 2003;19:2545-9.
- [171] Luo SZ, Xu J, Zhu ZY, Wu C, Liu SY. Phase transition behavior of unimolecular micelles with thermoresponsive poly(N-isopropylacrylamide) coronas. *Journal of Physical Chemistry B*. 2006;110:9132-9.
- [172] Lee SC, Chang JY. Thermosensitive Block Copolymers Consisting of Poly(N-isopropylacrylamide) and Star Shape Oligo(ethylene oxide). *Bulletin of the Korean Chemical Society*. 2009;30:1521-5.

- [173] Geever LM, Nugent MJD, Higginbotham CL. The effect of salts and pH buffered solutions on the phase transition temperature and swelling of thermoresponsive pseudogels based on N-isopropylacrylamide. *Journal of Materials Science*. 2007;42:9845-54.
- [174] Vlachy N, Jagoda-Cwiklik B, Vacha R, Touraud D, Jungwirth P, Kunz W. Hofmeister series and specific interactions of charged headgroups with aqueous ions. *Advances in Colloid and Interface Science*. 2009;146:42-7.
- [175] Zhang Y, Furyk S, Sagle LB, Cho Y, Bergbreiter DE, Cremer PS. Effects of Hofmeister anions on the LCST of PNIPAM as a function of molecular weight. *Journal of Physical Chemistry C*. 2007;111:8916-24.
- [176] Jhon YK, Bhat RR, Jeong C, Rojas OJ, Szleifer I, Genzer J. Salt-induced depression of lower critical solution temperature in a surface-grafted neutral thermoresponsive polymer. *Macromolecular Rapid Communications*. 2006;27:697-701.
- [177] Thormann E. On understanding of the Hofmeister effect: how addition of salt alters the stability of temperature responsive polymers in aqueous solutions. *Royal Society of Chemistry Advances*. 2012;2:8297-305.
- [178] Eeckman F, Amighi K, Moes AJ. Effect of some physiological and non-physiological compounds on the phase transition temperature of thermoresponsive polymers intended for oral controlled-drug delivery. *International Journal of Pharmaceutics*. 2001;222:259-70.
- [179] Du H, Wickramasinghe R, Qian X. Effects of Salt on the Lower Critical Solution Temperature of Poly (N-Isopropylacrylamide). *Journal of Physical Chemistry B*. 2010;114:16594-604.
- [180] Sadeghi R, Jahani F. Salting-In and Salting-Out of Water-Soluble Polymers in Aqueous Salt Solutions. *Journal of Physical Chemistry B*. 2012;116:5234-41.
- [181] Nair UB, Chang SSC, Armstrong DW, Rawjee YY, Eggleston DS, McArdle JV. Elucidation of vancomycin's enantioselective binding site using its copper complex. *Chirality*. 1996;8:590-5.
- [182] Brzezowska M, Kucharczyk-Klaminska M, Bernardi F, Valensin D, Gaggelli N, Gaggelli E, et al. Cu(II) ion interaction with teicoplanin-vancomycin's analog. *Journal of Inorganic Biochemistry*. 2010;104:193-8.
- [183] Aydin S. A short history, principles, and types of ELISA, and our laboratory experience with peptide/protein analyses using ELISA. *Peptides*. 2015;72:4-15.
- [184] Engvall E, Perlmann P. Enzyme-linked immunosorbent assay(ELISA) quantitative assay of immunoglobulin-G. *Immunochemistry*. 1971;8:871-74.

- [185] Jarvis WR. Selected aspects of the socioeconomic impact of nosocomial infections: Morbidity, mortality, cost, and prevention. *Infection Control and Hospital Epidemiology*. 1996;17:552-7.
- [186] Purcell K, Fergie J. Epidemic of community-acquired methicillin-resistant *Staphylococcus aureus* infections - A 14-year study at Driscoll Children's Hospital. *Archives of Pediatrics & Adolescent Medicine*. 2005;159:980-5.
- [187] Courvalin P. Vancomycin resistance in Gram-positive cocci. *Clinical Infectious Diseases*. 2006;42:S25-S34.
- [188] Peleg AY, Monga D, Pillai S, Mylonakis E, Moellering RC, Jr., Eliopoulos GM. Reduced Susceptibility to Vancomycin Influences Pathogenicity in *Staphylococcus aureus* Infection. *Journal of Infectious Diseases*. 2009;199:532-6.
- [189] Riedel S, Neoh KM, Eisinger SW, Dam LM, Tekle T, Carroll KC. Comparison of Commercial Antimicrobial Susceptibility Test Methods for Testing of *Staphylococcus aureus* and *Enterococci* against Vancomycin, Daptomycin, and Linezolid. *Journal of Clinical Microbiology*. 2014;52:2216-22.
- [190] Hayhurst EJ, Kailas L, Hobbs JK, Foster SJ. Cell wall peptidoglycan architecture in *Bacillus subtilis*. *Proceedings of the National Academy of Sciences of the United States of America*. 2008;105:14603-8.
- [191] Scherrer R, Gerhardt P. Molecular sieving by *Bacillus megaterium* cell wall and protoplast. *Journal of Bacteriology*. 1971;107:718-&.
- [192] Reifsteck F, Wee S, Wilkinson BJ. Hydrophobicity hydrophilicity of Staphylococci. *Journal of Medical Microbiology*. 1987;24:65-73.
- [193] Dmitriev BA, Holst O, Rietschel ET, Ehlers S. Tertiary structure of *Staphylococcus aureus* cell wall murein. *Journal of Bacteriology*. 2004;186:7141-8.
- [194] Lienkamp K, Kumar K-N, Som A, Nuesslein K, Tew GN. "Doubly Selective" Antimicrobial Polymers: How Do They Differentiate between Bacteria? *Chemistry-a European Journal*. 2009;15:11710-4.
- [195] Demchick P, Koch AL. The permeability of the wall fabric of *Escherichia coli* and *Bacillus subtilis*. *Journal of Bacteriology*. 1996;178:768-73.
- [196] Rosenberg M. Bacterial adherence to hydrocarbons-A useful technique for studying cell surface hydrophobicity. *Federation of European Microbiological Societies Microbiology Letters*. 1984;22:289-95.
- [197] Jonsson P, Wadstrom T. High surface hydrophobicity of *Staphylococcus aureus* as revealed by hydrophobic interaction chromatography. *Current Microbiology*. 1983;8:347-53.

- [198] Mesnage S, Dellarole M, Baxter NJ, Rouget J-B, Dimitrov JD, Wang N, et al. Molecular basis for bacterial peptidoglycan recognition by LysM domains. *Nature Communications*. 2014;5:4269.
- [199] Rosenberg M, Gutnick D, Rosenberg E. Adherence of bacteria to hydrocarbons- A simple method for measuring cell hydrophobicity. *Federation of European Microbiological Societies Microbiology Letters*. 1980;9:29-33.
- [200] Bae T, Baba T, Hiramatsu K, Schneewind O. Prophages of *Staphylococcus aureus* Newman and their contribution to virulence. *Molecular Microbiology*. 2006;62:1035-47.
- [201] Howden BP, Davies JK, Johnson PDR, Stinear TP, Grayson ML. Reduced Vancomycin Susceptibility in *Staphylococcus aureus*, Including Vancomycin-Intermediate and Heterogeneous Vancomycin-Intermediate Strains: Resistance Mechanisms, Laboratory Detection, and Clinical Implications. *Clinical Microbiology Reviews*. 2010;23:99-139.
- [202] Cooper MA, Fiorini MT, Abell C, Williams DH. Binding of vancomycin group antibiotics to D-alanine and D-lactate presenting self-assembled monolayers. *Bioorganic & Medicinal Chemistry*. 2000;8:2609-16.
- [203] Pinho MG, Errington J. Dispersed mode of *Staphylococcus aureus* cell wall synthesis in the absence of the division machinery. *Molecular Microbiology*. 2003;50:871-81.
- [204] Teratanatorn P, Hoskins R, Swift T, Douglas CWI, Shepherd J, Rimmer S. Binding of Bacteria to Poly(N-isopropylacrylamide) Modified with Vancomycin: Comparison of Behavior of Linear and Highly Branched Polymers. *Biomacromolecules*. 2017;18:2887-99.
- [205] Bertozzi CR, Kiessling LL. Chemical glycobiology. *Science*. 2001;291:2357-64.
- [206] Lather P, Mohanty AK, Jha P, Garsa AK. Contribution of Cell Surface Hydrophobicity in the Resistance of *Staphylococcus aureus* against Antimicrobial Agents. *Biochemistry research international*. 2016;2016:1091290.
- [207] Terada A, Yuasa A, Kushimoto T, Tsuneda S, Katakai A, Tamada M. Bacterial adhesion to and viability on positively charged polymer surfaces. *Microbiology-Sgm*. 2006;152:3575-83.
- [208] Wilson WW, Wade MM, Holman SC, Champlin FR. Status of methods for assessing bacterial cell surface charge properties based on zeta potential measurements. *Journal of Microbiological Methods*. 2001;43:153-64.
- [209] Poortinga AT, Bos R, Norde W, Busscher HJ. Electric double layer interactions in bacterial adhesion to surfaces. *Surface Science Reports*. 2002;47:3-32.

- [210] Soni KA, Balasubramanian AK, Beskok A, Pillai SD. Zeta potential of selected bacteria in drinking water when dead, starved, or exposed to minimal and rich culture media. *Current Microbiology*. 2008;56:93-7.
- [211] Duval JFL, Ohshima H. Electrophoresis of diffuse soft particles. *Langmuir*. 2006;22:3533-46.
- [212] Sonohara R, Muramatsu N, Ohshima H, Kondo T. Difference in surface properties between *Escherichia coli* and *Staphylococcus aureus* as revealed by electrophoretic mobility measurements. *Biophysical Chemistry*. 1995;55:273-7.
- [213] Ohshima H. Electrophoresis of soft particles. *Advances in Colloid and Interface Science*. 1995;62:189-235.
- [214] Abbasnezhad H, Gray MR, Foght JM. Two different mechanisms for adhesion of Gram-negative bacterium, *Pseudomonas fluorescens* LP6a, to an oil-water interface. *Colloids and Surfaces B-Biointerfaces*. 2008;62:36-41.
- [215] Carneiro-da-Cunha MG, Cerqueira MA, Souza BWS, Teixeira JA, Vicente AA. Influence of concentration, ionic strength and pH on zeta potential and mean hydrodynamic diameter of edible polysaccharide solutions envisaged for multilayered films production. *Carbohydrate Polymers*. 2011;85:522-8.
- [216] McConaughy SD, Stroud PA, Boudreaux B, Hester RD, McCormick CL. Structural characterization and solution properties of a galacturonate polysaccharide derived from *Aloe vera* capable of in situ gelation. *Biomacromolecules*. 2008;9:472-80.
- [217] Kiessling LL, Strong LE, Gestwicki JE. Principles for multivalent ligand design. *Annual Reports in Medicinal Chemistry*, Vol 35. 2000;35:321-30.
- [218] Gottenbos B, Grijpma DW, van der Mei HC, Feijen J, Busscher HJ. Antimicrobial effects of positively charged surfaces on adhering Gram-positive and Gram-negative bacteria. *Journal of Antimicrobial Chemotherapy*. 2001;48:7-13.
- [219] Komaromi I, Somogyi A, Dinya Z, Bogнар R, Sztaricskai F. The role of the carboxylate binding pocket of the vancomycin group of antibiotics in the antibacterial effect- A molecular mechanics study. *Journal of Molecular Structure-Computational and Theoretical Chemistry*. 1989;60:351-61.
- [220] Greenspan P, Mayer EP, Fowler SD. Nile red - A selective fluorescent stain for intracellular lipid droplets. *Journal of Cell Biology*. 1985;100:965-73.
- [221] Fowler SD, Greenspan P. Application of nile red, a fluorescent hydrophobic probe, for the detection of neutral lipid deposits in tissue selections comparison with oil red O. *Journal of Histochemistry & Cytochemistry*. 1985;33:833-6.

- [222] Swain J, Mishra AK. Nile red fluorescence for quantitative monitoring of micropolarity and microviscosity of pluronic F127 in aqueous media. *Photochemical & Photobiological Sciences*. 2016;15:1400-7.
- [223] Inal S, Koelsch JD, Chiappisi L, Janietz D, Gradzielski M, Laschewsky A, et al. Structure-related differences in the temperature-regulated fluorescence response of LCST type polymers. *Journal of Materials Chemistry C*. 2013;1:6603-12.
- [224] Cartwright SJ. Solvatochromic dyes detect the presence of homeopathic potencies. *Homeopathy*. 2016;105:55-65.
- [225] Lobnik A, Wolfbeis OS. Probing the polarity of sol-gels and ormosils via the absorption of Nile Red. *Journal of Sol-Gel Science and Technology*. 2001;20:303-11.
- [226] Chen W, Zhang C, Song L, Sommerfeld M, Hu Q. A high throughput Nile red method for quantitative measurement of neutral lipids in microalgae. *Journal of Microbiological Methods*. 2009;77:41-7.
- [227] Greenspan P, Fowler SD. Spectrofluorometric studies of the lipid probe, Nile red. *Journal of Lipid Research*. 1985;26:781-9.
- [228] Shim WJ, Song YK, Hong SH, Jang M. Identification and quantification of microplastics using Nile Red staining. *Marine Pollution Bulletin*. 2016;113:469-76.
- [229] Stuart MCA, van de Pas JC, Engberts J. The use of Nile Red to monitor the aggregation behavior in ternary surfactant-water-organic solvent systems. *Journal of Physical Organic Chemistry*. 2005;18:929-34.
- [230] Liu XM, Wang LS, Wang L, Huang JC, He CB. The effect of salt and pH on the phase-transition behaviors of temperature-sensitive copolymers based on N-isopropylacrylamide. *Biomaterials*. 2004;25:5659-66.
- [231] Burova TV, Grinberg NV, Dubovik AS, Tanaka K, Grinberg VY, Grosberg AY. Effects of ligand binding on relative stability of subchain conformations of weakly charged N-isopropylacrylamide gels in swollen and shrunken states. *Macromolecules*. 2003;36:9115-21.
- [232] Cooper A, McAuleyhecht KE. Microcalorimetry and the molecular recognition of peptides and proteins. *Philosophical Transactions of the Royal Society a-Mathematical Physical and Engineering Sciences*. 1993;345:23-35.
- [233] Graziano G. On the temperature-induced coil to globule transition of poly-N-isopropylacrylamide in dilute aqueous solutions. *International Journal of Biological Macromolecules*. 2000;27:89-97.

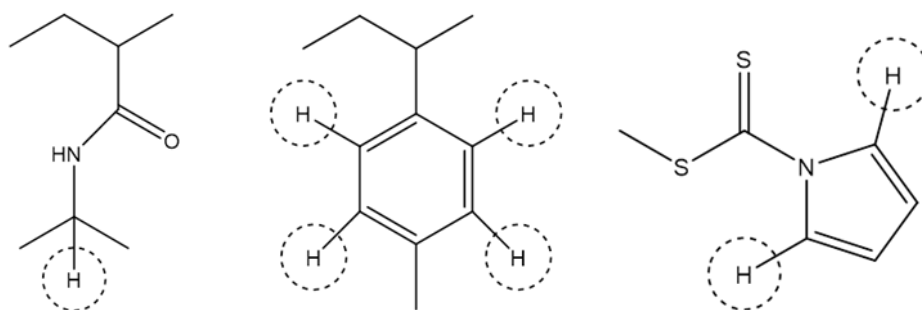
- [234] Constantin M, Cristea M, Ascenzi P, Fundueanu G. Lower critical solution temperature versus volume phase transition temperature in thermoresponsive drug delivery systems. *Express Polymer Letters*. 5:839-48.
- [235] Bergbreiter DE, Mijalis AJ, Fu H. Polymer Inverse Temperature-Dependent Solubility: A Visual Demonstration of the Importance of $T \Delta S$ in the Gibbs Equation. *Journal of Chemical Education*. 2012;89:675-7.
- [236] von Ah U, Wirz D, Daniels AU. Rapid differentiation of methicillin-susceptible *Staphylococcus aureus* from methicillin-resistant *S. aureus* and MIC determinations by isothermal microcalorimetry. *Journal of Clinical Microbiology*. 2008;46:2083-7.
- [237] McPhail D, Cooper A. Thermodynamics and kinetics of dissociation of ligand-induced dimers of vancomycin antibiotics. *Journal of the Chemical Society-Faraday Transactions*. 1997;93:2283-9.
- [238] Jiang L, Cao S, Cheung PP-H, Zheng X, Leung CWT, Peng Q, et al. Real-time monitoring of hydrophobic aggregation reveals a critical role of cooperativity in hydrophobic effect. *Nature Communications*. 2017;8:15639.
- [239] Aseyev V, Hietala S, Laukkanen A, Nuopponen M, Confortini O, Du Prez FE, et al. Mesoglobules of thermoresponsive polymers in dilute aqueous solutions above the LCST. *Polymer*. 2005;46:7118-31.

Appendix 1: NMR functionality calculations

For ^1H NMR functionality calculation the integrals of NIPAM isopropyl functional group, the benzyl group and the N-pyrrole hydrogens were compared, fixing the isopropyl NIPAM functionalities to 1 (results shown in figure 2.2-2.5). The ^1H values were calculated by dividing the integrals of isopropyl NIPAM by 6, benzyl by 4 and N-pyrrole by 2.

The distal hydrogen from pyrrole functional unit overlaps the benzyl peak. For this reason distal pyrroles were not used in functionality calculations.

Protons used in ^1H NMR functionality calculation for isopropyl NIPAM, benzyl and N-pyrrole

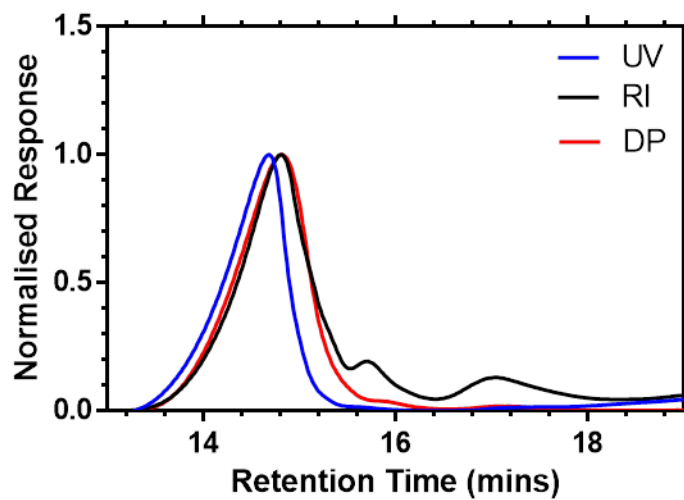


$$\% \text{Pyrrole functionality} = \frac{1H \text{ pyrrole}}{1H \text{ Benzyl}} \times 100$$

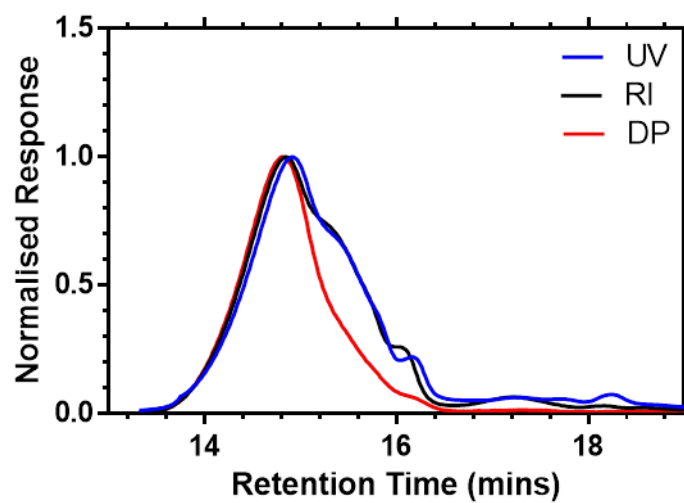
$$\text{Degree of Branching} = \frac{1H \text{ pyrrole}}{1H \text{ NIPAM} + 1H \text{ Benzyl} + 1H \text{ Pyrrole}}$$

Appendix 2 GPC chromatograms showing data from RI, UV (295 nm) and viscometric detectors of (a) L-PNIPAM-van and (b) HB-PNIPAM-van

a)



b)



Appendix 3: The size distribution of HB-PNIPAM-van and L-PNIPAM-van carried out on a Brookhaven Instrument Corporation ZetaPALS 90Plus at 25°C (pH 7.6)

